1-1-1967

Influence of opening on stresses in deep beams with plain and stiffened edges.

Muhammad Harunur Rashid
University of Windsor

INFLUENCE OF OPENING ON STRESSES IN DEEP BEAMS WITH PLAIN AND STIFFENED EDGES

A Dissertation
Submitted to the Faculty of Graduate Studies Through the
Department of Civil Engineering in Partial Fulfillment
of the Requirements for the Degree of
Doctor of Philosophy at the
University of Windsor

by

Muhammad Harunur Rashid
B.Sc. Engg., University of Dacca, 1956
M.S., University of Illinois, 1961
M.A.Sc., University of Toronto, 1967

Windsor, Ontario, Canada
1969

NSX 6708

APPROVED BY:

J. Kennedy

G. Abdel-Sayed

Thompson

A. L. Smith

275304

PREFACE

The utilization of computer techniques to solve large numbers of simultaneous equations has removed the long-standing restrictions applied to solutions in closed form of civil engineering problems primarily designed for hand calculations. More versatile methods can now be developed and utilized, without too many assumptions, applicable to wider range of problems, hitherto avoided because of the number of equations; one such approach, simple in concept but versatile in its applications, the displacement method, is demonstrated in this dissertation towards the solution of doubly connected deep beams.

The author is greatly indebted to Dr. J. B. Kennedy for his untiring advice, suggestions, encouragements and discussions. The author feels extremely fortunate to have studied under his guidance. The efforts of other members of the dissertation committee, specially Dr. G. Abdel-Sayed for his valuable suggestions are gratefully acknowledged.

The financial assistance of the Canadian Agency for International Development greatly made this study possible. Thanks are also due to the workshop staff, specially Mr. M. Aminzadeh for his assistance in setting up the equipment.

This dissertation represents the culmination of a great deal of effort and utmost dedication not only on the part of the author but also his entire family. Words cannot express enough gratitude

for the enormous sacrifice of the two children, Imran and Suzan and wife, Milly who has constantly provided technical, secretarial and inspirational assistance for the last several years.

ABSTRACT

This dissertation deals with the problem of doubly connected deep beams with or without stiffening around the outer edges. Without going through the application of customary Airy stress function for plane stress problems and the necessary corrections for the doubly-connected domain, the displacement method hitherto avoided for the increased number of simultaneous equations, was successfully applied. The versatile method of finite difference approximations, in transforming the partial differential equations in terms of displacements at discrete points into linear simultaneous equations containing the unknown variables, was used. A solid deep beam without any opening was studied to compare the results with those of the previous investigators, so as to prove the reliability and the utility of the method over the conventional Airy stress function applied to deep beam problems. A set of seven experiments were conducted on deep beams with unstiffened edges and with three different sizes of opening at the centre. The experimental results agree well with the theoretical ones.

Addition of stiffening around the outer edges creates a state of singularity along the interfaces. This is due to the abrupt change of cross-section. In order to avoid this, the problem was separated into two parts, the plate itself and the stiffening frame with equal and opposite forces as well as equal displacements and curvatures assumed to be acting. Instead of dividing the frame into a finite-difference mesh, the redurdant forces in the statically indeterminate frame were

determined through Castigliano's first theorem applied to linear frame analysis. The curvatures of the frame-members in terms of moments and the curvatures of the plate at a discrete point in terms of the displacements were equated to yield sufficient number of extranodal equations covering the unknown forces, assumed to be in the form of trigonometric series along the interfaces. Here again, a set of eight experiments on aluminum models were conducted. The agreement between theoretical and experimental results were not as good as that for the unstiffened cases. This is mainly due to the additional disturbing conditions that arise from the presence of interfaces. Also the linear frame analysis (in the absence of a suitable non-linear method) incorporates a limitation of the general use of the method, since it is not applicable to very slender stiffening frame. Here the axial strain will gain prominence over the bending moment, which in turn will question the validity of the linear frame analysis.

It was shown by the graphical results that the pursued method of displacement can be reliably applied to deep beams with openings with or without stiffened outer edges. With a finer meshwork better results can be obtained without the need of any further experimental verifications keeping in mind the fact that, unlike other numerical methods, too many assumptions are not necessary in this direct approach where only a minor modification in the differential equation itself is in effect. Although the computations far exceed the amount of other widely applied methods, the versatility of the present approach in its application to simply as well as doubly-connected plane stress problems, is sure to offset those arising from

the facilities offered by the computer techniques to handle precisely a large number of linear simultaneous equations.

TABLE OF CONTENTS

LIST OF FIGURES

Fig. 34 Longitudinal Stresses at Midsection of a Stiffened Rect. Deep Beam with a Small Opening.

Fig. 35 Longitudinal Stresses at Midsection of a Stiffened Rect. Deep Beam with a Small Opening.

LIST OF TABLES

CHAPTER I

INTRODUCTION

Beams whose depths are comparable to their spans are used in a variety of structures; the constructions of bins or hoppers, as well as in foundation walls or in cases in which walls are supported on individual columns or footings. The horizontal and vertical diaphra used to transmit wind forces in floors or walls of buildings are frequently of such dimensions as to represent deep beams. In reinforced concrete hipped plate construction, the plates of the structure proper or the vertical supporting diaphra often fall into this category. In bridge construction, the reinforced concrete pier or abutment wall as well as the vertical cross beams may also be called deep beams. Deep beams are also encountered in the construction of quay walls and retaining walls.

It is frequently necessary to provide openings in deep beams for utility or other purposes, whereas in case of bridge piers, these openings not only incur a substantial saving in material but also induce an aesthetic beauty in the structure itself.

The conventional design procedure for flexural members is based on Navier's hypothesis prescribing a linear stress distribution in any section of the member. This assumption closely represents the conditions that exist as long as the behaviour of the material is essentially elastic and the depth of the member is relatively small in comparison to its span. This assumption however, is not valid when the depth tc span ratio exceeds eight tenths for simply supported span

and four tenths for continuous girders. This limitation is based on Bay's findings and will be discussed in chapter II. (See page 6)

When the depth's dimension of a flexural member approaches that of its span, design based on the ordinary beam theory will be seriously in error. This is because of the fact that Navier's hypothesis does not consider the effect of the normal pressures on the top and bottom edges caused by loads and reactions. Furthermore, it does not take into account the deformation due to shear or the effect of Poisson's ratio on the stress in the depthwise and the widthwise directions. The effect of the normal pressures on the stress distribution of deep beam is such that the variation of bending stress along any vertical section is not linear and the distribution of shear is not parabolic. Consequently a transverse section which was plane before bending does not remain plane after bending. The neutral axis does not lie at the mid-depth, with maximum deviation from the mid-depth in the vicinity of the support, its position being shifted in a spanwise direction.

By introducing an opening, the whole system of stress distribution in a deep beam is further disturbed. Position as well as the magnitude of the maximum critical stresses are also changed, leaving aside with the existence of stress concentration around the periphery of the opening. Presently available results are not adequate for the design of such cases. On the other hand, the most widely used solutions of ordinary deep beams through Airy stress function cannot be directly applied to a deep beam with an opening, since in this case additional conditions are necessary to establish a relationship

between the assumed values of the stress function on the outer and the inner boundaries of the Deep Beam. This renders the doubly connected deep beam problem as a very much complex one.

In the work, presented herein, the direct method of displacements was applied to find the maximum stresses in solid deep beam, and to check the results with previous works. This method was further extended to obtain the maximum bending stresses in beams with openings. Deep beams with unstiffened and stiffened edges were examined. Thus an attempt is made to form a clear picture of the influence of openings on ordinary deep beams with unstiffened and stiffened edges.

CHAPTER II

LITERATURE SURVEY

In 1932, Franz Dischinger[1] contributed to the basic deep beam theory in the Zurich Symposium of the International Bridge and Structural Engineering Association. He assumed the boundary loading in a trigonometric series acting over a continuous beam of infinite length. An Airy stress function related to a plane stress problem was assumed in the form

$$\varphi = -\sum_{1}^{\infty} \frac{Bn}{\alpha^2} (1 + \alpha y) e^{-\alpha y} \cos \alpha x + \frac{Bo}{2} \cdot \frac{x^2}{2} \quad \ldots\ldots\ldots\ldots\ldots (2.1)$$

Accordingly, the stresses were represented by

$$\sigma_x = \sum_{1}^{\infty} B_n (1-\alpha y) e^{-\alpha y} \cos \alpha x \quad \ldots\ldots\ldots\ldots\ldots\ldots\ldots (2.2)$$

$$\sigma_y = \sum_{1}^{\infty} B_n (1 + \alpha y)\ e^{-\alpha y} \cos \alpha x + \frac{Bo}{2} \quad \ldots\ldots\ldots\ldots\ldots\ldots (2.3)$$

$$\tau_{xy} = \alpha y \sum_{1}^{\infty} B_n e^{-\alpha y} \operatorname{Sin} \alpha x \quad \ldots\ldots\ldots\ldots\ldots\ldots\ldots (2.4)$$

The constants were evaluated from the boundary conditions which state that at $y = 0$,

$$\sigma_y = \frac{Bo}{2} + \sum_{1}^{\infty} Bn \cos \alpha x = p_{xu} \quad \ldots\ldots\ldots\ldots\ldots\ldots\ldots (2.5)$$

$$\tau_{xy} = 0 \quad \ldots\ldots\ldots\ldots\ldots\ldots\ldots\ldots\ldots\ldots\ldots\ldots \quad (2.6)$$

and at $y = \infty$,

$$\sigma_y = \frac{Bo}{2} \quad \ldots\ldots\ldots\ldots\ldots\ldots\ldots\ldots\ldots\ldots\ldots \quad (2.7)$$

$$\tau_{xy} = 0 \quad \ldots\ldots\ldots\ldots\ldots\ldots\ldots\ldots\ldots\ldots\ldots\ldots \quad (2.8)$$

With the help of many worked-out examples Dischinger calculated, for several cases of loading, the bending stresses for various ratios of beam height to span; he also showed how the stresses in deep beams approached those of the slender beams. Dischinger also observed that the magnitude of the lever arm between the internal forces was more critical than the actual stress diagrams. The practical value of his work lay in determining these lever arms for several practical cases of loading. The lever arm of internal forces in a deep beam was no longer proportional to the height of the beam but to the span. It was further observed that there was a considerable difference between freely supported and continuous girders. In the former, the lever arm at which the internal forces acted was twice as great as in the case of continuous girders.

Based on these observations due to Dischinger, Portland Cement Association[2] later prepared an extended version of his paper and added solutions for simply supported spans in the form of many curves and figures. As the first comprehensive design guide in the English language on deep beams, this included Navier's hypothesis

with respect to depth to span ratios based on Dischinger's lever arm theory. Fig. 1a shows a continuous girder of Dischinger's type but for a specific case in which the length of support equals one-half of the theoretical span measured between centre-line of support. Since the length of support equals the clear span, the condition is that of a beam which is loaded alternately upward and downward with equal loads but which has no other supports. It is apparent that moment is zero at alternate points. There is no assurance that the moment is zero at everywhere in these sections, but the fact that the total moment is zero indicates that portions of the beam with length of L/2 between points of inflection may be in the same stress condition as in the simply supported beam. Accordingly it is assumed that the stress curves for moment are alike at mid-span of the two beams in Fig. 1c. Accordingly the ratio of H/L is twice as great for the single-span beam as for the continuous beam. Thus the Portland Cement Association used the curves for continuous beams for single-span beams when ratio of H/L for latter was computed to be H/2L.

In a different way almost at the same time, Bay[3] analyzed the case of continuous deep beams with supports of equal span, the spans being equal to or less than height of the beam. He used Filon's[4] solution together with methods of superposition and concluded that beams of infinite length with height greater than span of supports had similar stress distribution to beams with height equal to span. Thus he confirmed Dischinger's analysis.

In case of simply supported deep beams, although Fourier Series can be applied to represent any form of periodic loading, the boundary conditions at the two vertical edges can not be easily satisfied by this means. Since additional terms will have to be added changing the whole expression for the stress function to multiple Fourier series; this procedure will involve considerable labour. Iyengar's[5] attempt in this direction is worth mentioning.

Chow, Conway and Morgan[4] proposed a second stress function to eliminate, by means of superposition, the residual normal stresses at the vertical edges resulting from the first stress function. They used a second stress function in the form of polynomials with adjustable parameters. These were determined by applying the principle of least-work to the strain energy integral - a method developed by Timoshenko and used by Goodier in solving various problems. This method involved some approximations due to using only a finite number of terms in the infinite series for the second stress function.

Chow, Conway and Winter[6] analyzed simply supported deep beams as problems of plane stress by solving the differential equations by means of finite difference approximations. They used five different types of loading and three different span to depth ratios, but made no experimental verifications. In a subsequent discussion,[7] it was found out that a considerable amount of error existed because of the coarseness of the net and the inherent rounding off of peak values.

Elihu Geer[8] in his doctoral thesis, attempted to overcome these errors by using five point finite difference equations instead of customery three points for second derivatives. He also used a finer

mesh.

Archer and Kitchen[9,10] presented the solutions for a beam of rectangular cross-section, in which the thickness is small compared with the depth which is comparable to span, for symmetric loading. They employed the Rayleigh-Ritz method by expressing the stress function in two parts, the first one accounted for the elementary beam theory for straight line distribution of bending stress and parabolic distribution of shear stress. The second part was expressed in terms of polynomials. The minimization of the total strain energy led to equations for the determination of the parameters assumed. They also verified their results by experiments using 12 in. x 12 in. x 1/2 in. steel models supported at each end and loaded at the opposite edge. The strains at six points on the lower edge of each plate were measured using strain gages.

Guzman and Luisoni[11] applied Galerkin's variational method to the same problem and the results were tabulated in equation forms.

Saad and Hendry[12, 13] recently published papers on gravitational stresses in deep beams. Their results were based on a series of experiments using frozen stress method of photoelasticity. Gravitational loading was simulated in a large centrifuge. The stresses so obtained were in a form suitable for use in design and checked well with theoretical results obtained by means of an Airy stress function converted into finite difference pattern.

Durant and Garwood[14] presented a solution of deep beam including gravitational stresses by choosing a particular solution

for the bi-harmonic equation and then finding a polynomial which cancelled out the stresses on the vertical boundary implicit in the particular solution selected. This solution has the advantage of giving the results in a closed form; it has been noted [11] that the results are not very rapidly convergent nor are they very accurate.

Fox[15] discussed the application of relaxation method in plane stress problems with governing equations in terms of displacements. He observed that in bi-harmonic problems of mixed boundary conditions where photo-elastic methods were difficult to apply, this method might be valuable.

Recently, Coul[16] suggested a method of handling deep beam problems in which he transformed the two-dimensional plane stress problem into unidirectional by expressing the stresses in the form of Fourier series in one direction, the coefficients of the series being functions of the other co-ordinate only. After satisfying the equilibrium and boundary conditions, the coefficients were determined by minimization of the strain energy. For general loading case of an ordinary deep beam with unsymmetrical boundary stresses, the method had to incorporate two different co-ordinate axes - one for symmetrical case and the other for the antysymmetrical case thereby yielding additive results. The same method has been successfully applied in plate problems before.[17]

As early as in 1898, Kirsch[18] presented an approximate solution for the stress distribution around a circular hole in a plate subjected to uniform tension in one direction. In 1930, Tuzi[19] presented solutions for stress distribution in a beam, containing a

small circular hole on the neutral axis, subjected to pure bending. This load of pure bending was also applied by Sen[20] and Wolf[21] to find the effect of small elliptical holes and cracks on maximum bending stresses. Their works were essentially the extension of Tuzi's analytical solution.

Gupta[22] attempted a solution for a simple rectangular plate plane stress elastic cantilever problem, with the end shear load having a parabolic distribution. The effect was found by G. B. Jeffery's[23] original bi-polar solution, treating the rectangle as a semi-infinite in one direction (opening near the middle of the supporting infinite edge). Some values of stress at hole were given.

The other attempts worth mentioning are credited to Bickley[24] Hütter[26], Hengst[25], and Savin[27]. However, none of these treated the deep beam with opening.

CHAPTER III

THEORETICAL SOLUTIONS

(i) Governing Equations

If $u(x, y)$ and $v(x, y)$ are the displacement components in the x and y directions respectively, of any point (x, y) then the problem of in a plane state of stress can be defined by two displacement equations. In the absence of body forces, these equations are

$$2\frac{\partial^2 u}{\partial x^2} + (1-\upsilon)\frac{\partial^2 u}{\partial y^2} + (1+\upsilon)\frac{\partial^2 v}{\partial x \partial y} = 0$$

$$2\frac{\partial^2 v}{\partial y^2} + (1-\upsilon)\frac{\partial^2 v}{\partial x^2} + (1+\upsilon)\frac{\partial^2 u}{\partial x \partial y} = 0 \qquad (3.1)$$

These two equations, together with the appropriate boundary conditions, are sufficient to yield the solutions for displacements u and v, provided all the conditions pertaining to the state of plane stress are valid. The stresses, thereoff, at any point can be found by

$$\sigma_x = \frac{E}{1-\upsilon^2}\left(\frac{\partial u}{\partial x} + \upsilon\frac{\partial v}{\partial y}\right)$$

$$\sigma_y = \frac{E}{1-\upsilon^2}\left(\frac{\partial v}{\partial y} + \upsilon\frac{\partial u}{\partial x}\right) \qquad (3.2)$$

$$\tau_{xy} = \frac{E}{2(1+\upsilon)}\left(\frac{\partial v}{\partial x} + \frac{\partial u}{\partial y}\right)$$

All other stresses are zero.

On the boundary, either displacements or forces can be specified. The case of a force-free boundary is one in which there are no externally applied forces and the displacements are unknown.

In the case when boundary forces exist, equilibrium of an element of the surface demands that

$$T_x = \sigma_x \cos(n, x) + \tau_{xy} \cos(n, y)$$
$$T_y = \tau_{xy} \cos(n,x) + \sigma_y \cos(n,y) \qquad (3.2)$$

where T_x and T_y are the components of the stress vector applied to the boundary; (n, x) and (n, y) are the angles between the normal n at the surface and the coordinate x and y axis respectively.

Substituting Eqs. (3.2) in Eqs. (3.3), the required boundary conditions are obtained as,

$$T_x = \frac{E}{1 - \upsilon^2}\left(\frac{\partial u}{\partial x} + \upsilon \frac{\partial v}{\partial y}\right) \cos(n, x) + \frac{E}{2(1 + \upsilon)}\left(\frac{\partial u}{\partial y} + \frac{\partial v}{\partial x}\right) \cos(n, y)$$

$$T_y = \frac{E}{1 - \upsilon^2}\left(\frac{\partial v}{\partial y} + \upsilon \frac{\partial u}{\partial x}\right) \cos(n,y) + \frac{E}{2(1+\upsilon)}\left(\frac{\partial u}{\partial y} + \frac{\partial v}{\partial x}\right)\cos(n, x) \qquad (3.4)$$

If the boundary is free of applied forces, then $T_x = T_y = 0$ and Eqs. (3.4) become

$$2\left(\frac{\partial u}{\partial x} + \upsilon \frac{\partial u}{\partial y}\right) \cos(n, x) + (1 - \upsilon)\left(\frac{\partial u}{\partial y} + \frac{\partial v}{\partial x}\right) \cos(n, y) = 0$$

$$2\left(\frac{\partial v}{\partial y} + \upsilon \frac{\partial u}{\partial x}\right) \cos(n, y) + (1 - \upsilon)\left(\frac{\partial u}{\partial y} + \frac{\partial v}{\partial x}\right) \cos(n, x) = 0 \qquad (3.5)$$

For any point on the boundary, the angles (n, x), (n, y) can easily be obtained, and for any particular material the Poisson's ratio, υ is also known. Eqs. (3.5), therefore, are of the form

$$b_1 \frac{\partial u}{\partial x} + b_2 \frac{\partial u}{\partial y} + b_3 \frac{\partial v}{\partial x} + b_4 \frac{\partial v}{\partial y} = 0$$

$$c_1 \frac{\partial u}{\partial x} + c_2 \frac{\partial u}{\partial y} + c_3 \frac{\partial v}{\partial x} + c_4 \frac{\partial v}{\partial y} = 0 \qquad (3.6)$$

in which the coefficients b_i, c_i $(i = 1, 2, 3, 4)$ vary from point to point and may all be regarded as known.

(ii) Finite Difference Approximations in Plane Stress Problems

The partial differential equations representing the plane stress problems are seldom amenable to precise analytical solutions for general problems of practical importance such as the present case of deep beams. An approximate, numerical method of wide-spread application is provided by finite-difference techniques. Essentially these replace the linear governing equations and boundary conditions by finite-difference approximations in terms of a finite number of unknown quantities of the dependent

variables at discrete points within or just outside the domain of integration. The finite-difference equations form a set of linear algebric equations containing the unknown values of the dependent variables; the task of obtaining numerical solutions of the simultaneous equations can be achieved through the facilities offered by the digital computer. Thus the finite-difference approximation of attacking a plane stress problem is a direct approach and the approximation lies in changing the original differential equations and boundary conditions into a set of linear algebraic finite-difference equations.

There are quite a number of different approaches of formulating finite-difference equations in a unique way. These will lead to the following equations:[37]

$$\left(\frac{df}{dx}\right)_o \approx \frac{f_1 - f_{-1}}{2h}$$

$$\left(\frac{d^2f}{dx^2}\right)_o \approx \frac{f_1 - 2f_o + f_{-1}}{h^2}$$

and so on. Similarly for any point, say point 8 in Fig. 2,

$$\left(\frac{d^2f}{dxdy}\right) \approx \frac{f_{14} - f_4 + f_{12} - f_2}{4hH}$$

where H, h are all defined in Fig. 2.

The sets of equations are widely used primarily because of the simplicity of the difference operators and the ease by which boundary conditions can be handled.

(iii) Limitations of Finite-Difference Approximations

Finite-difference equations replace the original differential equations and the equations defining boundary conditions. This then reduces the problem to a set of simultaneous algebric equations which can be solved without mathematical difficulty. Thus the approximation is limited to a minor interference which breaks the curve at discrete points and joins them by a straight line. Hence, the finite-difference equations representing the original differential equations are valid as long as the parent equations are valid. Of course, finite-difference equations do not exactly represent the original governing equations; there is a residual. However, for all practical purposes, the error can be minimized by reducing the mesh size.

Finite-difference approximations, as in other approximate methods, is liable to be in great error especially in regions where stresses are subject to very rapid changes such as those near singularities caused by concentrated loads, corners, dislocations or sudden change in geometry. In fact when internal singularities exist, the indiscriminate use of finite-difference approximations may lead to completely erroneous results[32].

It should also be noted that the combined use of the centre and end difference patterns in the solution of any problem should be avoided. Experience has shown that this may lead to serious errors in results.

(iv) Plain Deep Beams

Since, the boundary lines are parallel to x and y coordinate axes, on side OA, (Fig. 2), the boundary conditions are, from Eqs. (3.4),

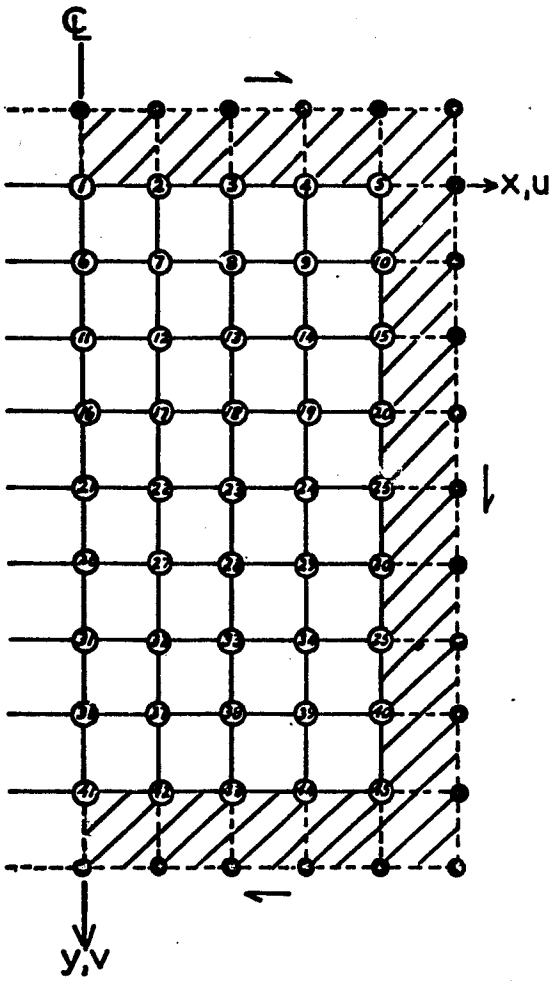

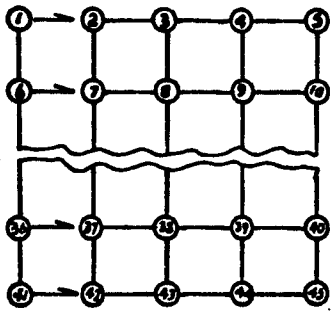

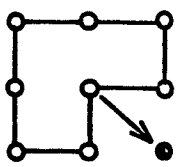

STEP 1

dv/dx & u along centre-line assumed to be zero

STEP 2

Fictitious points in black-dots are evaluated following the band around the boundary

STEP 3

Following the numerical order, the twin equations at each point are formulated. There will be single equation for points along the centre-line

In case of internal boundary, fictitious points around that will be included in STEP 2

$$T_y = \frac{E}{1 - \upsilon^2} \left(\upsilon \frac{\partial u}{\partial x} + \frac{\partial v}{\partial y}\right) = -p \qquad (3.7)$$

$$T_x = \frac{E}{2(1 + \upsilon)} \left(\frac{\partial v}{\partial x} + \frac{\partial u}{\partial y}\right) = 0 \qquad (3.8)$$

where p is the applied pressure in the y direction. For any point, say point 2 in Fig. 2, Eq. (3.7) will be in finite-difference terms,

$$-p\lambda = \upsilon \left(\frac{u_3 - u_1}{2h}\right) + \beta \left(\frac{v_7 - v_7'}{2h}\right)$$

when $\lambda = \frac{1 - \upsilon^2}{E}$ and $\beta = \frac{h}{H}$. Then

$$v_7' = v_7 + \frac{\upsilon}{\beta} (u_3 - u_1) + \frac{2ph\lambda}{\beta}$$

Because of symmetry, the u values are assumed to be zero on the centre-line. Then

$$v_7' = v_7 + \frac{\upsilon}{\beta} u_3 + \frac{2ph\lambda}{\beta} \qquad (3.9)$$

Similarly, for the same point 2, Eq. (3.8) gives

$$0 = \frac{v_3 - v_1}{2h} + \beta \left(\frac{u_7 - u_7'}{2h}\right)$$

Or,

$$u_7' = u_7 + \frac{1}{\beta} (v_3 - v_1) \qquad (3.10)$$

For point 3, from Eq. (3.7),

$$v_8' = v_8 + \frac{\upsilon}{\beta}(u_4 - u_2) + \frac{2ph\lambda}{\beta} \tag{3.11}$$

and from Eq. (3.8),

$$u_8' = u_8 + \frac{1}{\beta}(v_4 - v_2) \tag{3.12}$$

For point 1, because of symmetry along the centre-line,

$$v_6' = v_6 + \frac{2\upsilon}{\beta}\ u_2 + \frac{2ph\lambda}{\beta} \tag{3.13}$$

$$u_6' = u_6 = 0 \tag{3.14}$$

Similarly, at point 4,

$$v_9' = v_9 + \frac{\upsilon}{\beta}(u_5 - u_3) + \frac{2ph\lambda}{\beta} \tag{3.15}$$

$$v_9' = u_9 + \frac{1}{\beta}(v_5 - v_3) \tag{3.16}$$

At the corner point 5, there are six unknown fictitious values of u and v, but only three boundary equations are available. These are

$$\sigma_y = \frac{1}{\lambda}\left(\upsilon\frac{\partial u}{\partial x} + \frac{\partial v}{\partial y}\right) = -\frac{p}{2} \tag{3.17a}$$

$$\tau_{xy} = \frac{E}{2(1+\upsilon)} \left(\frac{\partial v}{\partial x} + \frac{\partial v}{\partial y}\right) = 0 \qquad (3.17b)$$

$$\sigma_x = \frac{1}{\lambda} \left(\frac{\partial u}{\partial x} + \upsilon \frac{\partial v}{\partial y}\right) = 0 \qquad (3.17c)$$

Differentiating Eq. (3.17a) along x, Eq. (3.17c) along y and Eq. (3.17b) along x and y, yields

$$\begin{aligned} \upsilon \frac{\partial^2 u}{\partial x^2} &= \frac{\partial^2 u}{\partial y^2} \\ \upsilon \frac{\partial^2 v}{\partial y^2} &= \frac{\partial^2 v}{\partial x^2} \\ \frac{\partial^2 v}{\partial x \partial y} &= -\frac{\partial^2 v}{\partial x^2} \\ \frac{\partial^2 u}{\partial x \partial y} &= -\frac{\partial^2 u}{\partial y^2} \end{aligned} \qquad (3.18)$$

Substituting Eqs. (3.18) in equilibrium equations, the modified governing equations are obtained for the point 5. These are

$$\frac{\partial^2 u}{\partial x^2} = 0 \qquad (3.19)$$

$$\frac{\partial^2 v}{\partial y^2} = 0 \qquad (3.20)$$

which then provide additional boundary conditions in the form of

$$\frac{\partial^2 u}{\partial y^2} = 0$$

$$\frac{\partial^2 v}{\partial x^2} = 0 \qquad (3.21)$$

that is, the curvatures at point 5 both in x and y directions are zero.

Hence from Eqs. (3.17) and Eqs. (3.21), the fictitious point u_4', v_4', u_{10}' and v_{10}' can be found as follows,

$$v_{10}' = v_{10} + \frac{1}{\beta(1-\upsilon^2)}\, ph\lambda$$

$$u_4' = u_4 + \frac{\upsilon}{1-\upsilon^2}\, ph\lambda \qquad (3.22)$$

$$u_{10}' = 2u_5 - u_{10}$$

$$v_4' = 2v_5 - v_4$$

After obtaining all the fictitious points along the boundary, they can be eliminated from the differential equations. Eqs. (3.1). These will be, with $\xi = \frac{1-\upsilon}{2}$ and $\eta = \frac{1+\upsilon}{2}$, as follows for point 3:

$$\frac{1}{h^2}(u_4 - 2u_3 + u_2) + \frac{\xi}{H^2}(u_8 - 2u_3 + u_8') + \frac{\eta}{4hH}(v_9 - v_7 + v_7' - v_9') = 0 \qquad (3.23a)$$

$$\frac{\xi}{h^2}(v_4 - 2v_3 + v_2) + \frac{1}{H^2}(v_8 - 2v_3 + v_8') + \frac{\eta}{4hH}(u_9 - u_7 - u_7' - u_9') = 0 \qquad (3.23b)$$

From eqs. (3.9) through Eqs. (3.16), the fictitious values of u_7', u_8',

u_9', v_7', v_8', v_9', can be substituted in Eqs. (3.23) which then will be

$$u_2-(2+2\xi\beta^2-.5\upsilon\eta)\,u_3+u_4-.25\upsilon\eta u_5+2\xi\beta^2 u_8-\xi\beta v_2+\xi\beta v_4 = 0$$

$$-\upsilon\beta(u_2-u_4)-.25\eta v_1+\xi v_2-(2\xi+2\beta^2-.5\eta)v_3+\xi v_4-.25\eta v_5+2\beta^2 v_8 = -2\beta ph\lambda \qquad (3.24)$$

Similarly the single equation at point 1 (since u_1 is zero) is

$$2\upsilon\beta u_2-(2\xi+2\beta^2-.5\eta)v_1+2\xi v_2-.5\eta v_3+2\beta^2 v_6 = -2\beta ph\lambda \qquad (3.25)$$

Equations at point 5 from Eqs. (3.20) are

$$2u_4 - 2u_5 = -\frac{\upsilon}{1-\upsilon^2}\,ph\lambda$$

$$-2v_5 + 2v_{10} = -\frac{1}{\beta(1-\upsilon 2)}\,ph\lambda \qquad (3.26)$$

For any interior point, say point 8, Eqs. (3.1) can be transformed in finite-difference terms,

$$\frac{1}{h^2}(u_7-2u_8+u_9) + \frac{\xi}{H^2}(u_{13}-2u_8+u_3) + \frac{\eta}{4hH}(v_{14}-v_{12}+v_2-v_4) = 0$$

$$\frac{\xi}{h^2}(v_7-2v_8+v_9) + \frac{1}{H^2}(v_{13}-2v_8+v_3) + \frac{\eta}{4hH}(u_{14}-u_{12}+u_2-u_4) = 0$$

Or,

$$\xi\beta^2 u_3+u_7-(2+2\xi\beta^2)u_8+u_9+\xi\beta^2 u_{13}+.25\eta\beta(v_2-v_4-v_{12}+v_{14}) = 0$$

$$.25\eta\beta(u_2-u_4-u_{12}+u_{14}) + \beta^2 v_3 + \xi v_7-(2\xi + 2\beta^2)v_8 + \xi v_9 + \beta^2 v_{13} = 0 \qquad (3.27)$$

Equations for all other points can be derived in the same way. Due to symmetry along the centre-line (OY), u values along OY are taken to be zero. v values on the left-hand side of this line are same as on the right-hand side whereas u values there are taken to be equal and opposite of those on the right-hand side.

In case of an opening, the points on the periphery as well as the corner point are treated in the same way as the top edge AB and point 5 with the applied forces taken to be zero there. Taking the line connecting points 11 and 13 as the top edge of the opening and point 13 as the corner point, the equations at points 11, 12 and 13 will be : at point 11,

$$-2\upsilon\beta.u_{12}+2\beta^2.v_6-(2\xi+2\beta^2-.5\eta)v_{11}+2\xi v_{12}-.5\eta v_{13} = 0 \qquad (3.28)$$

At point 12,

$$2\xi\beta^2 u_7 - (2+2\xi\beta^2-.5\upsilon\eta)u_{12}+u_{13}-.25\eta\beta v_8+\xi\beta(v_{11} - v_{13}) + .25\eta\beta v_{18} = 0$$

$$-.25\eta\beta u_8-\upsilon\beta u_{13} + .25\eta\beta u_{18} + 2\beta^2 v_7+ \xi v_{11}-(2\xi+2\beta^2)v_{12}+\xi v_{13} = 0 \qquad (3.29)$$

At point 13, which is the corner point, the equations are

$$u_{12} - 2u_{13} + u_{14} = 0$$

$$v_8 - 2v_{13} + v_{18} = 0 \qquad (3.30)$$

Equations at all other points, whether lying on the boundary or inside the boundary can be derived in the same way. Having formulated the equations of all the nodal points in finite-difference terms, these linear algebric equations were solved by the IBM 7094. To guard against round-off errors, all computations were carried to 16 significant figures. Results for a set of 16 programs were obtained and presented graphically in Figs. 7 through 30.

(v) Stiffened Deep Beams

In this case, the problem was divided in two parts: the plate itself and the stiffening frame.

1. The plate is assumed to be subjected to six unknown forces acting on its edges. These forces are the normal pressures and shear stresses on each face assumed to be varying in trigonometric series with unknown coefficients. Thus on top face, a normal negative (compressive) pressure of $\Sigma PA_m \cos m\pi x/2a$ in acting where 2a is the length

$m = 1, 3, 5 \ldots$

of the plate. Similarly, there will be also a shear stress of ΣTA_m Sin

$m = 1, 3, 5 \ldots$

$m\pi x/2a$ acting. A positive (tensile) pressure $\Sigma PB_n \cos m\pi x/2a$ and shear

$n = 1, 3, 5 \ldots$

$\Sigma TB_n \sin m\pi x/2a$ are assumed acting on the bottom face. On the vertical

$n = 1, 3, 5 \ldots$

faces normal pressures are $\Sigma PC_k \cos k\pi y/2b + \Sigma PD_\ell \sin \ell\pi y/2b$ and the

$k = 1, 3, 5 \ldots$ $\ell = 1, 3, 5 \ldots$

shear stresses are $\Sigma TC_k \cos k\pi y/2b + \Sigma TD_\ell \sin \ell\pi y/2b$. (See Fig. 3a)

$k = 1, 3, 5 \ldots$ $\ell = 1, 3, 5 \ldots$

From the equilibrium of the plate

$$\int_0^a PA_m \cos m\pi x/2a \, dx + \int_0^a PB_n \cos m\pi x/2a \, dx - \int_0^b TC_k \cos k\pi y/2b \, dy -$$

$$\int_0^b TD_\ell \sin \ell\pi y/2b \, dy = 0$$

Or,

$$\Sigma \frac{PA_m}{m} \sin \frac{m\pi}{2} + \frac{\Sigma PB_n}{n} \sin \frac{n\pi}{2} - \frac{\Sigma TC_k}{k} \sin \frac{k\pi}{2} - \Sigma \frac{TD_\ell}{\ell} = 0 \quad (3.31)$$

And also at corners,

$$\Sigma TA_m \operatorname{Sin} \frac{m\pi}{2} = \Sigma TC_k$$

$$\Sigma TB_n \operatorname{Sin} \frac{n\pi}{2} = \Sigma TD_\ell \operatorname{Sin} \frac{\ell\pi}{2} \quad (3.32)$$

The boundary conditions as well as the nodal equations can be derived in the same way as before, having a varying normal pressure and the presence of shear stress in this case.

Thus

$$v_8' = v_8 + \frac{\upsilon}{\beta}(u_4 - u_2) + \frac{2}{\beta}\Sigma PA_m h\lambda \cos\frac{m\pi}{4} \tag{3.33}$$

$$u_8' = u_8 + \frac{1}{\beta}(v_4 - v_2) - \frac{2}{\xi\beta}\Sigma TA_m h\lambda \sin\frac{m\pi}{4} \tag{3.34}$$

$$v_9' = v_9 + \frac{\upsilon}{\beta}(u_5 - u_3) + \frac{2}{\beta}\Sigma PA_m h\lambda \cos\frac{3m\pi}{4} \tag{3.35}$$

$$u_9' = u_9 + \frac{1}{\beta}(v_5 - v_3) - \frac{2}{\xi\beta}\Sigma TA_m h\lambda \sin\frac{3m\pi}{8} \tag{3.36}$$

$$v_{10}' = v_{10} - \frac{\upsilon}{\beta(1-\upsilon^2)}\Sigma PC_k h\lambda \tag{3.37}$$

$$u_4' = u_4 - \frac{1}{1-\upsilon^2}\Sigma PC_k h\lambda \tag{3.38}$$

Therefore, the governing differential equations, for point 3, will be, in finite-difference terms, as follows:

$$u_2 - (2 + 2\xi\beta^2 - \frac{\eta\upsilon}{2})u_3 + u_4 - \frac{\eta\upsilon}{4}u_5 + 2\xi\beta^2 v_8 - 2\beta\Sigma TA_m h\lambda \sin\frac{m\pi}{4} +$$

$$.5\eta(\Sigma PA_m h\lambda \cos\frac{m\pi}{8} - \Sigma PA_m h\lambda \cos\frac{3m\pi}{8} = 0 \tag{3.39}$$

$$-\upsilon\beta(u_2 - u_4) - .25\eta v_1 + \xi v_2 - (2\xi + 2\beta^2 - \frac{\eta}{2})v_3 + \xi v_4 - \frac{\eta}{4}v_5 + 2\beta^2 v_8$$

$$+ 2\beta\Sigma PA_m h\lambda \cos\frac{m\pi}{4} + \frac{.5\eta}{\xi}\{\Sigma TA_m h\lambda \sin\frac{3m\pi}{8} - \Sigma TA_m h\lambda \frac{m\pi}{8}\} = 0 \tag{3.40}$$

Similarly for point 4, these equations are

$$-\frac{\eta\upsilon}{4}u_2 + u_3 - \left(2 + 2\xi\beta^2 - \frac{\eta\upsilon}{4}\right)u_4 + u_5 + 2\xi\beta^2 u_9 - \xi\beta v_3 - 2\beta\Sigma TA_m h\lambda \sin\frac{3m\pi}{8}$$

$$+\frac{\eta}{2}\Sigma PA_m h\lambda \sin\frac{m\pi}{2} + \frac{\eta\upsilon}{4(1-\upsilon 2)}\Sigma PC_k h\lambda = 0 \qquad (3.41a)$$

$$-\upsilon\beta u_3 + (\upsilon\beta - .5\eta\beta)u_5 + \frac{\eta\upsilon}{2}u_{10} - \frac{\eta}{4}v_2 + \xi v_3 - \left(2\xi + 2\beta^2 - \frac{\eta}{4}\right)v_4 + 2\beta^2 v_9$$

$$+ 2\beta\Sigma PA_m \cos\frac{3m\pi}{8} + \frac{\eta\pi}{32\beta(1-\upsilon 2)}\Sigma mPA_m \sin\frac{m\pi}{2} - \frac{\eta}{2\xi}\Sigma TA_m \sin\frac{m\pi}{2} = 0 \quad (3.41b)$$

Since v at point 5, is assumed to be zero, there will only be one equation at that point, which is

$$2(1-\upsilon^2)(u_4-u_5) - \Sigma PC_k h\lambda + \frac{\upsilon\pi}{8}\Sigma mPA_m h\lambda \sin\frac{m\pi}{2} + \frac{\pi\beta}{16}\Sigma nTB_n = 0 \qquad (3.42)$$

whereas the nodal equations for any interior point still remain unchanged and will be the same as the plain deep beam.

2. For the frame portion (Fig. 3b) the same unknown forces are assumed to be acting but opposite in sign. Since the frame itself is statically indeterminate by two degrees, the redundant forces M_o and H_o at centre of the top member (see Fig. 3b) can be found out from Castigliano's first theorem[39] taking advantage of the state of symmetry. Because of symmetry, the slope at point 1, and also the horizontal displacement are taken to be zero. Neglecting axial shortening, the minimization of the total strain energy in bending with respect to

these redundant forces will be zero. Thus the unknown, M_o and H_o can be seperated from those two equations. These equations can be derived as follows:

Bending strain energy,

$$U = \frac{1}{2EI}\Big[\int_o^a \{M_o - \frac{q_o x^2}{2} + \Sigma\frac{4a^2}{m^2\pi^2} PA_m (1-\cos\frac{m\pi x}{2a})\}^2 dx + \int_o^a \{M_o - H_o b +$$

$$\Sigma\frac{4a^2 PA_m}{m^2\pi^2} + \Sigma\frac{2ab TA_m}{m\pi} + \Sigma\frac{4b^2 PC_k}{k^3\pi^2} - \Sigma\frac{4b^2 PD\ell}{\ell^2\pi^2}\sin\frac{\ell\pi}{2} - \Sigma\frac{4a^2 PB_n}{n^2\pi^2}\cos\frac{n\pi x}{2a}$$

$$+ \frac{q_o a^2}{2}\}^2 dx + \int_o^b \{M_o - \frac{q_o a^2}{2} + \Sigma\frac{4a^2}{m^2\pi^2} PA_m - H_o y + y\Sigma\frac{2aTA_m}{m\pi} + \Sigma\frac{4b^2 PC_k}{k^2\pi^2}$$

$$(1-\cos\frac{k\pi y}{2b}) - \Sigma\frac{4b^2 PD\ell}{\ell^2\pi^2}\sin\frac{\ell\pi y}{2b}\}^2 dy\Big] \qquad (3.43)$$

$$\frac{\partial U}{\partial M_o} = \frac{1}{EI}\int M\frac{\partial M}{\partial M_o} dx = 0$$

$$\therefore\ 2M_o a + \Sigma\frac{4a^2}{m^2\pi^2} PA_m - \Sigma\frac{8a^3}{m^3\pi^3} PA_m \sin\frac{m\pi}{2} - \frac{q_o a^3}{6} - H_o ab + \Sigma\frac{4a^3 PA_m}{m^2\pi^2} + \Sigma\frac{4b^3 PC_k}{k^2\pi^2}$$

$$+\Sigma\frac{2a^2 bTA_m}{m\pi} - \Sigma\frac{4ab^2 PD\ell}{\ell^2\pi^2}\sin\frac{\ell\pi}{2} - \frac{q_o a^3}{2} + \Sigma\frac{8a^3 PB_n}{n^3\pi^3}\sin\frac{n\pi}{2} + M_o b - \frac{q_o a^2 b}{2} + \Sigma\frac{4ab^2 PC_k}{k^2\pi^2}$$

$$+\Sigma\frac{4a^2 b}{m^2\pi^2} PA_m - \frac{H_o b^2}{2} + \Sigma\frac{ab^2}{m\pi} TA_m - \Sigma\frac{8b^3 PC_k}{k^3\pi^3}\sin\frac{k\pi}{2} - \Sigma\frac{8b^3 PD\ell}{\ell^3\pi^3} = 0 \qquad (3.43a)$$

$$\frac{\partial U}{\partial H_o} = \frac{1}{EI}\int M\frac{\partial M}{\partial H_o} dx = 0$$

$$\therefore\ M_o ab - H_o ab^2 + \Sigma\frac{4a^3 bPA_m}{m^2\pi^2} + \Sigma\frac{2a^2 b^2}{m\pi} TA_m + \Sigma\frac{4ab^3 PC_k}{k^2\pi^2} - \Sigma\frac{4ab^3 PD\ell}{\ell^2\pi^2}$$

$$\sin\frac{\ell\pi}{2} - q_{oa}\frac{3}{2}b + \Sigma\frac{8a^3b}{n^3\pi^3}PB_n\sin\frac{n\pi}{2} + \frac{M_o b^2}{2} - q_{oa}\frac{2}{4}b^2 + \Sigma\frac{2a^2b^2PA_m}{m^2\pi^2}$$

$$- \frac{H_o b^3}{3} + \Sigma\frac{2ab^3TA_m}{3m\pi} + \Sigma\frac{2b^4PC_k}{k^2\pi^2} - \Sigma\frac{8b^4}{k^3\pi^3}PC_k\sin\frac{k\pi}{2} + \Sigma\frac{16b^4PC_k}{k^4\pi^4}$$

$$- \Sigma\frac{8b^4PD_\ell}{\ell^3\pi^3} - \Sigma\frac{16b^4}{\ell^4\pi^4}PD_\ell\sin\frac{\ell\pi}{2} = 0 \qquad (3.43b)$$

Taking $\frac{2a}{b} = \beta$, and with the help of Eqs. (3.31) and (3.32), M_o and H_o can be seperated from Eqs. (3.43). These are as follows:

$$M_o = \frac{q_o a^2}{6}\left(\frac{3 + 8\beta + 3\beta^2}{1 + 4\beta + 3\beta^2}\right) - \frac{2a^2}{\pi}\left(\frac{\beta}{1 + 4\beta + 3\beta^2}\right)\Sigma\frac{PA_m}{m}\sin\frac{m\pi}{2} - \frac{4a^2}{\pi^2}$$

$$\Sigma\frac{PA_m}{m^2} + \frac{8a^2}{\pi^2}\left(\frac{2\beta + 3\beta^2}{1 + 4\beta + 3\beta^2}\right)\Sigma\frac{PA_m}{m^3}\sin\frac{m\pi}{2} - \frac{2a}{\pi}\left(\frac{\beta}{1 + 4\beta + 3\beta^2}\right)^2\Sigma\frac{PB_n}{n}$$

$$\sin\frac{n\pi}{2} + \frac{8a^2}{\pi^3}\left(\frac{\beta}{1 + 4\beta + 3\beta^2}\right)^2\Sigma\frac{PB_n}{n^3}\sin\frac{n\pi}{2} - \frac{4a^2}{\pi\beta^2}\left(\frac{\beta}{1 + 4\beta + 3\beta^2}\right)^2\Sigma\frac{TA_m}{m}$$

$$- \frac{16a^2}{\beta^2\pi^2}\left(\frac{1 + 2\beta}{1 + 4\beta + 3\beta^2}\right)^2\Sigma\frac{PC_k}{k^2} - \frac{64a^2}{\beta^3\pi^3}\left(\frac{\beta}{1 + 4\beta + 3\beta^2}\right)^2\Sigma\frac{PC_k}{k^3}\sin\frac{k\pi}{2} +$$

$$\frac{384a^2}{\beta^2n^4(1 + 3\beta)}\Sigma\frac{PC_k}{k^4} - \frac{16a^2}{\beta^2\pi^2}\left(\frac{\beta}{1 + 4\beta + 3\beta^2}\right)^2\Sigma\frac{PD_\ell}{\ell^2}\sin\frac{\ell\pi}{2} - \frac{64a^2}{\beta^3\pi^2}$$

$$\left(\frac{\beta}{1 + 4\beta + 3\beta^2}\right)^2\Sigma\frac{PD_\ell}{\ell^3} - \frac{384a^2}{\beta^2(1 + 3\beta)\pi^4}\Sigma\frac{PD_\ell}{\ell^4}\sin\frac{\ell\pi}{2} - \frac{4a^2}{\pi\beta}$$

$$\left(\frac{\beta}{1 + 4\beta + 3\beta^2}\right)^2\Sigma\frac{TB_n}{n} \qquad (3.44)$$

$$H_o = \frac{q_o a}{2}\left(\frac{\beta^2}{1 + 3\beta}\right) + \frac{3a}{\pi}\left(\frac{\beta^2}{1 + 3\beta}\right)\Sigma\frac{PA_m}{m}\sin\frac{m\pi}{2} - \frac{12a}{\pi^3}\left(\frac{\beta^2}{1 + 3\beta}\right)\Sigma\frac{PA_m}{m^3}$$

$$\sin\frac{m\pi}{2} + \frac{3a}{\pi}\left(\frac{\beta^2}{1+3\beta}\right)\Sigma\frac{PB_n}{n}\sin\frac{n\pi}{2} - \frac{12a}{\pi^3}\left(\frac{\beta^2}{1+3\beta}\right)\Sigma\frac{PB_n}{n^3}\sin\frac{n\pi}{2}$$

$$- \frac{2a}{\pi(1+3\beta)}\Sigma\frac{TA_m}{m} + \frac{6a}{\pi\beta}\left(\frac{\beta^2}{1+3\beta}\right)\Sigma\frac{TB_n}{n} - \frac{24a}{\pi^2(1+3\beta)}\Sigma\frac{PC_k}{k^2} + \frac{96a}{\pi^2\beta(1+3\beta)}\Sigma\frac{PC_k}{k^3}$$

$$\sin\frac{k\pi}{2} - \frac{384}{\pi^4\beta(1+3\beta)}\Sigma\frac{PC_k}{k^4} + \frac{24a}{\pi^2(1+3\beta)}\Sigma\frac{PD_\ell}{\ell^2}\sin\frac{\ell\pi}{2} + \frac{384a}{\pi^4\beta(1+3\beta)}\Sigma\frac{PD_\ell}{\ell^4}$$

$$\sin\frac{\ell\pi}{2} + \frac{96a}{\pi^3\beta(1+3\beta)}\Sigma\frac{PD_\ell}{\ell^4} \qquad (3.45)$$

Between the interfaces of the frame and the plate the following conditions must be satisfied:[32]

1. Normal and shear stresses will be equal and opposite.
2. Tangential stretching $(\frac{\partial u}{\partial x})$ must be the same.
3. The curvatures or $\frac{\partial^2 v}{\partial x^2}$ must be the same.

Conditions 1 and 2 are automatically satisfied by assuming equal and opposite forces acting on the interfaces and also by taking same strains there. In order to satisfy the third condition, $\frac{\partial^2 v}{\partial x^2}$ for the frame in terms of the moment and $\frac{\partial^2 v}{\partial x^2}$ for the plate in finite-difference terms are matched at points on the boundary.

Thus, at the centre of the top of the frame that is at point 1,

$$2v_2 - 2v_1 + \frac{M_o h^2}{EI} = 0 \qquad (3.46)$$

Similarly at point 2,

$$v_1 - 2v_2 + v_3 + \frac{M_o h^2}{EI} - \frac{qoh^2}{2} + \Sigma\frac{4PA_m a^2}{m^2\pi^2}\left(1 - \cos\frac{m\pi}{8}\right) = 0 \qquad (3.47)$$

and so on.

Four Fortran programs for the IBM 7094 were prepared, the results of which were graphically presented in Figs. 31 through 35.

CHAPTER IV

EXPERIMENTAL INVESTIGATION

(i) Materials and Apparatus

Fifteen tests were performed on 6061-T6 aluminum alloy[40] models. Two groups of structures were considered: (a) plain deep beams, (b) deep beams with stiffened edges. Seven tests were included in the first group and eight in the later. The geometries of these test specimens are given in table I and II. Eight to ten strain rosette gauges were installed in five basic test models, along the vertical mid-section. These rosette gauges are of the 2-legged 90^{o} rectangular type, having a gauge factor of 2.07 and a resistance of 120 ohms. At the corners three-legged rosettes were used. Most of the gauges used were of 1/8 inch gauge length. Terminal strips (type T-50) were used to connect the lead wires to the gauge tabs. All the lead wires were 16 feet long, made of No. 26 stranded copper wire and with vinyl insulation. To provide mechanical protection and water-proofing, the installed gauges were covered with gauge coat No. 1 (synthetic resin compound), gauge coat No. 2 (nitrite rubber) and gauge coat No. 5(a two-compound epoxy resin).

Application of compressive stress on the upright plate and avoiding eccentric loading was a major problem. To apply compressive loading in such a fashion so that there is no loss of pressure during the time of recording, a mechanical loading rig was designed and

employed as shown in Fig. 4a. The top member of this frame was of solid 4 inch x 6 inch steel section that housed the 2-inch diameter loading screw in a threaded hole at the centre. This top bar was supported on two vertical 10-inch at 12 pounds I-sections. The joints between the top bar and the two vertical members were screwed to facilitate future adjustments when necessary. The two vertical I - sections were welded at their lower ends with a horizontal I-section of 12-inch at 16 pounds which was lying on the floor and securely fastened to avoid any movement. A Budd load-cell (type LUD 10K) was attached at the lower end of the loading screw that acts through the threaded hole in the top bar. Beneath the load-cell, there were two cross-beams of solid 2-inch x 2-inch steel section, the top one resting on the bottom one through eight smooth ball-bearings of 3/4 inch diameter. These two cross-beams were kept in position by means of two 3/8 inch rods hung from the solid top member of the frame. At each end the cross-beams were supported by friction-less bearing-balls acting in two vertical slots in the inner flanges of the vertical I-sections, so that the cross-beams can freely move downward without any lateral displacement when released. The load-cell was calibrated before hand through a portable Budd Strain Indicator (model P-350) and the load factor in micro-inch/inch/lb. was found out and occasionally checked. The model was placed vertically on the bottom I-section on two roller supports to facilitate free horizontal movement. The cross-beams when released from hanging rested on the model. A half-inch thick rubber padding was attached at the under-side of the bottom cross-

beam. In order to eliminate friction between the rubber and the model, that may partially restrict the longitudinal strain of the top edge of the model, the lower edge of the rubber was cut at every inch into 3/8 inch deep cuts. This discontinuous edge of the rubber when under pressure from the cross-beams, was expected to simulate best the effects of uniformly distributed load on the top of the model. The upper edge of the model in contact with the rubber was also slightly lubricated.

During the tests, strains were measured by means of three switch and balancing units (model C-10T and C-10LTC, Budd Instrument Division), a digital strain indicator with an automatic print-out unit. To check any lateral deflection perpendicular to the plane of the plate, two 1/1000 inch dial indicators were installed at the back of the mid-depth of the model. Figs. 5a and 5b show the apparatus and the general set-up of the experiment.

(ii) Experimental Procedure

For each test-model, the plate was first cut smoothly to the required dimensions. In order to cut out the opening, holes were first drilled near the inner corners. Then these bore-holes were connected by means of a sabre-saw. Later the inner edges were smoothened by milling machine up to ten thousandth of an inch of the required dimensions. The plate was then cleaned with acetone and the locations of the strain gauges were laid with reference to the sides. Care was taken to ensure that all the gauges are in proper alignment with respect to the axis which are parallel to the outer edges. The installation of these rosette gauges followed a set pattern.

Next, gauge lead wires from the rosette gauges were soldered to tin 5-channel receptacles especially provided for three switch and balancing units. Unit strains for any loading were automatically recorded by a precise digital strain indicator and printer.

After placing the model in position, the cross-beams were released to rest on the top edge of the model through the rubber padding. By turning the loading-screw, the load-cell while moving downward exerted a compressive pointed load at the centre of the top cross-beam. This load was then transmitted through eight bearing-balls to the bottom cross-beam. The load was further distributed as uniform load through the rubber padding on to the model. The compressed load-cell coupled with the portable strain indicator (Budd model P-350) indicated the strain in the load-cell in mocro-inch/inch corresponding to the particular pressure applied. The deflecto-meters set at the back indicated lateral deflection (perpendicular to the plane of the plate) due to eccentric loading, which was corrected by shifting the position of the plate after releasing the load. Again the loading was applied and the deflecto-meter readings were checked. By trial and error method in this fashion, the eccentricity was eliminated as far as possible. When no eccentricity was noted, the strains were then recorded through the automatic strain recorder.

For each test, six sets of strain readings were taken independently. The final test results, reported herein, were the average of these readings. After completion of the first set of seven tests a frame made of similar aluminum alloy was welded to the plate around the outer edges to yield the deep beams with stiffened edges. In order to avoid excessive heat due to welding that could damage the

already existing gauges, the welding was discontinued at the interfaces and a structural adhesive was used in lieu of welding.

CHAPTER V

DISCUSSION OF RESULTS

(i) Plain Deep Beams

Experimental and theoretical results for the longitudinal stresses at the mid-section of a solid square deep beam under uniformly distributed load acting on the top edge are presented in Fig. 7a. Theoretical results obtained from the works of Winter[6] and Geer[8] based on the Airy stress function are also shown to facilitate comparison. From this figure it is noted that the theoretical results are in close agreement with the experimental ones. This confirms the suitability of the present method in solving plane-stress problems. This comparison also justifies the results of the previous investigators[6,8] who did not verify their findings experimentally. However, it is also observed that the magnitude of the present maximum stresses exceeds those of the others[6,8]. This discrepancy can be attributed to the difference in support width used. The previous investigators used a support width one eightth and one tenth of span respectively whereas it is only one sixteenth of the span in the present case. By increasing the width to one eightth of span, it is found both experimentally and theoretically that the magnitude of the maximum longitudinal stress decreases by an amount of 35% for a square deep beam and by 44% for a rectangular one having the depth greater than the span. However, for a rectangular deep beam whose length exceeds the depth, this decrease is negligible.

Thus it can be assumed that the width of the support has a direct bearing on the stress distribution in a deep beam.

In Fig. 7b, the longitudinal stresses at the mid-section of a square deep beam due to the uniformly distributed load acting along the bottom edge are shown and compared with those found by Winter.[6] The influence of the support-width on the magnitude of the maximum longitudinal stress is also clearly evident in this case. However, in the discussion[7] of Winter's paper[6], it was pointed out that an error of the magnitude of 10 to 17% might exist in those results. If this is the case, the present investigation is advantageously conservative as indicated by the results presented.

Figures 8a and 8b show the distribution of the longitudinal stresses on the mid-section of rectangular deep beams due to uniformly distributed load acting on the top edge, whereas Fig. 9 exhibits the same for uniform load at the bottom edge. To facilitate comparison of stress values obtained from the linear beam theory as well as Winter's results[6] are also plotted. It is interesting to note that the maximum deviation of the longitudinal stress from the linear beam theory is prominent in a rectangular deep beam whose span is approximately 30% less than the depth. When the span exceeds the depth by the same amount, the deviation is almost negligible. This observation indicates that in a solid deep beam the most severe condition will occur not in a square panel but in a rectangular one having a span slightly smaller than the depth. This also confirms that the charecterization

of a solid deep beam could be based on the dimension-ratios (ratios of span to depth) falling in between 2/3 to 3/2. Unfortunately none of the previous investigators laid any emphasis on this particular aspect. However, this behaviour can be attributed to the fact that the narrow support produces a very severe stress concentration which is almost solely responsible for the stress-distribution in a true deep beam and not the bending moment. The adjustment and redistribution of this severe stress-concentration on the support has a profoundly significant effect on the entire stress-system in a deep beam and not the bending moment. This is also confirmed by Fig. 10 where the shear stress at a quarter point of the span is plotted. The shear stress results for a rectangular deep beam having a span less than the depth vary in a distinct manner with a peak value not at mid-depth but somewhat closer to the bottom surface. This also indicates that the peak point is due to a sort of 'attraction' towards the support in the same manner as the longitudinal stresses are attracted, for any rectangular deep beam having a depth greater than span. In case of a span exceeding the depth, this behaviour is not at all prominent when the shear stress diagram resembles that obtained from linear beam theory.

The longitudinal stresses at mid-section of a square deep beam with a small opening at the centre for uniform load on the top

edge are given in Fig. 11. Figures 12 and 13 represent the same for rectangular beams. The area of the opening is 4% of the total area of the deep beam. It is interesting to note that the magnitude of the maximum tension in these cases is less than that in a solid deep beam. This indicates that the opening relieves the maximum tension at the centre of the span. This behaviour is apparently linked up with the same criterion that is responsible for the tension in a solid deep beam.

In view of the principle of St. Venant the effect of the intense field of stress set up in the immediate vicinity of the point of application of a so-called point load (and reaction) on the bending of a simple beam is ignored. This is justifiably so for any beam which is long compared with its depth because the disturbance of this simple distribution is very local and has insignificant effect on the overall pattern. However, for any deep beam this is otherwise.

A beam of typical proportion is shown in Fig. 6a. To bring out the origin of tensile stresses, a few stress trajectories are shown. At point A, this line, being compressive, produces an outward resultant force C as shown in Fig. 6b. There are many such trajectories in this vicinity, all producing outward resultant forces. The free left boundary can furnish no reactive force and consequently the cumulative effect is a tension in the direction of the dotted line. Thus it is readily seen in a qualitative way that the action of a beam of this proportions is mainly one of the distribution of a localised force which is totally insignificant in an ordinary beam. By choosing

a narrow support-width the intensity of this localised force is added on.

Introducing a small opening at the centre of the member, some of this trajectories close to the opening may not remain concave inward. This means that the trajectory line close to A (Fig. 6b) will not be compressive but tensile whereas others will remain as before. The most probable picture will be as in Fig. 6c; this situation causes a decrease in the magnitude of the cumulative tensile stress at the centre.

However, increase in the size of the opening causes stress trajectories near the centre to move further away towards the support. This action is analogus to decreasing the support-width. Because of the fact that the vertical force-free faces can not provide any reactive horizontal stresses, the resulting tensile stresses are increased. This has been verified by the experimental as well as theoretical results shown in Figs. 14 to 16, where an increased tension at the bottom of the mid-section is observed due to a large opening having an area approximately 6% of the total area of the deep beam.

For a still larger opening, about 25% of the area of the beam, the theoretical results become unreliable. This is because of the fact that in such a case, the deep beam closely resembles a deep frame. The axial stresses in such cases may be of such magnitude that their presence will void the use of the principle of super position; such cases can not be represented in two-dimensional plane-stress system.

Figs. 17 to 19 indicate that for a uniformly distributed load acting on the top surface the bottom tensile stress attains maximum value not at the centre of the span but closer to the support. Furthermore, the size of the opening and also the shape of the beam itself, whether square or rectangular, dictate the position and magnitude of this tension. In a square deep beam with a small opening the difference between the tension at the centre and its maximum value near the support is noticeable. In the case of a larger opening (θ = 6 1/4%) the variation of the tensile stress is almost linear. Fig. 20 represents the variation of the bottom tensile stress along the span for uniformly distributed load acting at the bottom edge. It is interesting to note that the shapes of these curves are similar for a particular size of opening irrespective of the ratio of the sides.

The behaviour of a deep beam is also influenced by the kind of loading applied. Figs. 21 to 23 show the distribution of the longitudinal stresses at mid-section due to a single concentrated load acting at the centre of top edge. The magnitude of the maximum tension as well as the manner of variation are significantly different from those due to uniform load. The centre-tension is not as large as that due to uniform load in case of a square deep beam. The most severe cases are for any opening when the depth is greater than the span. This is also true for quarter point loads shown in Figs. 24 to 26. This indicates that the loads acting near the support augment the particular deep beam action that causes the severity in a deep beam with depth slightly more than span.

Figs. 27 to 30 present a summary of the variation of the centre-tension with respect to size of the opening, shape of the deep beam and the type of loading applied. It is interesting to note that the maximum tension at the centre occurs in a rectangular deep beam with a depth 30% more than span having an opening of approximately 6% of the total area of the beam. This is for the case of a uniformly distributed load acting at the top. However, if the uniform load acts at the bottom edge, the maximum tension accurs in the solid rectangular deep beam of the same aspect ratio. Whereas for a concentrated load, whether acting at centre or at quarter points of the span, the maximum tension will develop with an opening of approximately 6% of the area of the beam having a depth 30 % greater than span.

(ii) Stiffened Deep Beams

By stiffening a deep beam by means of a frame around it, its behaviour changes significantly depending on the degree of stiffeners added and the area of the opening included. This is illustrated in Figs. 31 through 35.

For a small cross-section of the stiffening frame denoted by $\zeta = \frac{512I}{tL^3} = 0.074$, the stiffened deep beam without any opening behaves as an ordinary deep beam with reduction in stresses. However, the introduction of a small opening with an area of approximately 4%, the behaviour changes. The influence of the stiffening frame predominates the actual deep beam behaviour. This predominant frame action is more prominent in the case of a rectangular deep beam with greater depth than span.

For a larger cross-section of the stiffening frame ($\zeta = 0.25$) absence of any opening renders the action of the member as that of an ordinary stiffening block (Fig. 31), save and except a small amount of localized tension at the centre of the unsupported edge. Whereas the presence of an opening transforms it into a stiff frame irrespective of the aspect ratio (β). However, for a larger opening, $\theta = 25\%$ or more, the stiffened deep beam behaves as a deep frame irrespective of span to depth ratio. This behaviour is also independent of the degree of stiffening (Figs. 34 and 35).

It should be noted that for a slender stiffening section ($\zeta = .07$), the theoretical approach is not valid (Fig. 31). This is because of the fact that instead of tackling the problem with finite-difference approximations for both the plate and frame portions, the frame portion has been analyzed by means of ordinary linear structural frame analysis. This was performed to avoid error due to singularity at the interfaces where there is an abrupt change in cross-section. In linear structural analysis the axial strain is always neglected as the rotation is neglected in braced-frame (truss) analysis. Furthermore, while membrane stress is neglected, in plate analysis, it is predominant in other structures. The slender section of the stiffening frame under a heavy axial strain will, not act as a frame but as an elastic band. This will void the calculations of the redundant forces as performed here. This fact also contributes to the non-linearity of the load-deflection relationship which violates not only the principles of ordinary structural analysis (linear) but also the conditions of the plane

state of stress.

There are three different cases of non-linearity in the behaviour of structures. The first one arises from the non-linear behaviour of the material of which the structure is made. The second case is referred to as gross deformation.

In linear structural analysis, it is essential to assume that the deformation is small compared with the dimensions, so that the overall shape of the structure is not significantly altered by the process of loading. More significantly, it is assumed valid to use the equilibrium equations with the lengths, angles etc. for the undistorted structure whereas strictly speaking these equations must hold in the distorted structure.

The third case of non-linear behaviour which is important in the present case, can be a particular case of the second one. This is the effect which axial forces have on the bending stiffness of members in rigid-jointed frames and trusses. If the axial force in a member is compressive, the bending stiffness is reduced, while if it is tensile the stiffnes is increased. The effect may in extreme cases cause a structure to be unstable while the material is within its elastic region.

The limitation of the theory of elasticity to isotropic homogeneous materials leads to a number of simplifying conclusions enabling one to express stress in terms of strain or vice versa irrespective of the orientation of the material with respect to coordinate axes viz: stress-strain relations are invariant to transfor-

nation of coordinates. From this follows the principle of superposition of stresses in elastic system leading to the conclusion that the strain ϵ_x is linearly dependent upon all three stresses by

$$\epsilon_x = \frac{1}{E}[\sigma_x - \upsilon(\sigma_y + \sigma_z)]$$

and so on. This is the principle of superposition which not only allows the state of strain at a point to be derived in this way, but is equally applicable to distributions of stress and strain generally. However, this principle is valid only for a linear case. Thus the present attempt is limited to linear cases only.

(iii) Sources of Error

In the theoretical approach, the probably sources of error lie in the moderately coarse mesh incorporated in the finite-difference equations. There are errors also due to singularity at points directly under the loads. Because of this, the magnitude of maximum tension at bottom-centre when the load is acting at the bottom are less precise than the same for load on the top edge. However, it is expected that the errors in theoretical results will not exceed 10 %. This observation is based on the favourable comparison made between the results obtained herein and those reported by previous investigators. The actual stress-concentration around the periphery of the openings, specially at the corners, can not be accounted for by the present approach. Due to singularity, the results will be totally erroneous.

In case of experimental investigations, the probable sources of error can be classified in three groups; fabrication errors, loading errors, instrumentation errors.

Fabrication errors arise due to preparation of the specimens, uneven thickness of the materials and possible change of elastic properties and residual stresses due to welding. The thickness of the model itself is liable to incur a significant error, since the rigorous fulfillment of the plane-stress conditions demands a thickness tending to zero. Also because of the variation in thickness, a small amount of lateral deflection may be induced and will contribute to the magnitude of the measured strains, hence the calculated stresses may have significant errors inspite of the fact that an effort was made to eliminate the lateral deflections as far as possible. This type of error might have been associated in results shown in Fig. 31.

Experience has also shown that the heat due to machining appreciably changed the elastic properties of the tension specimen. Keeping this in mind, the process of welding causing alternate heating and cooling was sure not only to change the elastic properties but also to induce residual stresses. This is expected to incur a significant error in stress-values. The effect of the manufacturers' deficiency such as unevenness of the thickness and quality control are still unknown and overlooked.

Instrumentation errors arising from the strain gauges in their alignament and their readings may not be as significant as those in the first group. However, the small strain readings are liable to involve

error which has been distributed by taking the average of several readings.

The maximum error involved in the experimental investigations is expected in the loading device. The loading rig was designed in such a fashion so that it could apply a uniformly distributed load on the upper edge of the specimen. However, the results shown by all the experimental stress-diagrams indicate that the applied load may not truly represent a uniformly distributed nature. This is evident from the fact that those stress-diagrams assumed slightly different shape at the top from the theoretical curves as well as from those of the previous investigators. It was also noted that because of the mechanical device in loading, the load could not be applied without any jerk or vibration. This may also be a critical source of error.

From all these considerations, it is expected that the experimental results involved a significant amount of error, which may be in some cases as high as 30 % as shown in Fig. 15. Since the experimental observations were used mainly to verify the theoretical approach and since the theoretical results are in good agreement with those of the previous investigators, the experimental results do substantiate the theoretical approach.

However, it is expected that the finite-element method may be adequately suitable in this type of problems dealing with singularities due to change in cross-sections, opening and concentrated loading. This method could also arrest the magnitude of stress-concentration around the periphery as well as the inner corners where the method of finite-difference is liable to yield totally erroneous results.

CHAPTER VII

CONCLUDING REMARKS

As a result of this theoretical and experimental investigation on the behaviour of plain and stiffened deep beams with or without opening, the following conclusions may be made:

1. For the limiting case where the plain deep beam is without an opening, the displacement method yields results which are in good agreement with the findings of previous investigators.
2. For deep beams with small openings, the stresses obtained by model tests and theoretical analysis are in reasonable agreement, confirming the validity of the theoretical approach to doubly-connected plane-stress system.
3. For a plain deep beam having a small opening at the centre, the maximum longitudinal tension at the centre is significantly less than that in a solid deep beam without an opening; if the opening area is further increased the tension, however, increases abruptly.
4. For a still larger opening, having an area of about 25% of the total area of the member itself, the behaviour will be similar to that of a frame, not that of a deep beam proper.
5. The maximum longitudinal tension in a solid deep beam

occurs not in a square deep beam but when the depth is slightly larger than the span. This is also true in the case when an opening is introduced.

6. The distribution of longitudinal stresses in the mid-section of a deep beam with or without opening is nearly linear when the span is more than 30% of the depth.
7. For any deep beam critical stress condition will not exist at the centre of the span, but somewhere closer to the support.
8. The type of loading and its point of application will not only determine the maximum longitudinal stress but also the position of the neutral axis.
9. By introducing a frame around the outer edges of a deep beam, its behaviour is totally changed; it behaves neither as a deep beam nor as a deep frame, depending on the span-depth ratio, size of opening and the degree of stiffening added.
10. For a stiffened deep beam without an opening, the mid-section is subjected to a small tensile stress at the centre of the bottom edge; while an increased stiffening area will render it to almost a stiff compression block with a small localized tension at the bottom.
11. Presence of an opening influences the behaviour of a stiffened deep beam in such a manner that bending action becomes more prominent.

It should be pointed out, however, that for a slender stiffening frame the theoretical approach is not valid, as was discussed before. Although the present approach involves a very large amount of arithmatic, its versatility in solutions of doubly connected deep beams is sure to offset the labour.

REFERENCES

1. F. Dischinger - 'Beitrag zur Theorie der Halbscheibe und des Wandartigen Balkans.' Publications, International Assoc. of Bridge and Structural Engineering I, Zurich, 1932.
2. Portland Cement Association - 'Design of Deep Girders'. Pamphlet No. ST66.
3. Harmann Bay- 'Uber den Spannungszustand in Hohen Tragern und die Bewehrung von Eisenbetontragwanden (Dissertation), Stuttgart, 1931.
4. Conway, Chow and Morgan - 'Analysis of Deep Beams' Journal of Applied Mechanics, V. 18, No. 2, June 1951.
5. K. Iyengar - 'Analysis of Deep Beams', Proceedings, Second Congress of Applied Mechanics, New Delhi, 1956.
6. Chow, Conway and Winter - 'Stresses in Deep Beams'. Proc. ASCE V. 78 Seperate No. 127, May 1952.
7. A. M. Guzman and C. Luisoni - Discussion on 'Stresses in Deep Beams', Proc. ASCE, February 1953.
8. Elihu Geer - 'Stresses in Deep Beams', Journal of American Concrete Institute, January 1960.
9. F. Archer and E. Kitchen - 'Stresses in Deep Beams', Civil Engineering, London, V55, N643, Feb. 1960.
10. F. Archer and E. Kitchen - 'Strain Energy Methods for solutions of Deep Beams.' Civil Engineering, London V52, N618, Dec. 1957.
11. A. M. Guzman and C. J. Luisoni - 'Soluciono Varacional del problema

de la viga Rectangular Simplementi Apoyada de Gran Altura,' Ciencia y Lecnica, Buenos Aires, Argentina, Vol 111, 1956.

12. S. Saad and A. W. Hendry - 'Gravitational Stresses in Deep Beams,' The Structural Engineer, June 1961.
13. S. Saad and A. W. Hendry - 'Stresses in Deep Beams with Central Concentrated Loads.' Experimental Mechanics, V1, N6, June 1961.
14. N. J. Durant and F. Garwood - Ministry of Works, Technical Nate No. 78, London, October 1947.
15. L. Fox - 'Mixed Boundary Conditions in the Relaxation Treatment of Biharmonic Problems (plane-strain Problems)' Proc. Royal Society, London (A), 189, 1947.
16. A. Coul - 'Stress Analysis of Deep Beams and Walls,' The Engineer, Feb. 1966.
17. J. B. Kennedy - Personal Communications
18. S. Timoshenko and J. N. Goodier - Theory of Elasticity. McGraw-Hill, New York, 1951
19. B. Sen - 'Two-dimensional Boundary-value Problems of Elasticity,' Proc. Royal Society, London (A) 1946.
20. A. Tuzi - 'Effect of a Circular Hole on the Stress Distribution in a Beam under Uniform Bending Moment.' Philosophical Magazine. London, Seventh Series, V9, Jan - June 1930.
21. Karl Wolf - 'Beitrog zur ebenen Elastizitatstheorie,' Z. Techn. Phys. 2, 1921.

22. D. Gupta - 'Effect of Small Circular Hole on Stress Distribution on a Deep Rectangular Beam Subject to Flexure under Shear,' Indian Journal of Theoretical Physics, V10 N2 nd 3 1962.

23. M. A. Jeffery - 'Plane-Stress and Plane Strain in Bipolar Coordinates' Royal Society. London (A), V221, March 1921.

24. W. G. Bickley - 'Infinite Plate with Circular Holes', Royal Society London (A), V227 January 1928.

25. H. Hengst - 'Beitrag zur Berechnung von Stegblechen mit Sparlochern,' Stahlbau 15, 61 (1942)

26. A. Hutter - 'Die Spannungs spitzen in gelochten Blechscheiben und Striefen', Z. angew. Math. Mech. 22, 322 (1942)

27. G. N. Savin - Stress Concentration Around Holes.' Pergamon Press, New York, 1966.

28. G. B. Airy - 'On the Strains in the Interior of Beams' Trans.Royal Society,London 153, 1863.

29. P.P. Teodorescu - 'Hundred Years of Investigations in the Plane Problems of the Theory of Elasticity', Applied Mechanics Review, V 17, N3, March 1964.

30. de G. Allen - Relaxation Methods in Engineering and Science, McGraw-Hill, New York, 1954.

31. M. Hetenyi - Handbook of Experimental Stress Analysis, John Wiley and Sons, New York, 1950. pp. 751 - 770.

32. O. C. Zienkiewicz - Stress Analysis, John Wiley and Sons, 1965.

33. Hugh Ford - Advanced Mechanics of Materials, Longman, 1962.

34. Chi-Teh Wang - Applied Elasticity, McGraw-Hill, New York, 1953.

35. Ray W. Clough - 'The Finite Element Method in Plane Stress Analysis', ASCE, Second Conference on Electronic Computations, Nov. 1962.

36. Ray W. Clough - 'The Finite Element Method in Structural Mechanics' Stress Analysis, John Wiley and Sons, New York, 1965.

37. F. S. Shaw - Relaxation Methods, Dover, 1953.

38. N. M. Newmark - Class Notes on Numerical Analysis, University of Illinois, 1960.

39. S. Timoshenko and D. H. Young - Theory of Structures, McGraw-Hill, 1962.

40. Aluminum Company of Canada - Strength of Aluminum, 1968 Edition, Toronto.

41. G. N. J. Kani - Class Notes and Personal Communications, 1966.

42. J. B. Kennedy and S. F. Ng - 'Linear and Non-linear Analysis of Skew Plates' Journal of Applied Mechanics, June 1967.

43. J. B. Kennedy-Class notes on Theory of Elasticity I & II, University of Windsor, 1966-67.

NOMENCLATURE

A = Area of the Deep Beam

a' = Area of Opening

L, $2a$ = Span of the Deep Beam

H, D = Depth of the Deep Beam

$\theta = a'/A$

α = Side of Opening/Side of Beam

$\beta = L/D$

t = Thickness of Beam

I = Moment of Inertia of Frame Cross-Section

$\partial = \frac{512I}{t\,L^3}$

p = Applied Pressure in p.s.i.

q_o = Applied Pressure in lbs. per in.

P = Pointed Load at Centre in lbs.

Q = Pointed Load acting at a Quarter Point of the Span

σ_x, σ_y, τ_{xy} = Stresses at a Point

u,v = Displacement Components Parallel to x and y directions respectively

E = Young's Modulus of Elasticity

υ = Poisson's Ratio

$\lambda = (1 - \upsilon^2)/E$

$\xi = (1 - \upsilon)/2$

$\eta = (1 + \upsilon)/2$

VITA AUCTORIS

1933 Muhammad Harunur Rashid was born in November in Dinajpur, East Pakistan.

1940 Attended Harvey Primary School, Santahar, for his elementary Education.

1950 Graduated from Chuadanga Victoria Jubilee High School and was enrolled in Pabna Edward College the same year.

1952 Obtained Intermediate Science Certificate with a Senior Scholorship and got admitted at the Ahsanullah Engineering College, Dacca, the same year.

1957 In September, married Hosne Ara (Milly) while she was an undergraduate at the Holy Cross College, Dacca.

1958 In January, joined The Engineers Ltd, Dacca as an Assistant Engineer and was responsible for the design of 36 R. C. road bridges over the canal network of the G. K. Irrigation Project. Son Imran was born in July.

1959 In November, came back to teaching in Ahsanullah Engg. College.

1960 Sent on deputation to the University of Illinois on a one-year programme of higher studies jointly sponsored by the Ahsanullah Engg. College and Texas A and M. College.

1961 Completed coursework requirements and obtained an M.S. from the University of Illinois and returned to Dacca to teaching in August.

1962 Became Assistant Professor in the East Pakistan University of Engg. and Technology, Dacca, that absorbed the Ahsanullah Engineering College. Daughter Suzan was born in July.

1965 Sent to Canada for higher studies towards a Ph.D., presumably to head Civil Engineering in newly created Rajshahi Engg. College on return on a three-year programme sponsored by the Govt. of Canada.

1966 Completed requirements for an M.A.Sc. at the University of Toronto and was enrolled as a Ph.D. student at the University of Windsor under the guidance of Dr. J. B. Kennedy.

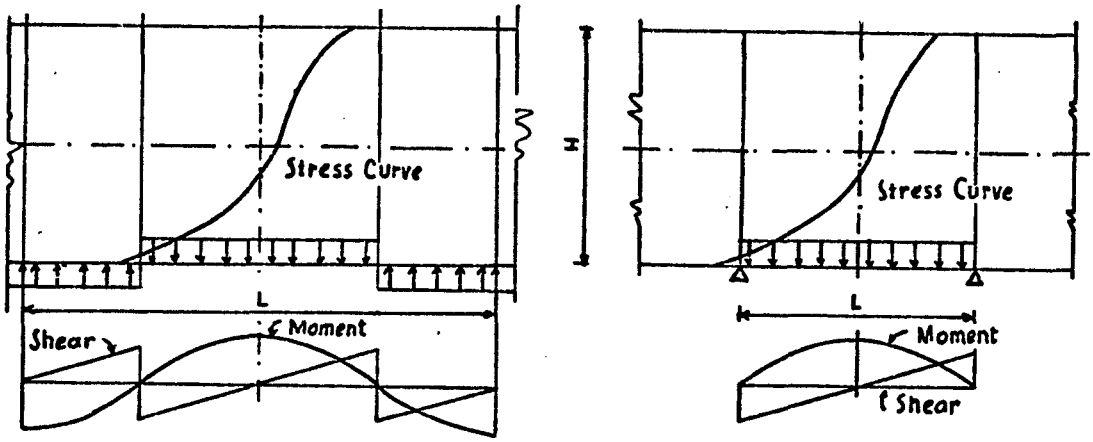

(a) Continuous Span

(b) Single Span

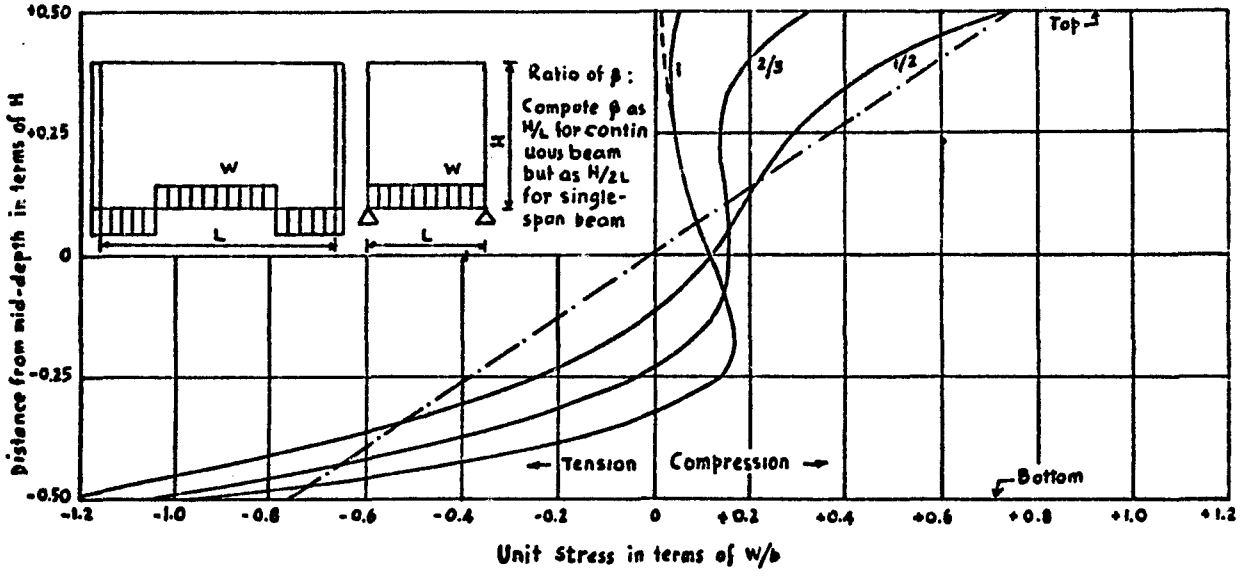

(c)

Fig. 1

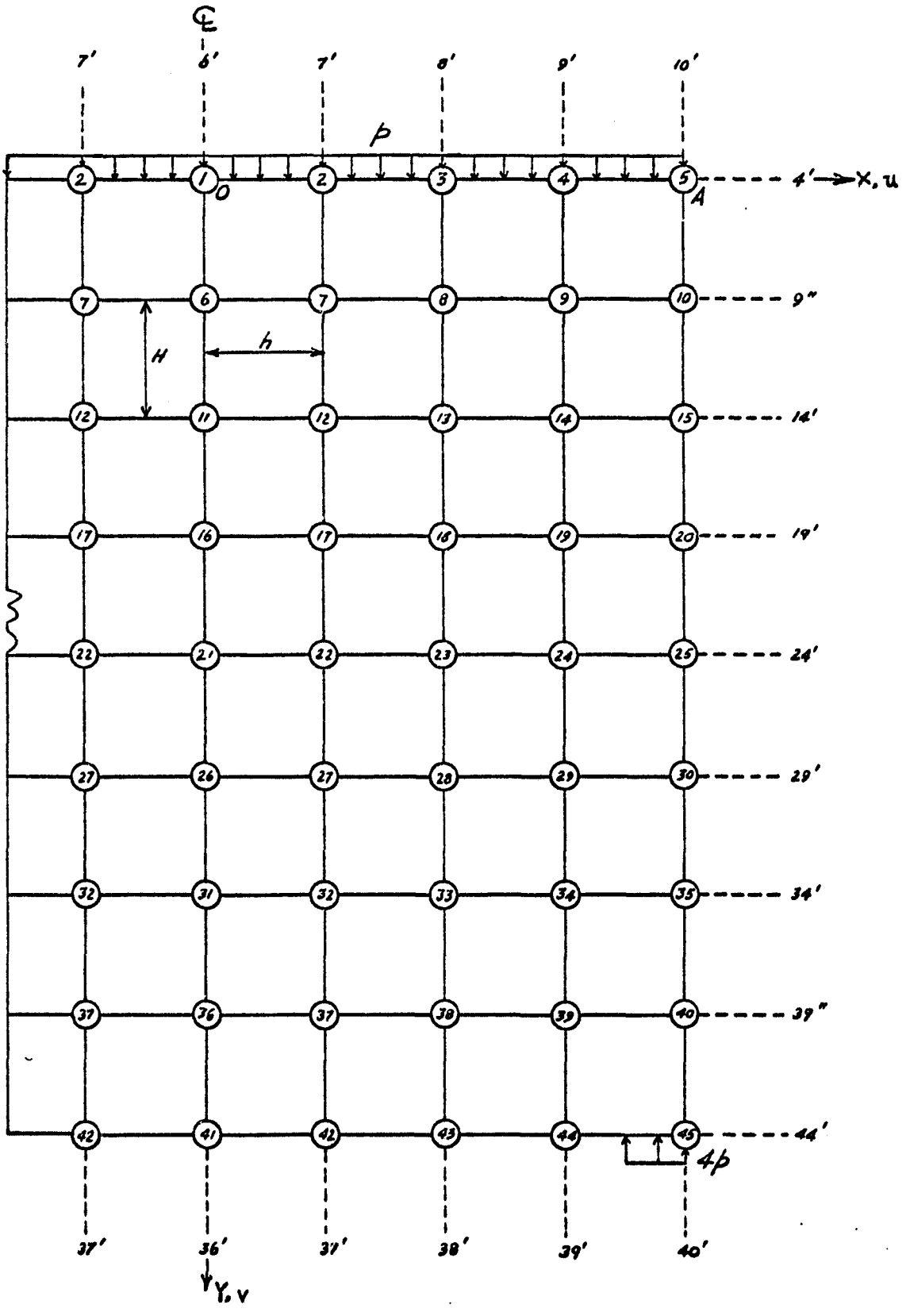
℄
7'
6'
7'
8'
9'
10'
p
2
1
0
2
3
4
5
A
4'
X, u
7
6
7
8
9
10
9"
H
h
12
11
12
13
14
15
14'
17
16
17
18
19
20
19'
22
21
22
23
24
25
24'
27
26
27
28
29
30
29'
32
31
32
33
34
35
34'
37
36
37
38
39
40
39"
42
41
42
43
44
45
44'
4p
37'
36'
37'
38'
39'
40'
Y, v

Fig. 2

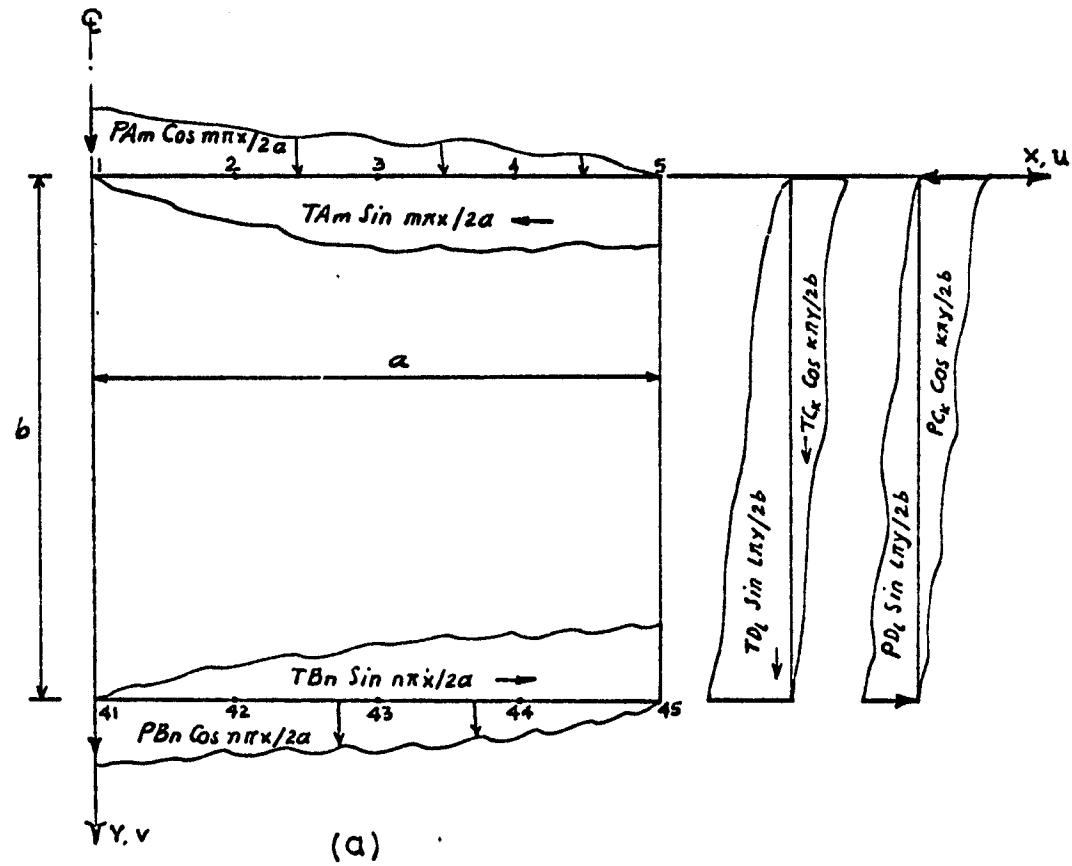
PAm Cos mπx/2a
1
2
3
4
5
x, u
TAm Sin mπx/2a
a
b
TQ_k Sin kπy/2b
TC_k Cos kπy/2b
PD_k Sin kπy/2b
PC_k Cos kπy/2b
TBn Sin nπx/2a
41
42
43
44
45
PBn Cos nπx/2a
Y, v

(a)

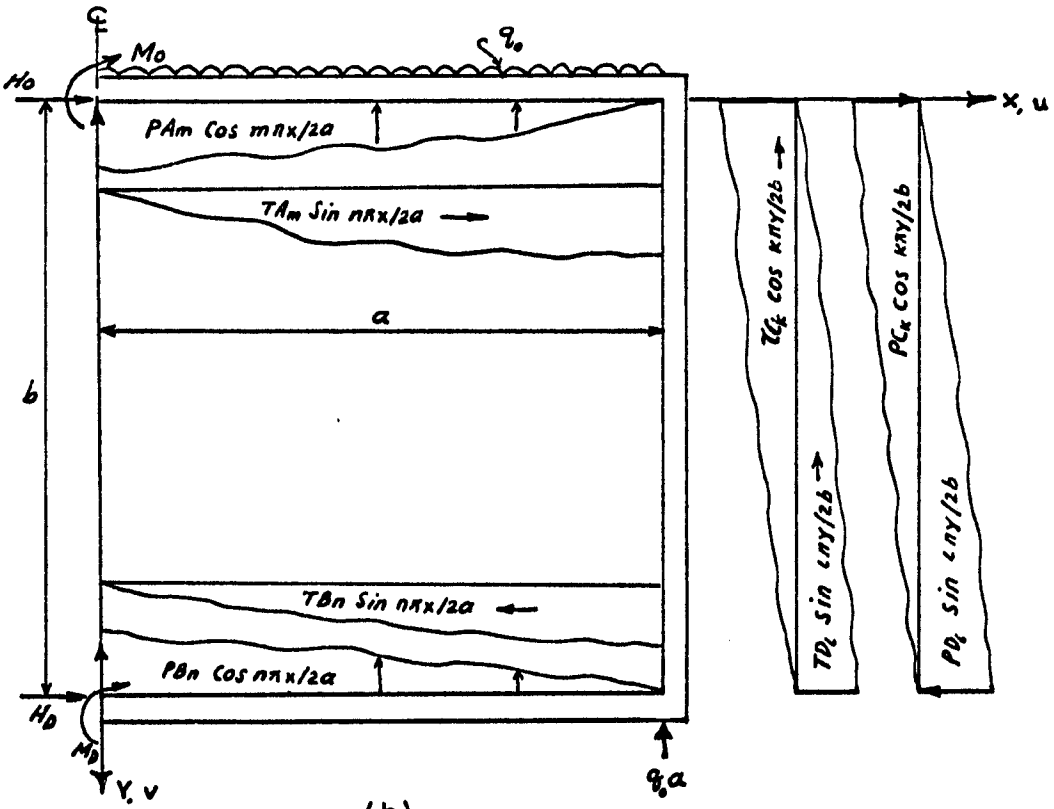
Mo
qo
Ho
x, u
PAm Cos mπx/2a
TAm Sin mπx/2a
a
b
TQ_k Cos kπy/2b
PC_k Cos kπy/2b
TQ_k Sin kπy/2b
PD_k Sin kπy/2b
TBn Sin nπx/2a
PBn Cos nπx/2a
Ho
Mo
Y, v
qo a

(b)

Fig.3

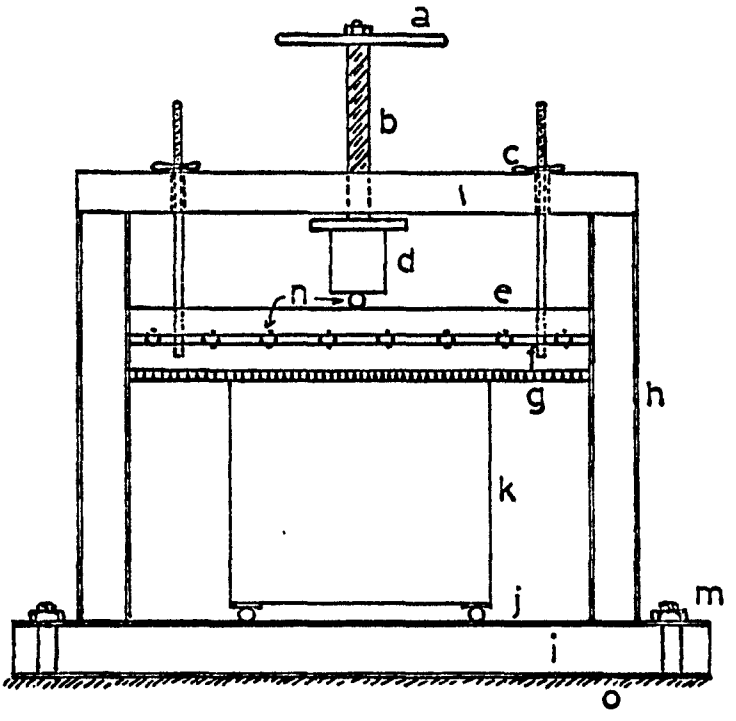

FIG. 4a LOADING FRAME

a LOADING BAR
b LOADING SCREW
c HOLDING BAR
d LOAD CELL
ef CROSS BEAMS
g RUBBER
h VERTICAL MEMBER
l BOTTOM I-BEAM
j ROLLER SUPPORT
k MODEL
l SOLID TOP BEAM
m FIXING NUT
n 3/4" DIAMETER BALL
o FLOOR

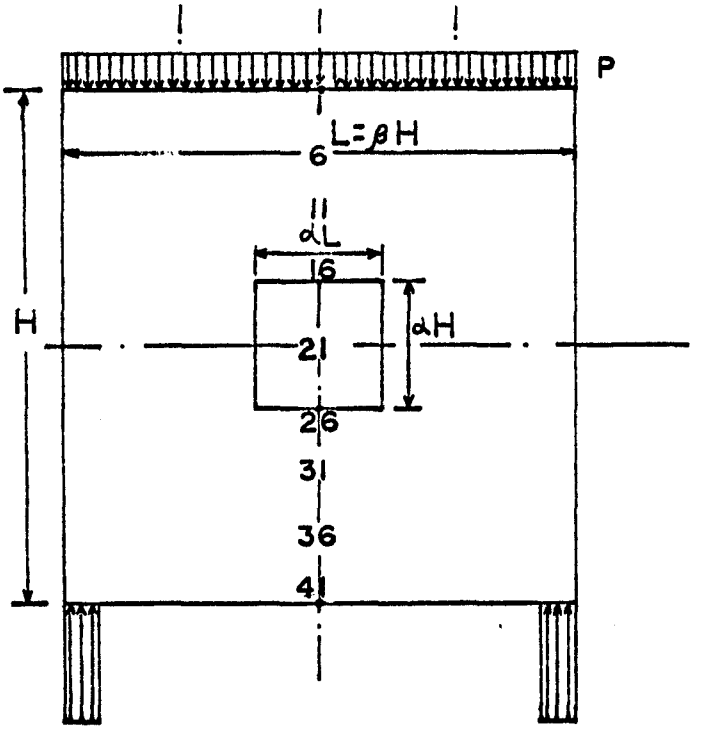

FIG. 4b MODEL

CASES STUDIED
P-UDL AT TOP
P-UDL AT BOTTOM
Q-AT CENTRE
Q-AT QT. POINTS
β = L/H = 2/3, 1, 3/2
α = 0, 1/4, 1/5, 1/2
SUPPORT WIDTH L/16
ONE CASE L/8
ONE CASE L/20

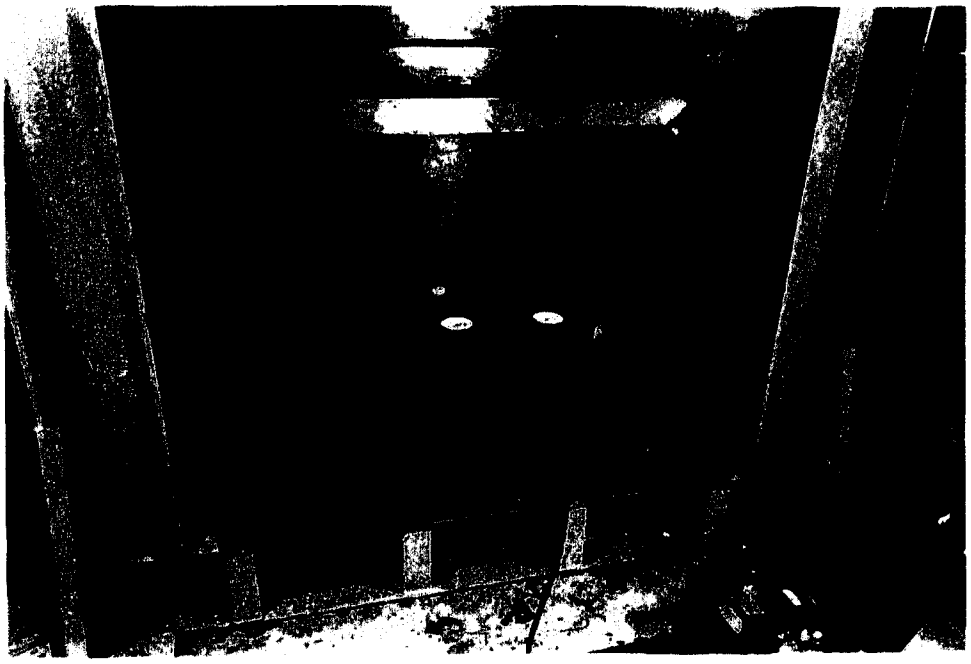

(a)

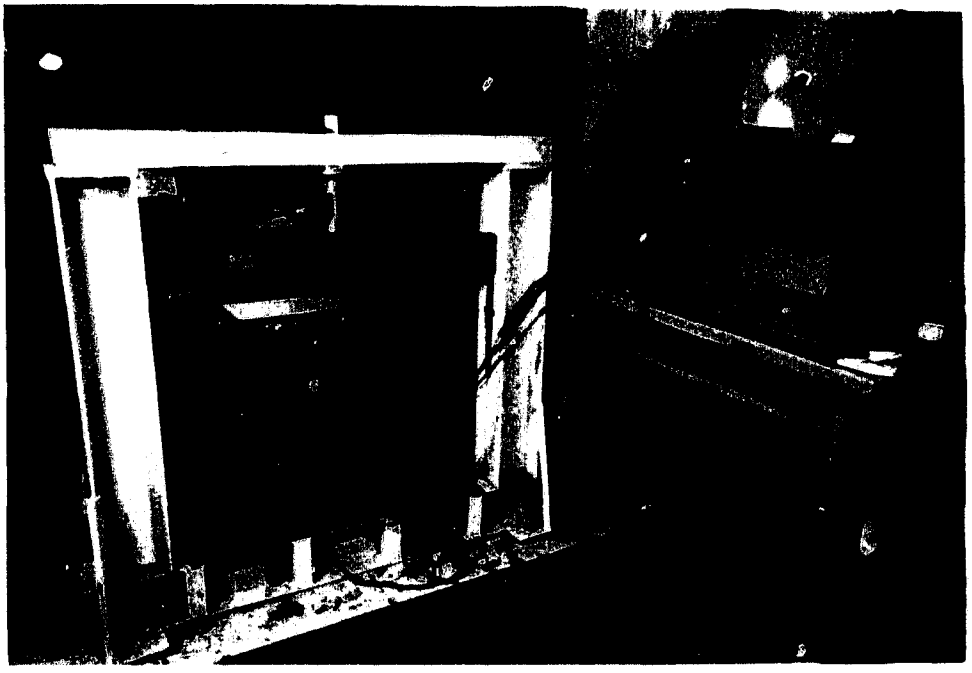

(b)

Fig.5

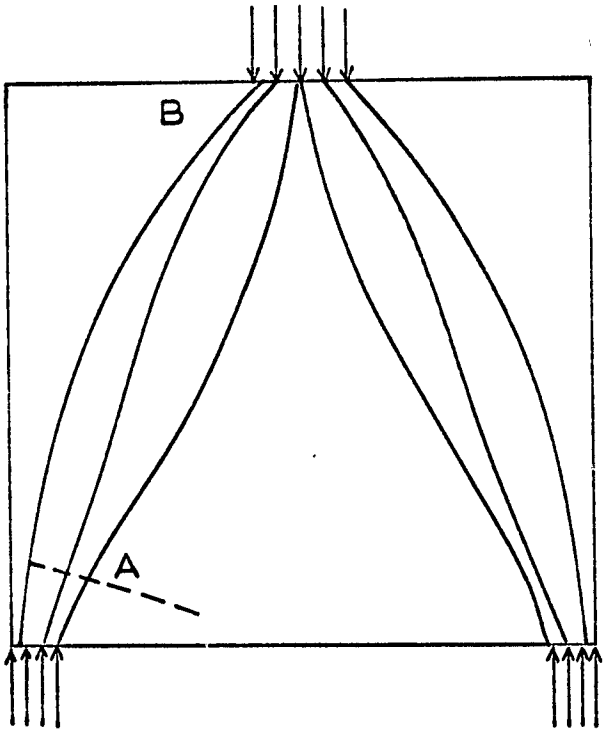

(a)

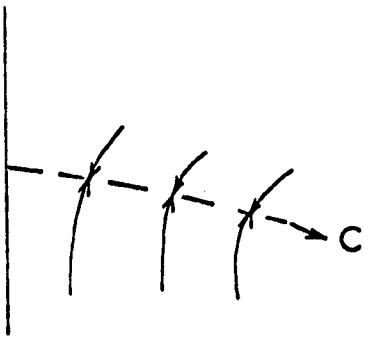

(b)

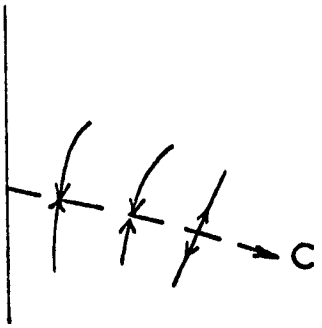

(c)

Fig. 6

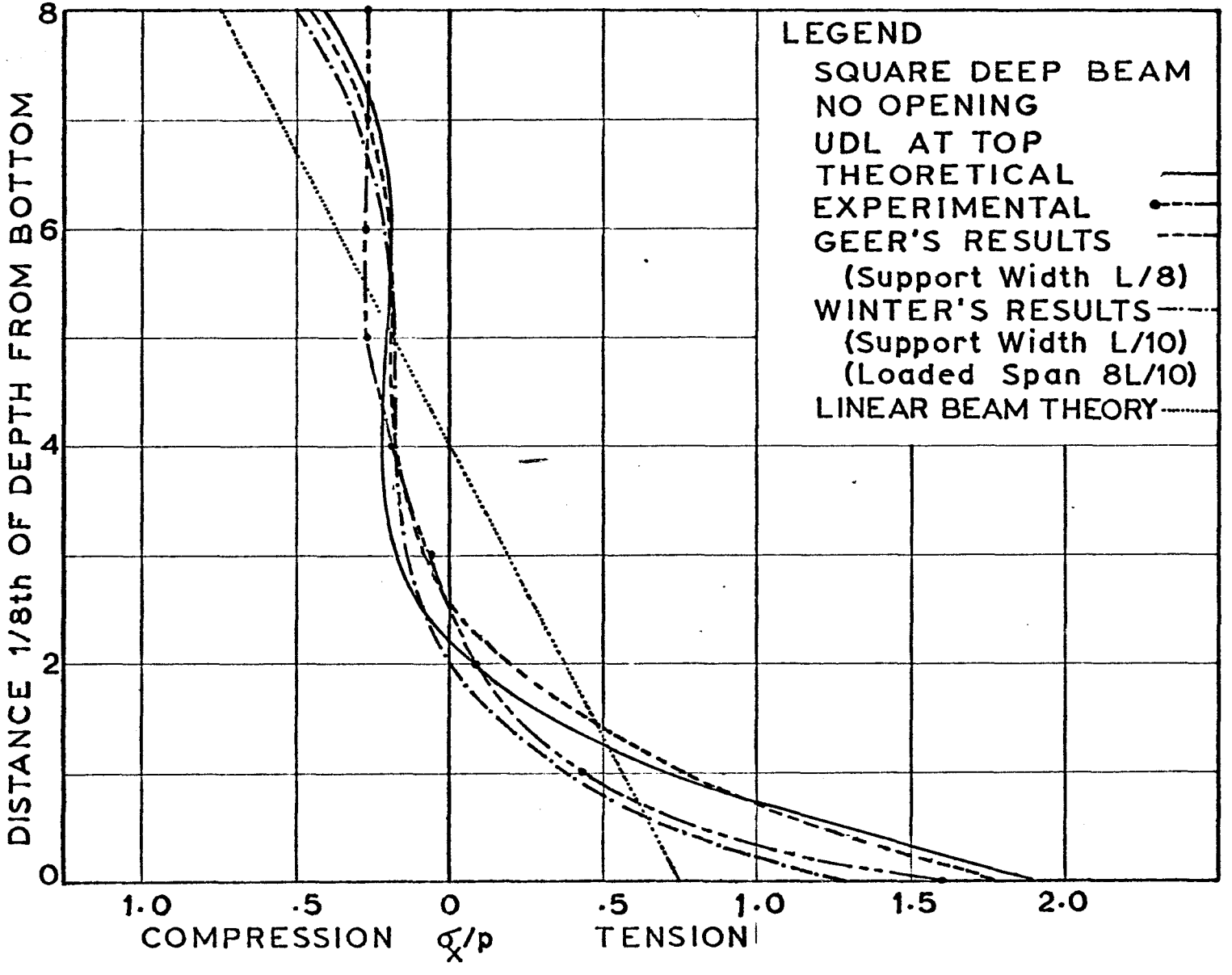

Fig.7a. Longitudinal Stresses at mid-section of a Solid Square Deep Beam for UDL at Top

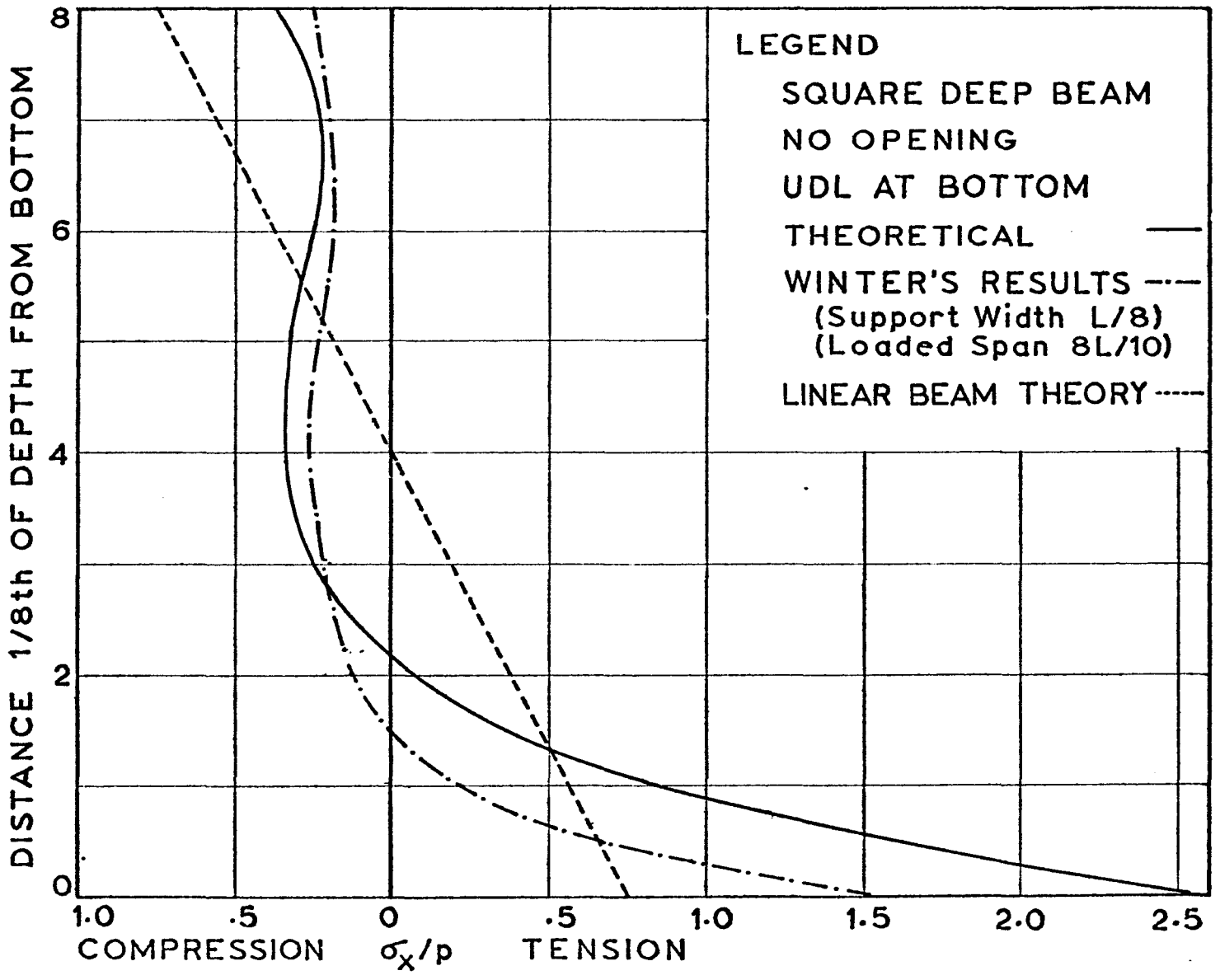

Fig. 7b. Longitudinal Stresses at mid-section of a Square Beam for UDL at Bottom

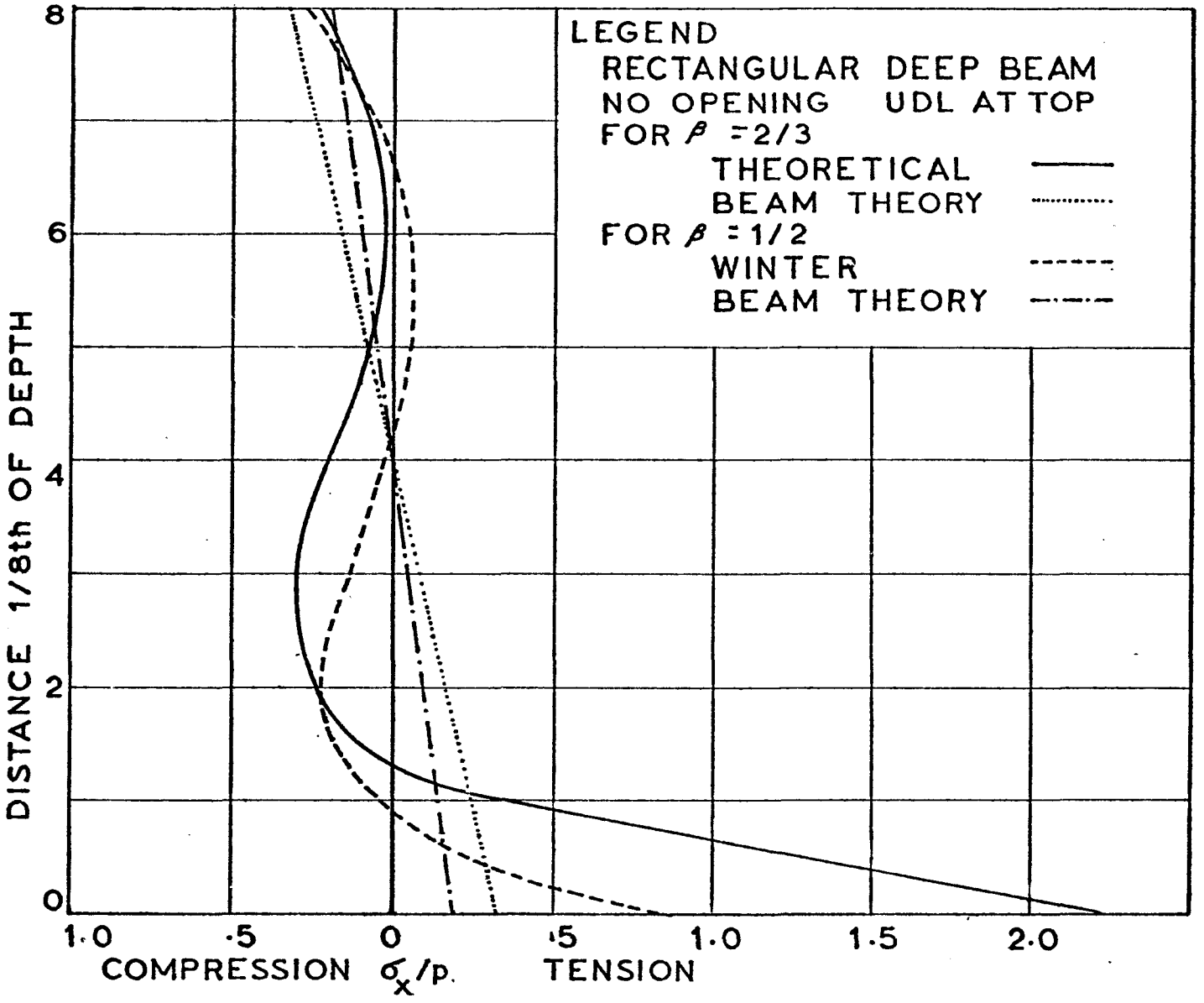

Fig.8a. Longitudinal Stresses at mid-section of a Solid Rectangular Deep Beam

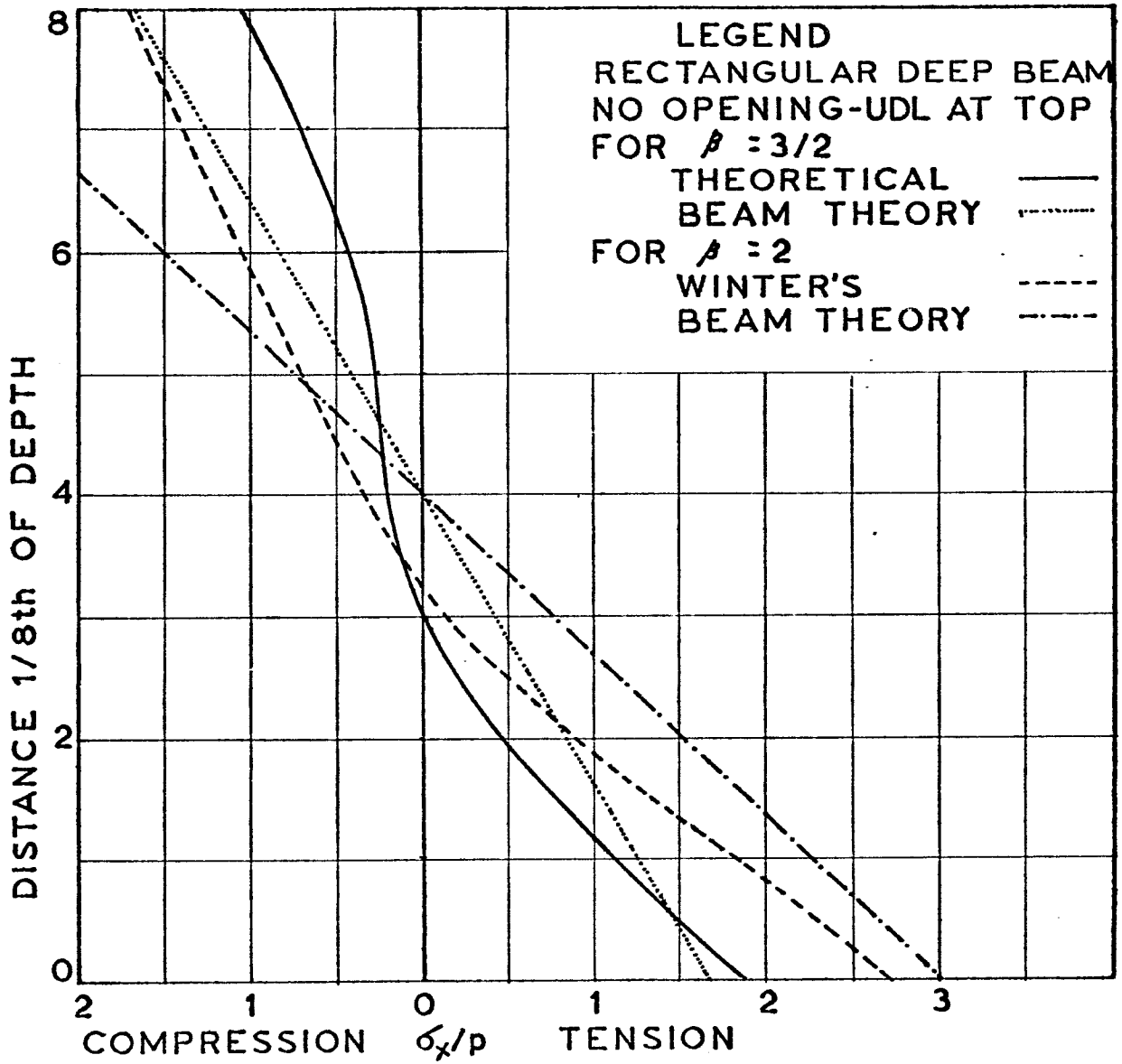

Fig.8b. Longitudinal Stresses at mid-section of a Solid Rectangular Deep Beam

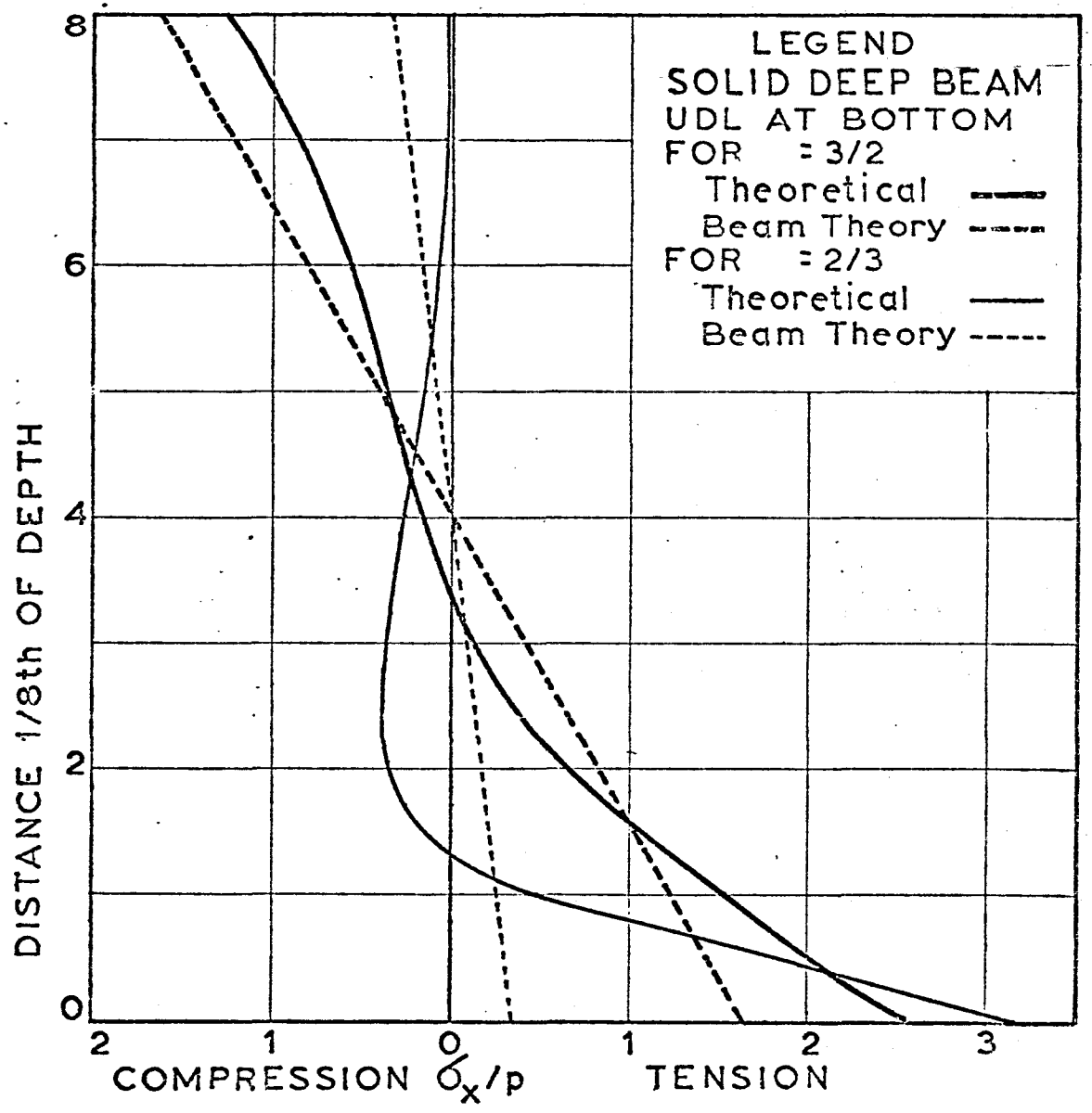

Fig.9. Longitudinal Stresses at mid-section of a Solid Rect. Deep Beam for UDL at Bottom

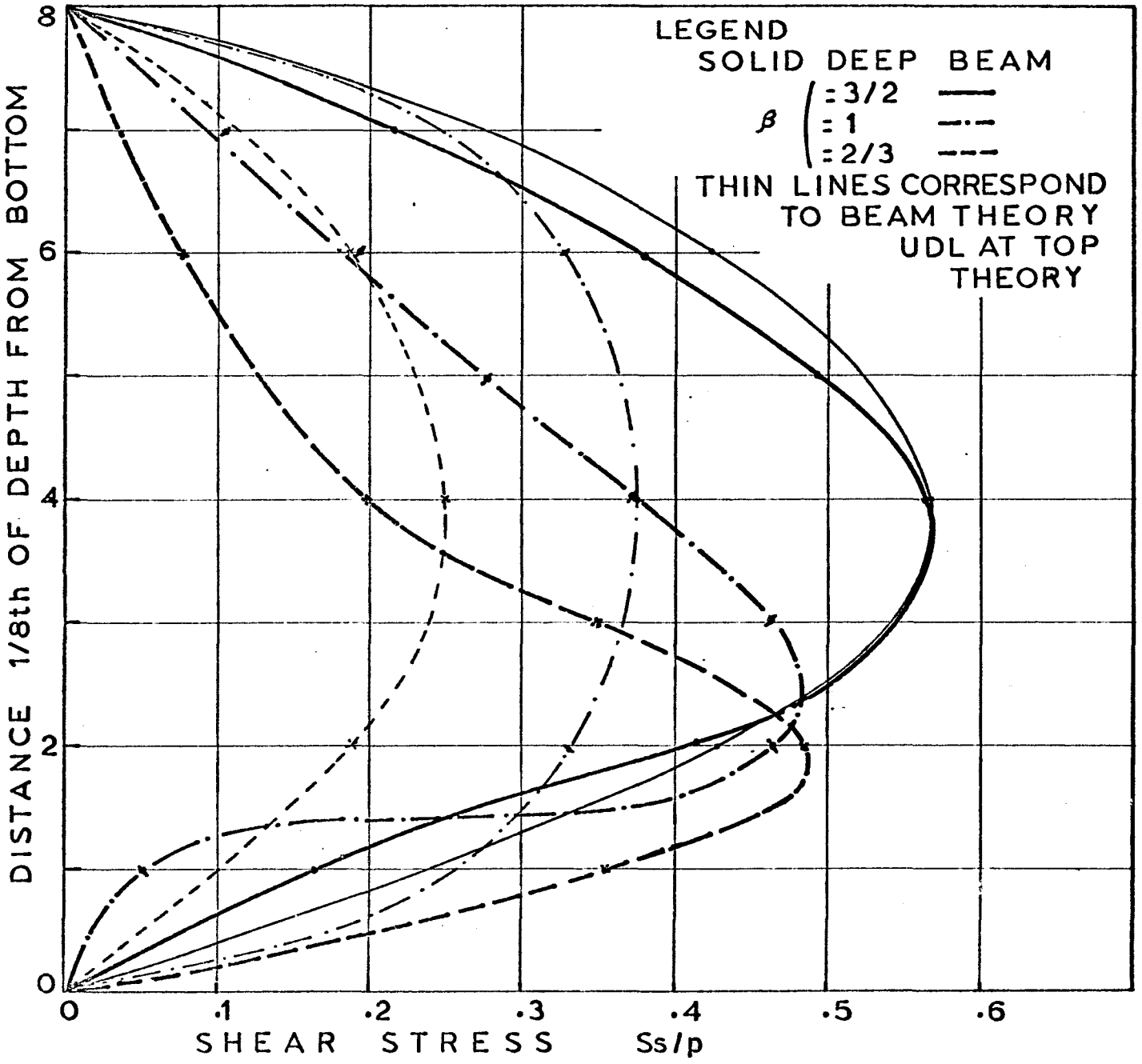

Fig.10 Shear Stress at Quarter Point for UDL at Top

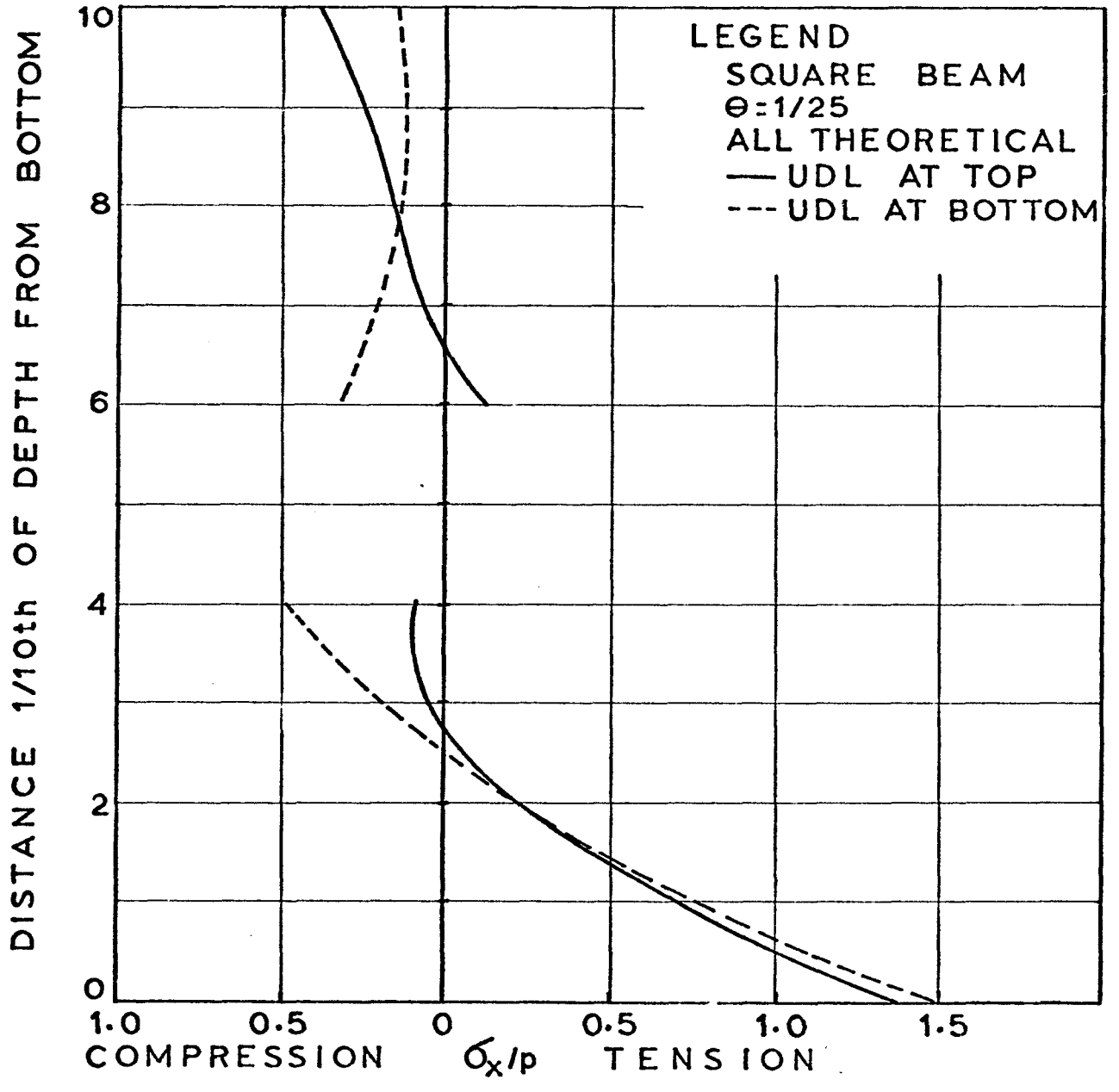

Fig.11 Longitudinal Stresses at mid-section Of Square Deep Beam with an Opening

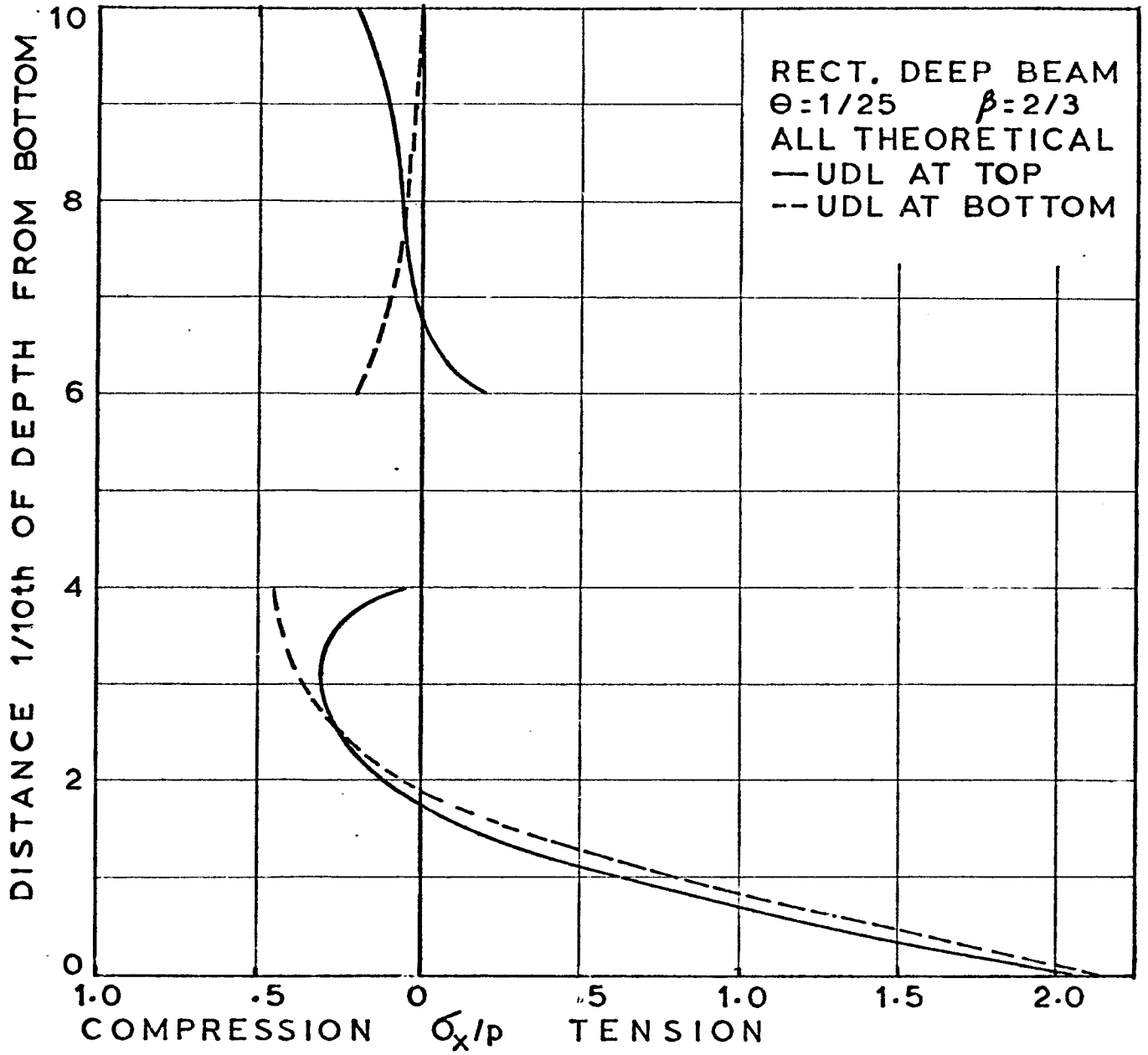

Fig.12 Longitudinal Stresses for a Rectangular Deep Beam with a Small Opening

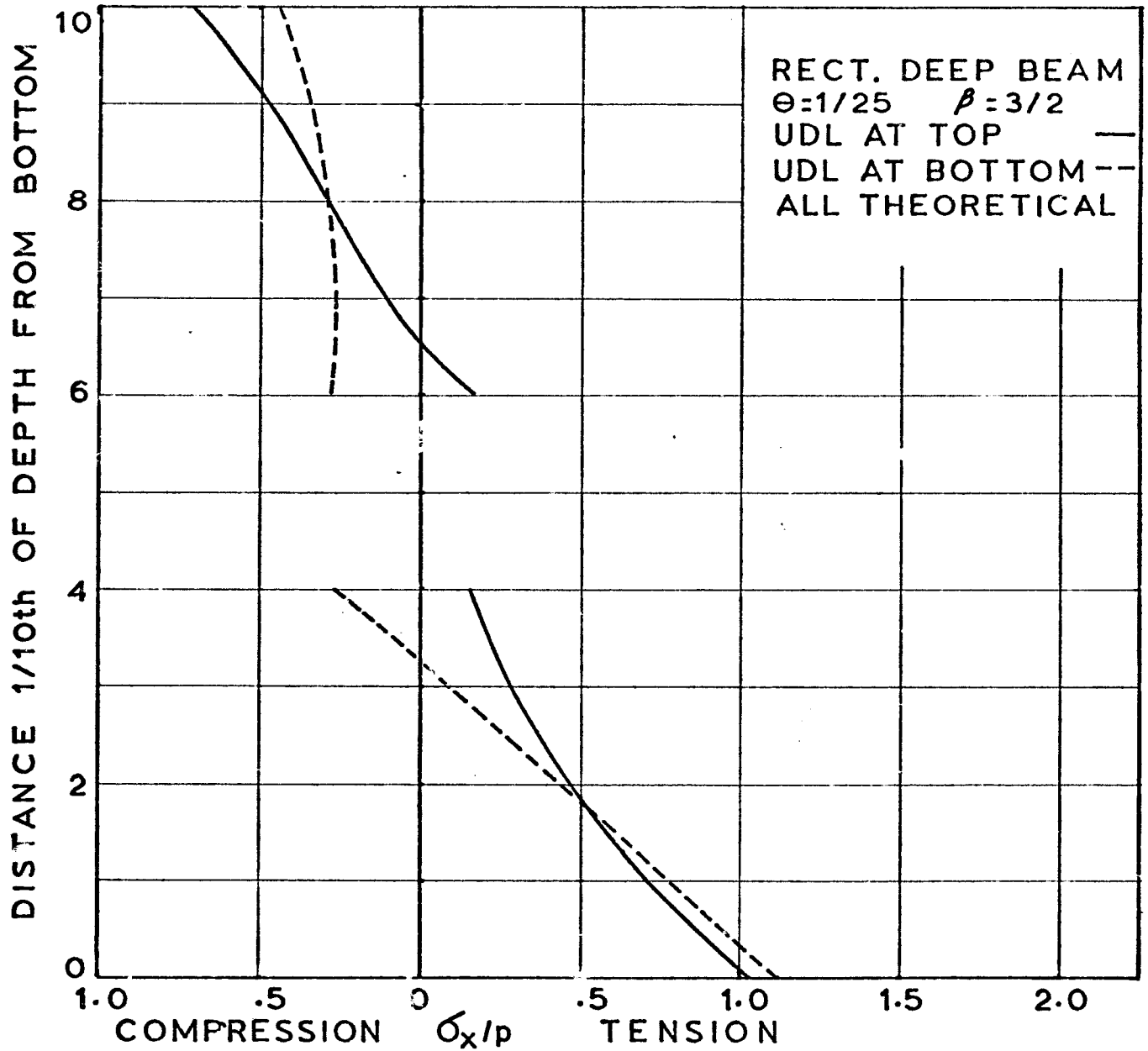

Fig.13 Longitudinal Stresses at mid-section of a Rect. Beam with a Small Opening

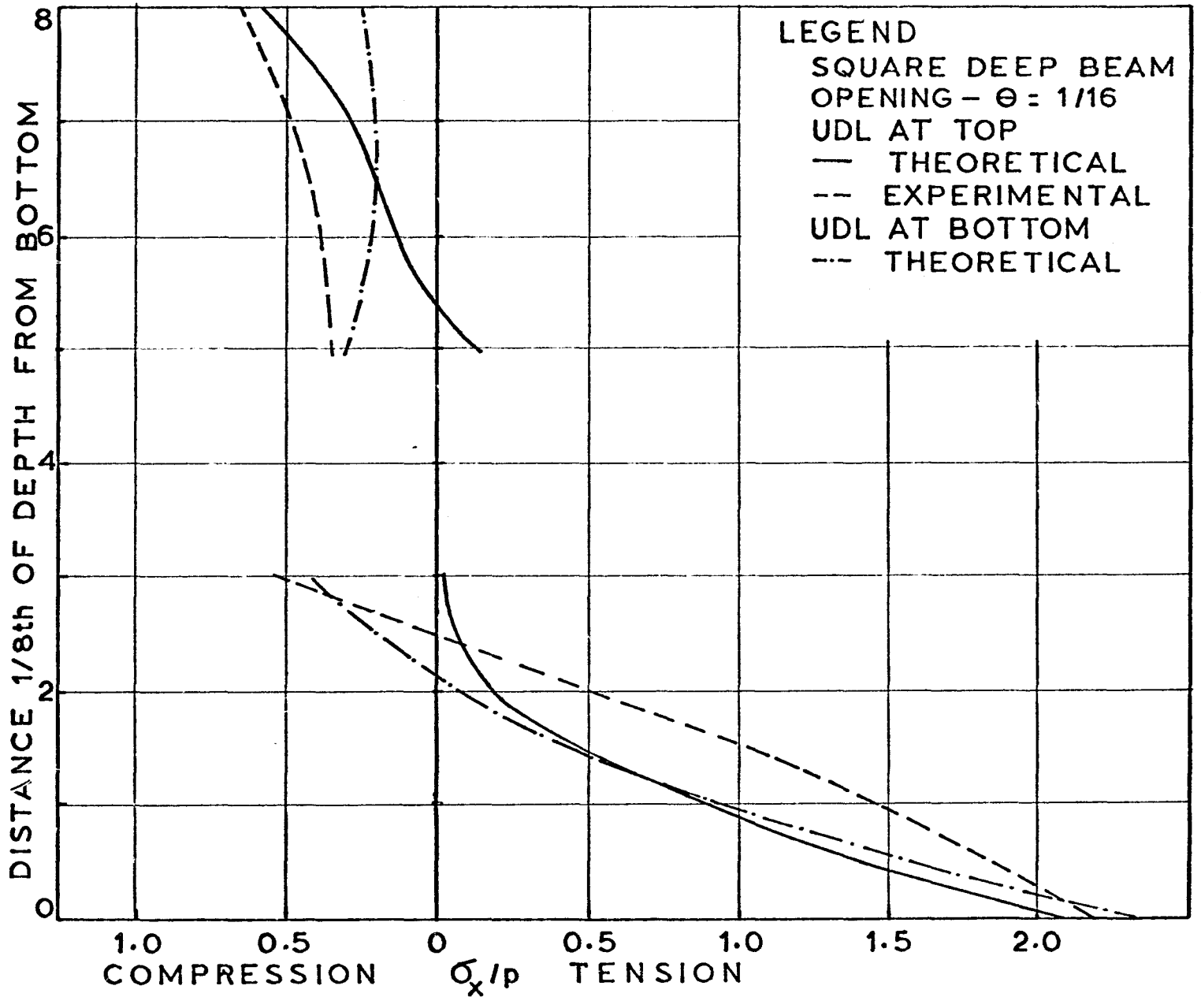

Fig.14 Longitudinal Stresses at mid-section of a Square Deep Beam with an Opening

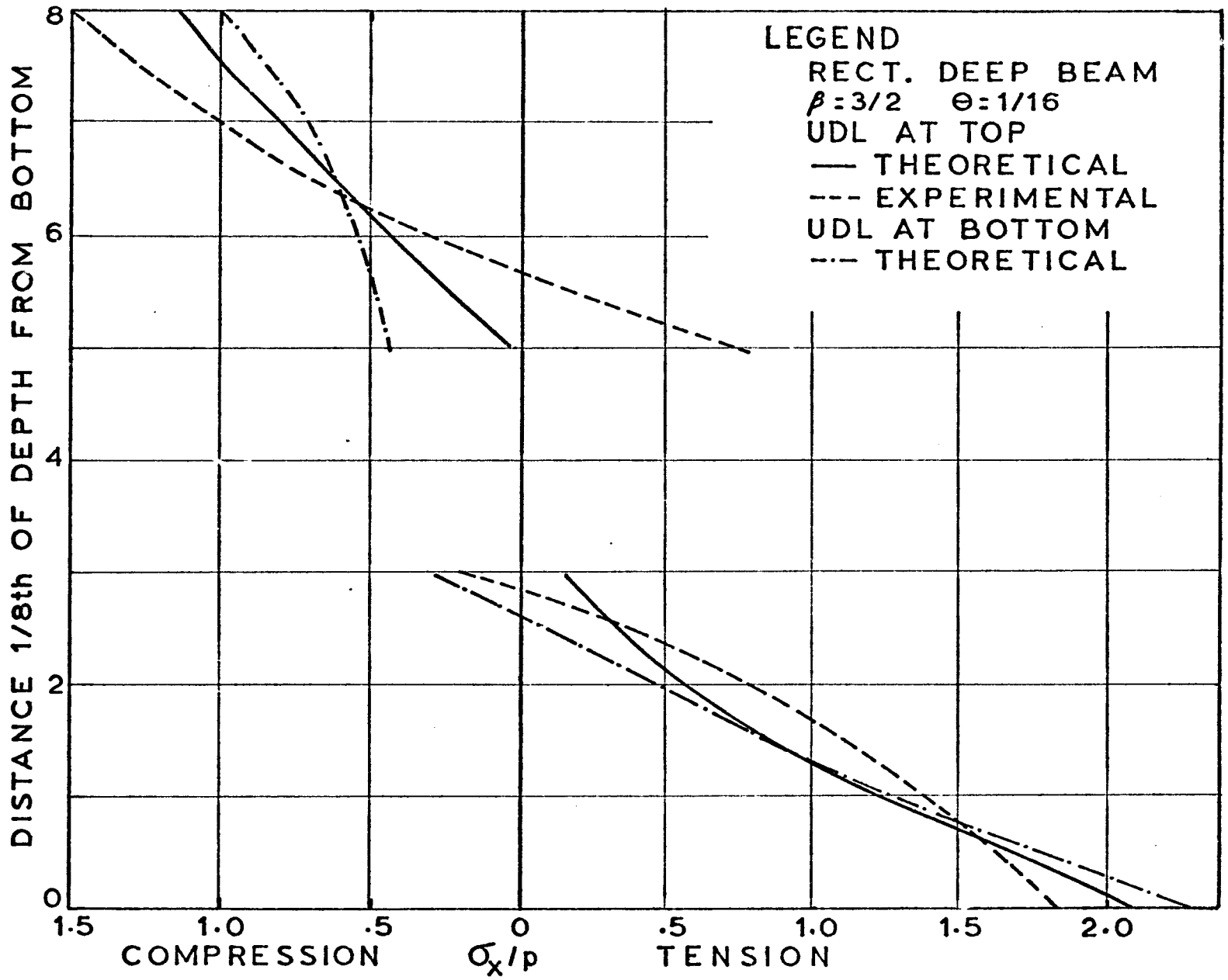

Fig.15 Longitudinal Stresses at mid-section of a Rect. Deep Beam with an Opening

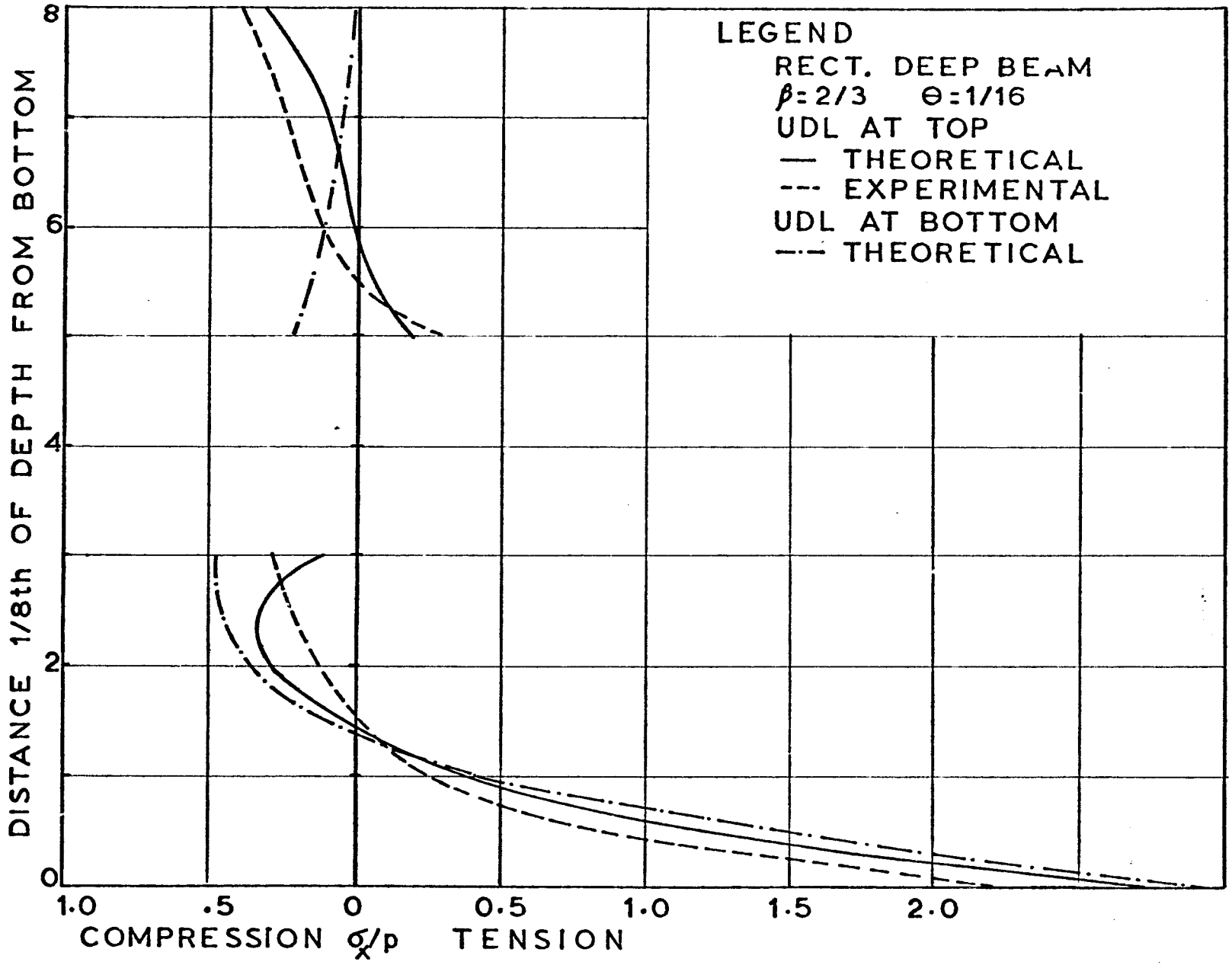

Fig.16 Longitudinal Stresses at mid-section of a Rect. Deep Beam with an Opening

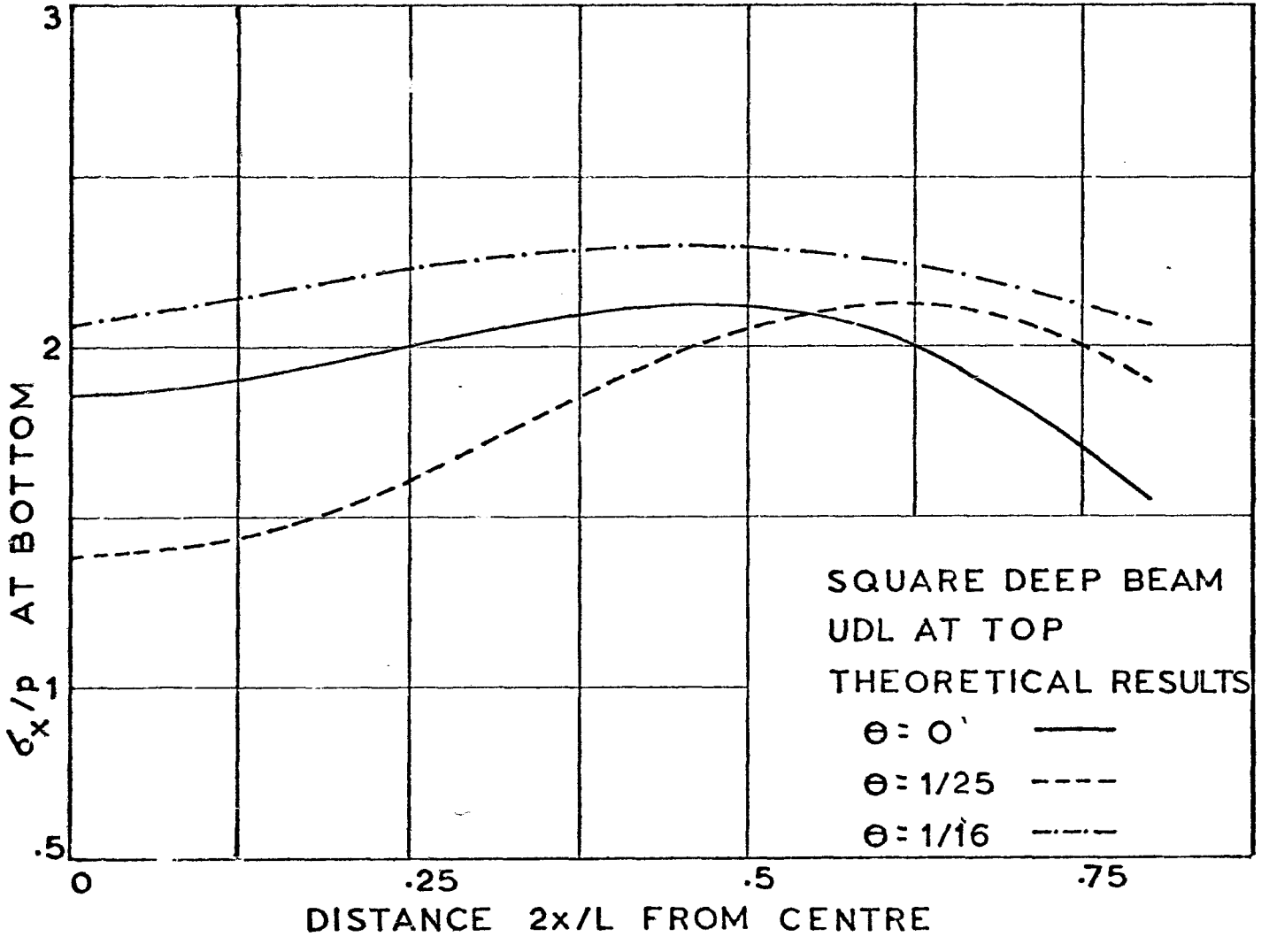

Fig.17 Variation of Bottom Tensile Stress of a Square Deep Beam along the Span

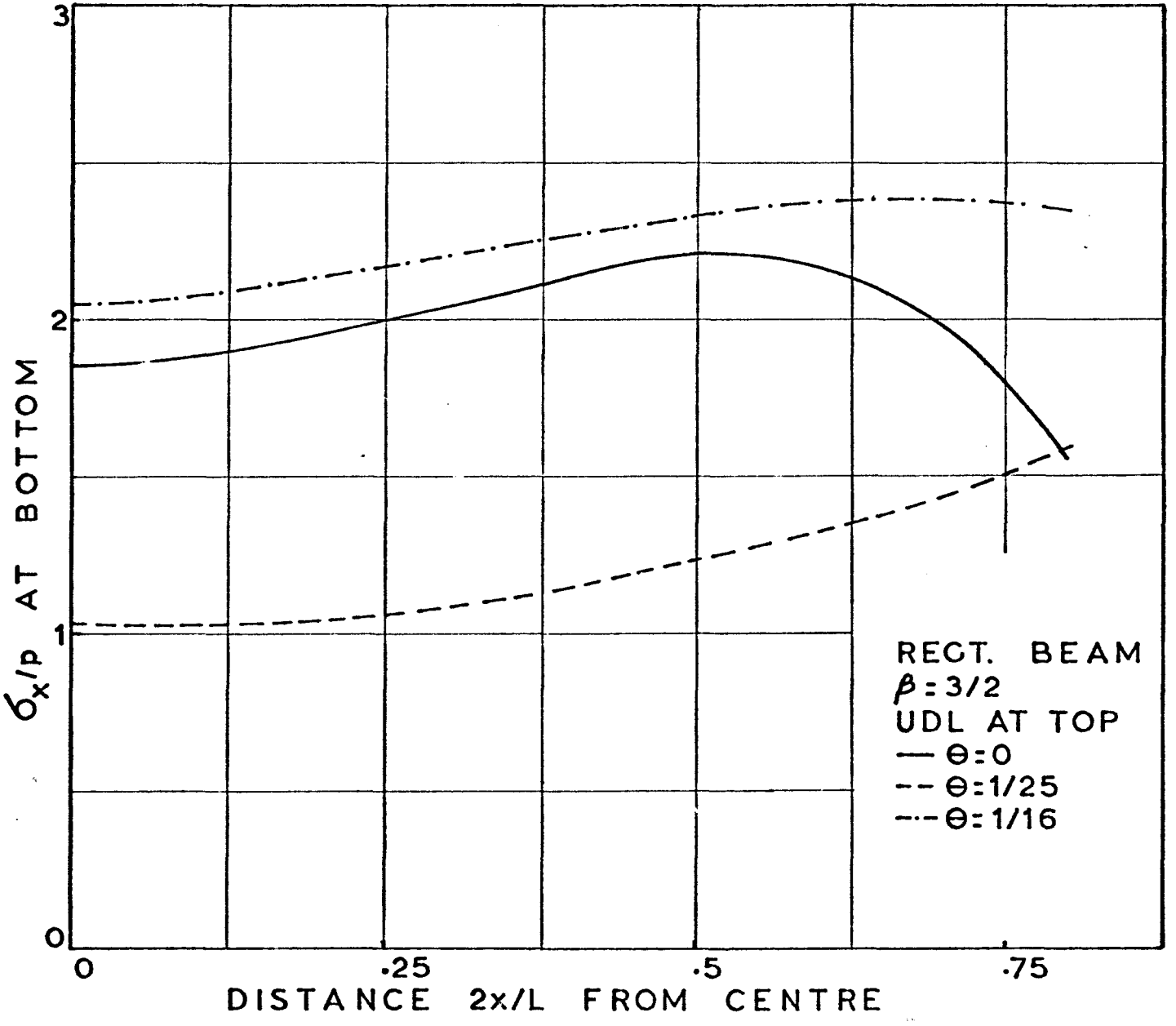

Fig.18 Variation of the Bottom Tensile Stress along the Span of a Rect. Deep Beam.

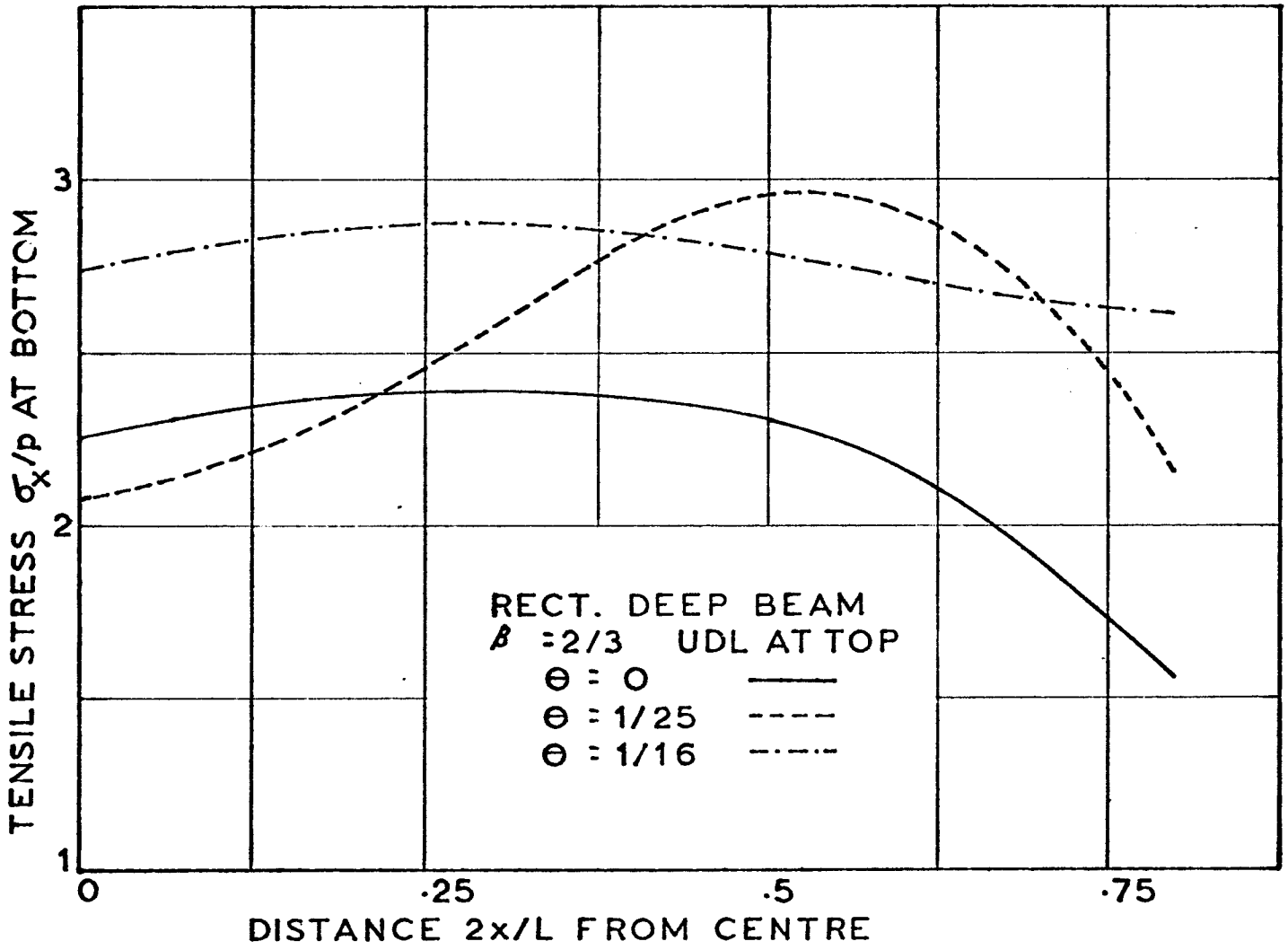

Fig.19 Variation of Bottom Tensile Stress of a Rect. Deep Beam along the Span

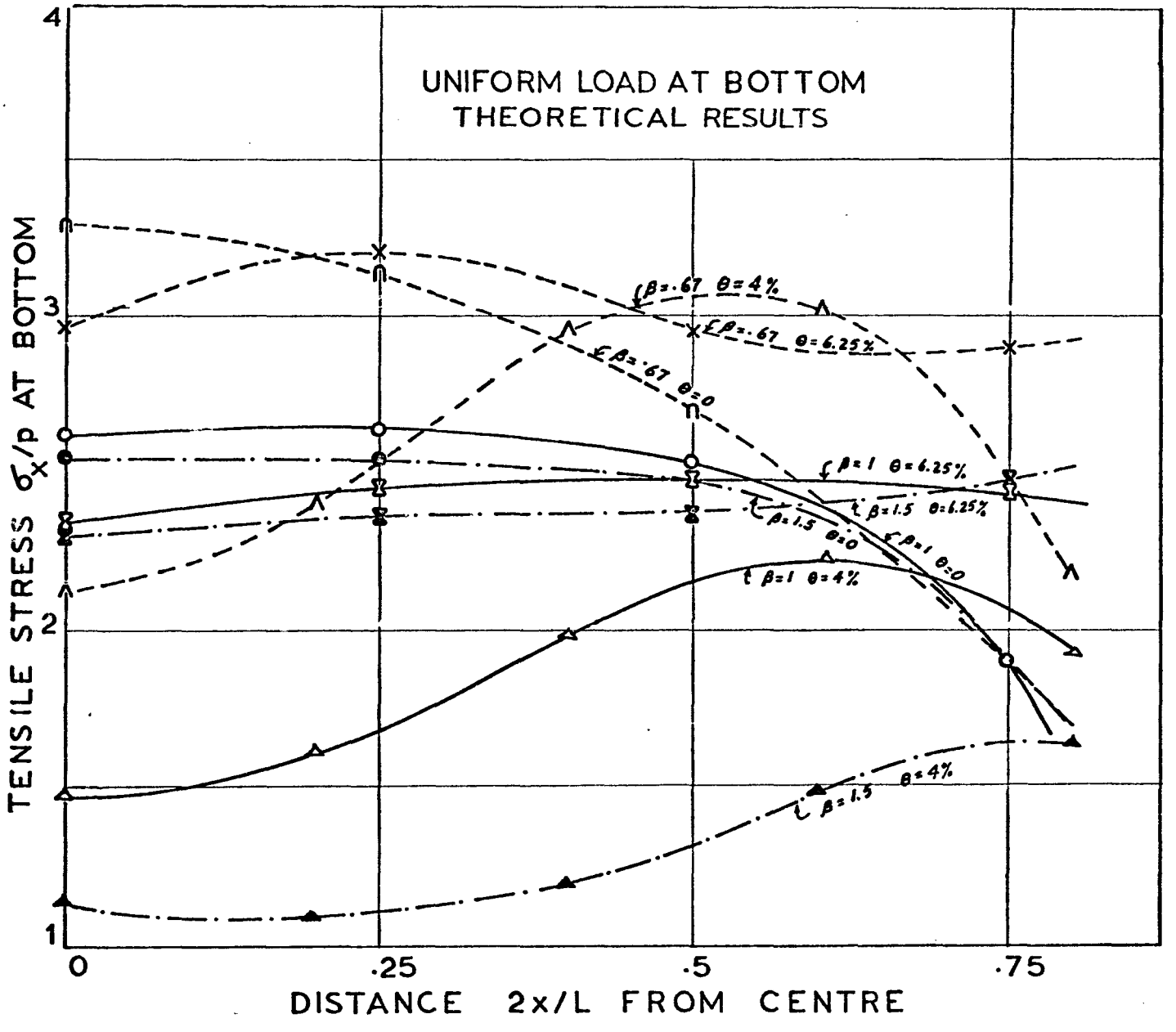

Fig.20 Variation of the Tensile Stress of a Deep Beam under UDL at Bottom

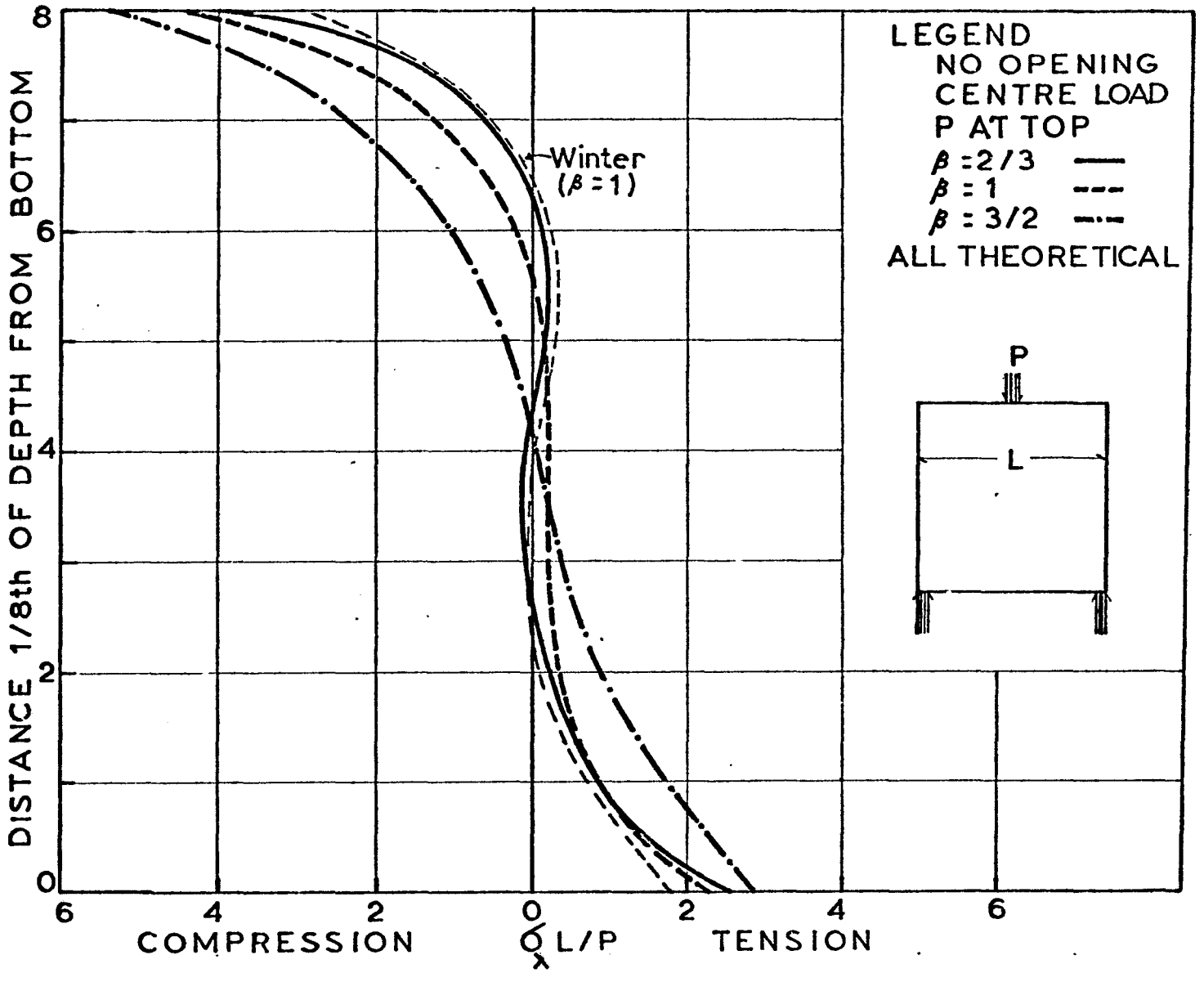

Fig.21 Longitudinal Stresses at mid-section of a Solid Deep Beam for a Pointed Load at Centre

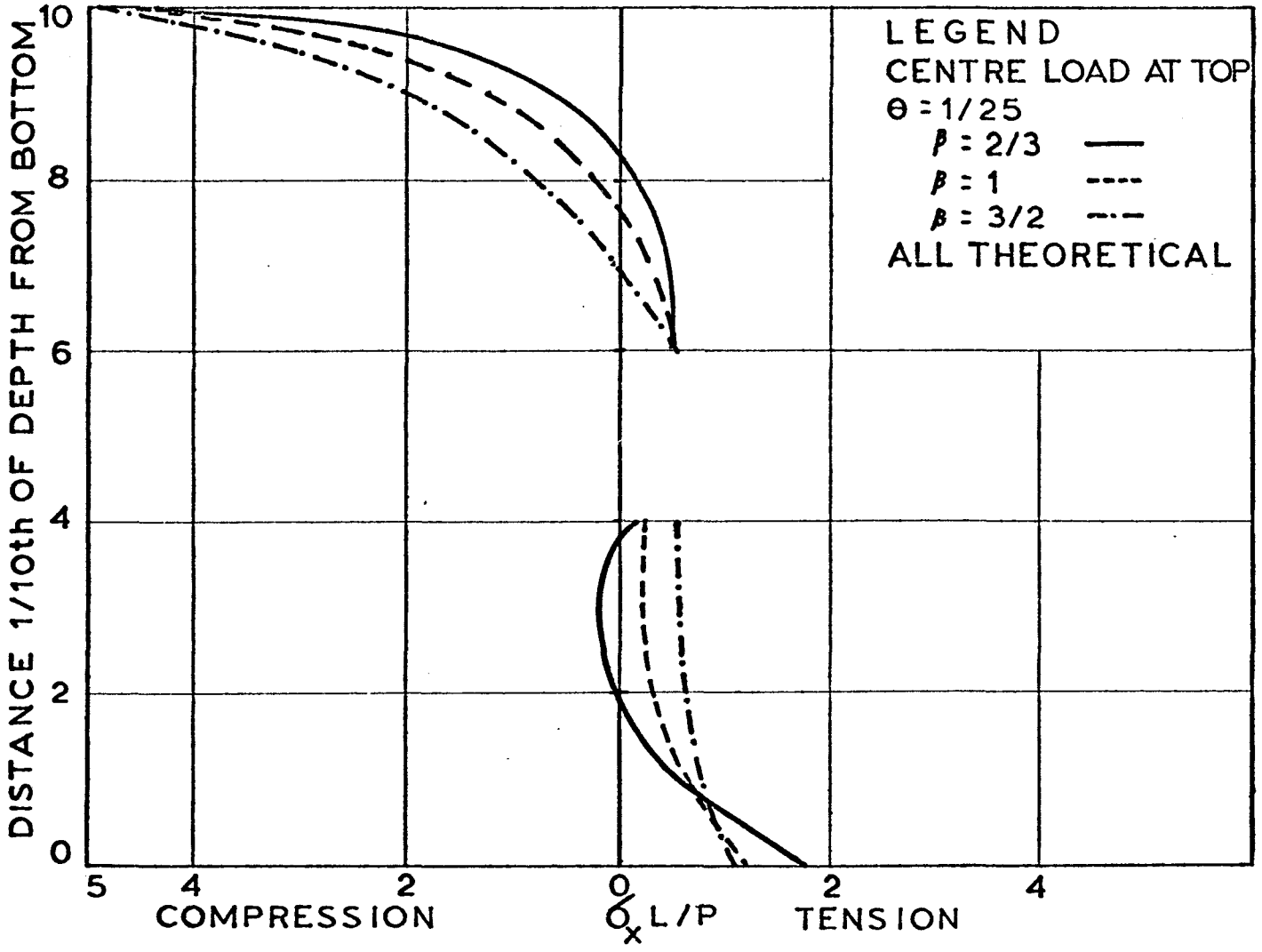

Fig.22 Longitudinal Stresses at mid-section of a Beam with a Small Opening for Load at centre

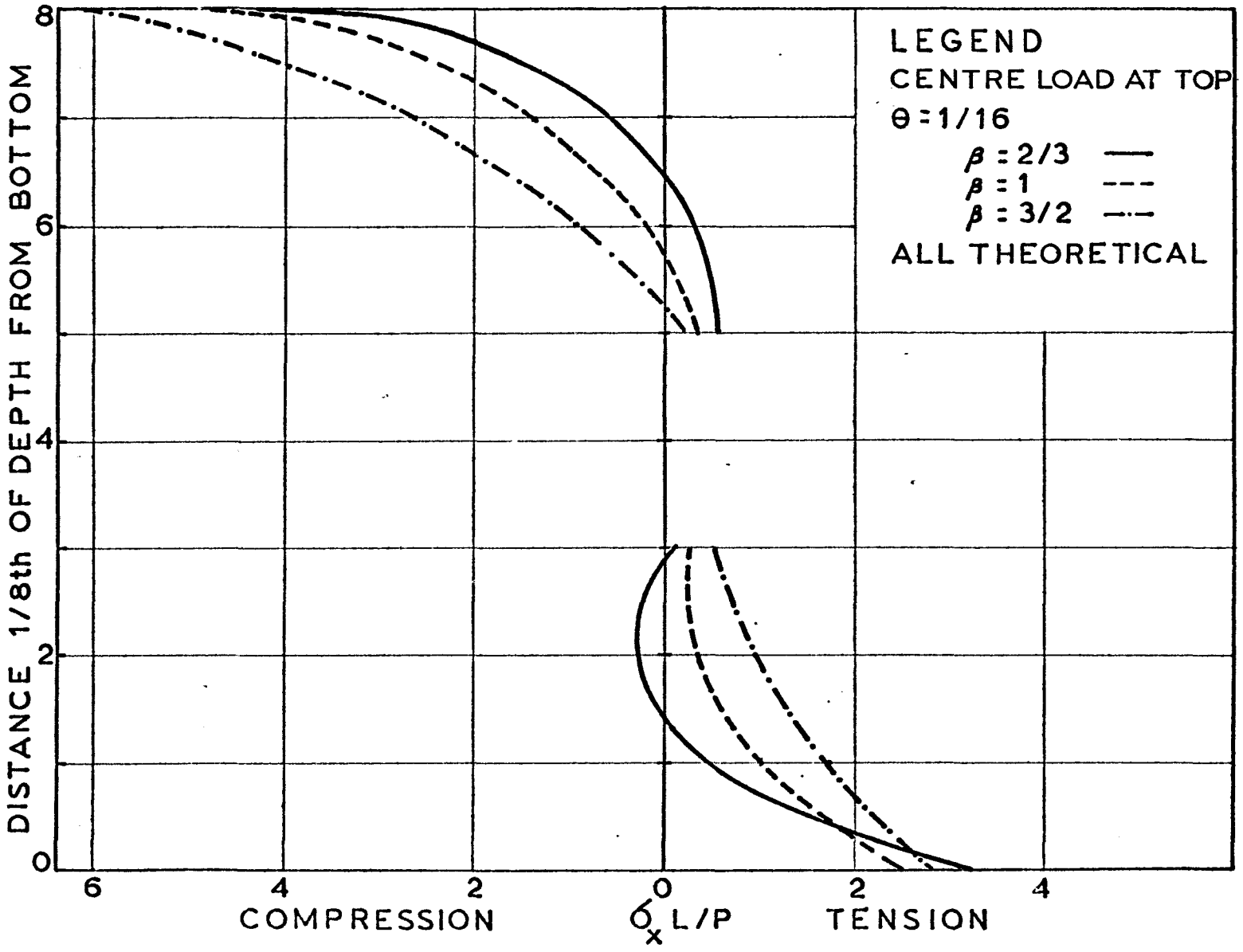

Fig.23 Longitudinal Stresses at mid-section for a Pointed Load at Centre.

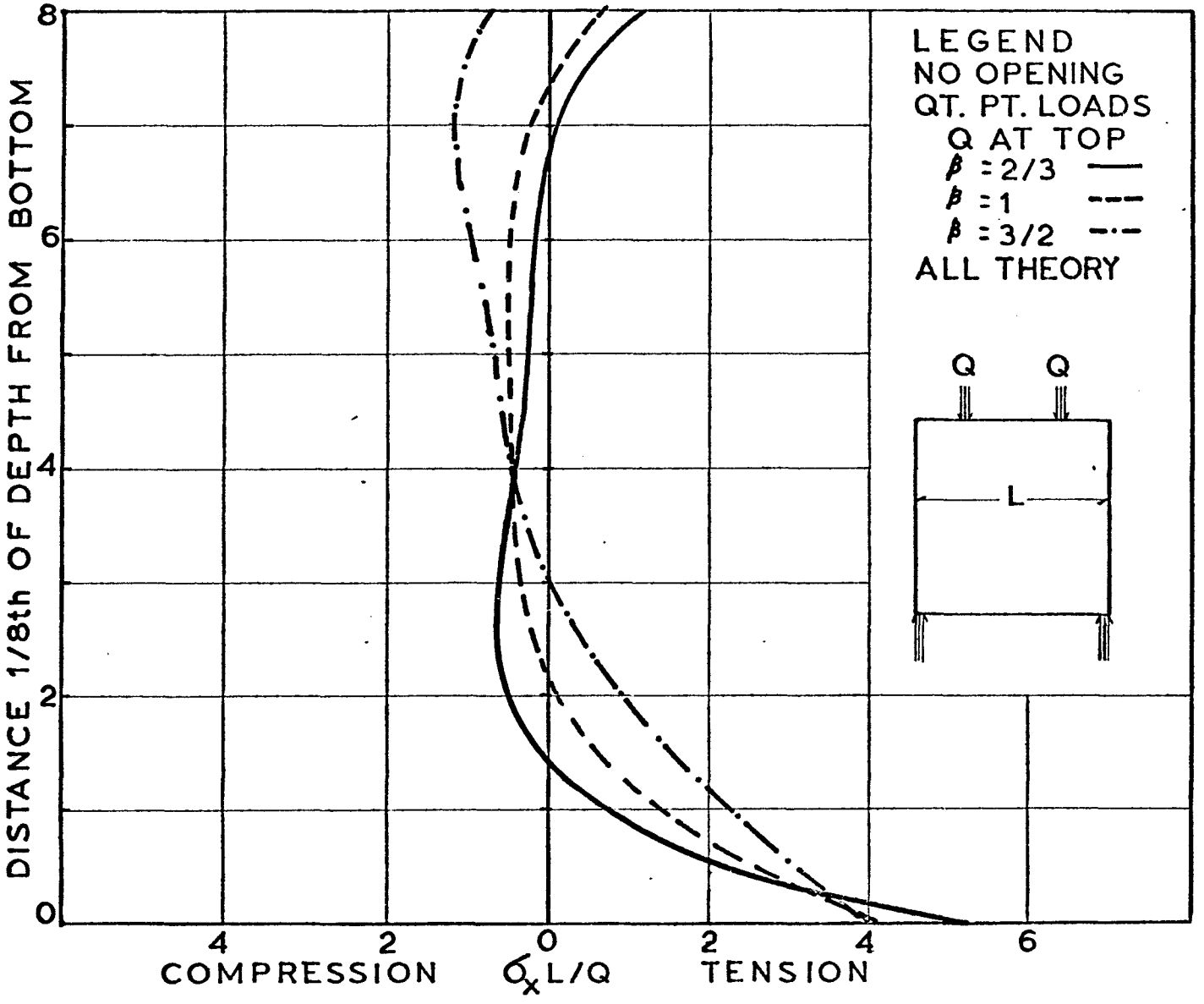

Fig.24 Longitudinal Stresses at mid-section of a Beam under Quarter Point Loads

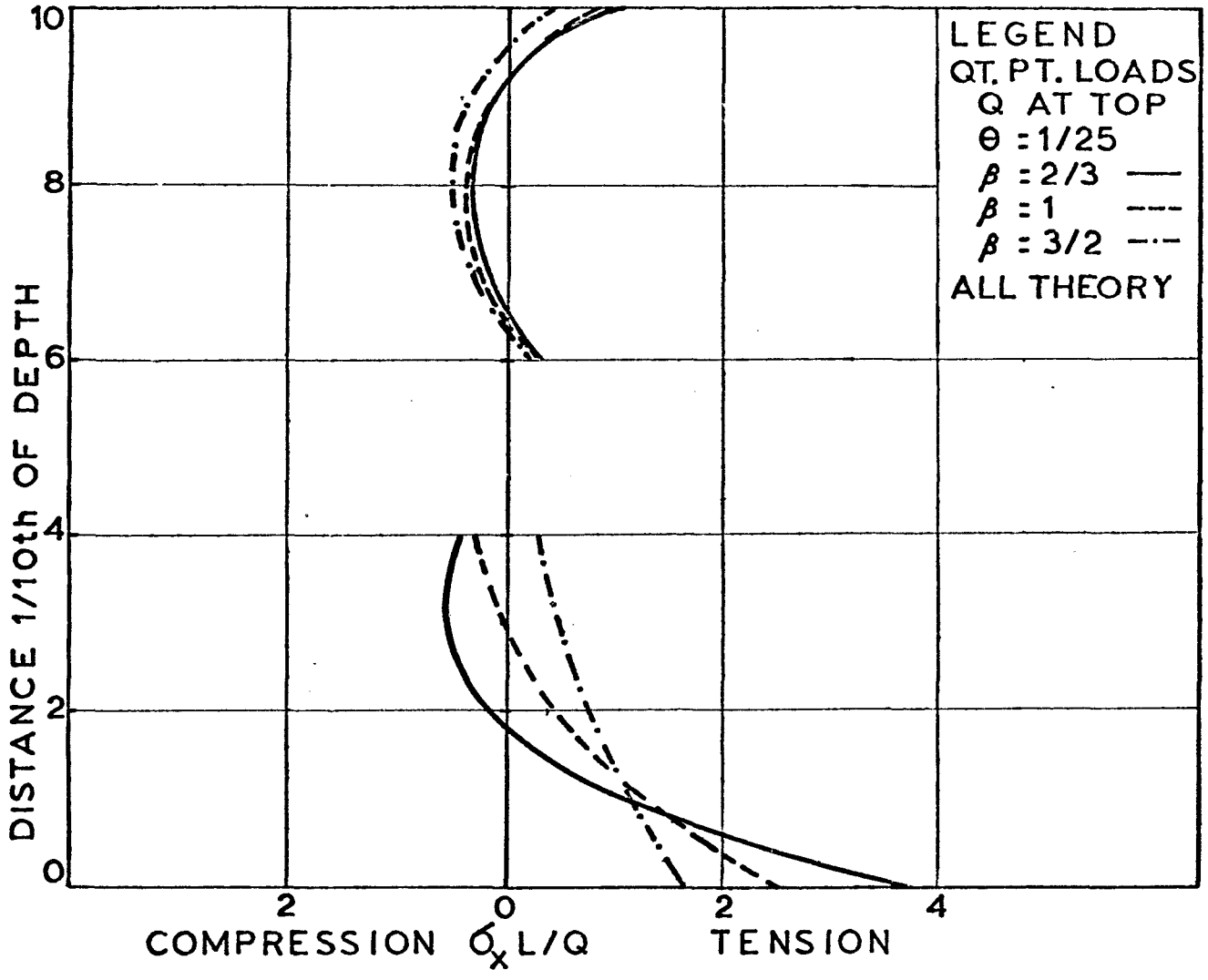

Fig.25 Longitudinal Stresses at mid-section of a Beam with an Opening

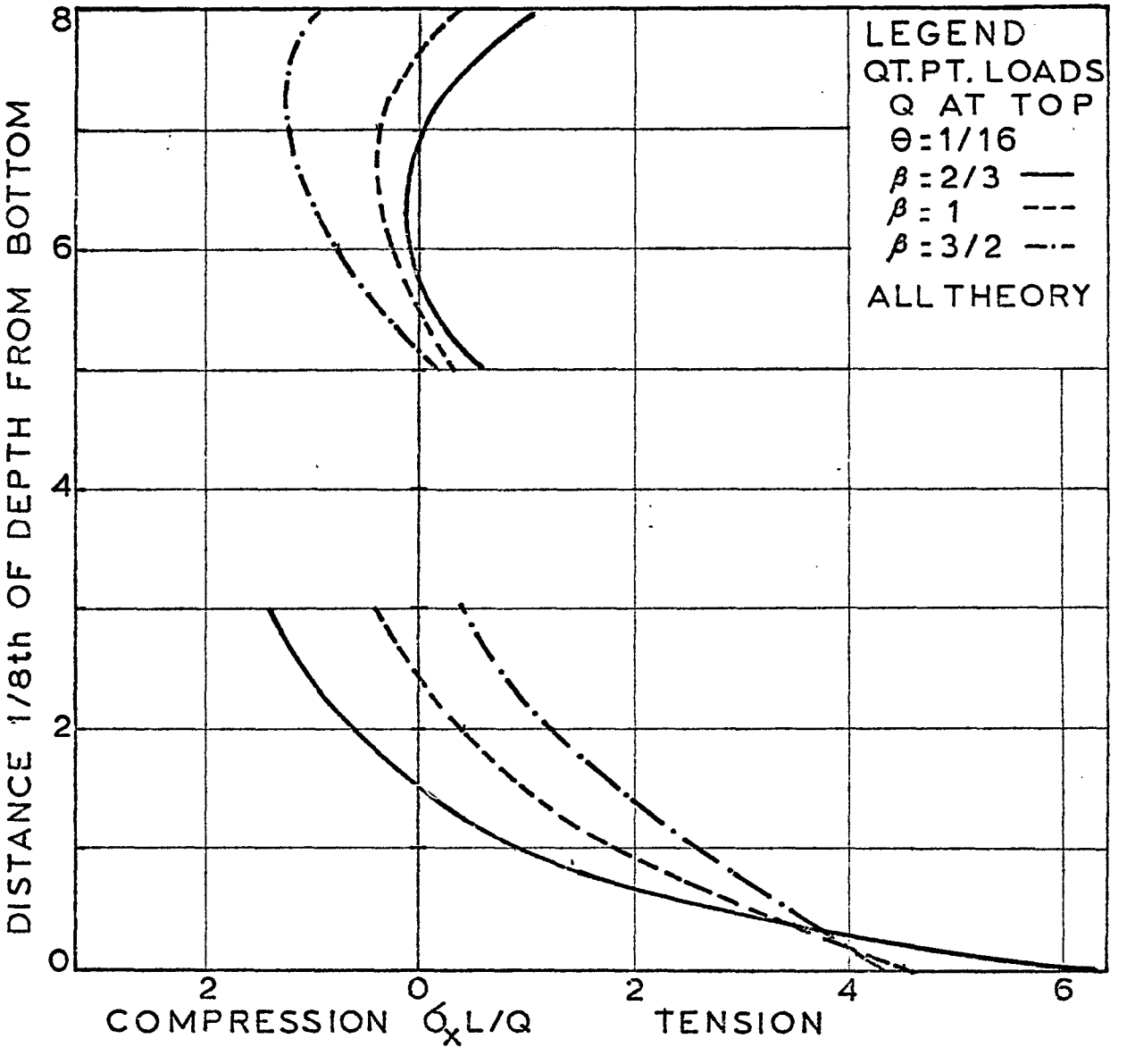

Fig.26 Longitudinal Stresses at mid-section for Qt. Point Loads

INFLUENCE OF OPENING ON STRESSES IN DEEP BEAMS WITH PLAIN AND STIFFENED EDGES

A Dissertation
Submitted to the Faculty of Graduate Studies.Through the
Department of Civil Engineering in Partial Fulfillment
of the Requirements for the Degree of
Doctor of Philosophy at the
University of Windsor

by

Muhammad Harunur Rashid
B.Sc. Engg., University of Dacca, 1956
M.S., University of Illinois, 1961
M.A.Sc., University of Toronto, 1967

Windsor, Ontario, Canada
1969

NSX 6708

APPROVED BY:

J. Kennedy

G. Abdel-Sayed

Thompson

A. L. Smith

275364

PREFACE

The utilization of computer techniques to solve large numbers of simultaneous equations has removed the long-standing restrictions applied to solutions in closed form of civil engineering problems primarily designed for hand calculations. More versatile methods can now be developed and utilized, without too many assumptions, applicable to wider range of problems, hitherto avoided because of the number of equations; one such approach, simple in concept but versatile in its applications, the displacement method, is demonstrated in this dissertation towards the solution of doubly connected deep beams.

The author is greatly indebted to Dr. J. B. Kennedy for his untiring advice, suggestions, encouragements and discussions. The author feels extremely fortunate to have studied under his guidance. The efforts of other members of the dissertation committee, specially Dr. G. Abdel-Sayed for his valuable suggestions are gratefully acknowledged.

The financial assistance of the Canadian Agency for International Development greatly made this study possible. Thanks are also due to the workshop staff, specially Mr. M. Aminzadeh for his assistance in setting up the equipment.

This dissertation represents the culmination of a great deal of effort and utmost dedication not only on the part of the author but also his entire family. Words cannot express enough gratitude

for the enormous sacrifice of the two children, Imran and Suzan and wife, Milly who has constantly provided technical, secretarial and inspirational assistance for the last several years.

ABSTRACT

This dissertation deals with the problem of doubly connected deep beams with or without stiffening around the outer edges. Without going through the application of customary Airy stress function for plane stress problems and the necessary corrections for the doubly-connected domain, the displacement method hitherto avoided for the increased number of simultaneous equations, was successfully applied. The versatile method of finite difference approximations, in transforming the partial differential equations in terms of displacements at discrete points into linear simultaneous equations containing the unknown variables, was used. A solid deep beam without any opening was studied to compare the results with those of the previous investigators, so as to prove the reliability and the utility of the method over the conventional Airy stress function applied to deep beam problems. A set of seven experiments were conducted on deep beams with unstiffened edges and with three different sizes of opening at the centre. The experimental results agree well with the theoretical ones.

Addition of stiffening around the outer edges creates a state of singularity along the interfaces. This is due to the abrupt change of cross-section. In order to avoid this, the problem was separated into two parts, the plate itself and the stiffening frame with equal and opposite forces as well as equal displacements and curvatures assumed to be acting. Instead of dividing the frame into a finite-difference mesh, the redurdant forces in the statically indeterminate frame were

determined through Castigliano's first theorem applied to linear frame analysis. The curvatures of the frame-members in terms of moments and the curvatures of the plate at a discrete point in terms of the displacements were equated to yield sufficient number of extranodal equations covering the unknown forces, assumed to be in the form of trigonometric series along the interfaces. Here again, a set of eight experiments on aluminum models were conducted. The agreement between theoretical and experimental results were not as good as that for the unstiffened cases. This is mainly due to the additional disturbing conditions that arise from the presence of interfaces. Also the linear frame analysis (in the absence of a suitable non-linear method) incorporates a limitation of the general use of the method, since it is not applicable to very slender stiffening frame. Here the axial strain will gain prominence over the bending moment, which in turn will question the validity of the linear frame analysis.

It was shown by the graphical results that the pursued method of displacement can be reliably applied to deep beams with openings with or without stiffened outer edges. With a finer meshwork better results can be obtained without the need of any further experimental verifications keeping in mind the fact that, unlike oti numerical methods, too many assumptions are not necessary in this direct approach where only a minor modification in the differential equation itself is in effect. Although the computations far exceed the amount of other widely applied methods, the versatility of the present approach in its application to simply as well as doubly-connected plane stress problems, is sure to offset those arising from

the facilities offered by the computer techniques to handle precisely a large number of linear simultaneous equations.

TABLE OF CONTENTS

LIST OF FIGURES

Fig. 34 Longitudinal Stresses at Midsection of a Stiffened Rect. Deep Beam with a Small Opening.

Fig. 35 Longitudinal Stresses at Midsection of a Stiffened Rect. Deep Beam with a Small Opening.

LIST OF TABLES

CHAPTER I

INTRODUCTION

Beams whose depths are comparable to their spans are used in a variety of structures; the constructions of bins or hoppers, as well as in foundation walls or in cases in which walls are supported on individual columns or footings. The horizontal and vertical diaphra used to transmit wind forces in floors or walls of buildings are frequently of such dimensions as to represent deep beams. In reinforced concrete hipped plate construction, the plates of the structure proper or the vertical supporting diaphra often fall into this category. In bridge construction, the reinforced concrete pier or abutment wall as well as the vertical cross beams may also be called deep beams. Deep beams are also encountered in the construction of quay walls and retaining walls.

It is frequently necessary to provide openings in deep beams for utility or other purposes, whereas in case of bridge piers, these openings not only incur a substantial saving in material but also induce anaesthetic beauty in the structure itself.

The conventional design procedure for flexural members is based on Navier's hypothesis prescribing a linear stress distribution in any section of the member. This assumption closely represents the conditions that exist as long as the behaviour of the material is essentially elastic and the depth of the member is relatively small in comparison to its span. This assumption however, is not valid when the depth tc span ratio exceeds eight tenths for simply supported span

and four tenths for continuous girders. This limitation is based on Bay's findings and will be discussed in chapter II. (See page 6)

When the depth's dimension of a flexural member approaches that of its span, design based on the ordinary beam theory will be seriously in error. This is because of the fact that Navier's hypothesis does not consider the effect of the normal pressures on the top and bottom edges caused by loads and reactions. Furthermore, it does not take into account the deformation due to shear or the effect of Poisson's ratio on the stress in the depthwise and the widthwise directions. The effect of the normal pressures on the stress distribution of deep beam is such that the variation of bending stress along any vertical section is not linear and the distribution of shear is not parabolic. Consequently a transverse section which was plane before bending does not remain plane after bending. The neutral axis does not lie at the mid-depth, with maximum deviation from the mid-depth in the vicinity of the support, its position being shifted in a spanwise direction.

By introducing an opening, the whole system of stress distribution in a deep beam is further disturbed. Position as well as the magnitude of the maximum critical stresses are also changed, leaving aside with the existence of stress concentration around the periphery of the opening. Presently available results are not adequate for the design of such cases. On the other hand, the most widely used solutions of ordinary deep beams through Airy stress function cannot be directly applied to a deep beam with an opening, since in this case additional conditions are necessary to establish a relationship

between the assumed values of the stress function on the outer and the inner boundaries of the Deep Beam. This renders the doubly connected deep beam problem as a very much complex one.

In the work, presented herein, the direct method of displacements was applied to find the maximum stresses in solid deep beam, and to check the results with previous works. This method was further extended to obtain the maximum bending stresses in beams with openings. Deep beams with unstiffened and stiffened edges were examined. Thus an attempt is made to form a clear picture of the influence of openings on ordinary deep beams with unstiffened and stiffened edges.

CHAPTER II

LITERATURE SURVEY

In 1932, Franz Dischinger[1] contributed to the basic deep beam theory in the Zurich Symposium of the International Bridge and Structural Engineering Association. He assumed the boundary loading in a trigonometric series acting over a continuous beam of infinite length. An Airy stress function related to a plane stress problem was assumed in the form

$$\varphi = -\sum_{1}^{\infty} \frac{Bn}{\alpha^2} (1 + \alpha y) e^{-\alpha y} \cos \alpha x + \frac{Bo}{2} \cdot \frac{x^2}{2} \quad \ldots\ldots\ldots\ldots\ldots (2.1)$$

Accordingly, the stresses were represented by

$$\sigma_x = \sum_{1}^{\infty} B_n (1-\alpha y) e^{-\alpha y} \cos \alpha x \quad \ldots\ldots\ldots\ldots\ldots\ldots\ldots (2.2)$$

$$\sigma_y = \sum_{1}^{\infty} B_n (1 + \alpha y)\, e^{-\alpha y} \cos \alpha x + \frac{Bo}{2} \quad \ldots\ldots\ldots\ldots\ldots\ldots (2.3)$$

$$\tau_{xy} = \alpha y \sum_{1}^{\infty} B_n e^{-\alpha y} \operatorname{Sin} \alpha x \quad \ldots\ldots\ldots\ldots\ldots\ldots\ldots (2.4)$$

The constants were evaluated from the boundary conditions which state that at $y = 0$,

$$\sigma_y = \frac{Bo}{2} + \sum_{1}^{\infty} Bn \cos \alpha x = p_{xu} \quad \ldots\ldots\ldots\ldots\ldots\ldots\ldots (2.5)$$

$$\tau_{xy} = 0 \quad \ldots\ldots\ldots\ldots\ldots\ldots\ldots\ldots\ldots\ldots\ldots\ldots \quad (2.6)$$

and at $y = \infty$,

$$\sigma_y = \frac{Bo}{2} \quad \ldots\ldots\ldots\ldots\ldots\ldots\ldots\ldots\ldots\ldots\ldots \quad (2.7)$$

$$\tau_{xy} = 0 \quad \ldots\ldots\ldots\ldots\ldots\ldots\ldots\ldots\ldots\ldots\ldots\ldots \quad (2.8)$$

With the help of many worked-out examples Dischinger calculated, for several cases of loading, the bending stresses for various ratios of beam height to span; he also showed how the stresses in deep beams approached those of the slender beams. Dischinger also observed that the magnitude of the lever arm between the internal forces was more critical than the actual stress diagrams. The practical value of his work lay in determining these lever arms for several practical cases of loading. The lever arm of internal forces in a deep beam was no longer proportional to the height of the beam but to the span. It was further observed that there was a considerable difference between freely supported and continuous girders. In the former, the lever arm at which the internal forces acted was twice as great as in the case of continuous girders.

Based on these observations due to Dischinger, Portland Cement Association[2] later prepared an extended version of his paper and added solutions for simply supported spans in the form of many curves and figures. As the first comprehensive design guide in the English language on deep beams, this included Navier's hypothesis

with respect to depth to span ratios based on Dischinger's lever arm theory. Fig. 1a shows a continuous girder of Dischinger's type but for a specific case in which the length of support equals one-half of the theoretical span measured between centre-line of support. Since the length of support equals the clear span, the condition is that of a beam which is loaded alternately upward and downward with equal loads but which has no other supports. It is apparent that moment is zero at alternate points. There is no assurance that the moment is zero at everywhere in these sections, but the fact that the total moment is zero indicates that portions of the beam with length of L/2 between points of inflection may be in the same stress condition as in the simply supported beam. Accordingly it is assumed that the stress curves for moment are alike at mid-span of the two beams in Fig. 1c. Accordingly the ratio of H/L is twice as great for the single-span beam as for the continuous beam. Thus the Portland Cement Association used the curves for continuous beams for single-span beams when ratio of H/L for latter was computed to be H/2L.

In a different way almost at the same time, Bay[3] analyzed the case of continuous deep beams with supports of equal span, the spans being equal to or less than height of the beam. He used Filon's[4] solution together with methods of superposition and concluded that beams of infinite length with height greater than span of supports had similar stress distribution to beams with height equal to span. Thus he confirmed Dischinger's analysis.

In case of simply supported deep beams, although Fourier Series can be applied to represent any form of periodic loading, the boundary conditions at the two vertical edges can not be easily satisfied by this means. Since additional terms will have to be added changing the whole expression for the stress function to multiple Fourier series; this procedure will involve considerable labour. Iyengar's[5] attempt in this direction is worth mentioning.

Chow, Conway and Morgan[4] proposed a second stress function to eliminate, by means of superposition, the residual normal stresses at the vertical edges resulting from the first stress function. They used a second stress function in the form of polynomials with adjustable parameters. These were determined by applying the principle of least-work to the strain energy integral - a method developed by Timoshenko and used by Goodier in solving various problems. This method involved some approximations due to using only a finite number of terms in the infinite series for the second stress function.

Chow, Conway and Winter[6] analyzed simply supported deep beams as problems of plane stress by solving the differential equations by means of finite difference approximations. They used five different types of loading and three different span to depth ratios, but made no experimental verifications. In a subsequent discussion,[7] it was found out that a considerable amount of error existed because of the coarseness of the net and the inherent rounding off of peak values.

Elihu Geer[8] in his doctoral thesis, attempted to overcome these errors by using five point finite difference equations instead of customery three points for second derivatives. He also used a finer

mesh.

Archer and Kitchen[9,10] presented the solutions for a beam of rectangular cross-section, in which the thickness is small compared with the depth which is comparable to span, for symmetric loading. They employed the Rayleigh-Ritz method by expressing the stress function in two parts, the first one accounted for the elementary beam theory for straight line distribution of bending stress and parabolic distribution of shear stress. The second part was expressed in terms of polynomials. The minimization of the total strain energy led to equations for the determination of the parameters assumed. They also verified their results by experiments using 12 in. x 12 in. x 1/2 in. steel models supported at each end and loaded at the opposite edge. The strains at six points on the lower edge of each plate were measured using strain gages.

Guzman and Luisoni[11] applied Galerkin's variational method to the same problem and the results were tabulated in equation forms.

Saad and Hendry[12, 13] recently published papers on gravitational stresses in deep beams. Their results were based on a series of experiments using frozen stress method of photoelasticity. Gravitational loading was simulated in a large centrifuge. The stresses so obtained were in a form suitable for use in design and checked well with theoretical results obtained by means of an Airy stress function converted into finite difference pattern.

Durant and Garwood[14] presented a solution of deep beam including gravitational stresses by choosing a particular solution

for the bi-harmonic equation and then finding a polynomial which cancelled out the stresses on the vertical boundary implicit in the particular solution selected. This solution has the advantage of giving the results in a closed form; it has been noted [11] that the results are not very rapidly convergent nor are they very accurate.

Fox[15] discussed the application of relaxation method in plane stress problems with governing equations in terms of displacements. He observed that in bi-harmonic problems of mixed boundary conditions where photo-elastic methods were difficult to apply, this method might be valuable.

Recently, Coul[16] suggested a method of handling deep beam problems in which he transformed the two-dimensional plane stress problem into unidirectional by expressing the stresses in the form of Fourier series in one direction, the coefficients of the series being functions of the other co-ordinate only. After satisfying the equilibrium and boundary conditions, the coefficients were determined by minimization of the strain energy. For general loading case of an ordinary deep beam with unsymmetrical boundary stresses, the method had to incorporate two different co-ordinate axes - one for symmetrical case and the other for the antysymmetrical case thereby yielding additive results. The same method has been successfully applied in plate problems before.[17]

As early as in 1898, Kirsch[18] presented an approximate solution for the stress distribution around a circular hole in a plate subjected to uniform tension in one direction. In 1930, Tuzi[19] presented solutions for stress distribution in a beam, containing a

small circular hole on the neutral axis, subjected to pure bending. This load of pure bending was also applied by Sen[20] and Wolf[21] to find the effect of small elliptical holes and cracks on maximum bending stresses. Their works were essentially the extension of Tuzi's analytical solution.

Gupta[22] attempted a solution for a simple rectangular plate plane stress elastic cantilever problem, with the end shear load having a parabolic distribution. The effect was found by G. B. Jeffery's[23] original bi-polar solution, treating the rectangle as a semi-infinite in one direction (opening near the middle of the supporting infinite edge). Some values of stress at hole were given.

The other attempts worth mentioning are credited to Bickley[24] Hütter[26], Hengst[25], and Savin[27]. However, none of these treated the deep beam with opening.

CHAPTER III

THEORETICAL SOLUTIONS

(i) Governing Equations

If $u(x, y)$ and $v(x, y)$ are the displacement components in the x and y directions respectively, of any point (x, y) then the problem of in a plane state of stress can be defined by two displacement equations. In the absence of body forces, these equations are

$$2\frac{\partial^2 u}{\partial x^2} + (1 - \upsilon)\frac{\partial^2 u}{\partial y^2} + (1 + \upsilon)\frac{\partial^2 v}{\partial x \partial y} = 0$$

$$2\frac{\partial^2 v}{\partial y^2} + (1 - \upsilon)\frac{\partial^2 v}{\partial x^2} + (1 + \upsilon)\frac{\partial^2 u}{\partial x \partial y} = 0 \qquad (3.1)$$

These two equations, together with the appropriate boundary conditions, are sufficient to yield the solutions for displacements u and v, provided all the conditions pertaining to the state of plane stress are valid. The stresses, thereoff, at any point can be found by

$$\sigma_x = \frac{E}{1 - \upsilon^2}\left(\frac{\partial u}{\partial x} + \upsilon \frac{\partial v}{\partial y}\right)$$

$$\sigma_y = \frac{E}{1 - \upsilon^2}\left(\frac{\partial v}{\partial y} + \upsilon \frac{\partial u}{\partial x}\right) \qquad (3.2)$$

$$\tau_{xy} = \frac{E}{2(1 + \upsilon)}\left(\frac{\partial v}{\partial x} + \frac{\partial u}{\partial y}\right)$$

All other stresses are zero.

On the boundary, either displacements or forces can be specified. The case of a force-free boundary is one in which there are no externally applied forces and the displacements are unknown.

In the case when boundary forces exist, equilibrium of an element of the surface demands that

$$T_x = \sigma_x \cos(n, x) + \tau_{xy} \cos(n, y)$$

$$T_y = \tau_{xy} \cos(n,x) + \sigma_y \cos(n,y) \qquad (3.2)$$

where T_x and T_y are the components of the stress vector applied to the boundary; (n, x) and (n, y) are the angles between the normal n at the surface and the coordinate x and y axis respectively.

Substituting Eqs. (3.2) in Eqs. (3.3), the required boundary conditions are obtained as,

$$T_x = \frac{E}{1 - \upsilon^2} \left(\frac{\partial u}{\partial x} + \upsilon \frac{\partial v}{\partial y}\right) \cos(n, x) + \frac{E}{2(1 + \upsilon)} \left(\frac{\partial u}{\partial y} + \frac{\partial v}{\partial x}\right) \cos(n, y)$$

$$T_y = \frac{E}{1 - \upsilon^2} \left(\frac{\partial v}{\partial y} + \upsilon \frac{\partial u}{\partial x}\right) \cos(n,y) + \frac{E}{2(1+\upsilon)} \left(\frac{\partial u}{\partial y} + \frac{\partial v}{\partial x}\right) \cos(n, x) \qquad (3.4)$$

If the boundary is free of applied forces, then $T_x = T_y = 0$ and Eqs. (3.4) become

$$2\left(\frac{\partial u}{\partial x} + \upsilon \frac{\partial u}{\partial y}\right) \cos(n, x) + (1 - \upsilon)\left(\frac{\partial u}{\partial y} + \frac{\partial v}{\partial x}\right) \cos(n, y) = 0$$

$$2\left(\frac{\partial v}{\partial y} + \upsilon \frac{\partial u}{\partial x}\right) \cos(n, y) + (1 - \upsilon)\left(\frac{\partial u}{\partial y} + \frac{\partial v}{\partial x}\right) \cos(n, x) = 0 \qquad (3.5)$$

For any point on the boundary, the angles (n, x), (n, y) can easily be obtained, and for any particular material the Poisson's ratio, υ is also known. Eqs. (3.5), therefore, are of the form

$$b_1 \frac{\partial u}{\partial x} + b_2 \frac{\partial u}{\partial y} + b_3 \frac{\partial v}{\partial x} + b_4 \frac{\partial v}{\partial y} = 0$$

$$c_1 \frac{\partial u}{\partial x} + c_2 \frac{\partial u}{\partial y} + c_3 \frac{\partial v}{\partial x} + c_4 \frac{\partial v}{\partial y} = 0 \qquad (3.6)$$

in which the coefficients b_i, c_i $(i = 1, 2, 3, 4)$ vary from point to point and may all be regarded as known.

(ii) Finite Difference Approximations in Plane Stress Problems

The partial differential equations representing the plane stress problems are seldom amenable to precise analytical solutions for general problems of practical importance such as the present case of deep beams. An approximate, numerical method of wide-spread application is provided by finite-difference techniques. Essentially these replace the linear governing equations and boundary conditions by finite-difference approximations in terms of a finite number of unknown quantities of the dependent

variables at discrete points within or just outside the domain of integration. The finite-difference equations form a set of linear algebric equations containing the unknown values of the dependent variables; the task of obtaining numerical solutions of the simultaneous equations can be achieved through the facilities offered by the digital computer. Thus the finite-difference approximation of attacking a plane stress problem is a direct approach and the approximation lies in changing the original differential equations and boundary conditions into a set of linear algebraic finite-difference equations.

There are quite a number of different approaches of formulating finite-difference equations in a unique way. These will lead to the following equations:[37]

$$\left(\frac{df}{dx}\right)_o \approx \frac{f_1 - f_{-1}}{2h}$$

$$\left(\frac{d^2f}{dx^2}\right)_o \approx \frac{f_1 - 2f_o + f_{-1}}{h^2}$$

and so on. Similarly for any point, say point 8 in Fig. 2,

$$\left(\frac{d^2f}{dxdy}\right) \approx \frac{f_{14} - f_4 + f_{12} - f_2}{4hH}$$

where H, h are all defined in Fig. 2.

The sets of equations are widely used primarily because of the simplicity of the difference operators and the ease by which boundary conditions can be handled.

(iii) Limitations of Finite-Difference Approximations

Finite-difference equations replace the original differential equations and the equations defining boundary conditions. This then reduces the problem to a set of simultaneous algebric equations which can be solved without mathematical difficulty. Thus the approximation is limited to a minor interference which breaks the curve at discrete points and joins them by a straight line. Hence, the finite-difference equations representing the original differential equations are valid as long as the parent equations are valid. Of course, finite-difference equations do not exactly represent the original governing equations; there is a residual. However, for all practical purposes, the error can be minimized by reducing the mesh size.

Finite-difference approximations, as in other approximate methods, is liable to be in great error especially in regions where stresses are subject to very rapid changes such as those near singularities caused by concentrated loads, corners, dislocations or sudden change in geometry. In fact when internal singularities exist, the indiscriminate use of finite-difference approximations may lead to completely erroneous results[32].

It should also be noted that the combined use of the centre and end difference patterns in the solution of any problem should be avoided. Experience has shown that this may lead to serious errors in results.

(iv) Plain Deep Beams

Since, the boundary lines are parallel to x and y coordinate axes, on side OA, (Fig. 2), the boundary conditions are, from Eqs. (3.4),

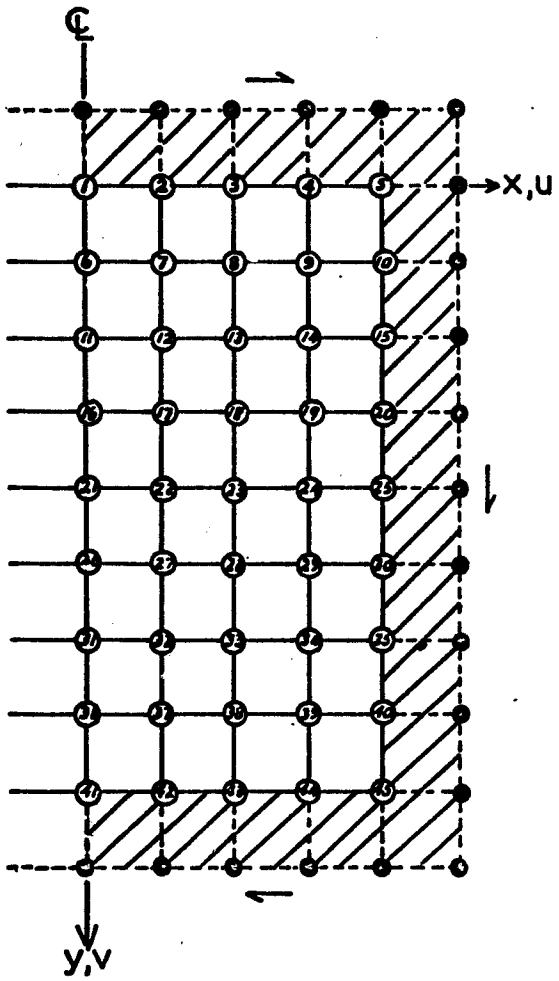

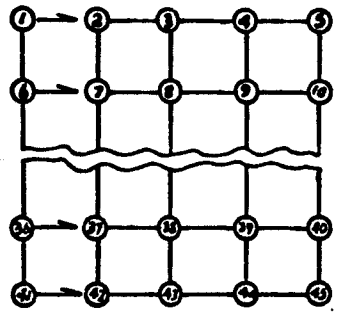

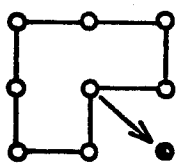

STEP 1

dv/dx & u along centre-line assumed to be zero

STEP 2

Fictitious points in black-dots are evaluated following the band around the boundary

STEP 3

Following the numerical order, the twin equations at each point are formulated. There will be single equation for points along the centre-line

In case of internal boundary, fictitious points around that will be included in STEP 2

$$T_y = \frac{E}{1 - \upsilon^2} \left(\upsilon \frac{\partial u}{\partial x} + \frac{\partial v}{\partial y}\right) = -p \qquad (3.7)$$

$$T_x = \frac{E}{2(1 + \upsilon)} \left(\frac{\partial v}{\partial x} + \frac{\partial u}{\partial y}\right) = 0 \qquad (3.8)$$

where p is the applied pressure in the y direction. For any point, say point 2 in Fig. 2, Eq. (3.7) will be in finite-difference terms,

$$-p\lambda = \upsilon \left(\frac{u_3 - u_1}{2h}\right) + \beta \left(\frac{v_7 - v_7'}{2h}\right)$$

when $\lambda = \frac{1 - \upsilon^2}{E}$ and $\beta = \frac{h}{H}$. Then

$$v_7' = v_7 + \frac{\upsilon}{\beta} (u_3 - u_1) + \frac{2ph\lambda}{\beta}$$

Because of symmetry, the u values are assumed to be zero on the centre-line. Then

$$v_7' = v_7 + \frac{\upsilon}{\beta} u_3 + \frac{2ph\lambda}{\beta} \qquad (3.9)$$

Similarly, for the same point 2, Eq. (3.8) gives

$$0 = \frac{v_3 - v_1}{2h} + \beta \left(\frac{u_7 - u_7'}{2h}\right)$$

Or,

$$u_7' = u_7 + \frac{1}{\beta} (v_3 - v_1) \qquad (3.10)$$

For point 3, from Eq. (3.7),

$$v_8' = v_8 + \frac{\upsilon}{\beta}(u_4 - u_2) + \frac{2ph\lambda}{\beta} \tag{3.11}$$

and from Eq. (3.8),

$$u_8' = u_8 + \frac{1}{\beta}(v_4 - v_2) \tag{3.12}$$

For point 1, because of symmetry along the centre-line,

$$v_6' = v_6 + \frac{2\upsilon}{\beta}\ u_2 + \frac{2ph\lambda}{\beta} \tag{3.13}$$

$$u_6' = u_6 = 0 \tag{3.14}$$

Similarly, at point 4,

$$v_9' = v_9 + \frac{\upsilon}{\beta}(u_5 - u_3) + \frac{2ph\lambda}{\beta} \tag{3.15}$$

$$v_9' = u_9 + \frac{1}{\beta}(v_5 - v_3) \tag{3.16}$$

At the corner point 5, there are six unknown fictitious values of u and v, but only three boundary equations are available. These are

$$\sigma_y = \frac{1}{\lambda}\left(\upsilon\frac{\partial u}{\partial x} + \frac{\partial v}{\partial y}\right) = -\frac{p}{2} \tag{3.17a}$$

$$\tau_{xy} = \frac{E}{2(1+\upsilon)} \left(\frac{\partial v}{\partial x} + \frac{\partial v}{\partial y}\right) = 0 \qquad (3.17b)$$

$$\sigma_x = \frac{1}{\lambda} \left(\frac{\partial u}{\partial x} + \upsilon \frac{\partial v}{\partial y}\right) = 0 \qquad (3.17c)$$

Differentiating Eq. (3.17a) along x, Eq. (3.17c) along y and Eq. (3.17b) along x and y, yields

$$\begin{aligned} \upsilon \frac{\partial^2 u}{\partial x^2} &= \frac{\partial^2 u}{\partial y^2} \\ \upsilon \frac{\partial^2 v}{\partial y^2} &= \frac{\partial^2 v}{\partial x^2} \\ \frac{\partial^2 v}{\partial x \partial y} &= -\frac{\partial^2 v}{\partial x^2} \\ \frac{\partial^2 u}{\partial x \partial y} &= -\frac{\partial^2 u}{\partial y^2} \end{aligned} \qquad (3.18)$$

Substituting Eqs. (3.18) in equilibrium equations, the modified governing equations are obtained for the point 5. These are

$$\frac{\partial^2 u}{\partial x^2} = 0 \qquad (3.19)$$

$$\frac{\partial^2 v}{\partial y^2} = 0 \qquad (3.20)$$

which then provide additional boundary conditions in the form of

$$\frac{\partial^2 u}{\partial y^2} = 0$$

$$\frac{\partial^2 v}{\partial x^2} = 0 \qquad (3.21)$$

that is, the curvatures at point 5 both in x and y directions are zero.

Hence from Eqs. (3.17) and Eqs. (3.21), the fictitious point u_4', v_4', u_{10}' and v_{10}' can be found as follows,

$$v_{10}' = v_{10} + \frac{1}{\beta(1-\upsilon^2)}\, ph\lambda$$

$$u_4' = u_4 + \frac{\upsilon}{1-\upsilon 2}\, ph\lambda \qquad (3.22)$$

$$u_{10}' = 2u_5 - u_{10}$$

$$v_4' = 2v_5 - v_4$$

After obtaining all the fictitious points along the boundary, they can be eliminated from the differential equations. Eqs. (3.1). These will be, with $\xi = \frac{1-\upsilon}{2}$ and $\eta = \frac{1+\upsilon}{2}$, as follows for point 3:

$$\frac{1}{h}2\,(u_4-2u_3+u_2) + \frac{\xi}{H}2(u_8-2u_3+u_8') + \frac{\eta}{4hH}\,(v_9-v_7+v_7'-v_9') = 0 \qquad (3.23a)$$

$$\frac{\xi}{h}2(v_4-2v_3+v_2) + \frac{1}{H}2\,(v_8-2v_3+v_8') + \frac{\eta}{4hH}\,(u_9-u_7-u_7'-u_9') = 0 \qquad (3.23b)$$

From eqs. (3.9) through Eqs. (3.16), the fictitious values of u_7', u_8',

u_9', v_7', v_8', v_9', can be substituted in Eqs. (3.23) which then will be

$$u_2-(2+2\xi\beta^2-.5\upsilon\eta)\,u_3+u_4-.25\upsilon\eta u_5+2\xi\beta^2 u_8-\xi\beta v_2+\xi\beta v_4 = 0$$

$$-\upsilon\beta(u_2-u_4)-.25\eta v_1+\xi v_2-(2\xi+2\beta^2-.5\eta)v_3+\xi v_4-.25\eta v_5+2\beta^2 v_8 = -2\beta ph\lambda \qquad (3.24)$$

Similarly the single equation at point 1 (since u_1 is zero) is

$$2\upsilon\beta u_2-(2\xi+2\beta^2-.5\eta)v_1+2\xi v_2-.5\eta v_3+2\beta^2 v_6 = -2\beta ph\lambda \qquad (3.25)$$

Equations at point 5 from Eqs. (3.20) are

$$2u_4 - 2u_5 = -\frac{\upsilon}{1-\upsilon^2}\,ph\lambda$$

$$-2v_5 + 2v_{10} = -\frac{1}{\beta(1-\upsilon 2)}ph\lambda \qquad (3.26)$$

For any interior point, say point 8, Eqs. (3.1) can be transformed in finite-difference terms,

$$\frac{1}{h^2}(u_7-2u_8+u_9) + \frac{\xi}{H^2}(u_{13}-2u_8+u_3) + \frac{\eta}{4hH}(v_{14}-v_{12}+v_2-v_4) = 0$$

$$\frac{\xi}{h^2}(v_7-2v_8+v_9) + \frac{1}{H^2}(v_{13}-2v_8+v_3) + \frac{\eta}{4hH}(u_{14}-u_{12}+u_2-u_4) = 0$$

Or,

$$\xi\beta^2 u_3+u_7-(2+2\xi\beta^2)u_8+u_9+\xi\beta^2 u_{13}+.25\eta\beta(v_2-v_4-v_{12}+v_{14}) = 0$$

$$.25\eta\beta(u_2-u_4-u_{12}+u_{14}) + \beta^2 v_3 + \xi v_7-(2\xi + 2\beta^2)v_8 + \xi v_9 + \beta^2 v_{13} = 0 \qquad (3.27)$$

Equations for all other points can be derived in the same way. Due to symmetry along the centre-line (OY), u values along OY are taken to be zero. v values on the left-hand side of this line are same as on the right-hand side whereas u values there are taken to be equal and opposite of those on the right-hand side.

In case of an opening, the points on the periphery as well as the corner point are treated in the same way as the top edge AB and point 5 with the applied forces taken to be zero there. Taking the line connecting points 11 and 13 as the top edge of the opening and point 13 as the corner point, the equations at points 11, 12 and 13 will be : at point 11,

$$-2\upsilon\beta.u_{12}+2\beta^2.v_6-(2\xi+2\beta^2-.5\eta)v_{11}+2\xi v_{12}-.5\eta v_{13} = 0 \qquad (3.28)$$

At point 12,

$$2\xi\beta^2 u_7 - (2+2\xi\beta^2-.5\upsilon\eta)u_{12}+u_{13}-.25\eta\beta v_8+\xi\beta(v_{11} - v_{13}) + .25\eta\beta v_{18} = 0$$

$$-.25\eta\beta u_8-\upsilon\beta u_{13} + .25\eta\beta u_{18} + 2\beta^2 v_7+ \xi v_{11}-(2\xi+2\beta^2)v_{12}+\xi v_{13} = 0 \qquad (3.29)$$

At point 13, which is the corner point, the equations are

$$u_{12} - 2u_{13} + u_{14} = 0$$

$$v_8 - 2v_{13} + v_{18} = 0 \qquad (3.30)$$

Equations at all other points, whether lying on the boundary or inside the boundary can be derived in the same way. Having formulated the equations of all the nodal points in finite-difference terms, these linear algebric equations were solved by the IBM 7094. To guard against round-off errors, all computations were carried to 16 significant figures. Results for a set of 16 programs were obtained and presented graphically in Figs. 7 through 30.

(v) Stiffened Deep Beams

In this case, the problem was divided in two parts: the plate itself and the stiffening frame.

1. The plate is assumed to be subjected to six unknown forces acting on its edges. These forces are the normal pressures and shear stresses on each face assumed to be varying in trigonometric series with unknown coefficients. Thus on top face, a normal negative (compressive) pressure of $\Sigma PA_m \cos m\pi x/2a$ in acting where 2a is the length

$m = 1, 3, 5 \ldots$

of the plate. Similarly, there will be also a shear stress of ΣTA_m Sin

$m = 1, 3, 5 \ldots$

$m\pi x/2a$ acting. A positive (tensile) pressure $\Sigma PB_n \cos m\pi x/2a$ and shear

$n = 1, 3, 5 \ldots$

$\Sigma TB_n \sin m\pi x/2a$ are assumed acting on the bottom face. On the vertical

$n = 1, 3, 5 \ldots$

faces normal pressures are $\Sigma PC_k \cos k\pi y/2b + \Sigma PD_\ell \sin \ell\pi y/2b$ and the

$k = 1, 3, 5 \ldots$ $\ell = 1, 3, 5 \ldots$

shear stresses are $\Sigma TC_k \cos k\pi y/2b + \Sigma TD_\ell \sin \ell\pi y/2b$. (See Fig. 3a)

$k = 1, 3, 5 \ldots$ $\ell = 1, 3, 5 \ldots$

From the equilibrium of the plate

$$\int_0^a PA_m \cos m\pi x/2a \, dx + \int_0^a PB_n \cos m\pi x/2a \, dx - \int_0^b TC_k \cos k\pi y/2b \, dy -$$

$$\int_0^b TD_\ell \sin \ell\pi y/2b \, dy = 0$$

Or,

$$\Sigma \frac{PA_m}{m} \sin \frac{m\pi}{2} + \frac{\Sigma PB_n}{n} \sin \frac{m\pi}{2} - \frac{\Sigma TCk}{k} \sin \frac{k\pi}{2} - \Sigma \frac{TD_\ell}{\ell} = 0 \quad (3.31)$$

And also at corners,

$$\Sigma TA_m \operatorname{Sin} \frac{m\pi}{2} = \Sigma TC_k$$

$$\Sigma TB_n \operatorname{Sin} \frac{m\pi}{2} = \Sigma TD_\ell \operatorname{Sin} \frac{\ell\pi}{2} \quad (3.32)$$

The boundary conditions as well as the nodal equations can be derived in the same way as before, having a varying normal pressure and the presence of shear stress in this case.

Thus

$$v_8' = v_8 + \frac{\upsilon}{\beta}(u_4 - u_2) + \frac{2}{\beta}\Sigma PA_m h\lambda \cos\frac{m\pi}{4} \tag{3.33}$$

$$u_8' = u_8 + \frac{1}{\beta}(v_4 - v_2) - \frac{2}{\xi\beta}\Sigma TA_m h\lambda \sin\frac{m\pi}{4} \tag{3.34}$$

$$v_9' = v_9 + \frac{\upsilon}{\beta}(u_5 - u_3) + \frac{2}{\beta}\Sigma PA_m h\lambda \cos\frac{3m\pi}{4} \tag{3.35}$$

$$u_9' = u_9 + \frac{1}{\beta}(v_5 - v_3) - \frac{2}{\xi\beta}\Sigma TA_m h\lambda \sin\frac{3m\pi}{8} \tag{3.36}$$

$$v_{10}' = v_{10} - \frac{\upsilon}{\beta(1-\upsilon^2)}\Sigma PC_k h\lambda \tag{3.37}$$

$$u_4' = u_4 - \frac{1}{1-\upsilon^2}\Sigma PC_k h\lambda \tag{3.38}$$

Therefore, the governing differential equations, for point 3, will be, in finite-difference terms, as follows:

$$u_2 - (2 + 2\xi\beta^2 - \frac{\eta\upsilon}{2})u_3 + u_4 - \frac{\eta\upsilon}{4}u_5 + 2\xi\beta^2 v_8 - 2\beta\Sigma TA_m h\lambda \sin\frac{m\pi}{4} +$$

$$.5\eta(\Sigma PA_m h\lambda \cos\frac{m\pi}{8} - \Sigma PA_m h\lambda \cos\frac{3m\pi}{8} = 0 \tag{3.39}$$

$$-\upsilon\beta(u_2 - u_4) - .25\eta v_1 + \xi v_2 - (2\xi + 2\beta^2 - \frac{\eta}{2})v_3 + \xi v_4 - \frac{\eta}{4}v_5 + 2\beta^2 v_8$$

$$+ 2\beta\Sigma PA_m h\lambda \cos\frac{m\pi}{4} + \frac{.5\eta}{\xi}\{\Sigma TA_m h\lambda \sin\frac{3m\pi}{8} - \Sigma TA_m h\lambda \frac{m\pi}{8}\} = 0 \tag{3.40}$$

Similarly for point 4, these equations are

$$-\frac{\eta\upsilon}{4}u_2 + u_3 - \left(2 + 2\xi\beta^2 - \frac{\eta\upsilon}{4}\right)u_4 + u_5 + 2\xi\beta^2 u_9 - \xi\beta v_3 - 2\beta\Sigma TA_m h\lambda \sin\frac{3m\pi}{8}$$

$$+\frac{\eta}{2}\Sigma PA_m h\lambda \sin\frac{m\pi}{2} + \frac{\eta\upsilon}{4(1-\upsilon 2)}\Sigma PC_k h\lambda = 0 \qquad (3.41a)$$

$$-\upsilon\beta u_3 + (\upsilon\beta - .5\eta\beta)u_5 + \frac{\eta\upsilon}{2}u_{10} - \frac{\eta}{4}v_2 + \xi v_3 - \left(2\xi + 2\beta^2 - \frac{\eta}{4}\right)v_4 + 2\beta^2 v_9$$

$$+ 2\beta\Sigma PA_m \cos\frac{3m\pi}{8} + \frac{\eta\pi}{32\beta(1-\upsilon 2)}\Sigma mPA_m \sin\frac{m\pi}{2} - \frac{\eta}{2\xi}\Sigma TA_m \sin\frac{m\pi}{2} = 0 \quad (3.41b)$$

Since v at point 5, is assumed to be zero, there will only be one equation at that point, which is

$$2(1-\upsilon^2)(u_4-u_5) - \Sigma PC_k h\lambda + \frac{\upsilon\pi}{8}\Sigma mPA_m h\lambda \sin\frac{m\pi}{2} + \frac{\pi\beta}{16}\Sigma nTB_n = 0 \qquad (3.42)$$

whereas the nodal equations for any interior point still remain unchanged and will be the same as the plain deep beam.

2. For the frame portion (Fig. 3b) the same unknown forces are assumed to be acting but opposite in sign. Since the frame itself is statically indeterminate by two degrees, the redundant forces M_o and H_o at centre of the top member (see Fig. 3b) can be found out from Castigliano's first theorem[39] taking advantage of the state of symmetry. Because of symmetry, the slope at point 1, and also the horizontal displacement are taken to be zero. Neglecting axial shortening, the minimization of the total strain energy in bending with respect to

these redundant forces will be zero. Thus the unknown, M_o and H_o can be seperated from those two equations. These equations can be derived as follows:

Bending strain energy,

$$U = \frac{1}{2EI}\Big[\int_o^a \{M_o - \frac{q_o x^2}{2} + \Sigma\frac{4a^2}{m^2\pi^2} PA_m (1-\cos\frac{m\pi x}{2a})\}^2 dx + \int_o^a \{M_o - H_o b +$$

$$\Sigma\frac{4a^2 PA_m}{m^2\pi^2} + \Sigma\frac{2ab TA_m}{m\pi} + \Sigma\frac{4b^2 PC_k}{k^3\pi^2} - \Sigma\frac{4b^2 PD\ell}{\ell^2\pi^2}\sin\frac{\ell\pi}{2} - \Sigma\frac{4a^2 PB_n}{n^2\pi^2}\cos\frac{n\pi x}{2a}$$

$$+ \frac{q_o a^2}{2}\}^2 dx + \int_o^b \{M_o - \frac{q_o a^2}{2} + \Sigma\frac{4a^2}{m^2\pi^2} PA_m - H_o y + y\Sigma\frac{2aTA_m}{m\pi} + \Sigma\frac{4b^2 PCk}{k^2\pi^2}$$

$$(1-\cos\frac{k\pi y}{2b}) - \Sigma\frac{4b^2 PD\ell}{\ell^2\pi^2}\sin\frac{\ell\pi y}{2b}\}^2 dy\Big] \qquad (3.43)$$

$$\frac{\partial U}{\partial M_o} = \frac{1}{EI}\int M\frac{\partial M}{\partial M_o} dx = 0$$

$$\therefore\ 2M_o a + \Sigma\frac{4a^2}{m^2\pi^2} PA_m - \Sigma\frac{8a^3}{m^3\pi^3} PA_m \sin\frac{m\pi}{2} - \frac{q_o a^3}{6} - H_o ab + \Sigma\frac{4a^3 PA_m}{m^2\pi^2} + \Sigma\frac{4b^3 PC_k}{k^2\pi^2}$$

$$+\Sigma\frac{2a^2 bTA_m}{m\pi} - \Sigma\frac{4ab^2 PD\ell}{\ell^2\pi^2}\sin\frac{\ell\pi}{2} - \frac{q_o a^3}{2} + \Sigma\frac{8a^3 PB_n}{n^3\pi^3}\sin\frac{n\pi}{2} + M_o b - \frac{q_{oa}{}^2 b}{2} + \Sigma\frac{4ab^2 PC_k}{k^2\pi^2}$$

$$+\Sigma\frac{4a^2 b}{m^2\pi^2} PA_m - \frac{H_o b^2}{2} + \Sigma\frac{ab^2}{m\pi} TA_m - \Sigma\frac{8b^3 PC_k}{k^3\pi^3}\sin\frac{k\pi}{2} - \Sigma\frac{8b^3 PD\ell}{\ell^3\pi^3} = 0 \qquad (3.43a)$$

$$\frac{\partial U}{\partial H_o} = \frac{1}{EI}\int M\frac{\partial M}{\partial H_o} dx = 0$$

$$\therefore\ M_o ab - H_o ab^2 + \Sigma\frac{4a^3 bPA_m}{m^2\pi^2} + \Sigma\frac{2a^2 b^2}{m\pi} TA_m + \Sigma\frac{4ab^3 PC_k}{k^2\pi^2} - \Sigma\frac{4ab^3 PD\ell}{\ell^2\pi^2}$$

$$\sin\frac{\ell\pi}{2} - q_{oa}\frac{3}{b}\frac{b}{2} + \Sigma\frac{8a^3b}{n^3\pi^3} PB_n \sin\frac{n\pi}{2} + \frac{M_o b^2}{2} - q_{oa}\frac{2}{b}\frac{2}{4} + \Sigma\frac{2a^2b^2PA_m}{m^2\pi^2}$$

$$- \frac{H_o b^3}{3} + \Sigma\frac{2ab^3TA_m}{3m\pi} + \Sigma\frac{2b^4PC_k}{k^2\pi^2} - \Sigma\frac{8b^4}{k^3\pi^3} PC_k \sin\frac{k\pi}{2} + \Sigma\frac{16b^4PC_k}{k^4\pi^4}$$

$$- \Sigma\frac{8b^4PD_\ell}{\ell^3\pi^3} - \Sigma\frac{16b^4}{\ell^4\pi^4} PD_\ell \sin\frac{\ell\pi}{2} = 0 \qquad (3.43b)$$

Taking $\frac{2a}{b} = \beta$, and with the help of Eqs. (3.31) and (3.32), M_o and H_o can be seperated from Eqs. (3.43). These are as follows:

$$M_o = \frac{q_o a^2}{6}\left(\frac{3 + 8\beta + 3\beta^2}{1 + 4\beta + 3\beta^2}\right) - \frac{2a^2}{\pi}\left(\frac{\beta}{1 + 4\beta + 3\beta^2}\right)\Sigma\frac{PA_m}{m}\sin\frac{m\pi}{2} - \frac{4a^2}{\pi^2}$$

$$\Sigma\frac{PA_m}{m^2} + \frac{8a^2}{\pi^2}\left(\frac{2\beta + 3\beta^2}{1 + 4\beta + 3\beta^2}\right)\Sigma\frac{PA_m}{m^3}\sin\frac{m\pi}{2} - \frac{2a}{\pi}\left(\frac{\beta}{1 + 4\beta + 3\beta^2}\right)\Sigma\frac{PB_n}{n}$$

$$\sin\frac{n\pi}{2} + \frac{8a^2}{\pi^3}\left(\frac{\beta}{1 + 4\beta + 3\beta^2}\right)\Sigma\frac{PB_n}{n^3}\sin\frac{n\pi}{2} - \frac{4a^2}{\pi\beta^2}\left(\frac{\beta}{1 + 4\beta + 3\beta^2}\right)\Sigma\frac{TA_m}{m}$$

$$- \frac{16a^2}{\beta^2\pi^2}\left(\frac{1 + 2\beta}{1 + 4\beta + 3\beta^2}\right)\Sigma\frac{PC_k}{k^2} - \frac{64a^2}{\beta^3\pi^3}\left(\frac{\beta}{1 + 4\beta + 3\beta^2}\right)\Sigma\frac{PC_k}{k^3}\sin\frac{k\pi}{2} +$$

$$\frac{384a^2}{\beta^2n^4(1 + 3\beta)}\Sigma\frac{PC_k}{k^4} - \frac{16a^2}{\beta^2\pi^2}\left(\frac{\beta}{1 + 4\beta + 3\beta^2}\right)\Sigma\frac{PD_\ell}{\ell^2}\sin\frac{\ell\pi}{2} - \frac{64a^2}{\beta^3\pi^2}$$

$$\left(\frac{\beta}{1 + 4\beta + 3\beta^2}\right)\Sigma\frac{PD_\ell}{\ell^3} - \frac{384a^2}{\beta^2(1 + 3\beta)\pi^4}\Sigma\frac{PD_\ell}{\ell^4}\sin\frac{\ell\pi}{2} - \frac{4a^2}{\pi\beta}$$

$$\left(\frac{\beta}{1 + 4\beta + 3\beta^2}\right)\Sigma\frac{TB_n}{n} \qquad (3.44)$$

$$H_o = \frac{q_o a}{2}\left(\frac{\beta^2}{1 + 3\beta}\right) + \frac{3a}{\pi}\left(\frac{\beta^2}{1 + 3\beta}\right)\Sigma\frac{PA_m}{m}\sin\frac{m\pi}{2} - \frac{12a}{\pi^3}\left(\frac{\beta^2}{1 + 3\beta}\right)\Sigma\frac{PA_m}{m^3}$$

$$\sin\frac{m\pi}{2} + \frac{3a}{\pi}\left(\frac{\beta^2}{1+3\beta}\right)\Sigma\frac{PB_n}{n}\sin\frac{n\pi}{2} - \frac{12a}{\pi^3}\left(\frac{\beta^2}{1+3\beta}\right)\Sigma\frac{PB_n}{\pi^3}\sin\frac{n\pi}{2}$$

$$- \frac{2a}{\pi(1+3\beta)}\Sigma\frac{TA_m}{\pi} + \frac{6a}{\pi\beta}\left(\frac{\beta^2}{1+3\beta}\right)\Sigma\frac{TB_n}{n} - \frac{24a}{\pi^2(1+3\beta)}\Sigma\frac{PC_k}{k^2} + \frac{96a}{\pi^2\beta(1+3\beta)}\Sigma\frac{PC_k}{k^3}$$

$$\sin\frac{k\pi}{2} - \frac{384}{\pi^4\beta(1+3\beta)}\Sigma\frac{PC_k}{k^4} + \frac{24a}{\pi^2(1+3\beta)}\Sigma\frac{PD_\ell}{\ell^2}\sin\frac{\ell\pi}{2} + \frac{384a}{\pi^4\beta(1+3\beta)}\Sigma\frac{PD_\ell}{\ell^4}$$

$$\sin\frac{\ell\pi}{2} + \frac{96a}{\pi^3\beta(1+3\beta)}\Sigma\frac{PD_\ell}{\ell^4} \qquad (3.45)$$

Between the interfaces of the frame and the plate the following conditions must be satisfied:[32]

1. Normal and shear stresses will be equal and opposite.
2. Tangential stretching $(\frac{\partial u}{\partial x})$ must be the same.
3. The curvatures or $\frac{\partial^2 v}{\partial x^2}$ must be the same.

Conditions 1 and 2 are automatically satisfied by assuming equal and opposite forces acting on the interfaces and also by taking same strains there. In order to satisfy the third condition, $\frac{\partial^2 v}{\partial x^2}$ for the frame in terms of the moment and $\frac{\partial^2 v}{\partial x^2}$ for the plate in finite-difference terms are matched at points on the boundary.

Thus, at the centre of the top of the frame that is at point 1,

$$2v_2 - 2v_1 + \frac{M_o h^2}{EI} = 0 \qquad (3.46)$$

Similarly at point 2,

$$v_1 - 2v_2 + v_3 + \frac{M_o h^2}{EI} - \frac{qoh^2}{2} + \Sigma\frac{4PA_m a^2}{m^2\pi^2}\left(1 - \cos\frac{m\pi}{8}\right) = 0 \qquad (3.47)$$

and so on.

Four Fortran programs for the IBM 7094 were prepared, the results of which were graphically presented in Figs. 31 through 35.

CHAPTER IV

EXPERIMENTAL INVESTIGATION

(i) Materials and Apparatus

Fifteen tests were performed on 6061-T6 aluminum alloy[40] models. Two groups of structures were considered: (a) plain deep beams, (b) deep beams with stiffened edges. Seven tests were included in the first group and eight in the later. The geometries of these test specimens are given in table I and II. Eight to ten strain rosette gauges were installed in five basic test models, along the vertical mid-section. These rosette gauges are of the 2-legged 90^{o} rectangular type, having a gauge factor of 2.07 and a resistance of 120 ohms. At the corners three-legged rosettes were used. Most of the gauges used were of 1/8 inch gauge length. Terminal strips (type T-50) were used to connect the lead wires to the gauge tabs. All the lead wires were 16 feet long, made of No. 26 stranded copper wire and with vinyl insulation. To provide mechanical protection and water-proofing, the installed gauges were covered with gauge coat No. 1 (synthetic resin compound), gauge coat No. 2 (nitrite rubber) and gauge coat No. 5(a two-compound epoxy resin).

Application of compressive stress on the upright plate and avoiding eccentric loading was a major problem. To apply compressive loading in such a fashion so that there is no loss of pressure during the time of recording, a mechanical loading rig was designed and

employed as shown in Fig. 4a. The top member of this frame was of solid 4 inch x 6 inch steel section that housed the 2-inch diameter loading screw in a threaded hole at the centre. This top bar was supported on two vertical 10-inch at 12 pounds I-sections. The joints between the top bar and the two vertical members were screwed to facilitate future adjustments when necessary. The two vertical I - sections were welded at their lower ends with a horizontal I-section of 12-inch at 16 pounds which was lying on the floor and securely fastened to avoid any movement. A Budd load-cell (type LUD 10K) was attached at the lower end of the loading screw that acts through the threaded hole in the top bar. Beneath the load-cell, there were two cross-beams of solid 2-inch x 2-inch steel section, the top one resting on the bottom one through eight smooth ball-bearings of 3/4 inch diameter. These two cross-beams were kept in position by means of two 3/8 inch rods hung from the solid top member of the frame. At each end the cross-beams were supported by friction-less bearing-balls acting in two vertical slots in the inner flanges of the vertical I-sections, so that the cross-beams can freely move downward without any lateral displacement when released. The load-cell was calibrated before hand through a portable Budd Strain Indicator (model P-350) and the load factor in micro-inch/inch/lb. was found out and occasionally checked. The model was placed vertically on the bottom I-section on two roller supports to facilitate free horizontal movement. The cross-beams when released from hanging rested on the model. A half-inch thick rubber padding was attached at the under-side of the bottom cross-

beam. In order to eliminate friction between the rubber and the model, that may partially restrict the longitudinal strain of the top edge of the model, the lower edge of the rubber was cut at every inch into 3/8 inch deep cuts. This discontinuous edge of the rubber when under pressure from the cross-beams, was expected to simulate best the effects of uniformly distributed load on the top of the model. The upper edge of the model in contact with the rubber was also slightly lubricated.

During the tests, strains were measured by means of three switch and balancing units (model C-10T and C-10LTC, Budd Instrument Division), a digital strain indicator with an automatic print-out unit. To check any lateral deflection perpendicular to the plane of the plate, two 1/1000 inch dial indicators were installed at the back of the mid-depth of the model. Figs. 5a and 5b show the apparatus and the general set-up of the experiment.

(ii) Experimental Procedure

For each test-model, the plate was first cut smoothly to the required dimensions. In order to cut out the opening, holes were first drilled near the inner corners. Then these bore-holes were connected by means of a sabre-saw. Later the inner edges were smoothened by milling machine up to ten thousandth of an inch of the required dimensions. The plate was then cleaned with acetone and the locations of the strain gauges were laid with reference to the sides. Care was taken to ensure that all the gauges are in proper alignment with respect to the axis which are parallel to the outer edges. The installation of these rosette gauges followed a set pattern.

Next, gauge lead wires from the rosette gauges were soldered to tin 5-channel receptacles especially provided for three switch and balancing units. Unit strains for any loading were automatically recorded by a precise digital strain indicator and printer.

After placing the model in position, the cross-beams were released to rest on the top edge of the model through the rubber padding. By turning the loading-screw, the load-cell while moving downward exerted a compressive pointed load at the centre of the top cross-beam. This load was then transmitted through eight bearing-balls to the bottom cross-beam. The load was further distributed as uniform load through the rubber padding on to the model. The compressed load-cell coupled with the portable strain indicator (Budd model P-350) indicated the strain in the load-cell in mocro-inch/inch corresponding to the particular pressure applied. The deflecto-meters set at the back indicated lateral deflection (perpendicular to the plane of the plate) due to eccentric loading, which was corrected by shifting the position of the plate after releasing the load. Again the loading was applied and the deflecto-meter readings were checked. By trial and error method in this fashion, the eccentricity was eliminated as far as possible. When no eccentricity was noted, the strains were then recorded through the automatic strain recorder.

For each test, six sets of strain readings were taken independently. The final test results, reported herein, were the average of these readings. After completion of the first set of seven tests a frame made of similar aluminum alloy was welded to the plate around the outer edges to yield the deep beams with stiffened edges. In order to avoid excessive heat due to welding that could damage the

already existing gauges, the welding was discontinued at the interfaces and a structural adhesive was used in lieu of welding.

CHAPTER V

DISCUSSION OF RESULTS

(i) Plain Deep Beams

Experimental and theoretical results for the longitudinal stresses at the mid-section of a solid square deep beam under uniformly distributed load acting on the top edge are presented in Fig. 7a. Theoretical results obtained from the works of Winter[6] and Geer[8] based on the Airy stress function are also shown to facilitate comparison. From this figure it is noted that the theoretical results are in close agreement with the experimental ones. This confirms the suitability of the present method in solving plane-stress problems. This comparison also justifies the results of the previous investigators[6,8] who did not verify their findings experimentally. However, it is also observed that the magnitude of the present maximum stresses exceeds those of the others[6,8]. This discrepancy can be attributed to the difference in support width used. The previous investigators used a support width one eightth and one tenth of span respectively whereas it is only one sixteenth of the span in the present case. By increasing the width to one eightth of span, it is found both experimentally and theoretically that the magnitude of the maximum longitudinal stress decreases by an amount of 35% for a square deep beam and by 44% for a rectangular one having the depth greater than the span. However, for a rectangular deep beam whose length exceeds the depth, this decrease is negligible.

Thus it can be assumed that the width of the support has a direct bearing on the stress distribution in a deep beam.

In Fig. 7b, the longitudinal stresses at the mid-section of a square deep beam due to the uniformly distributed load acting along the bottom edge are shown and compared with those found by Winter.[6] The influence of the support-width on the magnitude of the maximum longitudinal stress is also clearly evident in this case. However, in the discussion[7] of Winter's paper[6], it was pointed out that an error of the magnitude of 10 to 17% might exist in those results. If this is the case, the present investigation is advantageously conservative as indicated by the results presented.

Figures 8a and 8b show the distribution of the longitudinal stresses on the mid-section of rectangular deep beams due to uniformly distributed load acting on the top edge, whereas Fig. 9 exhibits the same for uniform load at the bottom edge. To facilitate comparison of stress values obtained from the linear beam theory as well as Winter's results[6] are also plotted. It is interesting to note that the maximum deviation of the longitudinal stress from the linear beam theory is prominent in a rectangular deep beam whose span is approximately 30% less than the depth. When the span exceeds the depth by the same amount, the deviation is almost negligible. This observation indicates that in a solid deep beam the most severe condition will occur not in a square panel but in a rectangular one having a span slightly smaller than the depth. This also confirms that the charecterization

of a solid deep beam could be based on the dimension-ratios (ratios of span to depth) falling in between 2/3 to 3/2. Unfortunately none of the previous investigators laid any emphasis on this particular aspect. However, this behaviour can be attributed to the fact that the narrow support produces a very severe stress concentration which is almost solely responsible for the stress-distribution in a true deep beam and not the bending moment. The adjustment and redistribution of this severe stress-concentration on the support has a profoundly significant effect on the entire stress-system in a deep beam and not the bending moment. This is also confirmed by Fig. 10 where the shear stress at a quarter point of the span is plotted. The shear stress results for a rectangular deep beam having a span less than the depth vary in a distinct manner with a peak value not at mid-depth but somewhat closer to the bottom surface. This also indicates that the peak point is due to a sort of 'attraction' towards the support in the same manner as the longitudinal stresses are attracted, for any rectangular deep beam having a depth greater than span. In case of a span exceeding the depth, this behaviour is not at all prominent when the shear stress diagram resembles that obtained from linear beam theory.

The longitudinal stresses at mid-section of a square deep beam with a small opening at the centre for uniform load on the top

edge are given in Fig. 11. Figures 12 and 13 represent the same for rectangular beams. The area of the opening is 4% of the total area of the deep beam. It is interesting to note that the magnitude of the maximum tension in these cases is less than that in a solid deep beam. This indicates that the opening relieves the maximum tension at the centre of the span. This behaviour is apparently linked up with the same criterion that is responsible for the tension in a solid deep beam.

In view of the principle of St. Venant the effect of the intense field of stress set up in the immediate vicinity of the point of application of a so-called point load (and reaction) on the bending of a simple beam is ignored. This is justifiably so for any beam which is long compared with its depth because the disturbance of this simple distribution is very local and has insignificant effect on the overall pattern. However, for any deep beam this is otherwise.

A beam of typical proportion is shown in Fig. 6a. To bring out the origin of tensile stresses, a few stress trajectories are shown. At point A, this line, being compressive, produces an outward resultant force C as shown in Fig. 6b. There are many such trajectories in this vicinity, all producing outward resultant forces. The free left boundary can furnish no reactive force and consequently the cumulative effect is a tension in the direction of the dotted line. Thus it is readily seen in a qualitative way that the action of a beam of this proportions is mainly one of the distribution of a localised force which is totally insignificant in an ordinary beam. By choosing

a narrow support-width the intensity of this localised force is added on.

Introducing a small opening at the centre of the member, some of this trajectories close to the opening may not remain concave inward. This means that the trajectory line close to A (Fig. 6b) will not be compressive but tensile whereas others will remain as before. The most probable picture will be as in Fig. 6c; this situation causes a decrease in the magnitude of the cumulative tensile stress at the centre.

However, increase in the size of the opening causes stress trajectories near the centre to move further away towards the support. This action is analogus to decreasing the support-width. Because of the fact that the vertical force-free faces can not provide any reactive horizontal stresses, the resulting tensile stresses are increased. This has been verified by the experimental as well as theoretical results shown in Figs. 14 to 16, where an increased tension at the bottom of the mid-section is observed due to a large opening having an area approximately 6% of the total area of the deep beam.

For a still larger opening, about 25% of the area of the beam, the theoretical results become unreliable. This is because of the fact that in such a case, the deep beam closely resembles a deep frame. The axial stresses in such cases may be of such magnitude that their presence will void the use of the principle of super position; such cases can not be represented in two-dimensional plane-stress system.

Figs. 17 to 19 indicate that for a uniformly distributed load acting on the top surface the bottom tensile stress attains maximum value not at the centre of the span but closer to the support. Furthermore, the size of the opening and also the shape of the beam itself, whether square or rectangular, dictate the position and magnitude of this tension. In a square deep beam with a small opening the difference between the tension at the centre and its maximum value near the support is noticeable. In the case of a larger opening (θ = 6 1/4%) the variation of the tensile stress is almost linear. Fig. 20 represents the variation of the bottom tensile stress along the span for uniformly distributed load acting at the bottom edge. It is interesting to note that the shapes of these curves are similar for a particular size of opening irrespective of the ratio of the sides.

The behaviour of a deep beam is also influenced by the kind of loading applied. Figs. 21 to 23 show the distribution of the longitudinal stresses at mid-section due to a single concentrated load acting at the centre of top edge. The magnitude of the maximum tension as well as the manner of variation are significantly different from those due to uniform load. The centre-tension is not as large as that due to uniform load in case of a square deep beam. The most severe cases are for any opening when the depth is greater than the span. This is also true for quarter point loads shown in Figs. 24 to 26. This indicates that the loads acting near the support augment the particular deep beam action that causes the severity in a deep beam with depth slightly more than span.

Figs. 27 to 30 present a summary of the variation of the centre-tension with respect to size of the opening, shape of the deep beam and the type of loading applied. It is interesting to note that the maximum tension at the centre occurs in a rectangular deep beam with a depth 30% more than span having an opening of approximately 6% of the total area of the beam. This is for the case of a uniformly distributed load acting at the top. However, if the uniform load acts at the bottom edge, the maximum tension accurs in the solid rectangular deep beam of the same aspect ratio. Whereas for a concentrated load, whether acting at centre or at quarter points of the span, the maximum tension will develop with an opening of approximately 6% of the area of the beam having a depth 30 % greater than span.

(ii) Stiffened Deep Beams

By stiffening a deep beam by means of a frame around it, its behaviour changes significantly depending on the degree of stiffeners added and the area of the opening included. This is illustrated in Figs. 31 through 35.

For a small cross-section of the stiffening frame denoted by $\zeta = \frac{512I}{tL^3} = 0.074$, the stiffened deep beam without any opening behaves as an ordinary deep beam with reduction in stresses. However, the introduction of a small opening with an area of approximately 4%, the behaviour changes. The influence of the stiffening frame predominates the actual deep beam behaviour. This predominant frame action is more prominent in the case of a rectangular deep beam with greater depth than span.

For a larger cross-section of the stiffening frame ($\zeta = 0.25$) absence of any opening renders the action of the member as that of an ordinary stiffening block (Fig. 31), save and except a small amount of localized tension at the centre of the unsupported edge. Whereas the presence of an opening transforms it into a stiff frame irrespective of the aspect ratio (β). However, for a larger opening, $\theta = 25\%$ or more, the stiffened deep beam behaves as a deep frame irrespective of span to depth ratio. This behaviour is also independent of the degree of stiffening (Figs. 34 and 35).

It should be noted that for a slender stiffening section ($\zeta = .07$), the theoretical approach is not valid (Fig. 31). This is because of the fact that instead of tackling the problem with finite-difference approximations for both the plate and frame portions, the frame portion has been analyzed by means of ordinary linear structural frame analysis. This was performed to avoid error due to singularity at the interfaces where there is an abrupt change in cross-section. In linear structural analysis the axial strain is always neglected as the rotation is neglected in braced-frame (truss) analysis. Furthermore, while membrane stress is neglected, in plate analysis, it is predominant in other structures. The slender section of the stiffening frame under a heavy axial strain will, not act as a frame but as an elastic band. This will void the calculations of the redundant forces as performed here. This fact also contributes to the non-linearity of the load-deflection relationship which violates not only the principles of ordinary structural analysis (linear) but also the conditions of the plane

state of stress.

There are three different cases of non-linearity in the behaviour of structures. The first one arises from the non-linear behaviour of the material of which the structure is made. The second case is referred to as gross deformation.

In linear structural analysis, it is essential to assume that the deformation is small compared with the dimensions, so that the overall shape of the structure is not significantly altered by the process of loading. More significantly, it is assumed valid to use the equilibrium equations with the lengths, angles etc. for the undistorted structure whereas strictly speaking these equations must hold in the distorted structure.

The third case of non-linear behaviour which is important in the present case, can be a particular case of the second one. This is the effect which axial forces have on the bending stiffness of members in rigid-jointed frames and trusses. If the axial force in a member is compressive, the bending stiffness is reduced, while if it is tensile the stiffness is increased. The effect may in extreme cases cause a structure to be unstable while the material is within its elastic region.

The limitation of the theory of elasticity to isotropic homogeneous materials leads to a number of simplifying conclusions enabling one to express stress in terms of strain or vice versa irrespective of the orientation of the material with respect to coordinate axes viz: stress-strain relations are invariant to transfor-

nation of coordinates. From this follows the principle of superposition of stresses in elastic system leading to the conclusion that the strain ϵ_x is linearly dependent upon all three stresses by

$$\epsilon_x = \frac{1}{E}[\sigma_x - \upsilon(\sigma_y + \sigma_z)]$$

and so on. This is the principle of superposition which not only allows the state of strain at a point to be derived in this way, but is equally applicable to distributions of stress and strain generally. However, this principle is valid only for a linear case. Thus the present attempt is limited to linear cases only.

(iii) Sources of Error

In the theoretical approach, the probably sources of error lie in the moderately coarse mesh incorporated in the finite-difference equations. There are errors also due to singularity at points directly under the loads. Because of this, the magnitude of maximum tension at bottom-centre when the load is acting at the bottom are less precise than the same for load on the top edge. However, it is expected that the errors in theoretical results will not exceed 10 %. This observation is based on the favourable comparison made between the results obtained herein and those reported by previous investigators. The actual stress-concentration around the periphery of the openings, specially at the corners, can not be accounted for by the present approach. Due to singularity, the results will be totally erroneous.

In case of experimental investigations, the probable sources of error can be classified in three groups; fabrication errors, loading errors, instrumentation errors.

Fabrication errors arise due to preparation of the specimens, uneven thickness of the materials and possible change of elastic properties and residual stresses due to welding. The thickness of the model itself is liable to incur a significant error, since the rigorous fulfillment of the plane-stress conditions demands a thickness tending to zero. Also because of the variation in thickness, a small amount of lateral deflection may be induced and will contribute to the magnitude of the measured strains, hence the calculated stresses may have significant errors inspite of the fact that an effort was made to eliminate the lateral deflections as far as possible. This type of error might have been associated in results shown in Fig. 31.

Experience has also shown that the heat due to machining appreciably changed the elastic properties of the tension specimen. Keeping this in mind, the process of welding causing alternate heating and cooling was sure not only to change the elastic properties but also to induce residual stresses. This is expected to incur a significant error in stress-values. The effect of the manufacturers' deficiency such as unevenness of the thickness and quality control are still unknown and overlooked.

Instrumentation errors arising from the strain gauges in their alignament and their readings may not be as significant as those in the first group. However, the small strain readings are liable to involve

error which has been distributed by taking the average of several readings.

The maximum error involved in the experimental investigations is expected in the loading device. The loading rig was designed in such a fashion so that it could apply a uniformly distributed load on the upper edge of the specimen. However, the results shown by all the experimental stress-diagrams indicate that the applied load may not truly represent a uniformly distributed nature. This is evident from the fact that those stress-diagrams assumed slightly different shape at the top from the theoretical curves as well as from those of the previous investigators. It was also noted that because of the mechanical device in loading, the load could not be applied without any jerk or vibration. This may also be a critical source of error.

From all these considerations, it is expected that the experimental results involved a significant amount of error, which may be in some cases as high as 30 % as shown in Fig. 15. Since the experimental observations were used mainly to verify the theoretical approach and since the theoretical results are in good agreement with those of the previous investigators, the experimental results do substantiate the theoretical approach.

However, it is expected that the finite-element method may be adequately suitable in this type of problems dealing with singularities due to change in cross-sections, opening and concentrated loading. This method could also arrest the magnitude of stress-concentration around the periphery as well as the inner corners where the method of finite-difference is liable to yield totally erroneous results.

CHAPTER VII

CONCLUDING REMARKS

As a result of this theoretical and experimental investigation on the behaviour of plain and stiffened deep beams with or without opening, the following conclusions may be made:

1. For the limiting case where the plain deep beam is without an opening, the displacement method yields results which are in good agreement with the findings of previous investigators.
2. For deep beams with small openings, the stresses obtained by model tests and theoretical analysis are in reasonable agreement, confirming the validity of the theoretical approach to doubly-connected plane-stress system.
3. For a plain deep beam having a small opening at the centre, the maximum longitudinal tension at the centre is significantly less than that in a solid deep beam without an opening; if the opening area is further increased the tension, however, increases abruptly.
4. For a still larger opening, having an area of about 25% of the total area of the member itself, the behaviour will be similar to that of a frame, not that of a deep beam proper.
5. The maximum longitudinal tension in a solid deep beam

occurs not in a square deep beam but when the depth is slightly larger than the span. This is also true in the case when an opening is introduced.

6. The distribution of longitudinal stresses in the mid-section of a deep beam with or without opening is nearly linear when the span is more than 30% of the depth.
7. For any deep beam critical stress condition will not exist at the centre of the span, but somewhere closer to the support.
8. The type of loading and its point of application will not only determine the maximum longitudinal stress but also the position of the neutral axis.
9. By introducing a frame around the outer edges of a deep beam, its behaviour is totally changed; it behaves neither as a deep beam nor as a deep frame, depending on the span-depth ratio, size of opening and the degree of stiffening added.
10. For a stiffened deep beam without an opening, the mid-section is subjected to a small tensile stress at the centre of the bottom edge; while an increased stiffening area will render it to almost a stiff compression block with a small localized tension at the bottom.
11. Presence of an opening influences the behaviour of a stiffened deep beam in such a manner that bending action becomes more prominent.

It should be pointed out, however, that for a slender stiffening frame the theoretical approach is not valid, as was discussed before. Although the present approach involves a very large amount of arithmatic, its versatility in solutions of doubly connected deep beams is sure to offset the labour.

REFERENCES

1. F. Dischinger - 'Beitrag zur Theorie der Halbscheibe und des Wandartigen Balkans.' Publications, International Assoc. of Bridge and Structural Engineering I, Zurich, 1932.
2. Portland Cement Association - 'Design of Deep Girders'. Pamphlet No. ST66.
3. Harmann Bay- 'Uber den Spannungszustand in Hohen Tragern und die Bewehrung von Eisenbetontragwanden (Dissertation), Stuttgart, 1931.
4. Conway, Chow and Morgan - 'Analysis of Deep Beams' Journal of Applied Mechanics, V. 18, No. 2, June 1951.
5. K. Iyengar - 'Analysis of Deep Beams', Proceedings, Second Congress of Applied Mechanics, New Delhi, 1956.
6. Chow, Conway and Winter - 'Stresses in Deep Beams'. Proc. ASCE V. 78 Seperate No. 127, May 1952.
7. A. M. Guzman and C. Luisoni - Discussion on 'Stresses in Deep Beams', Proc. ASCE, February 1953.
8. Elihu Geer - 'Stresses in Deep Beams', Journal of American Concrete Institute, January 1960.
9. F. Archer and E. Kitchen - 'Stresses in Deep Beams', Civil Engineering, London, V55, N643, Feb. 1960.
10. F. Archer and E. Kitchen - 'Strain Energy Methods for solutions of Deep Beams.' Civil Engineering, London V52, N618, Dec. 1957.
11. A. M. Guzman and C. J. Luisoni - 'Soluciono Varacional del problema

de la viga Rectangular Simplementi Apoyada de Gran Altura,' Ciencia y Lecnica, Buenos Aires, Argentina, Vol 111, 1956.

12. S. Saad and A. W. Hendry - 'Gravitational Stresses in Deep Beams,' The Structural Engineer, June 1961.
13. S. Saad and A. W. Hendry - 'Stresses in Deep Beams with Central Concentrated Loads.' Experimental Mechanics, V1, N6, June 1961.
14. N. J. Durant and F. Garwood - Ministry of Works, Technical Nate No. 78, London, October 1947.
15. L. Fox - 'Mixed Boundary Conditions in the Relaxation Treatment of Biharmonic Problems (plane-strain Problems)' Proc. Royal Society, London (A), 189, 1947.
16. A. Coul - 'Stress Analysis of Deep Beams and Walls,' The Engineer, Feb. 1966.
17. J. B. Kennedy - Personal Communications
18. S. Timoshenko and J. N. Goodier - Theory of Elasticity. McGraw-Hill, New York, 1951
19. B. Sen - 'Two-dimensional Boundary-value Problems of Elasticity,' Proc. Royal Society, London (A) 1946.
20. A. Tuzi - 'Effect of a Circular Hole on the Stress Distribution in a Beam under Uniform Bending Moment.' Philosophical Magazine. London, Seventh Series, V9, Jan - June 1930.
21. Karl Wolf - 'Beitrog zur ebenen Elastizitatstheorie,' Z. Techn. Phys. 2, 1921.

22. D. Gupta - 'Effect of Small Circular Hole on Stress Distribution on a Deep Rectangular Beam Subject to Flexure under Shear,' Indian Journal of Theoretical Physics, V10 N2 nd 3 1962.

23. M. A. Jeffery - 'Plane-Stress and Plane Strain in Bipolar Coordinates' Royal Society. London (A), V221, March 1921.

24. W. G. Bickley - 'Infinite Plate with Circular Holes', Royal Society London (A), V227 January 1928.

25. H. Hengst - 'Beitrag zur Berechnung von Stegblechen mit Sparlochern,' Stahlbau 15, 61 (1942)

26. A. Hutter - 'Die Spannungs spitzen in gelochten Blechscheiben und Striefen', Z. angew. Math. Mech. 22, 322 (1942)

27. G. N. Savin - Stress Concentration Around Holes.' Pergamon Press, New York, 1966.

28. G. B. Airy - 'On the Strains in the Interior of Beams' Trans.Royal Society,London 153, 1863.

29. P.P. Teodorescu - 'Hundred Years of Investigations in the Plane Problems of the Theory of Elasticity', Applied Mechanics Review, V 17, N3, March 1964.

30. de G. Allen - Relaxation Methods in Engineering and Science, McGraw-Hill, New York, 1954.

31. M. Hetenyi - Handbook of Experimental Stress Analysis, John Wiley and Sons, New York, 1950. pp. 751 - 770.

32. O. C. Zienkiewicz - Stress Analysis, John Wiley and Sons, 1965.

33. Hugh Ford - Advanced Mechanics of Materials, Longman, 1962.

34. Chi-Teh Wang - Applied Elasticity, McGraw-Hill, New York, 1953.

35. Ray W. Clough - 'The Finite Element Method in Plane Stress Analysis', ASCE, Second Conference on Electronic Computations, Nov. 1962.

36. Ray W. Clough - 'The Finite Element Method in Structural Mechanics' Stress Analysis, John Wiley and Sons, New York, 1965.

37. F. S. Shaw - Relaxation Methods, Dover, 1953.

38. N. M. Newmark - Class Notes on Numerical Analysis, University of Illinois, 1960.

39. S. Timoshenko and D. H. Young - Theory of Structures, McGraw-Hill, 1962.

40. Aluminum Company of Canada - Strength of Aluminum, 1968 Edition, Toronto.

41. G. N. J. Kani - Class Notes and Personal Communications, 1966.

42. J. B. Kennedy and S. F. Ng - 'Linear and Non-linear Analysis of Skew Plates' Journal of Applied Mechanics, June 1967.

43. J. B. Kennedy-Class notes on Theory of Elasticity I & II, University of Windsor, 1966-67.

NOMENCLATURE

A = Area of the Deep Beam

a' = Area of Opening

L, $2a$ = Span of the Deep Beam

H, D = Depth of the Deep Beam

θ = a'/A

α = Side of Opening/Side of Beam

β = L/D

t = Thickness of Beam

I = Moment of Inertia of Frame Cross-Section

∂ = $\frac{512I}{t\,L^3}$

p = Applied Pressure in p.s.i.

q_o = Applied Pressure in lbs. per in.

P = Pointed Load at Centre in lbs.

Q = Pointed Load acting at a Quarter Point of the Span

σ_x, σ_y, τ_{xy} = Stresses at a Point

u,v = Displacement Components Parallel to x and y directions respectively

E = Young's Modulus of Elasticity

υ = Poisson's Ratio

λ = $(1 - \upsilon^2)/E$

ξ = $(1 - \upsilon)/2$

η = $(1 + \upsilon)/2$

VITA AUCTORIS

1933 Muhammad Harunur Rashid was born in November in Dinajpur, East Pakistan.

1940 Attended Harvey Primary School, Santahar, for his elementary Education.

1950 Graduated from Chuadanga Victoria Jubilee High School and was enrolled in Pabna Edward College the same year.

1952 Obtained Intermediate Science Certificate with a Senior Scholorship and got admitted at the Ahsanullah Engineering College, Dacca, the same year.

1957 In September, married Hosne Ara (Milly) while she was an undergraduate at the Holy Cross College, Dacca.

1958 In January, joined The Engineers Ltd, Dacca as an Assistant Engineer and was responsible for the design of 36 R. C. road bridges over the canal network of the G. K. Irrigation Project. Son Imran was born in July.

1959 In November, came back to teaching in Ahsanullah Engg. College.

1960 Sent on deputation to the University of Illinois on a one-year programme of higher studies jointly sponsored by the Ahsanullah Engg. College and Texas A and M. College.

1961 Completed coursework requirements and obtained an M.S. from the University of Illinois and returned to Dacca to teaching in August.

1962 Became Assistant Professor in the East Pakistan University of Engg. and Technology, Dacca, that absorbed the Ahsanullah Engineering College. Daughter Suzan was born in July.

1965 Sent to Canada for higher studies towards a Ph.D., presumably to head Civil Engineering in newly created Rajshahi Engg. College on return on a three-year programme sponsored by the Govt. of Canada.

1966 Completed requirements for an M.A.Sc. at the University of Toronto and was enrolled as a Ph.D. student at the University of Windsor under the guidance of Dr. J. B. Kennedy.

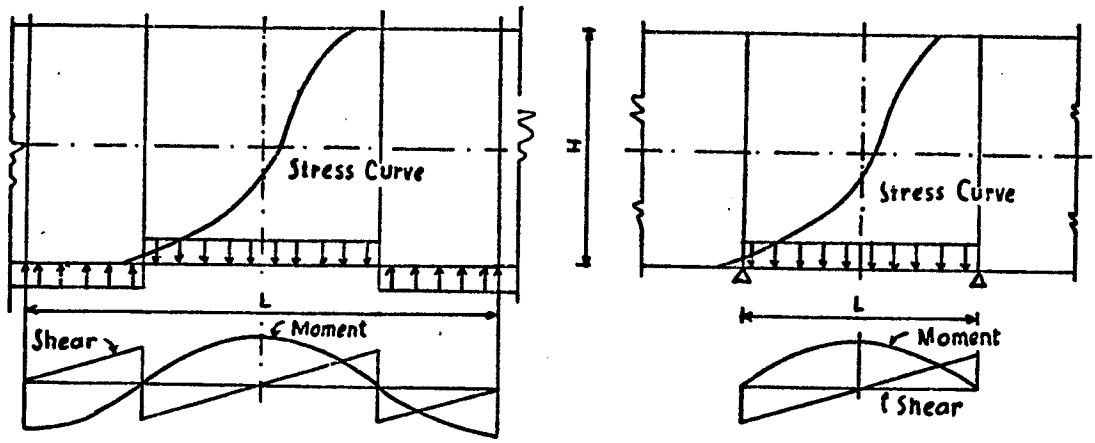

(a) Continuous Span

(b) Single Span

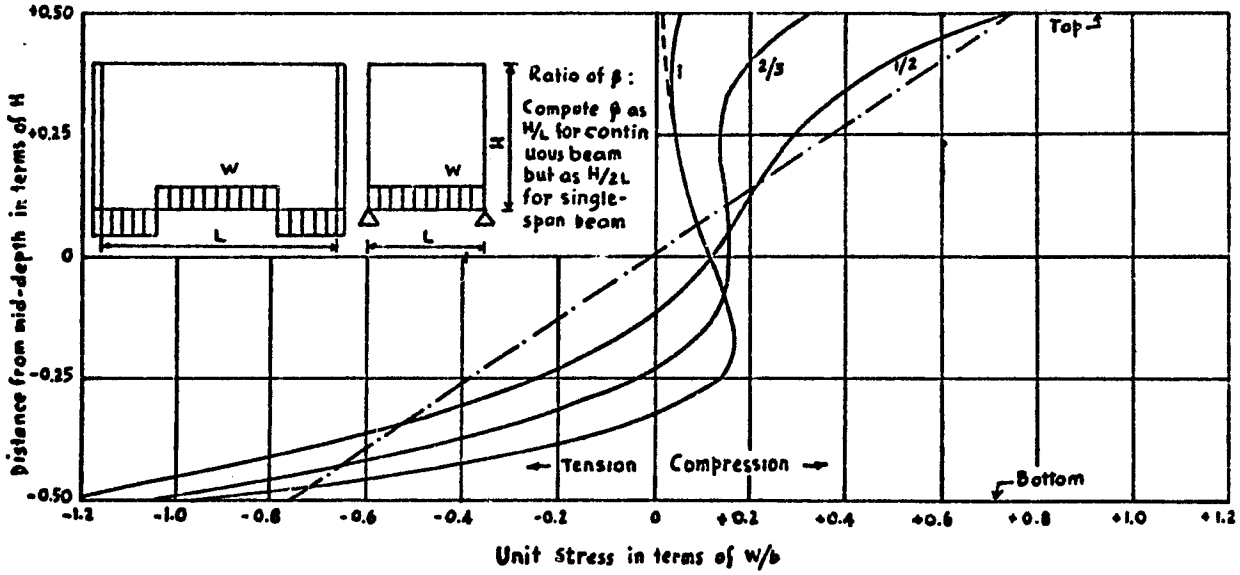

(c)

Fig. 1

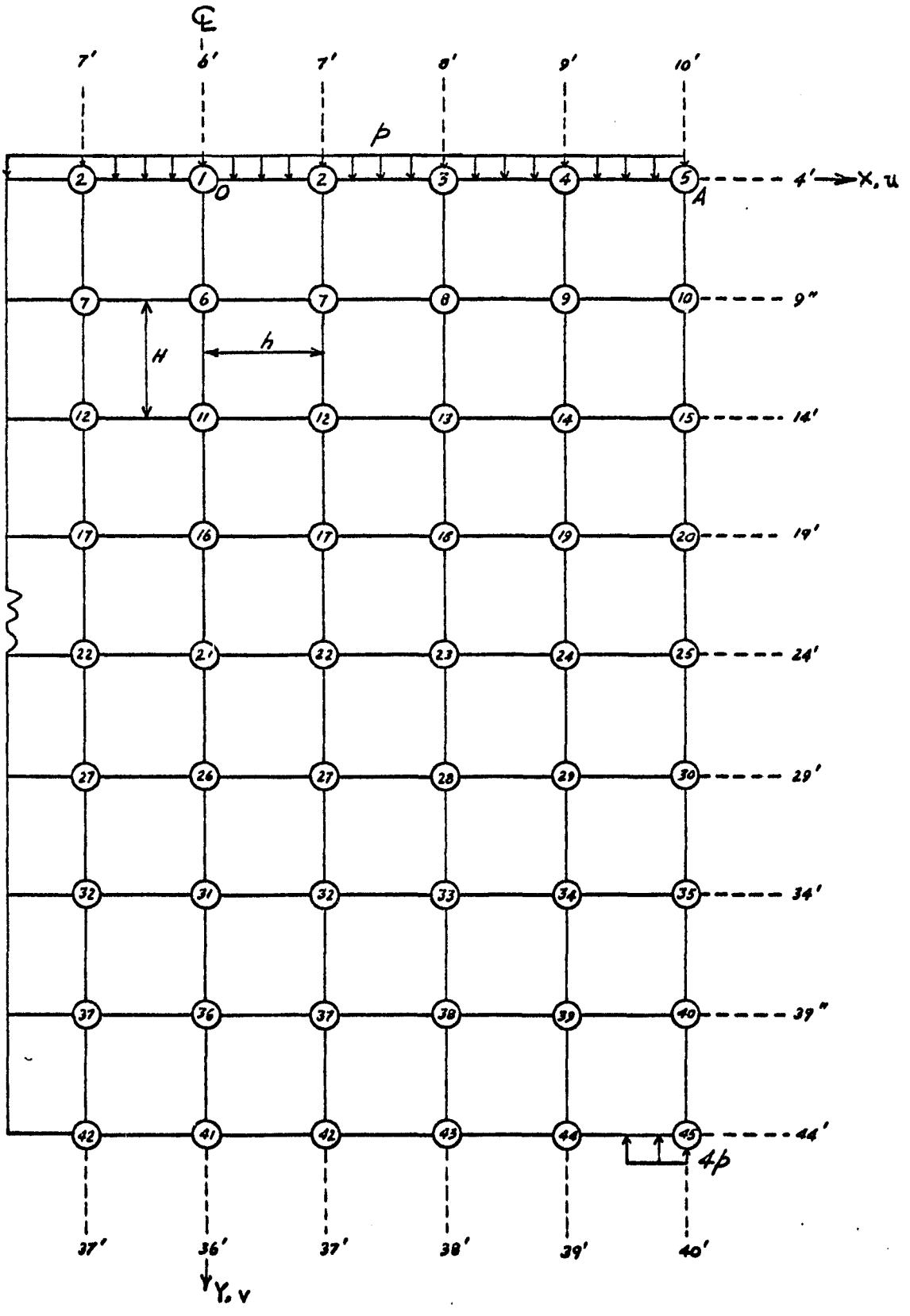
℄
7'
6'
7'
8'
9'
10'
p
2
1
O
2
3
4
5
A
4'
X, u
7
6
7
8
9
10
9"
H
h
12
11
12
13
14
15
14'
17
16
17
18
19
20
19'
22
21
22
23
24
25
24'
27
26
27
28
29
30
29'
32
31
32
33
34
35
34'
37
36
37
38
39
40
39"
42
41
42
43
44
45
44'
4p
37'
36'
37'
38'
39'
40'
Y, v

Fig. 2

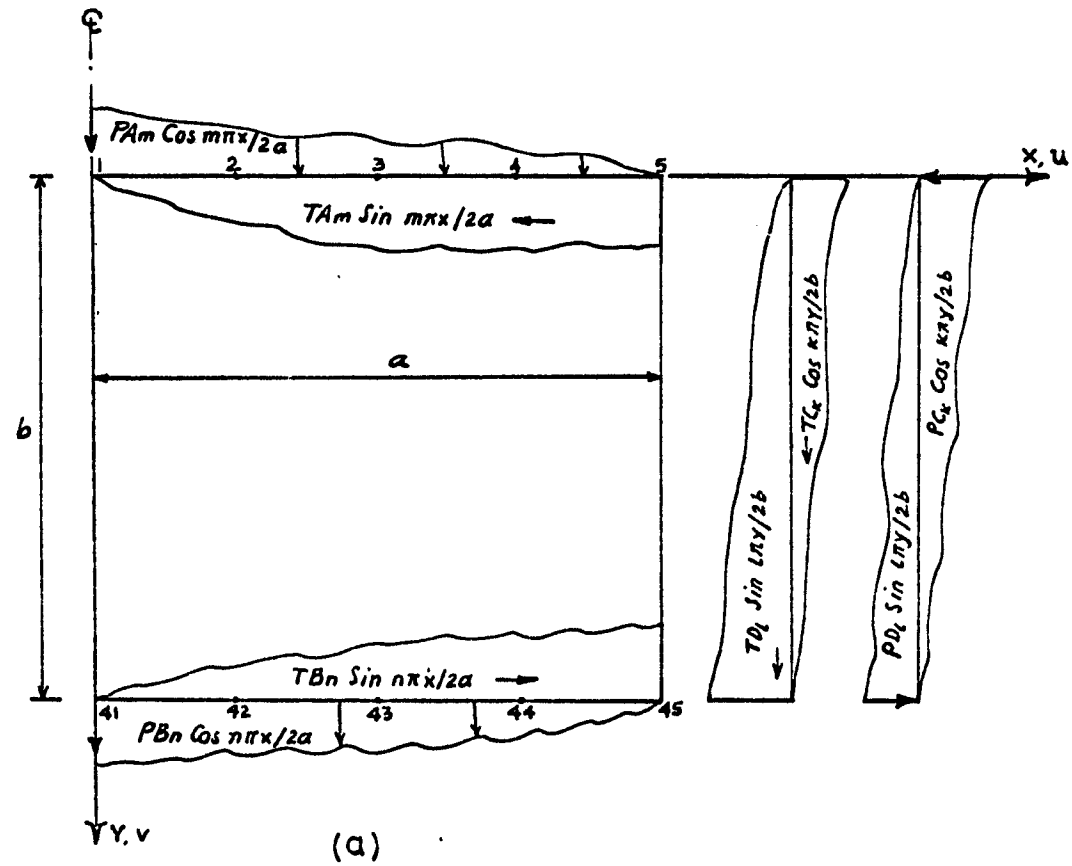
PAm Cos mπx/2a
TAm Sin mπx/2a
TBn Sin nπx/2a
PBn Cos nπx/2a
TCk Cos kπy/2b
TDℓ Sin ℓπy/2b
PCk Cos kπy/2b
PDℓ Sin ℓπy/2b
a
b
X, u
Y, v
1
2
3
4
5
41
42
43
44
45

(a)

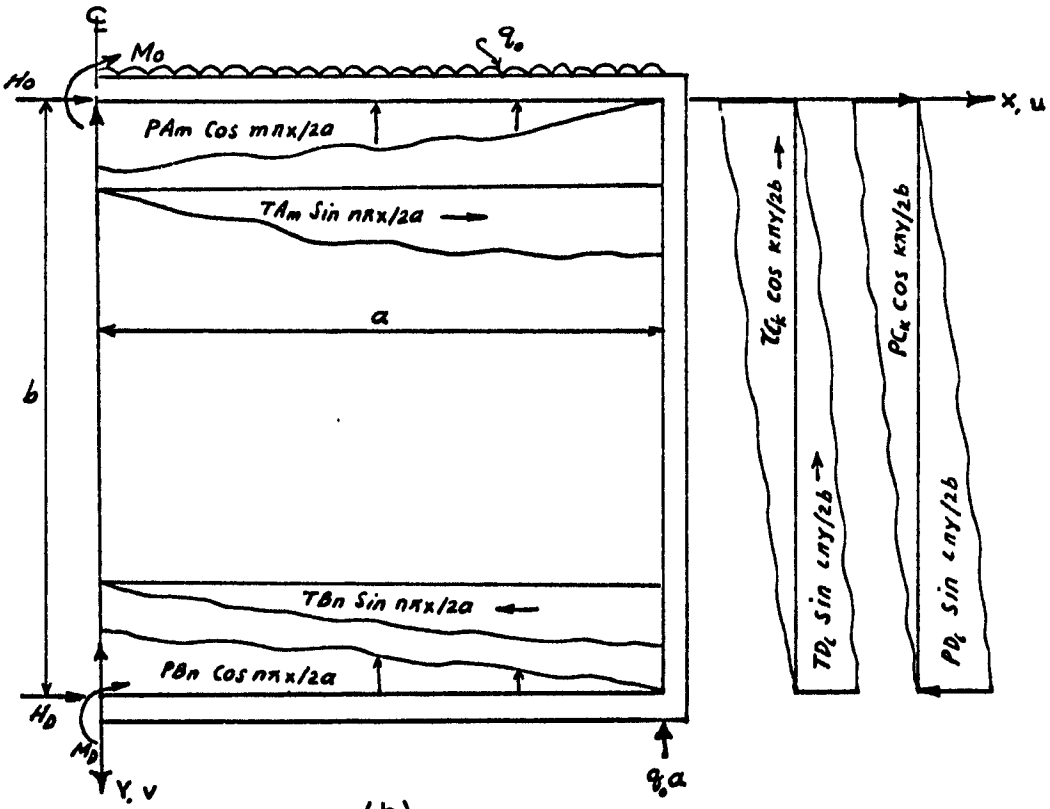
Mo
Ho
qo
PAm Cos mπx/2a
TAm Sin nπx/2a
TBn Sin nπx/2a
PBn Cos nπx/2a
TCk Cos kπy/2b
TDℓ Sin ℓπy/2b
PCk Cos kπy/2b
PDℓ Sin ℓπy/2b
a
b
X, u
Y, v
qoa

(b)

Fig.3

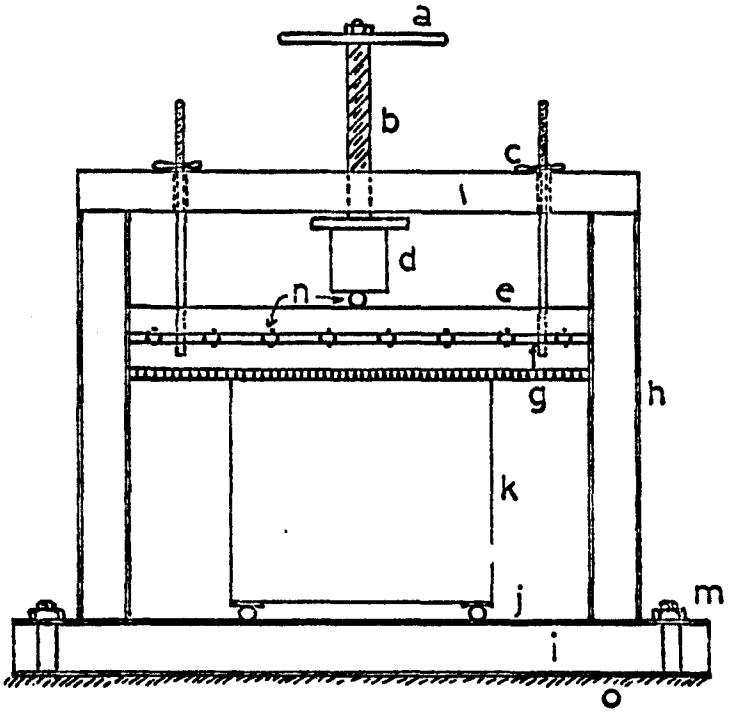

FIG. 4a LOADING FRAME

a LOADING BAR
b LOADING SCREW
c HOLDING BAR
d LOAD CELL
ef CROSS BEAMS
g RUBBER
h VERTICAL MEMBER
i BOTTOM I-BEAM
j ROLLER SUPPORT
k MODEL
l SOLID TOP BEAM
m FIXING NUT
n 3/4" DIAMETER BALL
o FLOOR

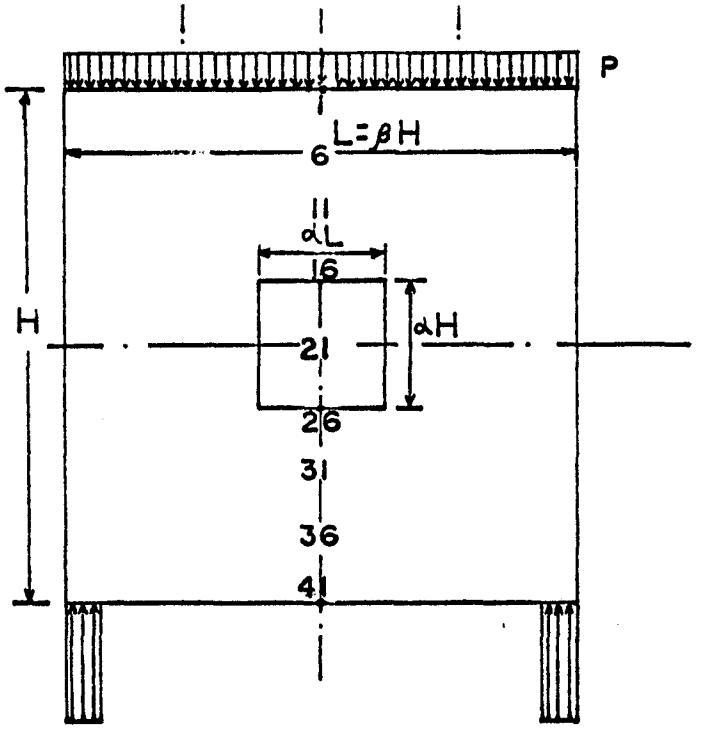

FIG. 4b MODEL

CASES STUDIED
P-UDL AT TOP
P-UDL AT BOTTOM
Q-AT CENTRE
Q-AT QT. POINTS
β = L/H = 2/3, 1, 3/2
α = 0, 1/4, 1/5, 1/2
SUPPORT WIDTH L/16
ONE CASE L/8
ONE CASE L/20

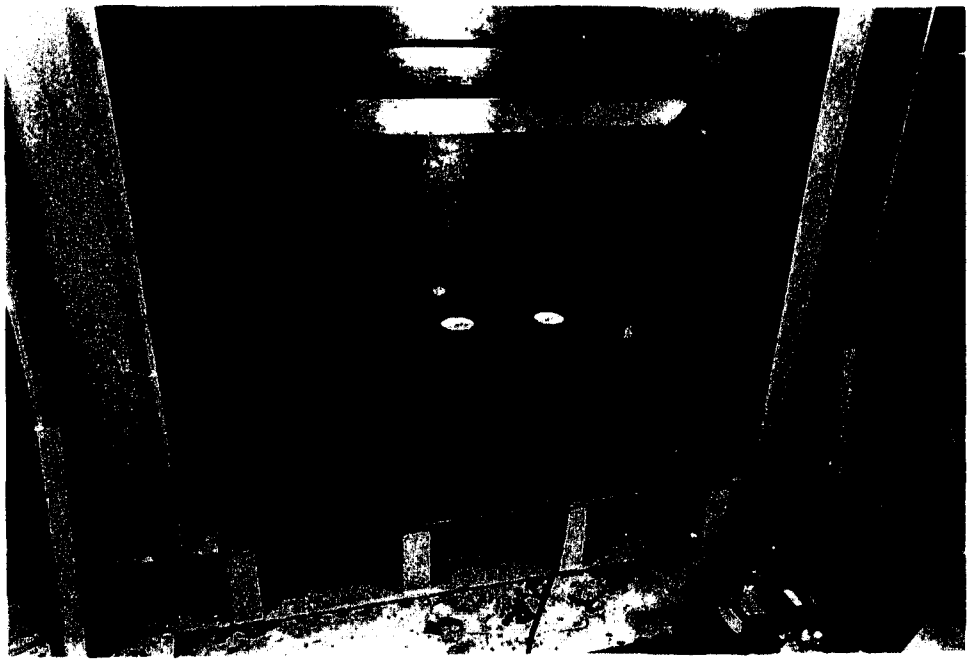

(a)

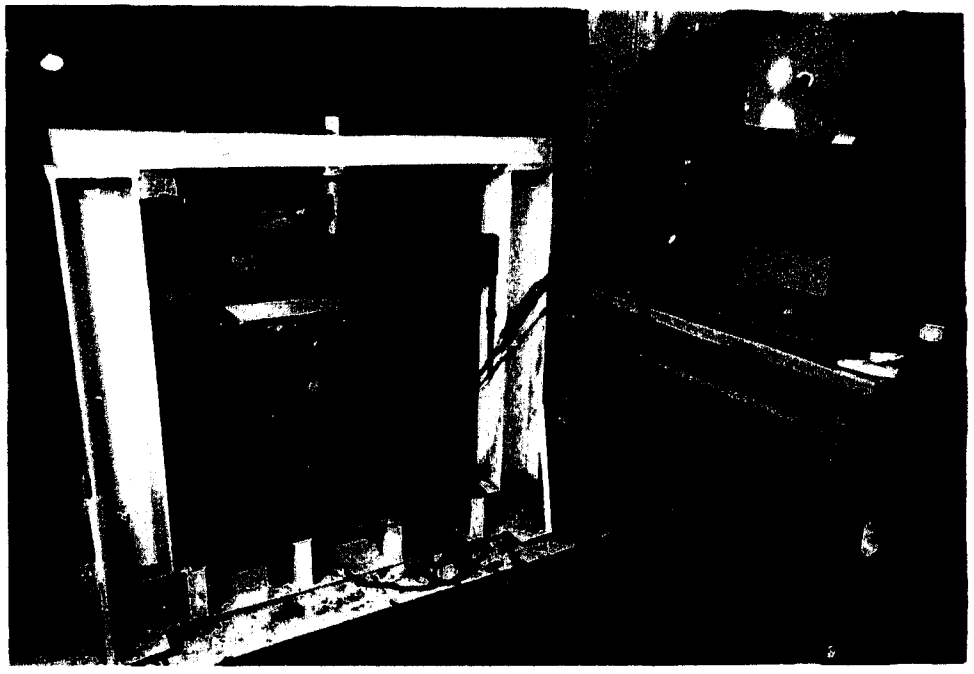

(b)

Fig.5

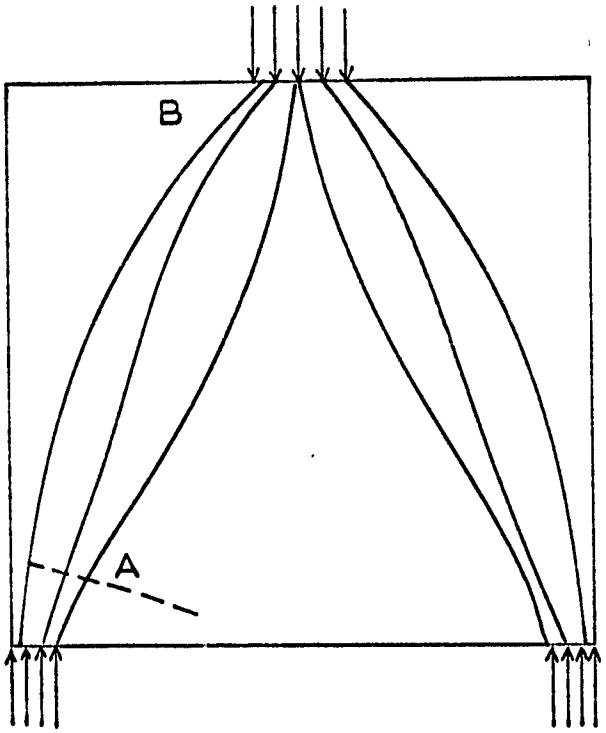

(a)

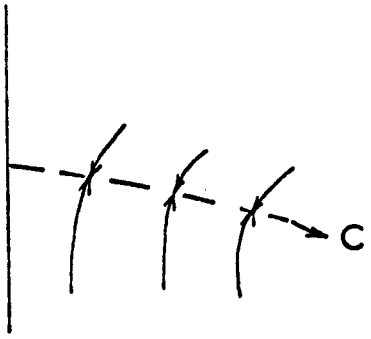

(b)

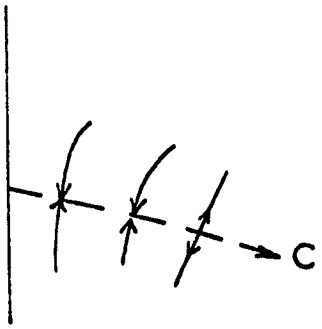

(c)

Fig. 6

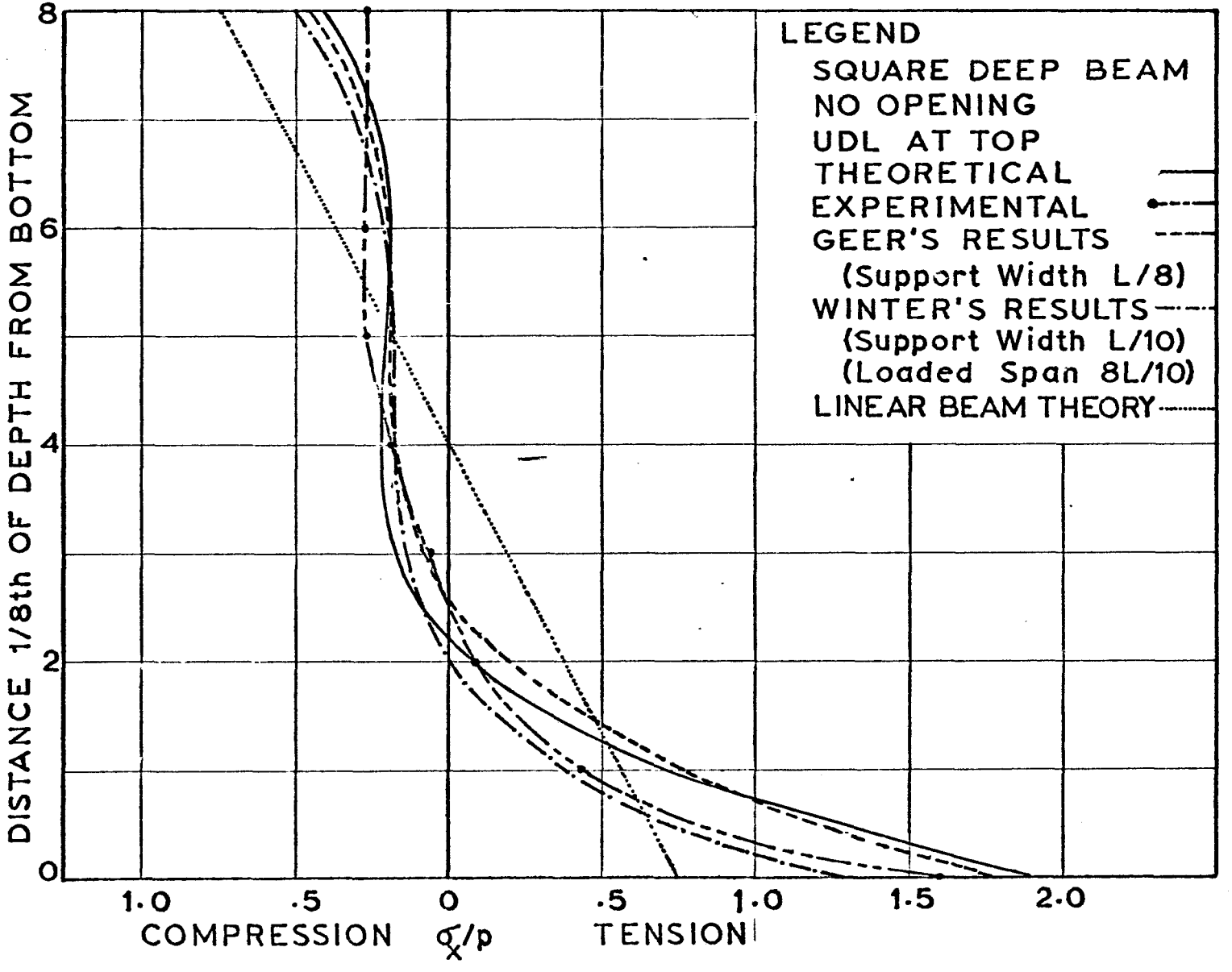

Fig.7a. Longitudinal Stresses at mid-section of a Solid Square Deep Beam for UDL at Top

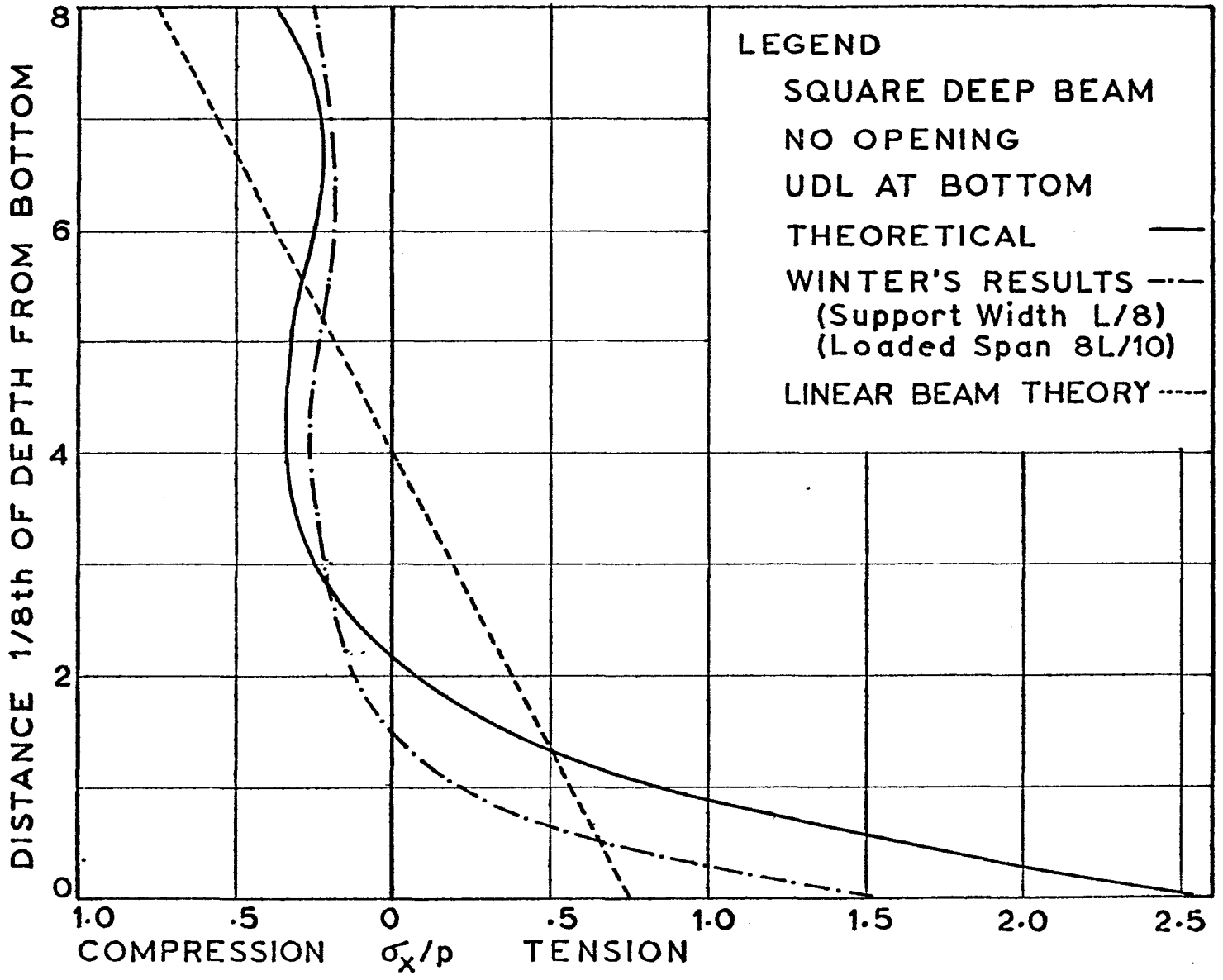

Fig. 7b. Longitudinal Stresses at mid-section of a Square Beam for UDL at Bottom

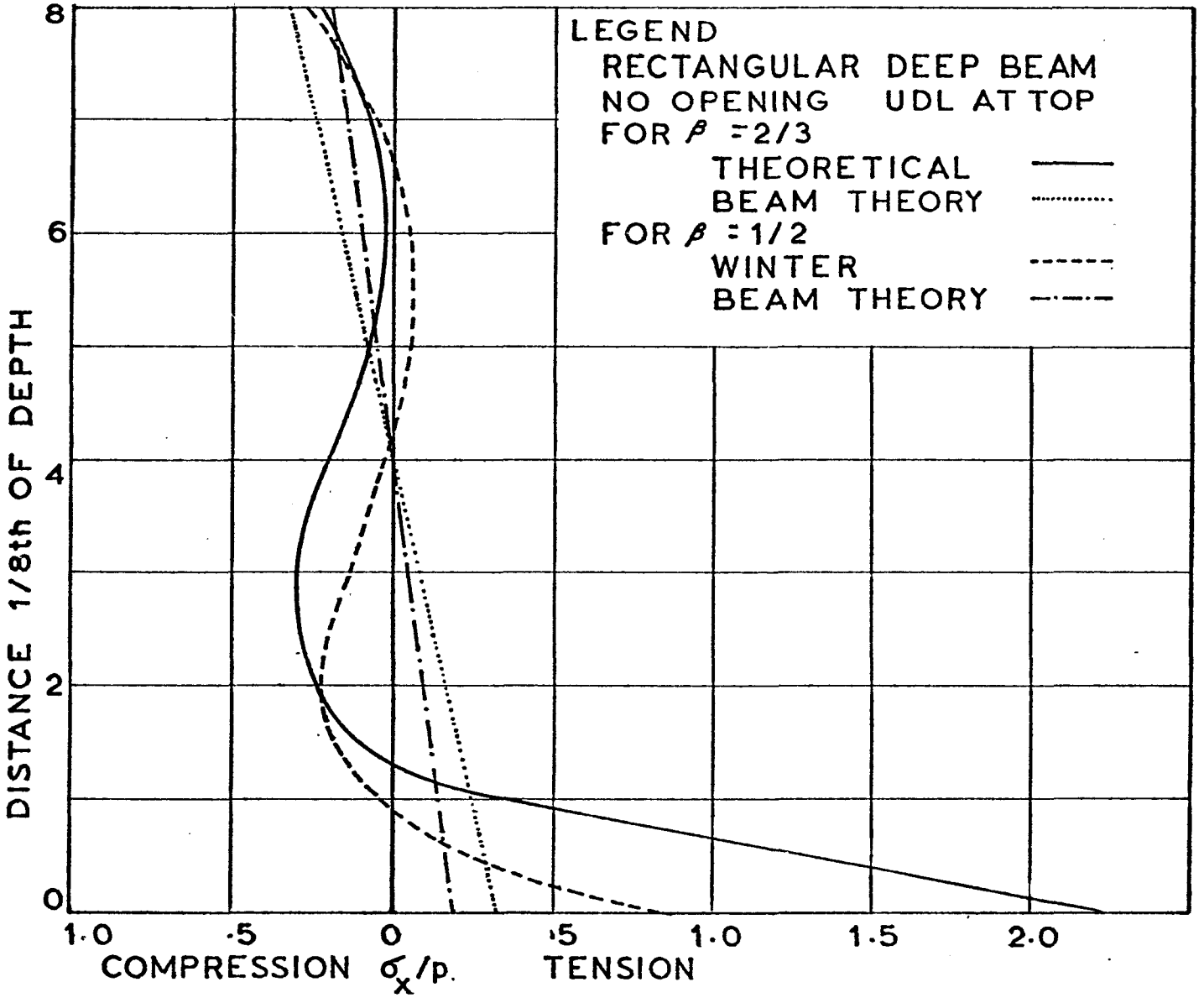

Fig.8a. Longitudinal Stresses at mid-section of a Solid Rectangular Deep Beam

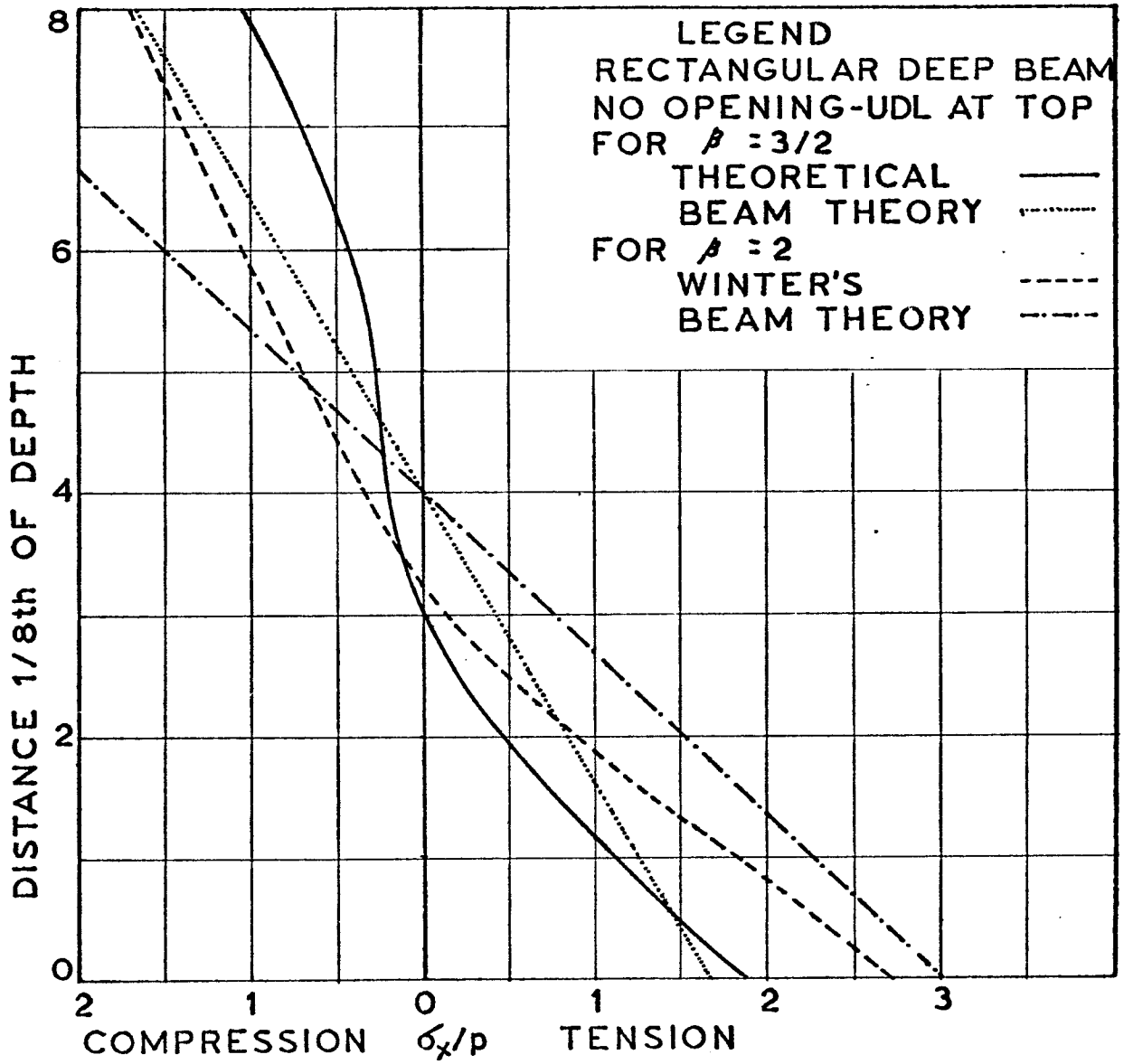

Fig.8b. Longitudinal Stresses at mid-section of a Solid Rectangular Deep Beam

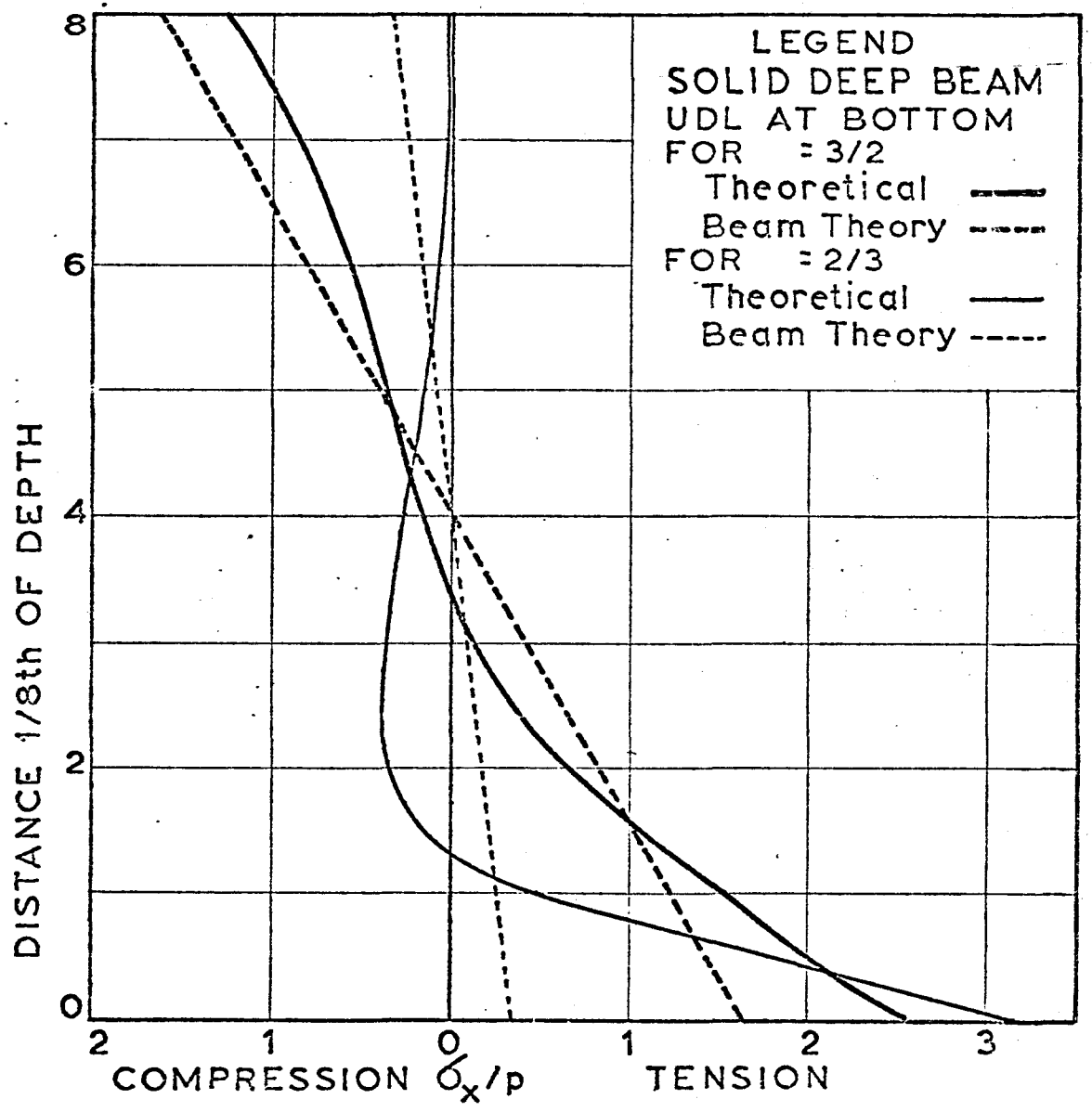

Fig.9. Longitudinal Stresses at mid-section of a Solid Rect. Deep Beam for UDL at Bottom

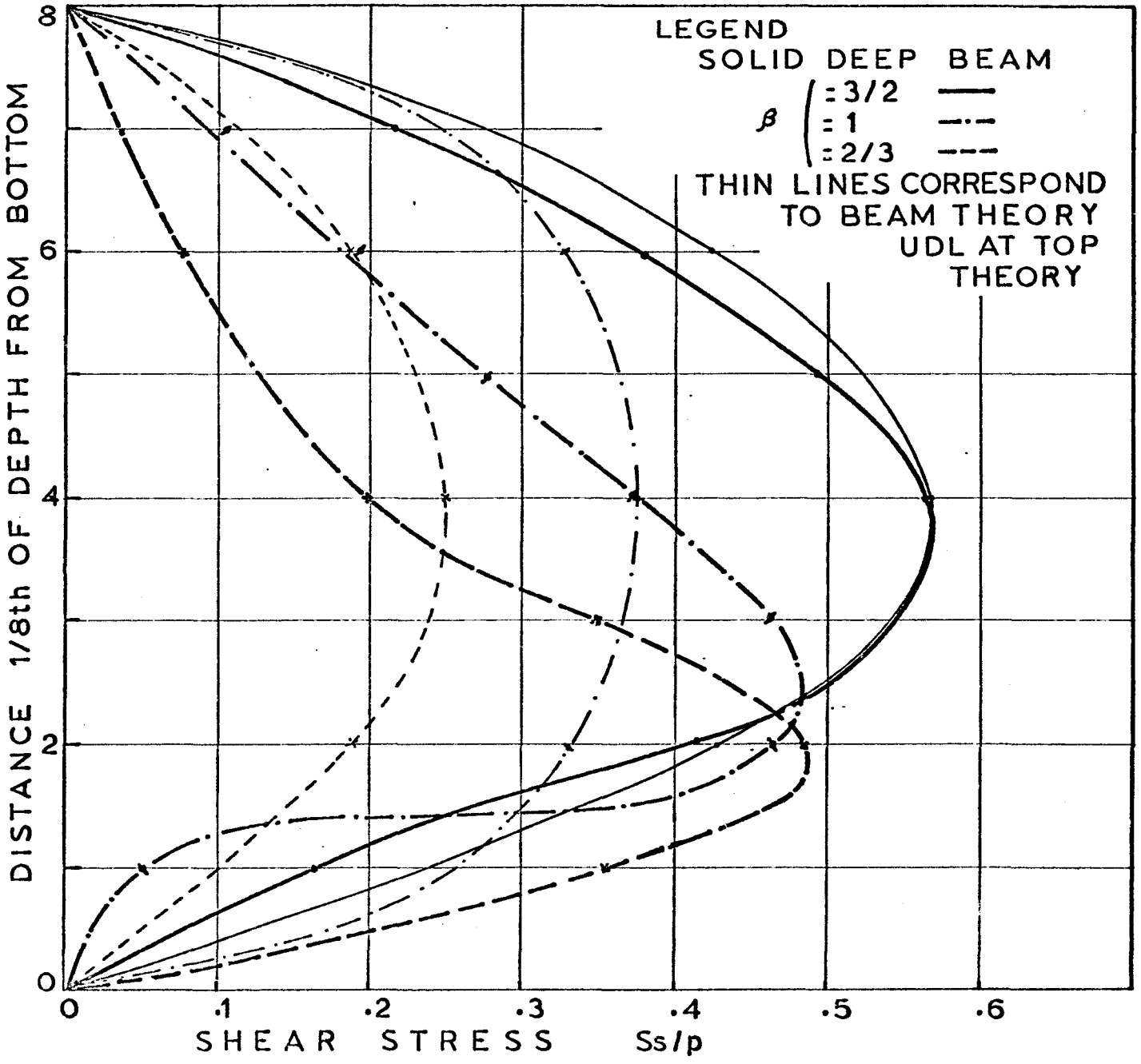

Fig.10 Shear Stress at Quarter Point for UDL at Top

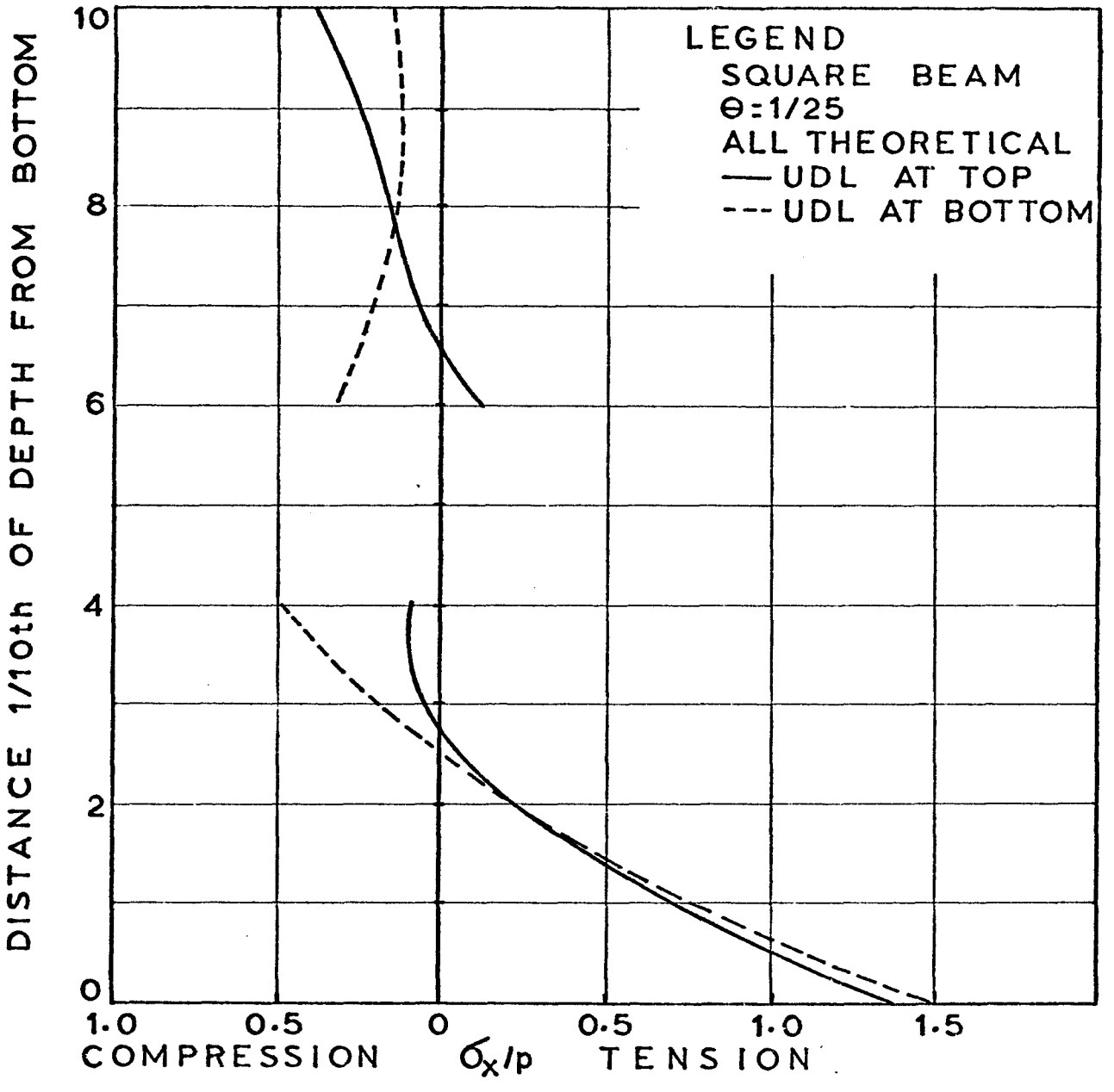

Fig.11 Longitudinal Stresses at mid-section Of Square Deep Beam with an Opening

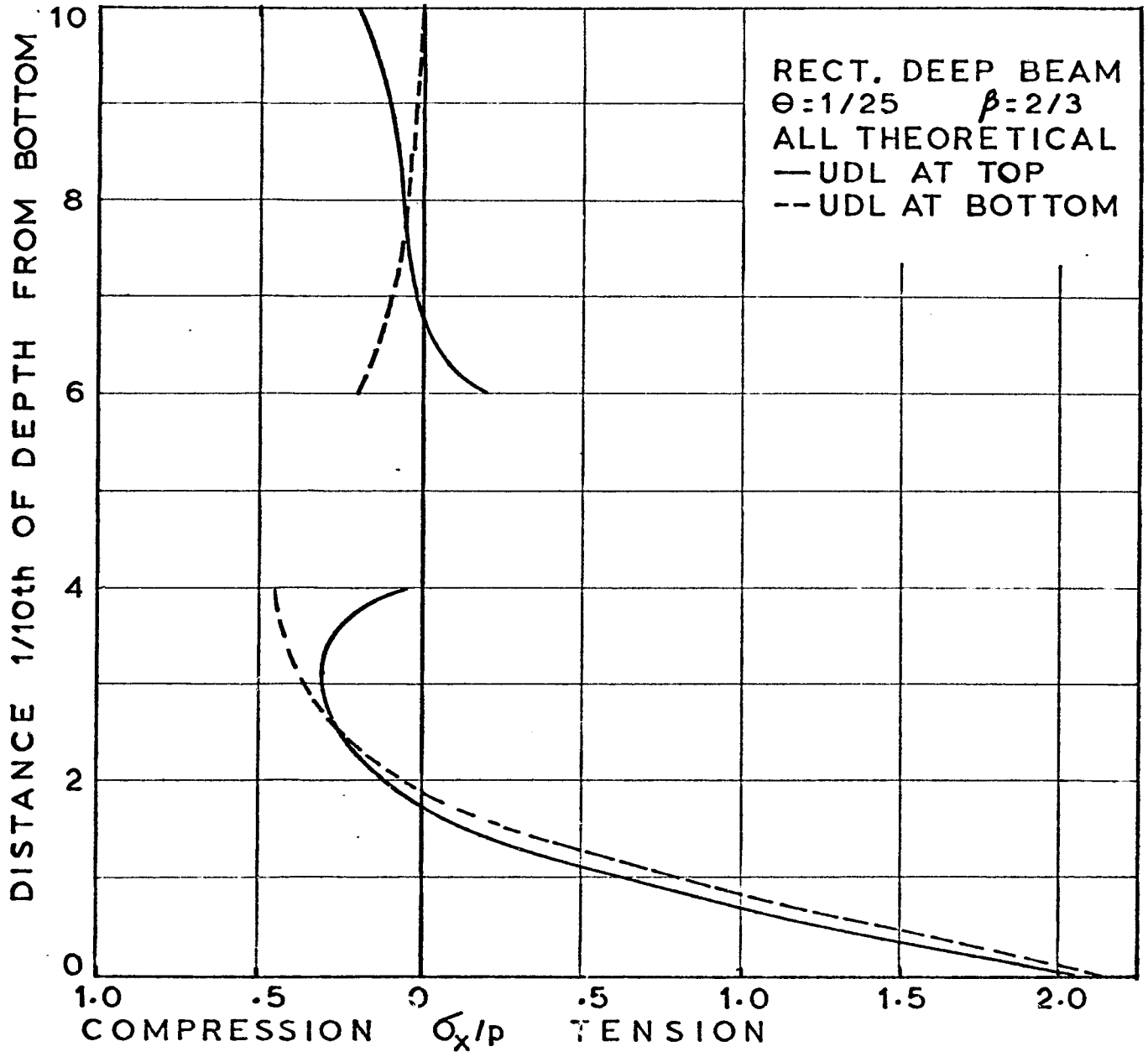

Fig.12 Longitudinal Stresses for a Rectangular Deep Beam with a Small Opening

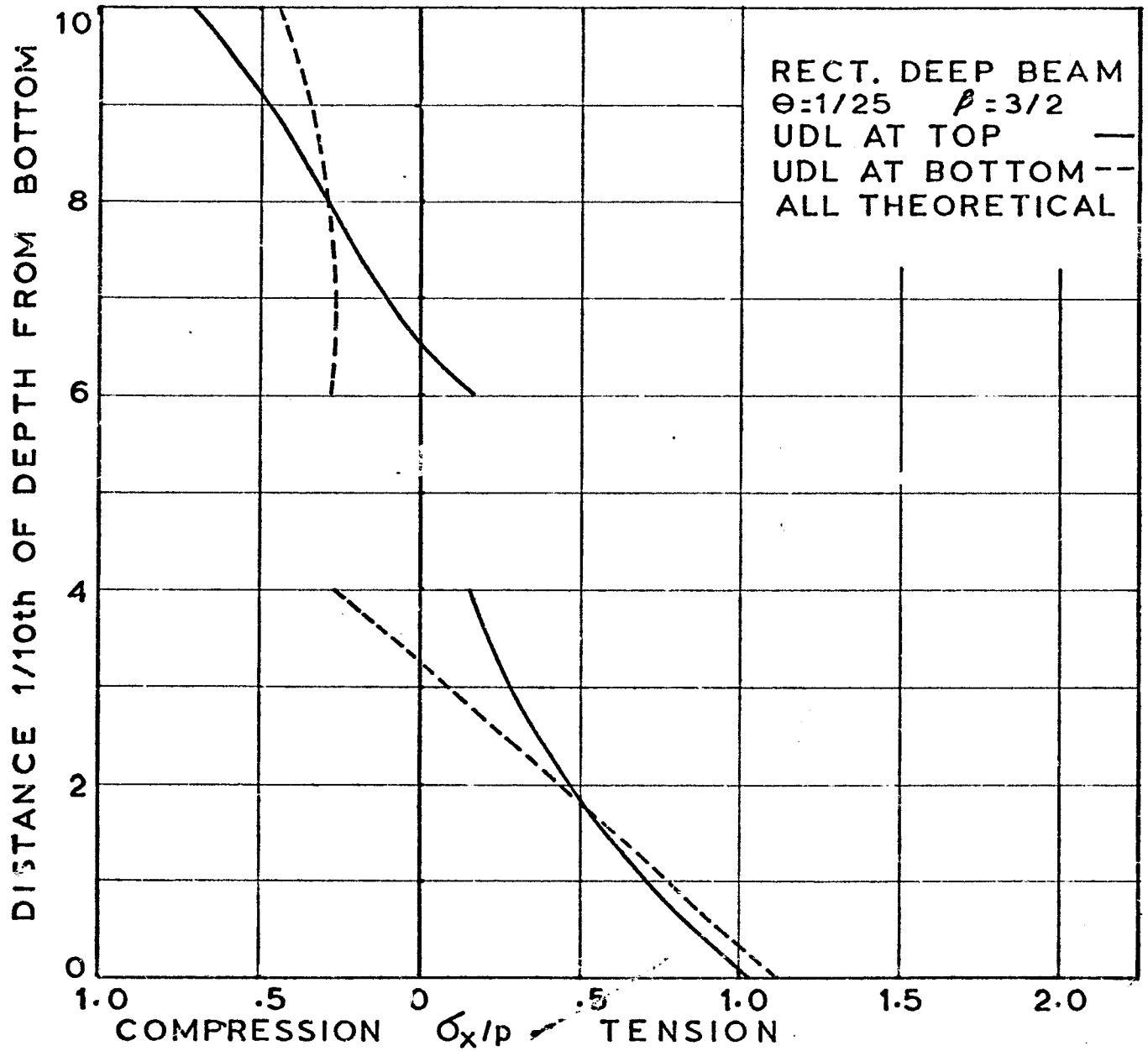

Fig.13 Longitudinal Stresses at mid-section of a Rect. Beam with a Small Opening

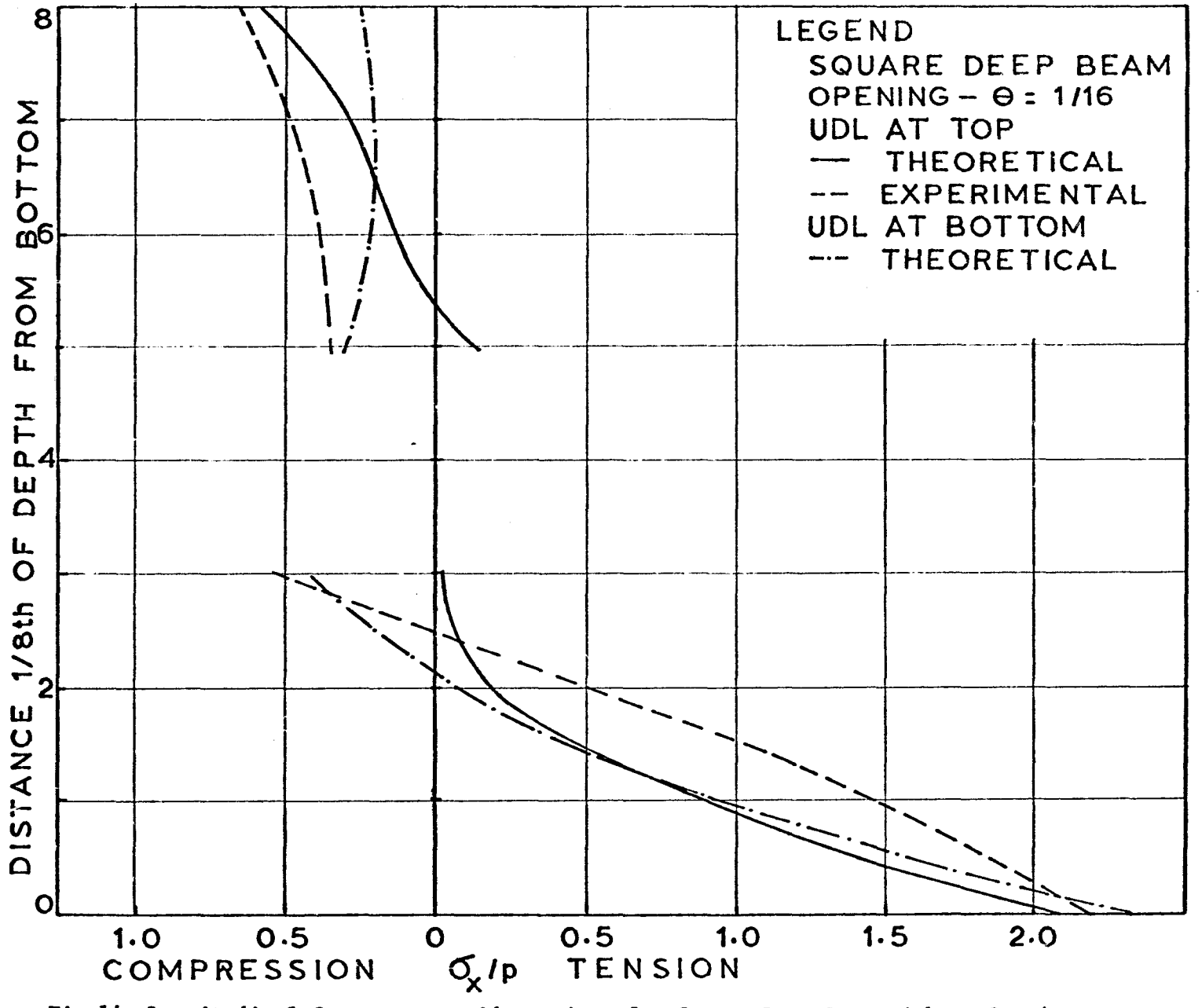

Fig.14 Longitudinal Stresses at mid-section of a Square Deep Beam with an Opening

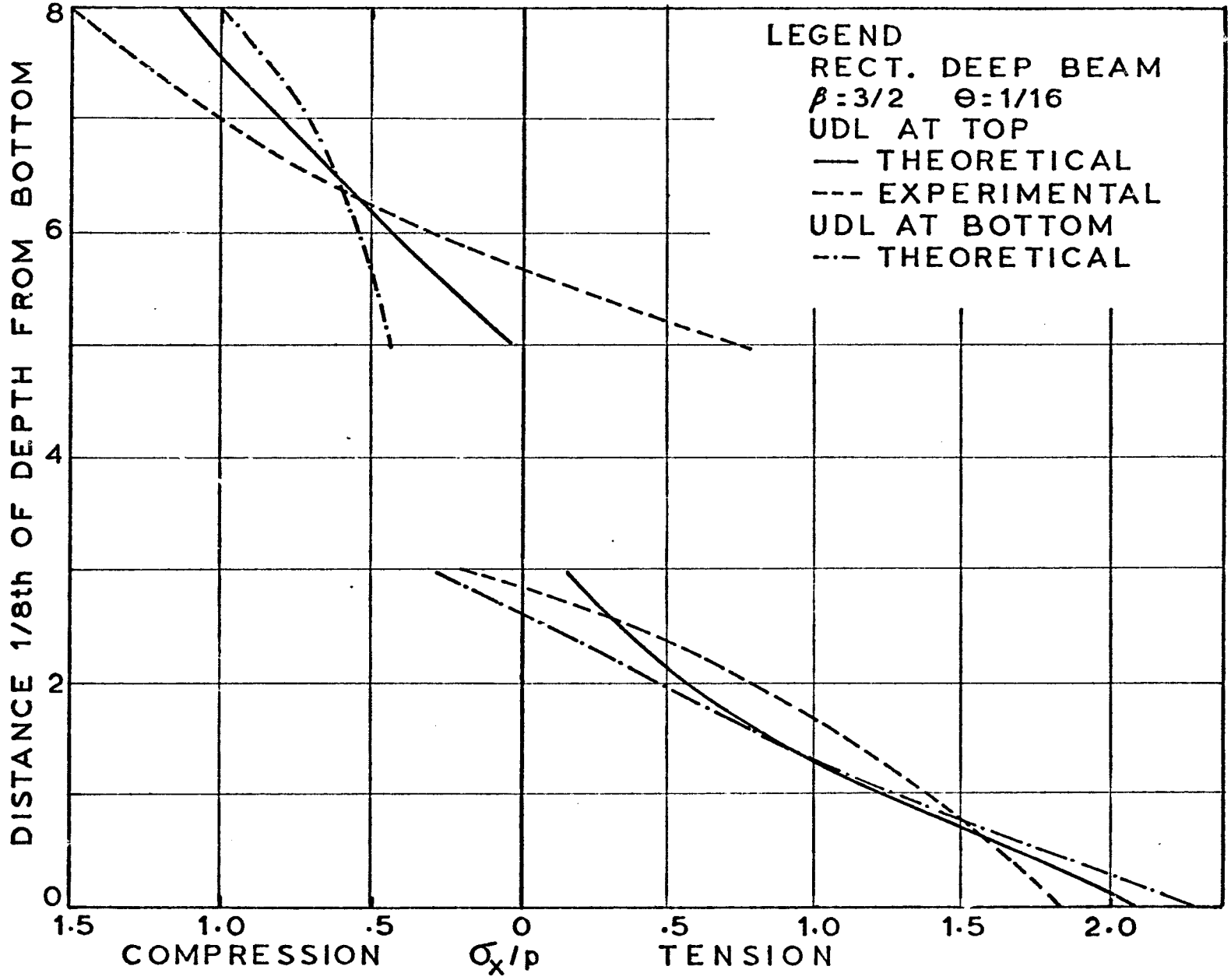

Fig.15 Longitudinal Stresses at mid-section of a Rect. Deep Beam with an Opening

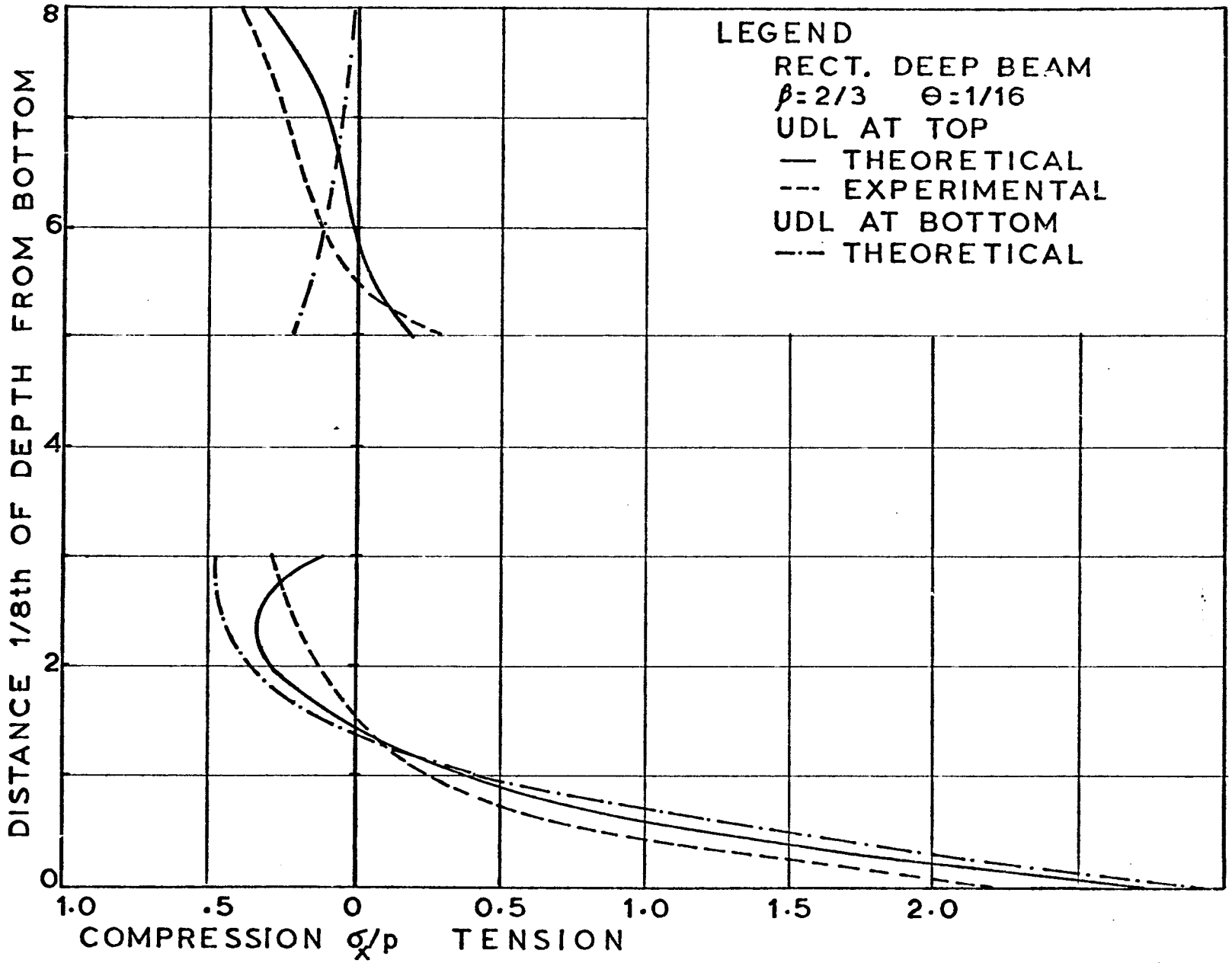

Fig.16 Longitudinal Stresses at mid-section of a Rect. Deep Beam with an Opening

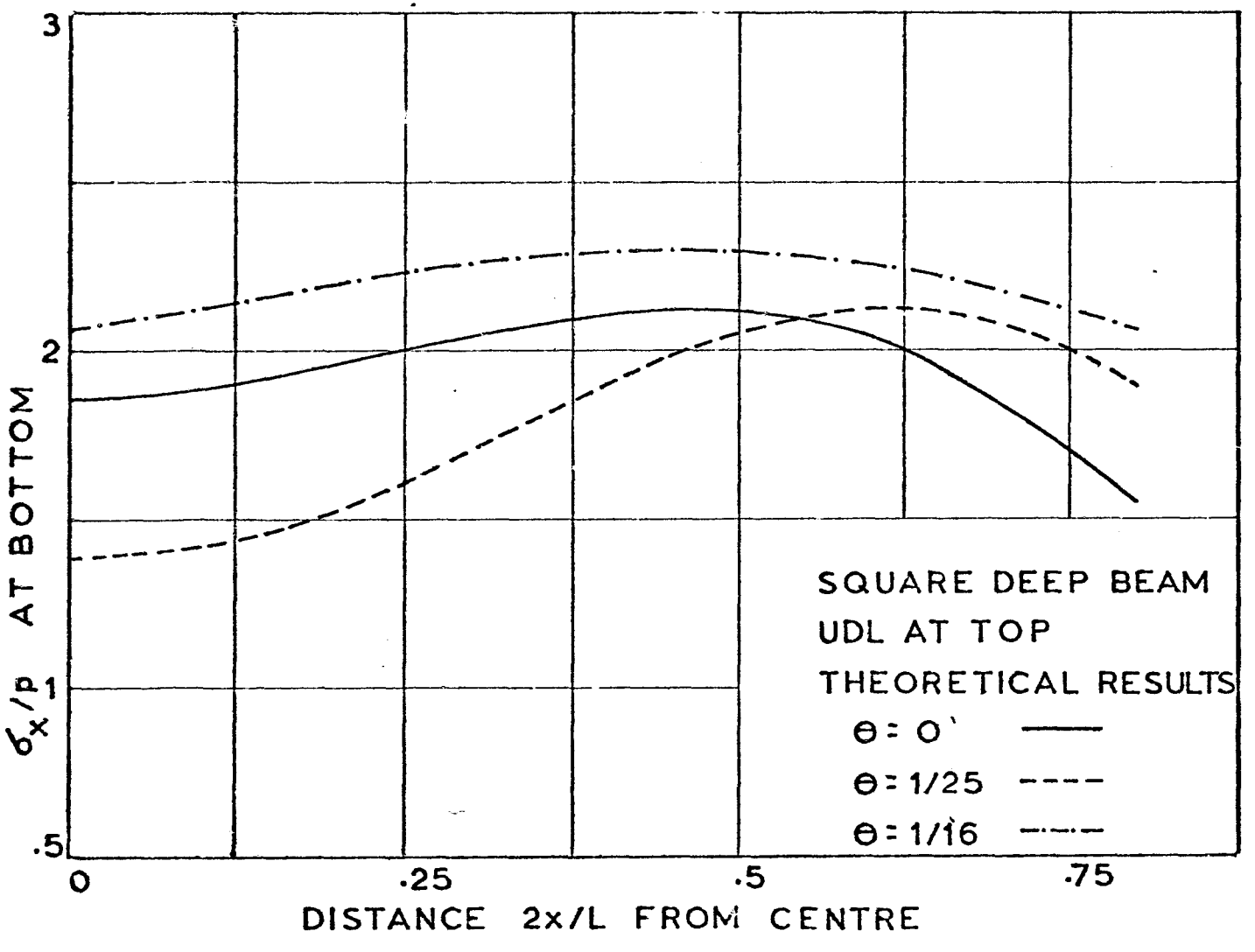

Fig.17 Variation of Bottom Tensile Stress of a Square Deep Beam along the Span

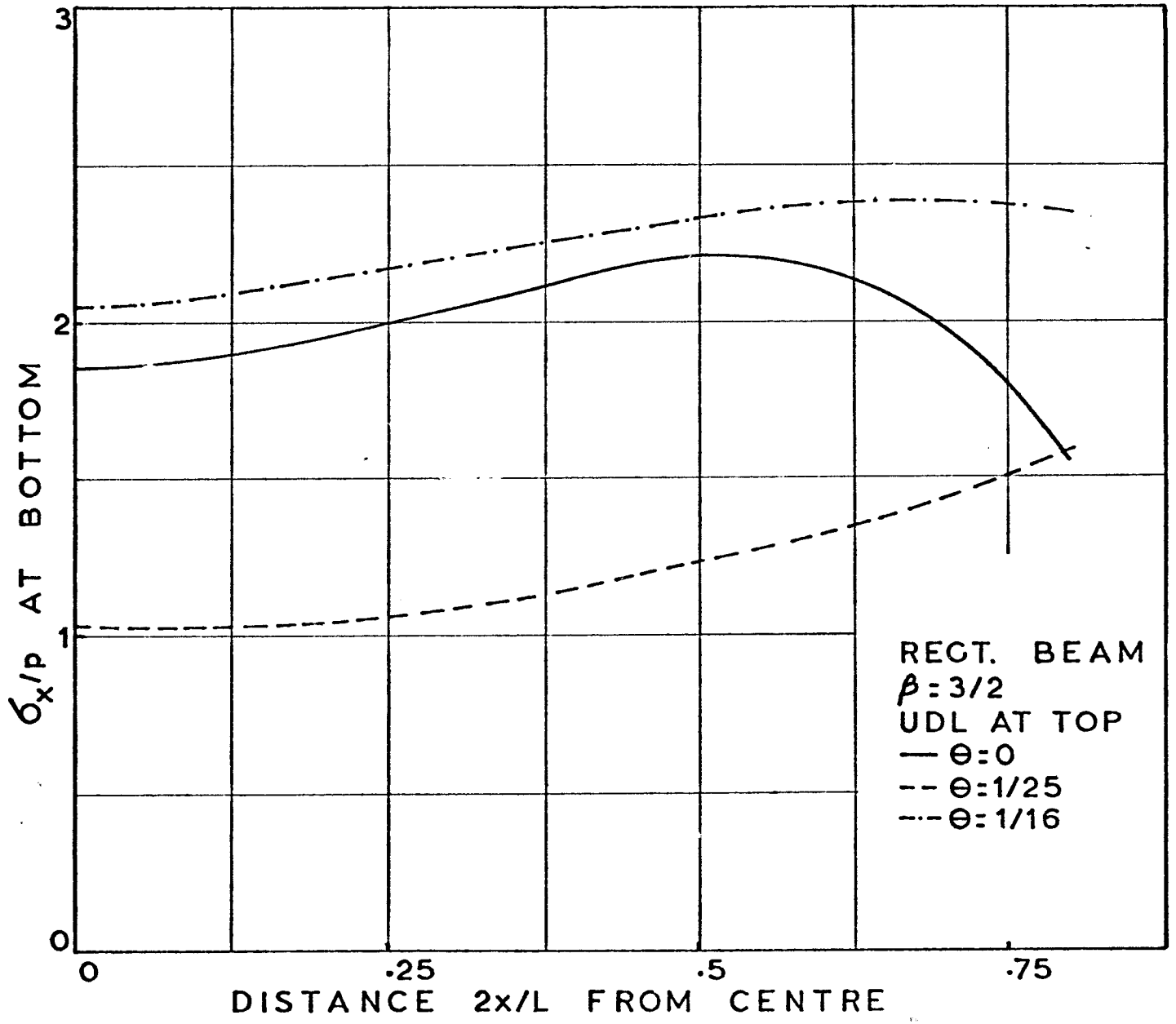

Fig.18 Variation of the Bottom Tensile Stress along the Span of a Rect. Deep Beam.

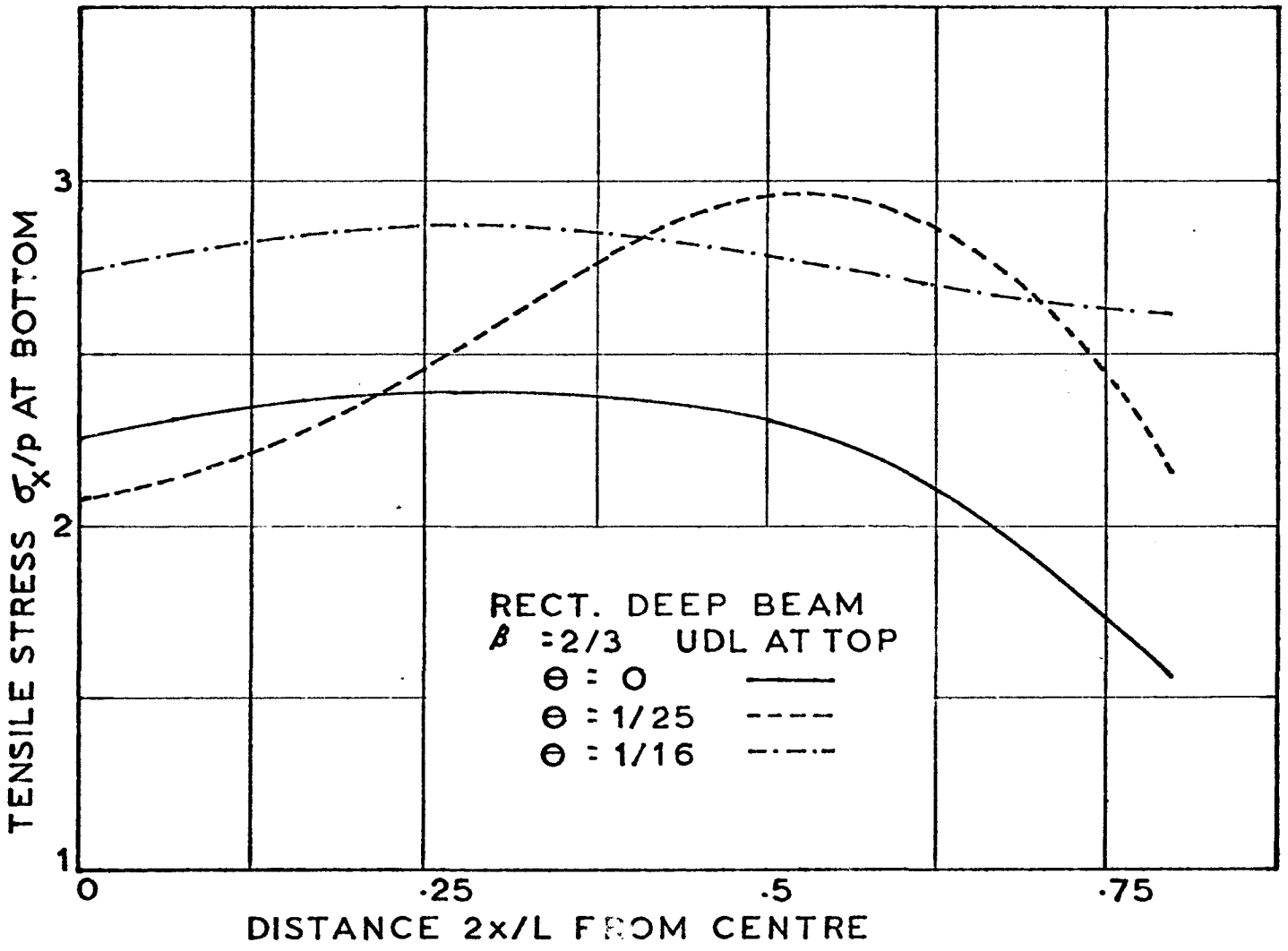

Fig.19 Variation of Bottom Tensile Stress of a Rect. Deep Beam along the Span

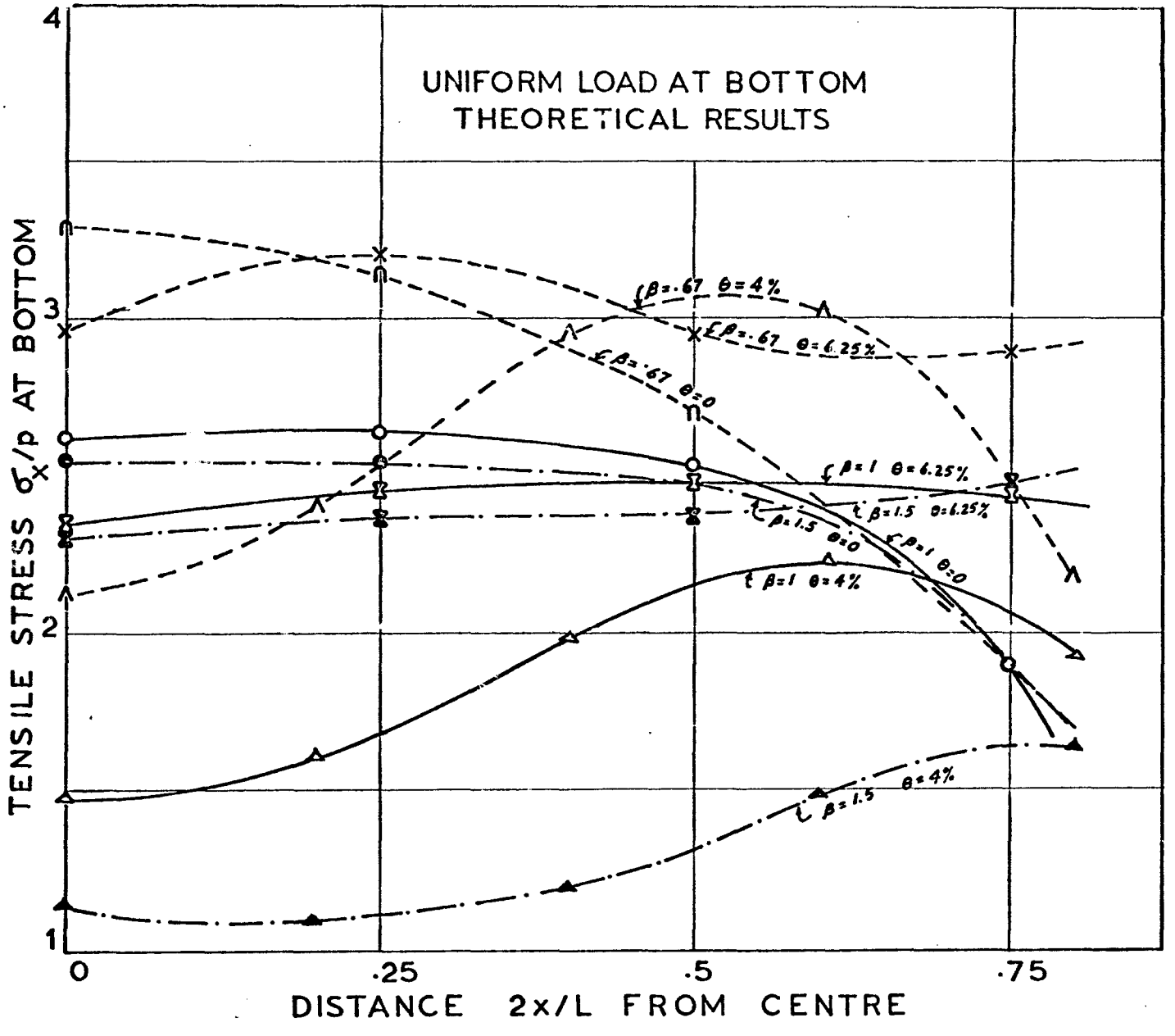

Fig.20 Variation of the Tensile Stress of a Deep Beam under UDL at Bottom

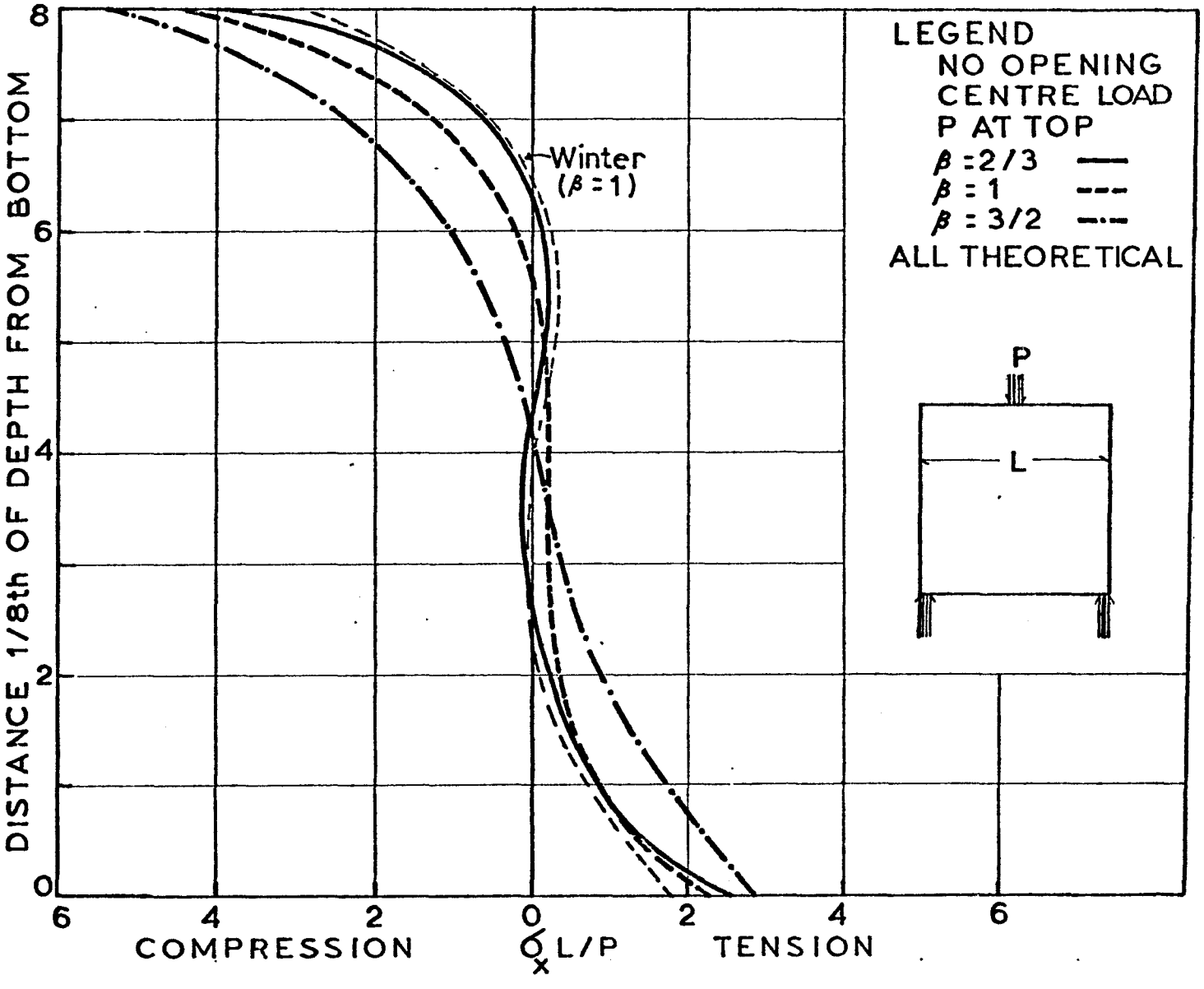

Fig.21 Longitudinal Stresses at mid-section of a Solid Deep Beam for a Pointed Load at Centre

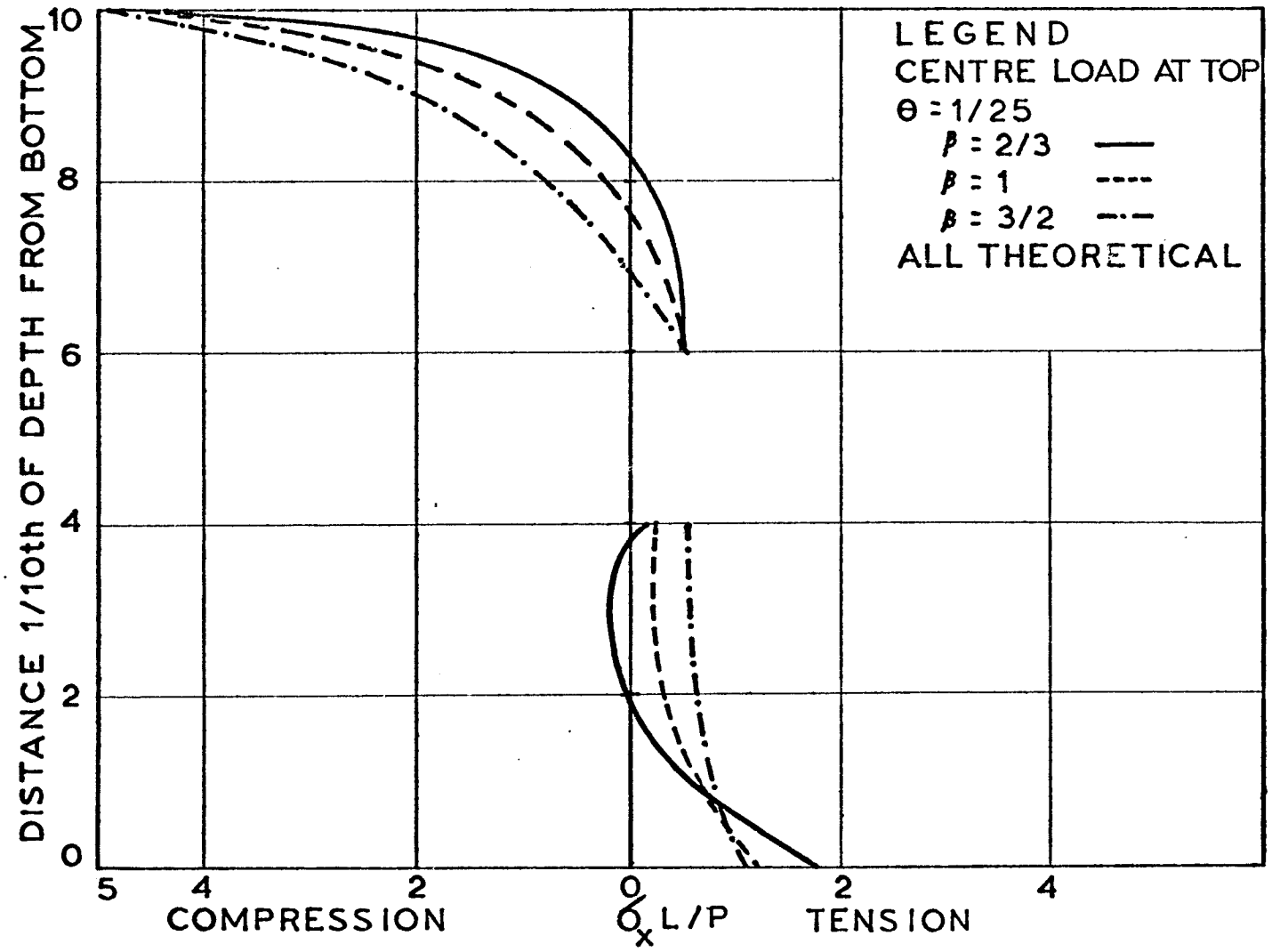

Fig.22 Longitudinal Stresses at mid-section of a Beam with a Small Opening for Load at centre

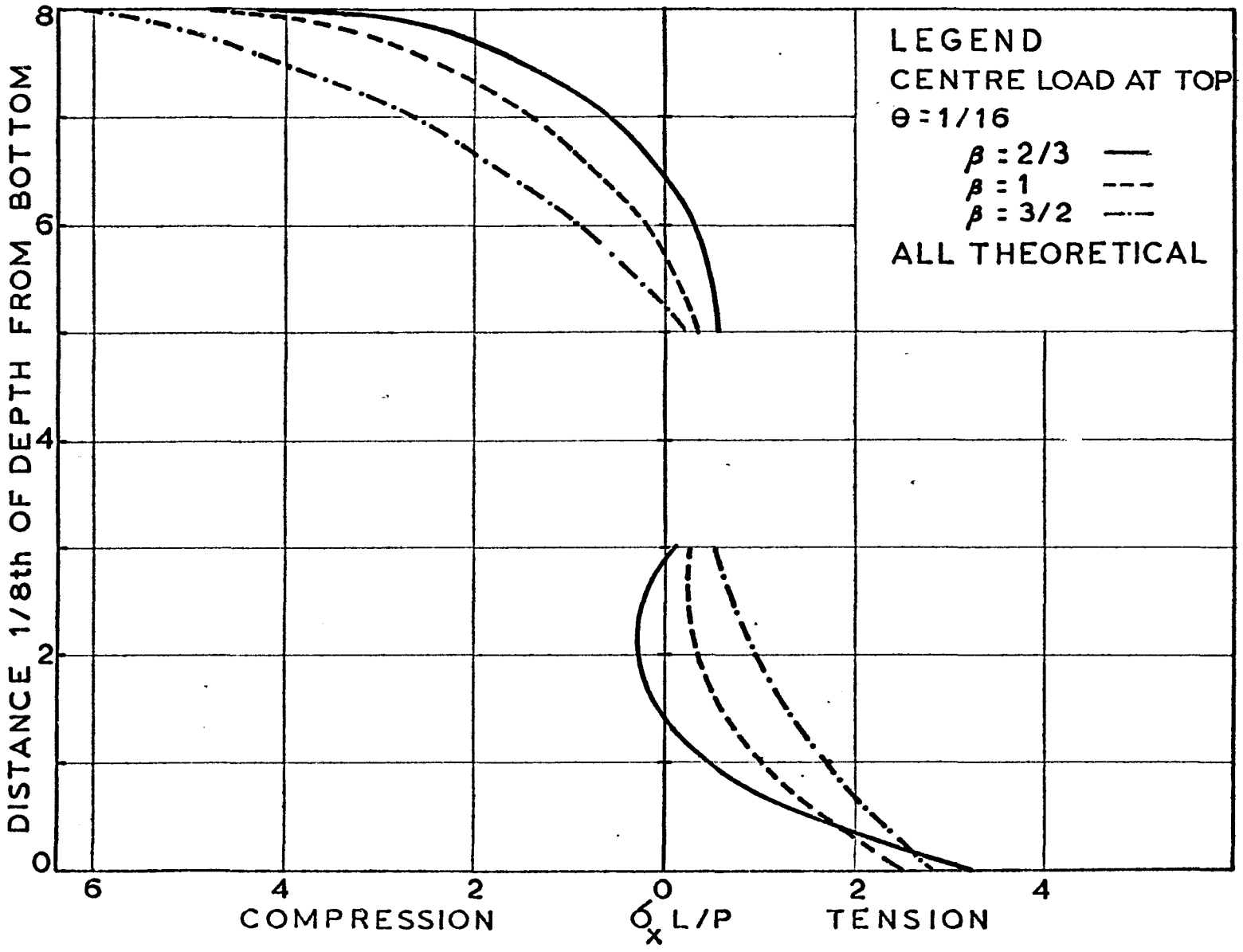

Fig.23 Longitudinal Stresses at mid-section for a Pointed Load at Centre.

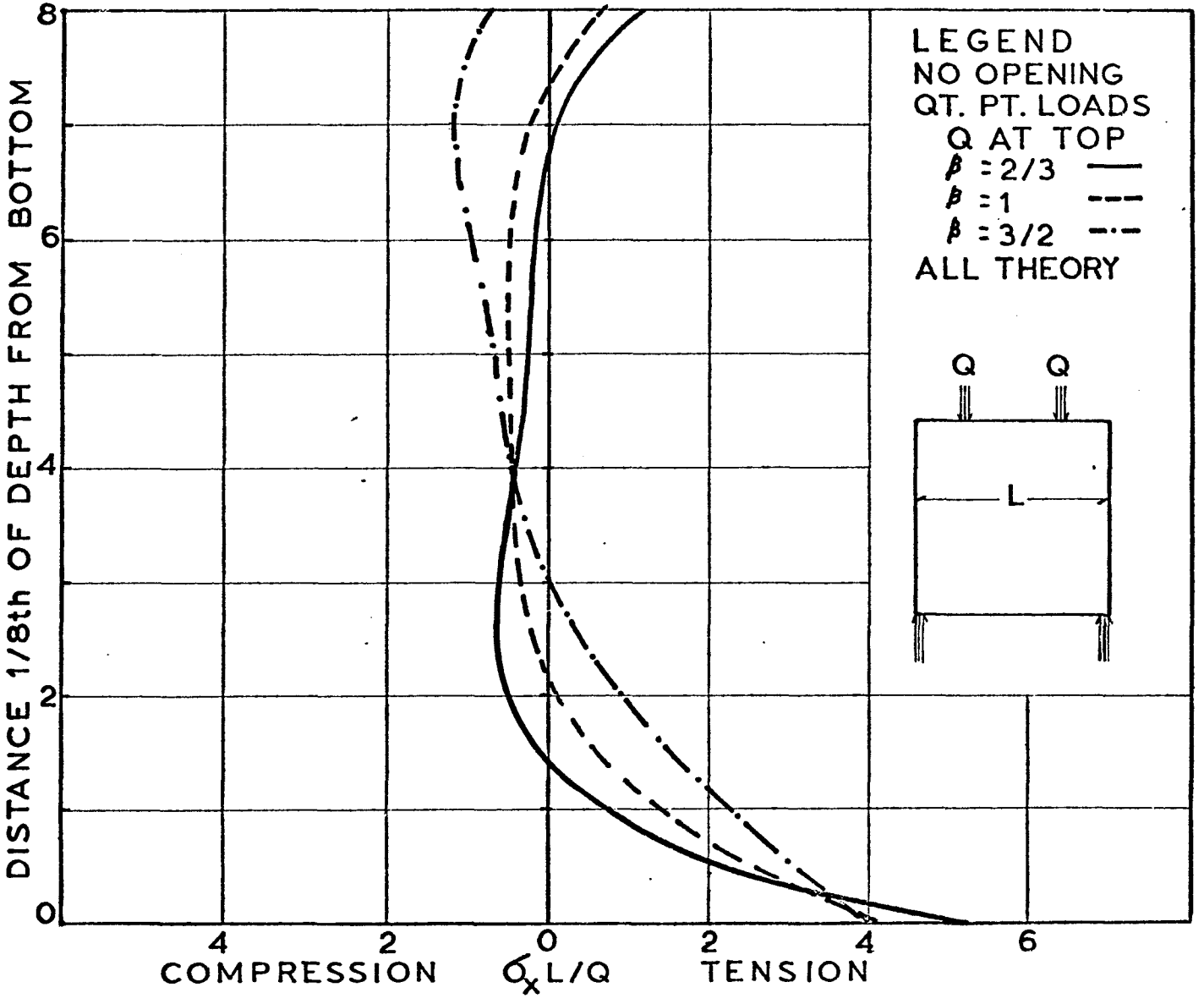

Fig.24 Longitudinal Stresses at mid-section of a Beam under Quarter Point Loads

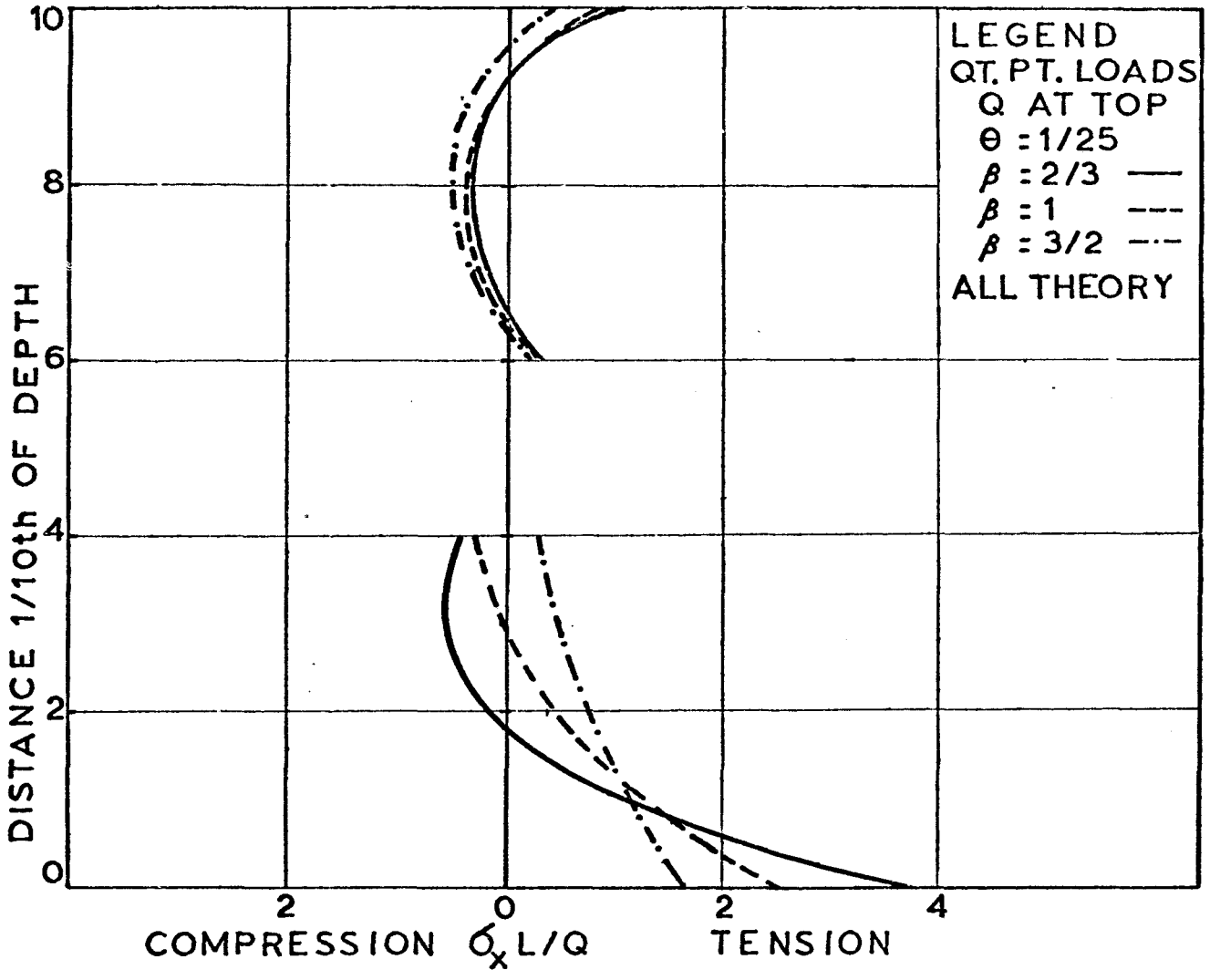

Fig.25 Longitudinal Stresses at mid-section of a Beam with an Opening

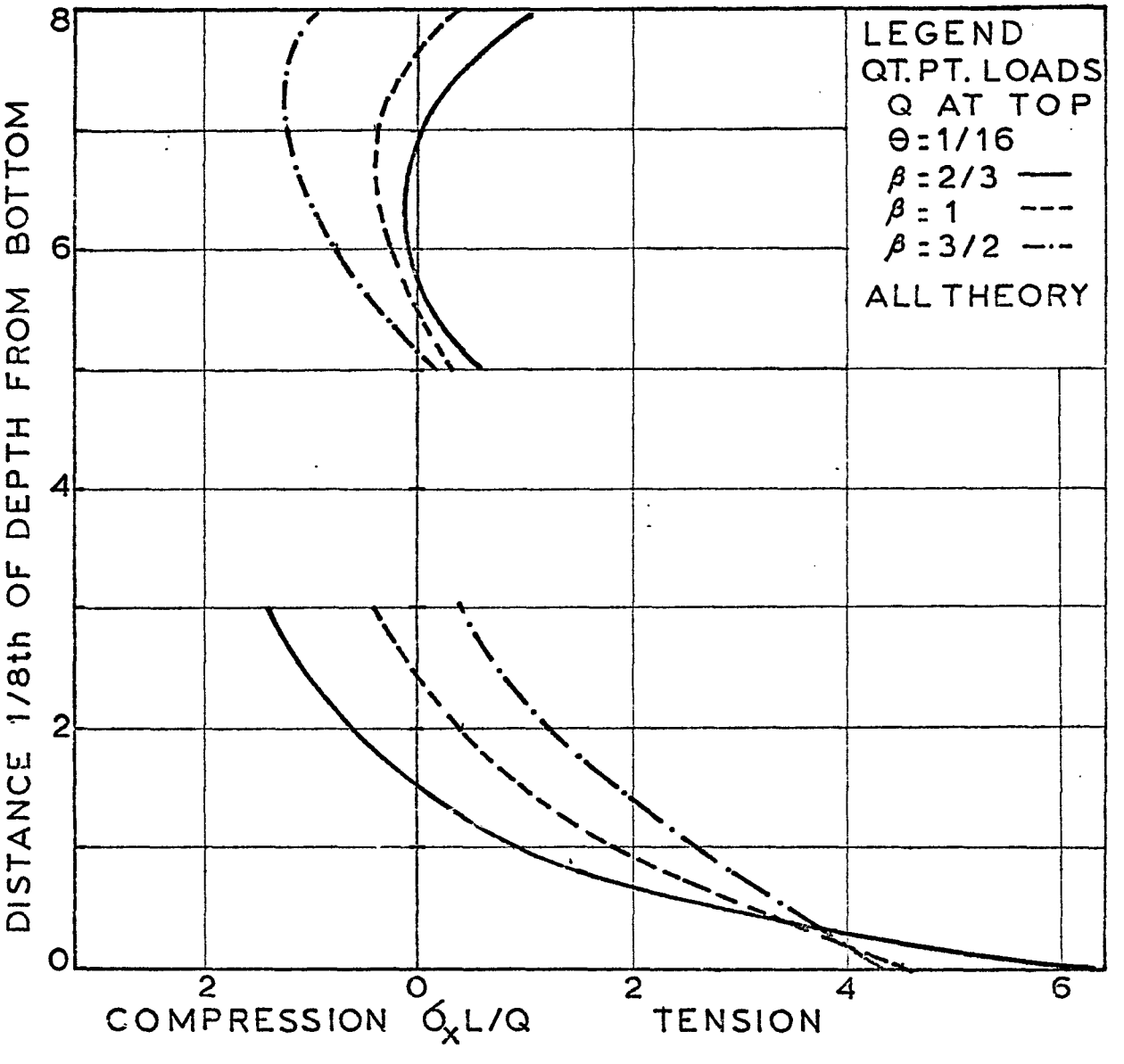

Fig.26 Longitudinal Stresses at mid-section for Qt. Point Loads

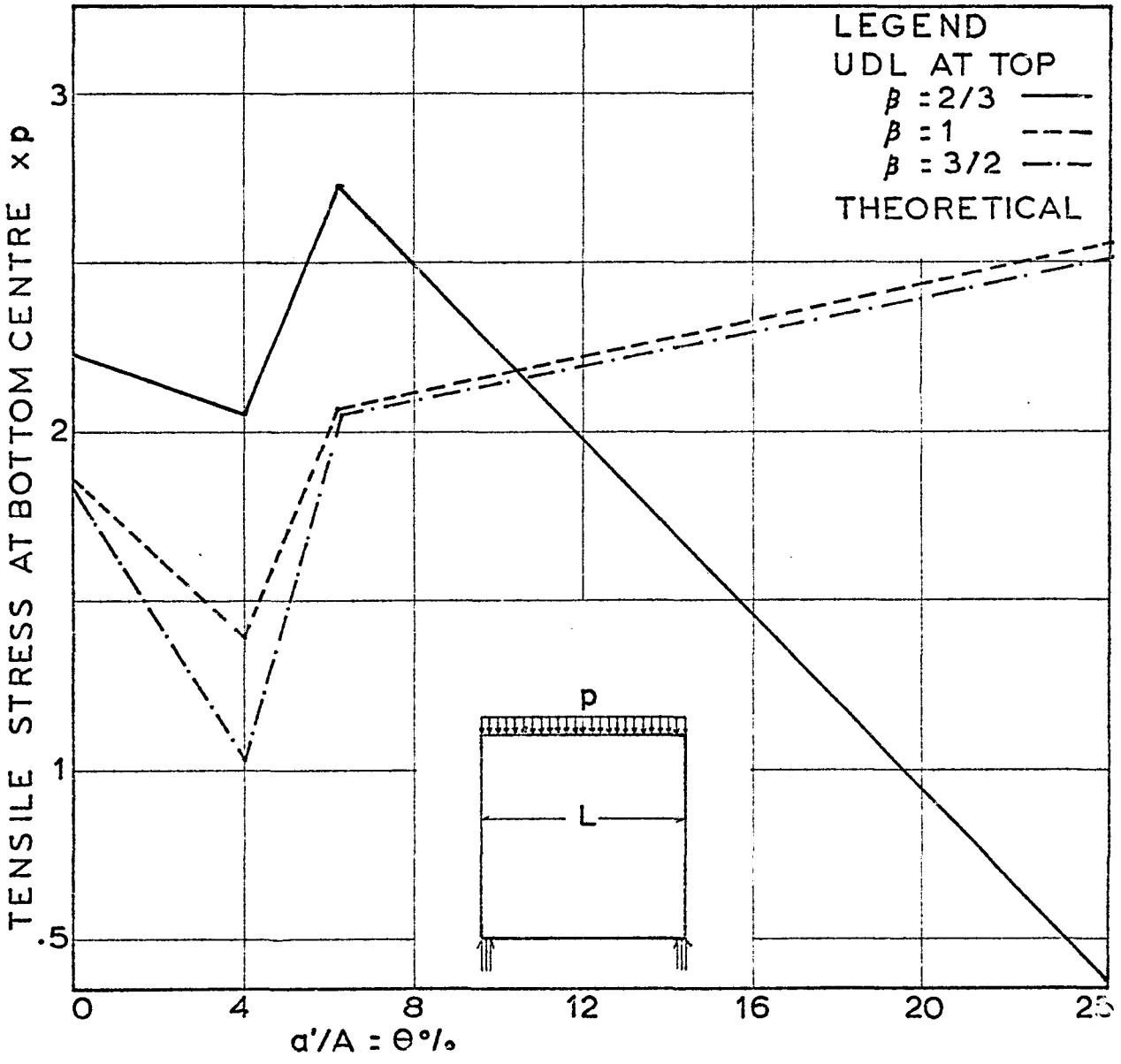

Fig.27 Variation of Centre-tension with Size of Opening for UDL at Top

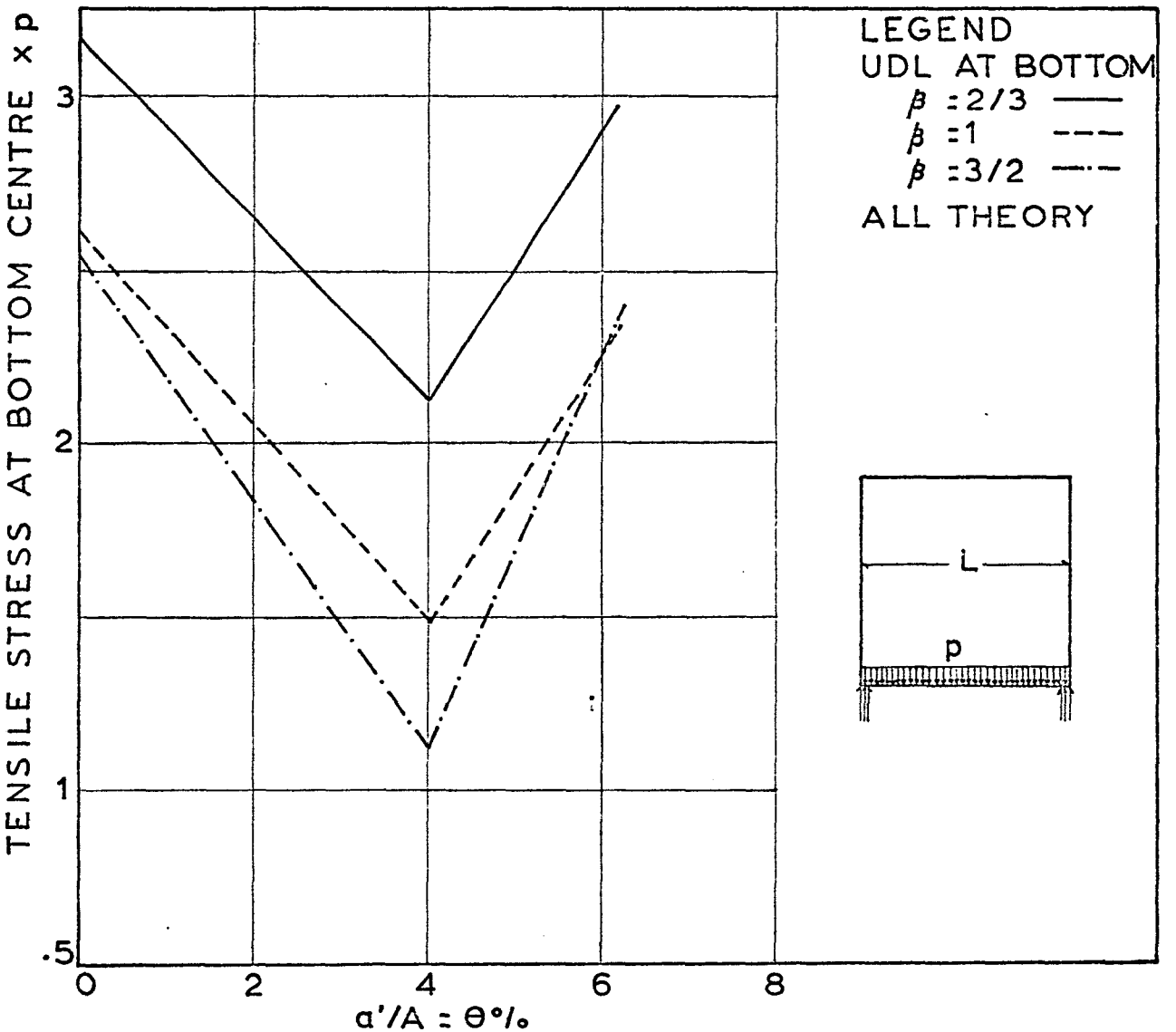

Fig.28 Variation of Centre-tension with Size of Opening for UDL at Bottom

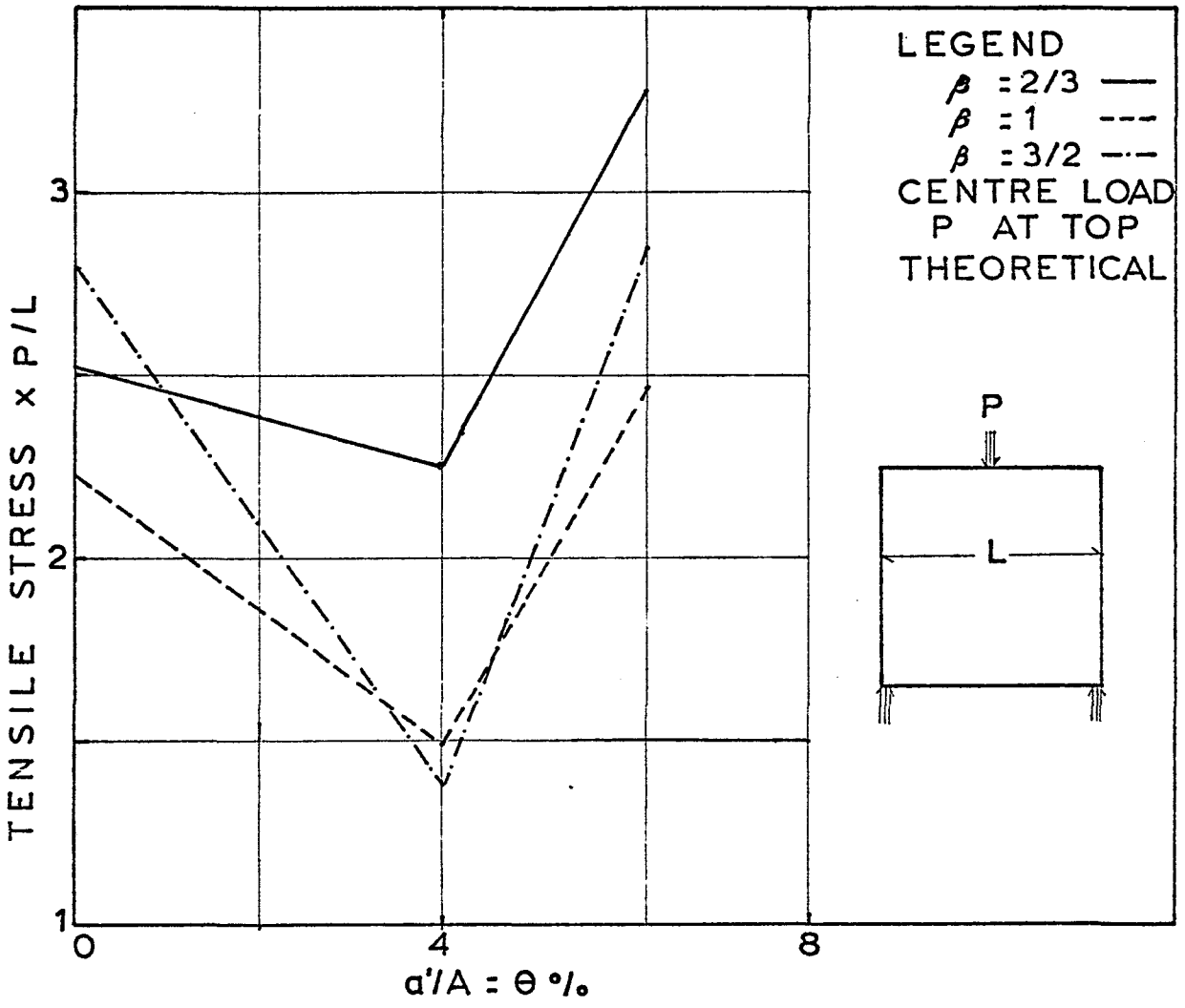

Fig.29 Variation of Centre-tension with Size of Opening for a Point Load at centre

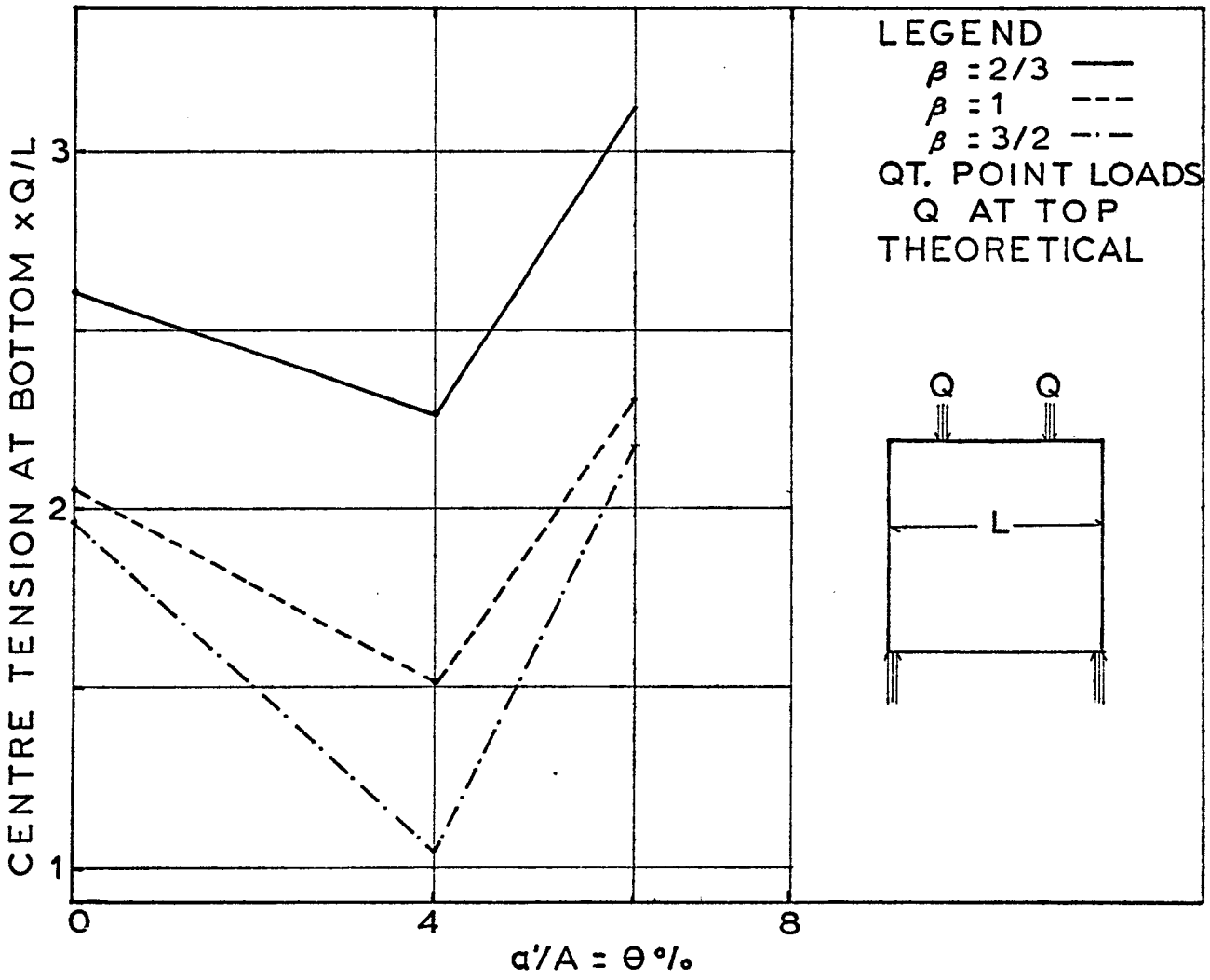

Fig.30 Variation of Centre-tension with Size of Opening for Quarter Point Loads

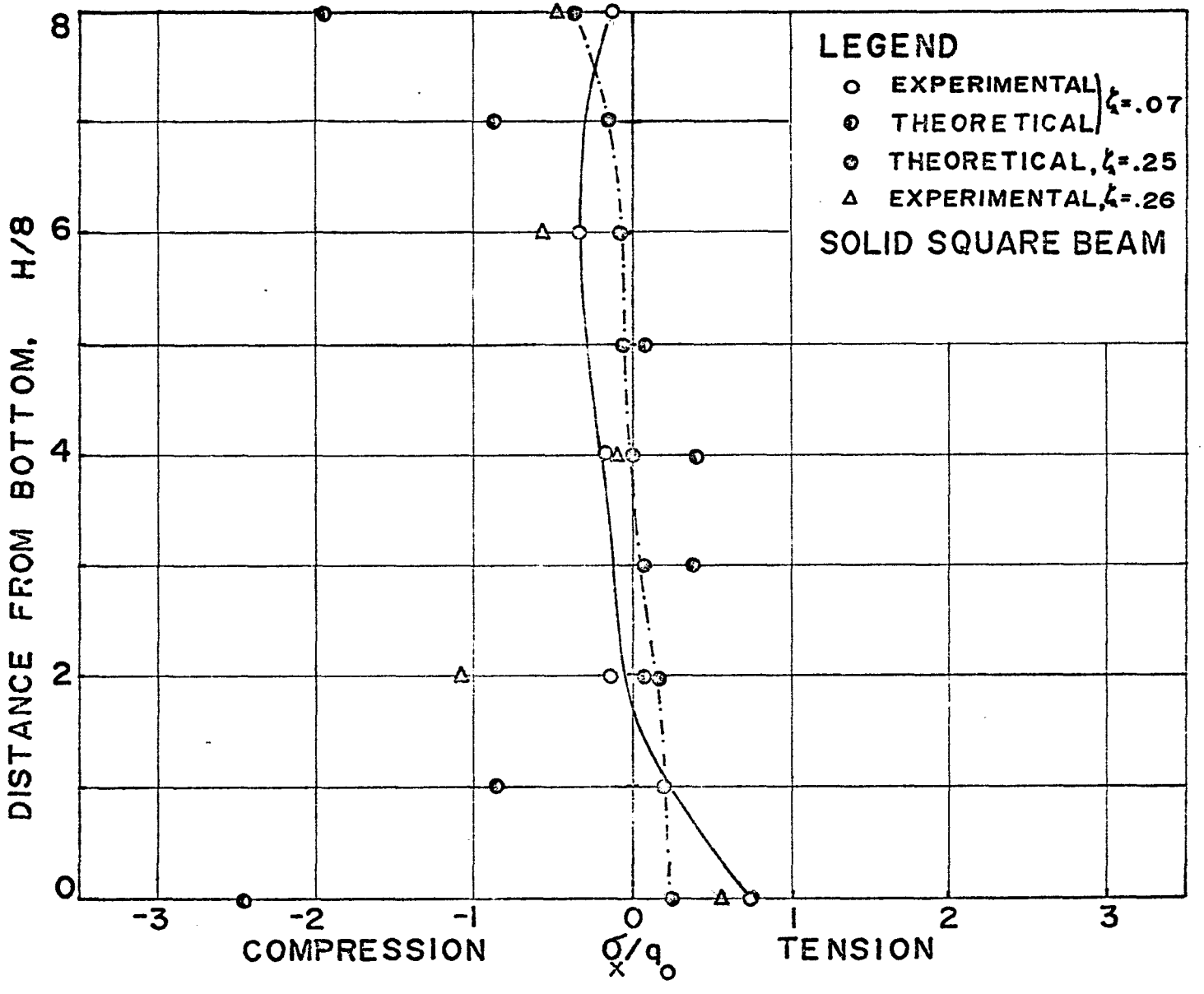

Fig.31 Longitudinal Stresses at mid-section of a Stiffened Sq. Deep Beam

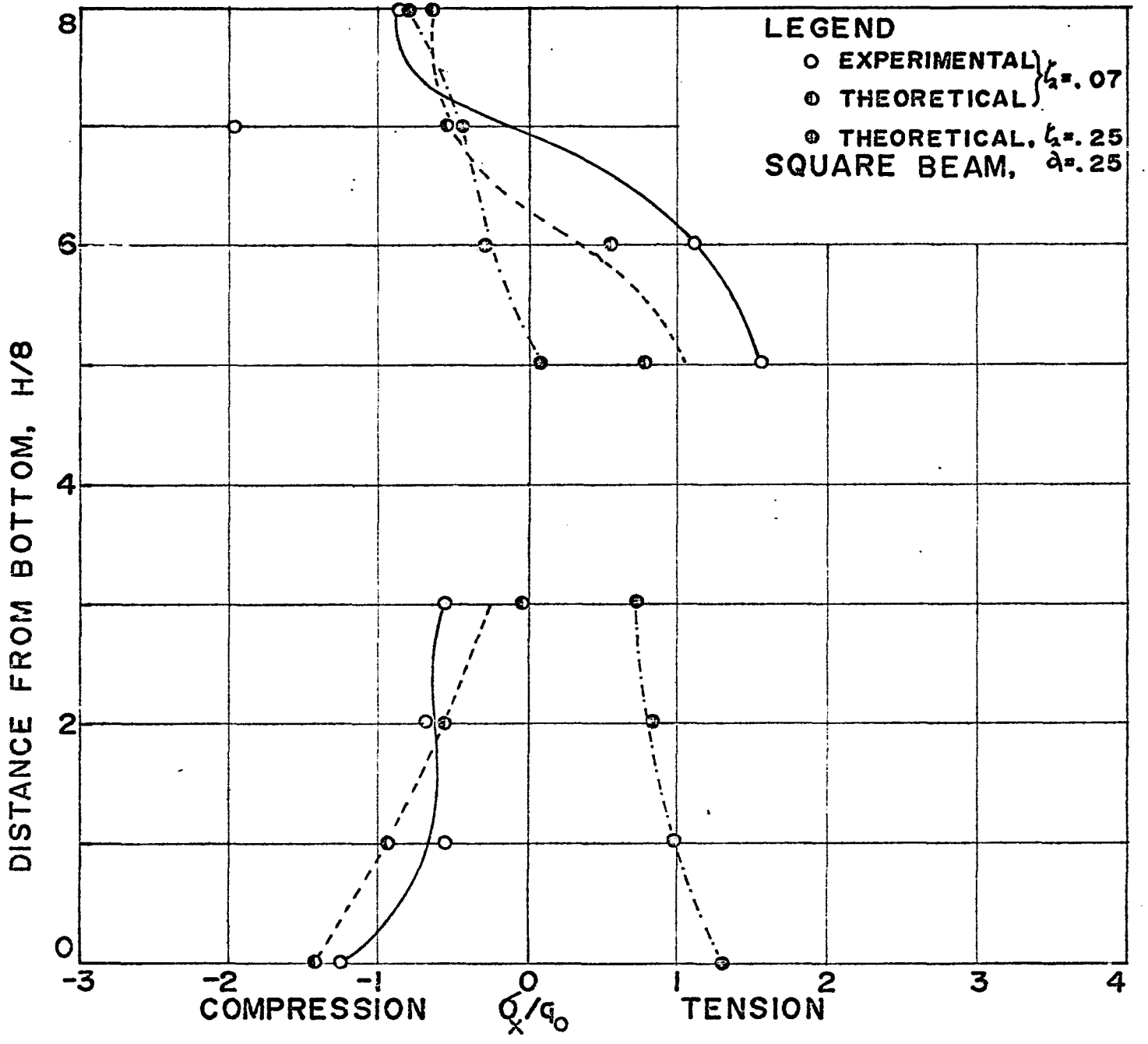

Fig.32 Longitudinal Stresses at mid-section of a Stiffened Sq. Beam with an Opening

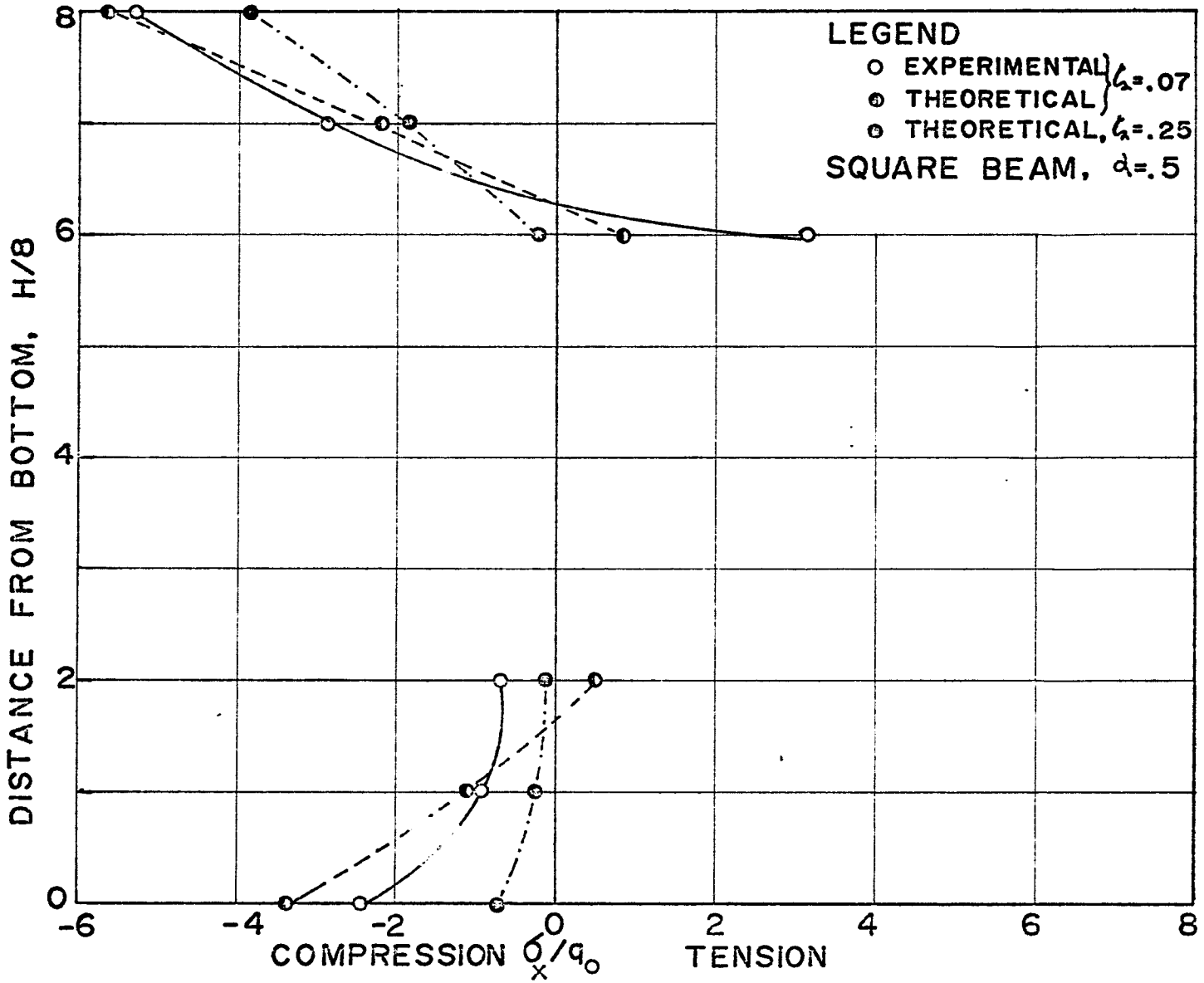

Fig.33 Longitudinal Stresses at mid-section of a Stiffened Sq. Beam with a Large Opening

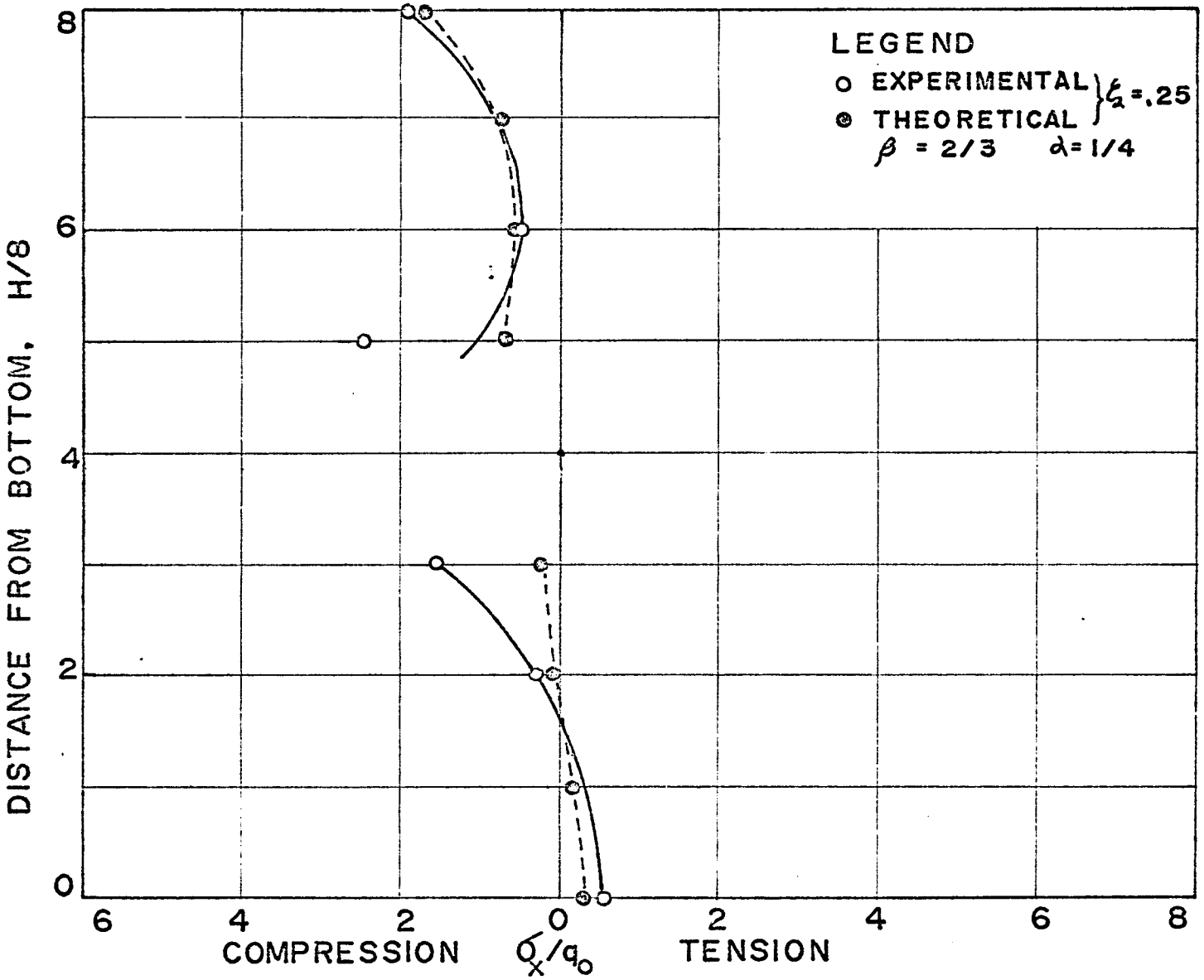

Fig.34 Longitudinal Stresses at mid-section of a Stiffened Rect. Beam with an Opening

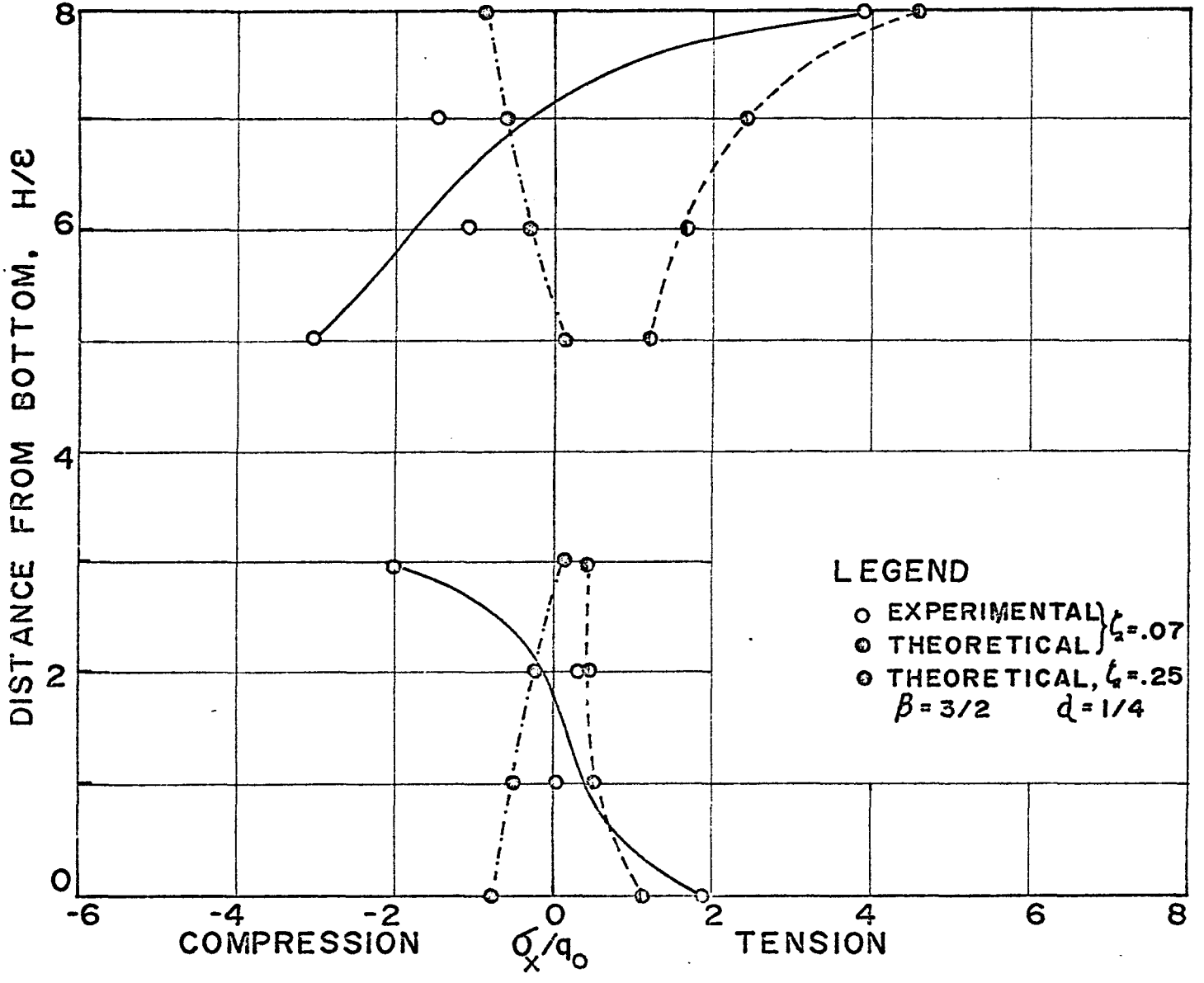

Fig.35 Longitudinal Stresses at mid-section of a Stiffened Rect. Beam with an Opening

APPENDIX I

TABLES OF RESULTS

GEOMETRY OF TEST MODELS

TABLE I

PLAIN DEEP BEAMS

TEST NO.	L in.	H in.	$\propto$ L in.	$\propto$ H in.	t in.
1	16	16	0	0	0.75
2	21	21	$5\frac{1}{4}$	$5\frac{1}{4}$	1.0
3	21	14	$5\frac{1}{4}$	$3\frac{1}{2}$	1.0
4	21	21	$10\frac{1}{2}$	$10\frac{1}{2}$	1.0
5	21	14	$10\frac{1}{2}$	7	1.0
6	14	21	$3\frac{1}{2}$	$5\frac{1}{4}$	1.0
7	14	21	7	$10\frac{1}{2}$	1.0

TABLE II

DEEP BEAMS WITH STIFFENED EDGES

TEST NO.	L in.	H in.	$\propto$ L in.	$\propto$ H in.	t in.	ζ
1	16	16	0	0	0.75	0.064
2	16	16	0	0	0.75	0.250
3	21	21	$5\frac{1}{4}$	$5\frac{1}{4}$	1.0	0.064
4	21	14	$5\frac{1}{4}$	$3\frac{1}{2}$	1.0	0.064
5	14	21	$3\frac{1}{2}$	$5\frac{1}{4}$	1.0	0.250
6	21	21	$10\frac{1}{2}$	$10\frac{1}{2}$	1.0	0.064
7	21	14	$10\frac{1}{2}$	7	1.0	0.064
8	14	21	7	$10\frac{1}{2}$	1.0	0.250

TABLE III
BENDING STRESSES AT MID SECTION

SQUARE BEAM $\beta = 1$	PT.	UDL AT TOP		UDL AT BOTTOM	CENTRE LOAD	¼T. POINT LOAD
		EXPERIMENT	THEORY	THEORY	THEORY	THEORY
$\theta = 0$	1	-0.260	-0.4132	-0.3545	-0.5561	+0.0872
	6	-	-0.236	-0.2414	-0.1626	-.0429
	11	-0.062	-0.1745	-0.2356	-0.0302	-0.0542
	16	-	-0.1873	-0.2810	+0.0005	-0.0611
	21	-0.350	-0.2154	-0.3233	+0.0008	-0.0686
	26	-	-0.000	-0.000	+0.000	-0.000
	31	+0.180	+0.0582	+0.0642	+0.0283	+0.0109
	36	-	+0.7044	+0.9953	+0.1152	+0.1940
	41	+1.804	+1.8525	+2.6020	+0.2787	+0.5186
	42	-	+2.0067	+2.6067	+0.2943	+0.5643
	43	-	+2.1094	+2.5023	+0.2963	+0.5962
$\theta = 1/25$	1	-	-0.3806	-0.1496	-0.5660	+0.1079
	7	-	-0.2296	-0.1288	-0.1541	-0.0358
	13	-	-0.1527	-0.1490	-0.0262	-0.0458
	19	-	-0.0957	-0.2076	+0.0205	-0.0316
	25	-	+0.1264	-0.3028	+0.0672	+0.0231
	37	-	-0.0432	-0.4707	+0.0324	-0.0129
	43	-	-0.0229	-0.1674	+0.0252	-0.0082
	49	-	+0.2345	+0.1932	+0.0400	+0.0492
	55	-	+0.7528	+0.7823	+0.0842	+0.1638
	61	-	+1.3922	+1.4770	+0.1475	+0.3044
	62	-	+1.5207	+1.6072	+0.1556	+0.3336

TABLE IV
BENDING STRESSES AT MID-SECTION

SQUARE BEAM $\beta = 1$	Pt.	UDL AT TOP		UDL AT BOTTOM	CENTRE LOAD	QT. POINT LOADS
		EXPERIMENT	THEORY	THEORY	THEORY	THEORY
$\theta = 1/16$	1	-0.580	-0.5581	-0.2490	-0.5993	+0.0515
	6	-0.510	-0.2790	-0.1898	-0.1742	-0.0490
	11	-	-0.1240	-0.2110	-0.0304	-0.0327
	16	-0.350	+0.1393	-0.2880	+0.0542	+0.0441
	26	-0.580	+0.0272	-0.4056	+0.0304	+0.0065
	31	-0.490	+0.1872	+0.0826	+0.0448	+0.0495
	36	+1.515	+0.8506	+0.9047	+0.1317	+0.2333
	41	+2.205	+2.0640	+2.3222	+0.3008	+0.5703
	42	-	+2.2195	+2.4360	+0.3188	+0.6149
	17	-	-0.1752	-0.2180	-0.0176	-0.0311
	27	-	-0.0940	-0.1424	+0.0068	-0.0251
$\theta = 1/4$	1	-2.17	-0.3322	-0.0001	-	-
	6	+1.05	-0.1918	-0.0001	-	-
	11	+1.16	-0.0113	-0.0004	-	-
	31	-1.04	-0.0015	-0.0281	-	-
	36	+2.23	+0.0041	+0.0831	-	-
	41	+2.55	-0.-194	+0.2827	-	-
	42	-	-0.0168	+0.2822	-	-

TABLE V
BENDING STRESSES AT MID-SECTION

β = 2/3	Pt.	UDL AT TOP	UDL AT BOTTOM	CENTRE LOAD	QT. PT. LOAD
		THEORY	THEORY	THEORY	THEORY
	1	-0.2158	-0.0243	-0.5253	+0.1516
	6	-0.0538	-0.0337	-0.0689	+0.0065
	11	-0.0029	-0.0721	+0.0224	-0.0147
	16	-0.0821	-0.1496	+0.0218	-0.0337
θ= 0	21	-0.1802	-0.2724	-0.0022	-0.0602
	26	-0.0000	-0.0000	-0.0000	-0.0000
	31	-0.2491	-0.3446	-0.0285	-0.0751
	36	+0.3411	+0.4953	+0.0499	+0.0975
	41	+2.2462	+3.1583	+0.3138	+0.6544
	42	+2.3736	+3.1373	+0.3313	+0.6916
	43	+2.2841	+2.7745	+0.3171	+0.6645
	1	-0.1967	+0.0053	-0.5448	+0.1483
	7	-0.0818	-0.0140	-0.0758	-0.0149
	13	-0.0363	-0.0429	+0.0199	-0.0219
	19	-0.0204	-0.0978	+0.0352	-0.0152
	25	+0.2053	-0.1950	+0.0620	+0.0388
θ= 1/25	37	-0.0370	-0.4642	+0.0105	-0.0213
	43	-0.3011	-0.3880	-0.0223	-0.0720
	49	-0.1128	-0.1438	-0.0077	-0.0274
	55	+0.6494	+0.6580	+0.0711	+0.1483
	61	+2.0576	+2.1246	+0.2212	+0.4729
	62	+2.2946	+2.3762	+0.2461	+0.5273

TABLE VI

BENDING STRESSES AT MID-SECTION

β =2/3	Pt.	UDL AT TOP		UDL AT BOTTOM	CENTRE LOAD	QT. POINT LOAD
		EXPERIMENT	THEORY	THEORY	THEORY	THEORY
θ =1/16	1	-0.369	-0.2978	-0.0042	-0.5477	+0.1320
	6	-0.099	-0.0804	-0.0307	-0.0772	+0.0012
	11	+0.119	-0.0099	-0.0832	+0.0238	-0.0068
	16	+0.179	+0.2240	-0.1956	+0.0731	+0.0588
	26	-0.150	-0.1039	-0.5239	+0.0017	-0.0344
	31	-0.109	-0.2695	-0.3573	-0.0322	-0.0801
	36	+0.281	+0.4084	+0.4246	+0.0631	+0.1155
	41	+2.262	+2.7261	+2.9557	+0.4055	+0.7832
	42	+2.448	+2.8843	+3.0991	+0.4286	+0.8287
	43	-	+2.7753	+2.9258	+0.4111	+0.7965
θ =1/4	1	-0.672	-0.3122	-0.0000		
	6	-0.178	-0.1722	+0.0000		
	11	-	-0.0147	-0.0002		
	31	-0.241	-0.0013	-0.0203		
	36	-0.100	+0.0273	+0.0851		
	41	+0.358	+0.0302	+0.2574		
	42	+0.449		+0.2643		
	43	+0.421		+0.2011		

TABLE VII

BENDING STRESSES AT MID-SECTION

β =3/2	Pt.	UDL AT TOP	UDL AT BOTTOM	CENTRE LOAD	QT. POINT LOAD
		THEORY	THEORY	THEORY	THEORY
θ = 0	1	-1.0662	-1.2668	-0.6751	-0.0871
	6	-0.6861	-0.8252	-0.2938	-0.1536
	11	-0.4444	-0.5601	-0.1252	-0.1260
	16	-0.2782	-0.3747	-0.0429	-0.0860
	21	-0.1225	-0.1843	+0.0053	-0.0423
	26	-0.0000	-0.0000	+0.0000	-0.0000
	31	+0.4929	+0.6458	+0.1158	+0.1278
	36	+1.1118	+1.5449	+0.2196	+0.2957
	41	+1.8606	+2.5456	+0.3554	+0.4947
	42	+1.9842	+2.4072	+0.3515	+0.5382
	43	+2.1128	+2.4541	+0.3239	0.5869
θ =1/25	1	-0.7036	-0.4423	-0.6177	+0.0517
	7	-0.4512	-0.3365	-0.2476	-0.0515
	13	-0.2848	-0.2838	-0.0891	-0.0612
	19	-0.1313	-0.2695	-0.0058	-0.0368
	25	+0.1525	-0.2706	+0.0688	+0.0299
	37	+0.1591	-0.2710	+0.0636	+0.0336
	43	+0.2958	+0.1036	+0.0726	+0.0612
	49	+0.4733	+0.4108	+0.0795	+0.0974
	55	+0.7317	+0.7619	+0.0992	+0.1497
	61	+1.0283	+1.1218	+0.1369	+0.2086
	62	+1.0330	+1.1001	+0.1217	+0.2116

TABLE VIII
BENDING STRESSES AT MID-SECTION

β =3/2	Pt.	UDL AT TOP		UDL AT BOTTOM	CENTRE LOAD	QT. POINT LOAD
		EXPERIMENT	THEORY	THEORY	THEORY	THEORY
θ =1/16	1	-1.511	-1.3206	-0.9971	-0.7672	-0.1125
	6	-0.962	-0.7838	-0.6958	-0.3292	-0.1537
	11	-0.378	-0.4146	-0.5298	-0.1193	-0.0981
	16	+0.837	-0.0145	-0.4498	+0.0225	+0.0135
	26	-	+0.1629	-0.2794	+0.0630	+0.0506
	31	+0.767	+0.5530	+0.4159	+0.1210	+0.1494
	36	+1.389	+1.2011	+1.2525	+0.2180	+0.3209
	41	+1.786	+2.0553	+2.3294	+0.3550	+0.5457
	42	+1.889	+2.1864	+2.3506	+0.3611	+0.5857
	43	-	+2.3301	+2.3737	+0.3661	+0.6361
θ =1/4	1	-1.886	-0.3429	-0.0000		
	6	-1.471	-0.1989	+0.0001		
	11	+2.929	+0.0307	-0.0000		
	31	+1.361	+0.0035	-0.0343		
	36	+2.024	+0.0025	+0.0998		
	41	+2.522	-0.0099	-0.0208		

TABLE IX
BENDING STRESSES AT MID SECTION
FOR SQUARE PLATE UNDER UDL

L/H=1	Pt.	ζ =512 I/tL^3=.074		ζ =.250
		EXPERIMENTAL	THEORETICAL	THEORETICAL
θ =1/16	1	-0.859	-0.6193	-0.8181
	6	-1.960	-0.5172	-0.4370
	11	1.110	0.5652	-0.2758
	16	1.540	0.7702	0.0966
	21	-	-	-
	26	-0.536	-0.0268	0.7114
	31	-0.692	-0.5440	0.8030
	36	-0.503	-0.9102	0.9858
	41	-1.280	-1.3549	1.3060
θ = 1/4	1	-5.310	-5.6108	-3.8583
	6	-2.870	-2.2024	-1.8713
	11	6.090	0.8432	-0.1844
	16	-	-	-
	21	-	-	-
	26	-	-	-
	31	-0.640	0.5476	-0.0595
	36	-0.911	-1.1658	-0.2135
	41	-2.420	-3.4722	-0.7163

TABLE X
BENDING STRESSES AT MID SECTION
FOR RECTANGULAR PLATE UNDER UDL

L/H= 1.5	Pt.	ζ = .074		ζ = .250
		EXPERIMENTAL	THEORETICAL	THEORETICAL
θ =1/16	1	3.920	3.7836	-0.8524
	6	-1.440	2.4695	-0.5808
	11	-1.120	1.7650	-0.2612
	16	-3.440	1.2737	0.1476
	21	-	-	-
	26	-4.900	0.4403	0.0778
	31	0.330	0.4096	-0.2328
	36	0.000	0.5477	-0.4518
	41	1.910	1.0627	-0.5842
θ = 1/4	1	-2.040	4.5026	3.7232
	6	-2.140	3.6804	3.0878
	11	2.030	3.7430	3.1588
	16	-	-	-
	21	-	-	-
	26	-	-	-
	31	0.120	1.7248	1.6990
	36	0.820	2.3777	1.6872
	41	1.130	3.5139	1.8142

TABLE XI

BENDING STRESSES AT MID SECTION

RECTANGULAR PLATE FOR UDL AT TOP

L/H=2/3	Pt.	ζ_1 = .074	ζ_1 = .250	
		THEORETICAL	EXPERIMENTAL	THEORETICAL
θ =1/16	1	-3.8529	-1.890	-1.8369
	6	-3.7978	-	-0.7401
	11	1.0998	-0.448	-0.5458
	16	9.3566	-2.483	-0.4272
	21	-	-	-
	26	1.8101	-2.000	-0.0532
	31	-9.6230	0 264	0.0022
	36	-14.3167	-	0.1479
	41	-15.8551	0.470	0.3165
θ = 1/4	1	-3.5411	-3.089	-3.9292
	6	-1.4228	0.640	-1.2810
	11	2.6234	2.680	0.5223
	16	-	-	-
	21	-	-	-
	26	-	-	-
	31	1.7469	-0.360	0.2521
	36	-1.2693	-0.580	0.8014
	41	-0.6054	-0.170	2.6891

TABLE XII
BENDING STRESSES AT MIDSECTION
SOLID DEEP BEAM FOR UDL AT TOP

θ = 0	Pt.	ζ = .074		ζ = .250	
		EXPERIMENT	THEORY	EXPERIMENT	THEORY
L/H = 1	1	-0.102	-1.9570	-0.446	-0.3718
	6	-	-0.8891	-	-0.1512
	11	-0.324	-0.3372	-0.589	-0.0689
	16	-	0.0938	-	-0.0418
	21	-0.166	0.4018	-0.100	-0.0052
	26	-	0.3994	-	0.0599
	31	-0.115	0.0273	-1.082	0.1400
	36	-	-0.8272	-	0.2083
	41	0.756	-2.958	0.568	0.2512
L/H=3/2	1	-	-2.6455	-	-0.7383
	6	-	-2.0992	-	-0.5384
	11	-	-1.7235	-	-0.3390
	16	-	-1.3404	-	-0.2014
	21	-	-0.8574	-	-0.1339
	26	-	-0.2858	-	-0.1338
	31	-	0.2998	-	-0.1864
	36	-	0.8323	-	-0.2513
	41	-	1.2971	-	-0.2290
L/H=2/3	1	-	-0.2065	-	2.9661
	6	-	-0.0792	-	2.6352
	11	-	0.0132	-	2.6328
	16	-	0.1244	-	2.5645
	21	-	0.2216	-	1.9258
	26	-	0.2436	-	0.7511
	31	-	0.1757	-	-0.3118
	36	-	-0.0244	-	-0.4401
	41	-	-0.6624	-	0.4288

APPENDIX II

SAMPLE PROGRAMS

```
 KENNEDY J.B.     UUWC78(STRESS     (C4(  06(    $
       $EXECUTE        IBJOB
IB VERSION 5 HAS CONTROL.
JOB
TC DK 001

       DK 001      -  EFN    SOURCE STATEMENT  -  IFN(S)  -

    D-III-A  UDL AT TOP HRASHID
'3 READ (5,2)0) ANU, BETA, EXA, ETA
C FORMAT (4F6.3)
   DOUBLE PRECISION A(8(,8(), B(8(), X(8(), SX(12), SY(7)
   WRITE (6,23) ANU, BETA, EXA, ETA
23 FORMAT (4F8.3)
   EQUIVALENCE (B,X)
   DO 201 I=1,8(
   DO 2(1 J=1,8(
)1 A(I,J)=(.
   A(1,1)=-2.-2.*EXA*BETA*BETA+.75*ANU*ETA
   A(1,2)=1.
   A(1,3)=-.25*ANU*ETA
   A(1,5)= 2.*EXA*BETA*BETA
   A(1,37)=-EXA*BETA
   A(1,39)= EXA*BETA
   A(2,1)= 1.
   A(2,2)= -2.-2.*EXA*BETA*BETA+.5*ANU*ETA
   A(2,3)= 1.
   A(2,4)=-.25*ANU*ETA
   A(2,6)= 2.*EXA*BETA*BETA
   A(2,38)=-EXA*BETA
   A(2,4(= EXA*BETA
   A(3,1)=-.25*ANU*ETA
   A(3,2)= 1.
   A(3,3)=-2.-2.*EXA*BETA*BETA+.25*ANU*ETA
   A(3,4)= 1.
   A(3,7)= 2.*EXA*BETA*BETA
   A(3,39)=-EXA*BETA
   A(3,41)= EXA*BETA
   A(4,3)= 2.
   A( 4,4)=-2.
   A(5,1)= EXA*BETA*BETA
   A(5,5)=-2.-2.*EXA*BETA*BETA
   A(5,6)= 1.
   A(5,9)= EXA*BETA*BETA
   A(5,37)= .25*ETA*BETA
   A(5,39)=-.25*ETA*BETA
   A(5,47)=-.25*ETA*BETA
   A(5,49)= .25*ETA*BETA
   A(6,2)= EXA*BETA*BETA
   A(6,5)= 1.
   A(6,6)=-2.-2.*EXA*BETA*BETA
   A(6,7)= 1.
   A(6,1(= EXA*BETA*BETA
```

```
A(6,38)= .25*ETA*BETA
A(6,40)=-.25*ETA*BETA
A(6,48)=-.25*ETA*BETA
A(6,50)= .25*ETA*BETA
A(7,3)= EXA*BETA*BETA
A(7,6)= 1.
A(7,7)=-2.-2.*EXA*BETA*BETA
A(7,8)= 1.
A(7,11)= EXA*BETA*BETA
A(7,39)= .25*ETA*BETA
A(7,41)=-.25*ETA*BETA
A(7,49)=-.25*ETA*BETA
A(7,51)= .25*ETA*BETA
A(8,4)= EXA*BETA*BETA
A(8,7)= 2.
A( 8, 8)=-2.-2.*EXA*BETA*BETA+.25*ETA*BETA*BETA
A(8,12)= EXA*BETA*BETA
A(8,16)=-.25*ETA*BETA*BETA
A(8,40)= .5*ETA*BETA
A(8,41)= ANU*BETA-.5*ETA*BETA
A(8,51)=-BETA*ANU
A(9,5)= EXA*BETA*BETA
A(9,9)=-2.-2.*EXA*BETA*BETA
A(9,10)= 1.
A(9,13)= EXA*BETA*BETA
A(9,42)= .25*ETA*BETA
A(9,44)=-.25*ETA*BETA
A(9,52)=-.25*ETA*BETA
A(9,54)= .25*ETA*BETA
A(10,6)= EXA*BETA*BETA
A(10,9)= 1.
A(10,10)=-2.-2.*EXA*BETA*BETA
A(10,11)=1.
A(10,14)= EXA*BETA*BETA
A(10,43)= .25*ETA*BETA
A(10,45)=-.25*ETA*BETA
A(10,53)=-.25*ETA*BETA
A(10,55)= .25*ETA*BETA
A(11,7)= EXA*BETA*BETA
A(11,10)= 1.
A(11,11)=-2.-2.*EXA*BETA*BETA
A(11,12)= 1.
A(11,15)= EXA*BETA*BETA
A(11,44)= .25*ETA*BETA
A(11,46)=-.25*ETA*BETA
A(11,54)=-.25*ETA*BETA
A(11,56)= .25*ETA*BETA
A(12,4)=-.25*ETA*BETA*BETA
A(12,8)=EXA*BETA*BETA
A(12,11)= 2.
A(12,12)=-2.-2.*EXA*BETA*BETA+.5*ETA*BETA*BETA
A(12,16)= EXA*BETA*BETA
A(12,20)=-.25*ETA*BETA*BETA
A(12,46)= BETA*ANU
A(12,56)=-BETA*ANU
A(13,9)= EXA*BETA*BETA
```

```
A(13,13)=-2.-2.*EXA*BETA*BETA
A(13,14)= 1.
A(13,17)= EXA*BETA*BETA
A(13,47)= .25*ETA*BETA
A(13,49)=-.25*ETA*BETA
A(13,57)=-.25*ETA*BETA
A(13,59)= .25*ETA*BETA
A(14,10)= EXA*BETA*BETA
A(14,13)= 1.
A(14,14)=-2.-2.*EXA*BETA*BETA
A(14,15)= 1.
A(14,18)= EXA*BETA*BETA
A(14,48)= .25*ETA*BETA
A(14,50)=-.25*ETA*BETA
A(14,58)=-.25*ETA*BETA
A(14,60)= .25*ETA*BETA
A(15,11)= EXA*BETA*BETA
A(15,14)= 1.
A(15,15)=-2.-2.*EXA*BETA*BETA
A(15,16)= 1.
A(15,19)= EXA*BETA*BETA
A(15,49)= .25*ETA*BETA
A(15,51)=-.25*ETA*BETA
A(15,59)=-.25*ETA*BETA
A(15,61)= .25*ETA*BETA
A(16,8)=-.25*ETA*BETA*BETA
A(16,12)= EXA*BETA*BETA
A(16,15)= 2.
A(16,16)=-2.-2.*EXA*BETA*BETA+.5*ETA*BETA*BETA
A(16,20)= EXA*BETA*BETA
A(16,24)=-.25*ETA*BETA*BETA
A(16,51)= ANU*BETA
A(16,61)=-ANU*BETA
A(17,13)= EXA*BETA*BETA
A(17,17)=-2.-2.*EXA*BETA*BETA
A(17,18)= 1.
A(17,21)= EXA*BETA*BETA
A(17,52)= .25*ETA*BETA
A(17,54)=-.25*ETA*BETA
A(17,62)=-.25*ETA*BETA
A(17,64)= .25*ETA*BETA
A(18,14)= EXA*BETA*BETA
A(18,17)= 1.
A(18,18)=-2.-2.*EXA*BETA*BETA
A(18,19)= 1.
A(18,22)= EXA*BETA*BETA
A(18,53)= .25*ETA*BETA
A(18,55)=-.25*ETA*BETA
A(18,63)=-.25*ETA*BETA
A(18,65)= .25*ETA*BETA
A(19,15)= EXA*BETA*BETA
A(19,18)= 1.
A(19,19)=-2.-2.*EXA*BETA*BETA
A(19,20)= 1.
A(19,23)= EXA*BETA*BETA
A(19,54)= .25*ETA*BETA
```

```
A(19,56)=-.25*ETA*BETA
A(19,64)=-.25*ETA*BETA
A(19,66)= .25*ETA*BETA
A(20,12)=-.25*ETA*BETA*BETA
A(20,16)= EXA*BETA*BETA
A(20,19) =2.
A(20,20)=-2.-2.*EXA*BETA*BETA+.5*ETA*BETA*BETA
A(20,24)= EXA*BETA*BETA
A(20,28)=-.25*ETA*BETA*BETA
A(20,56)= ANU*BETA
A(20,66)=-ANU*BETA
A(21,17)= EXA*BETA*BETA
A(21,21)=-2.-2.*EXA*BETA*BETA
A(21,22)= 1.
A(21,25)= EXA*BETA*BETA
A(21,57)= .25*ETA*BETA
A(21,59)=-.25*ETA*BETA
A(21,67)=-.25*ETA*BETA
A(21,69)= .25* ETA*BETA
A(22,18)= EXA*BETA*BETA
A(22,21)= 1.
A(22,22)=-2.-2.*EXA*BETA*BETA
A(22,23)= 1.
A(22,26)= EXA*BETA*BETA
A(22,58)= .25*ETA*BETA
A(22,60)=-.25*ETA*BETA
A(22,68)=-.25*ETA*BETA
A(22,70)= .25*ETA*BETA
A(23,19)= EXA*BETA*BETA
A(23,22)= 1.
A(23,23)=-2.-2.*EXA*BETA*BETA
A(23,24)= 1.
A(23,27)= EXA*BETA*BETA
A(23,59)= .25*ETA*BETA
A(23,61)=-.25*ETA*BETA
A(23,69)=-.25*ETA*BETA
A(23,71)= .25*ETA*BETA
A(24,16)=-.25*ETA*BETA*BETA
A(24,20)= EXA*BETA*BETA
A(24,23)= 2.
A(24,24)=-2.-2.*EXA*BETA*BETA+.5*ETA*BETA*BETA
A(24,28)= EXA*BETA*BETA
A(24,32)=-.25*ETA*BETA*BETA
A(24,61)=ANU*BETA
A(24,71)=-ANU*BETA
A(25,21)= EXA*BETA*BETA
A(25,25)=-2.-2.*EXA*BETA*BETA
A(25,26)= 1.
A(25,29)= EXA*BETA*BETA
A(25,62)= .25*ETA*BETA
A(25,64)=-.25*ETA*BETA
A(25,72)=-.25*ETA*BETA
A(25,74)= .25*ETA*BETA
A(26,22)= EXA*BETA*BETA
A(26,25)= 1.
A(26,26)=-2.-2.*EXA*BETA*BETA
```

```
A(26,27)= 1.
A(26,30)= EXA*BETA*BETA
A(26,63)= .25*ETA*BETA
A(26,65)=-.25*ETA*BETA
A(26,73)=-.25*ETA*BETA
A(26,75)= .25*ETA*BETA
A(27,23)= EXA*BETA*BETA
A(27,26)= 1.
A(27,27)=-2.-2.*EXA*BETA*BETA
A(27,28)= 1.
A(27,31)= EXA*BETA*BETA
A(27,64)= .25*ETA*BETA
A(27,66)=-.25*ETA*BETA
A(27,74)=-.25*ETA*BETA
A(27,76)= .25*ETA*BETA
A(28,20)=-.25*ETA*BETA*BETA
A(28,24)= EXA*BETA*BETA
A(28,27)= 2.
A(28,28)=-2.-2.*EXA*BETA*BETA+.5*ETA*BETA*BETA
A(28,32)= EXA*BETA*BETA
A(28,36)=-.25*ETA*BETA*BETA
A(28,66)= ANU*BETA
A(28,76)=-ANU*BETA
A(29,25)= EXA*BETA*BETA
A(29,29)=-2.-2.*EXA*BETA*BETA
A(29,30)= 1.
A(29,33)= EXA*BETA*BETA
A(29,67)= .25*ETA*BETA
A(29,69)=-.25*ETA*BETA
A(29,77)=-.25*ETA*BETA
A(29,79)= .25*ETA*BETA
A(30,26)= EXA*BETA*BETA
A(30,29)= 1.
A(30,30)=-2.-2.*EXA*BETA*BETA
A(30,31)= 1.
A(30,34)= EXA*BETA*BETA
A(30,68)= .25*ETA*BETA
A(30,70)=-.25*ETA*BETA
A(30,78)=-.25*ETA*BETA
A(30,80)=.25*ETA*BETA
A(31,27)= EXA*BETA*BETA
A(31,30)= 1.
A(31,31)=-2.-2.*EXA*BETA*BETA
A(31,32)= 1.
A(31,35)= EXA*BETA*BETA
A(31,69)= .25*ETA*BETA
A(31,71)=-.25*ETA*BETA
A(31,79)=-.25*ETA*BETA
A(32,24)= -.25*ETA*BETA*BETA
A(32,28)= EXA*BETA*BETA
A(32,31)= 2.
A(32,32)=-2.-2.*EXA*BETA*BETA+.25*ETA*BETA*BETA
A(32,36)= EXA*BETA*BETA
A(32,80)=-.5*ETA*BETA
A(32,71)= ANU*BETA
A(33,29)= 2.*EXA*BETA*BETA
```

```
A(33,33)=-2.-2.*EXA*BETA*BETA+.75*ETA*ANU
A(33,34)= 1.
A(33,35)=-.25*ETA*ANU
A(33,77)= EXA*BETA
A(33,79)=-EXA*BETA
A(34,30)= 2.*EXA*BETA*BETA
A(34,33)= 1.
A(34,34)=-2.-2.*EXA*BETA*BETA+.5*ETA*ANU
A(34,35)= 1.
A(34,36)=-.25*ETA*ANU
A(34,78)= EXA*BETA
A(34,80)=-EXA*BETA
A(35,31)= 2.*EXA*BETA*BETA
A(35,33)=-.25*ETA*ANU
A(35,34)= 1.
A(35,35)=-2.-2.*EXA*BETA*BETA+.25*ANU*ETA
A(35,36)= 1.
A(35,79)= EXA*BETA
A(36,35)= 2.
A(36,36)=-2.
A(37,1)= 2.*ANU*BETA
A(37,37)=-2.*EXA-2.*BETA*BETA+.5*ETA
A(37,38)= 2.*EXA
A(37,39)=-.5*ETA
A(37,42)= 2.*BETA*BETA
A(38,2)= ANU*BETA
A(38,37)= EXA
A(38,38)= -2.*EXA-2.*BETA*BETA+.25*ETA
A(38,39)= EXA
A(38,40)=-.25*ETA
A(38,43)= 2.*BETA*BETA
A(39,1)=-BETA*ANU
A(39,3)= BETA*ANU
A(39,37)=-.25*ETA
A(39,38)= EXA
A(39,39)=-2.*EXA-2.*BETA*BETA+.5*ETA
A(39,40)= EXA
A(39,41)= -.25*ETA
A(39,44)= 2.*BETA*BETA
A(40,2)= -BETA*ANU
A(40, 4)= ANU*BETA-.5*ETA*BETA
A(40, 8)= .5*ETA*BETA
A(40,38)=-.25*ETA
A(40,39)= EXA
A(40,40)=-2.*EXA-2.*BETA*BETA+.25*ETA
A(40,41)= EXA
A(40,45)= 2.*BETA*BETA
A(41,41)=-2.
A(41,46)= 2.
A(42,1)= -.5*ETA*BETA
A(42,9)= .5*ETA*BETA
A(42,37)= BETA*BETA
A(42,42)=-2.*EXA-2.*BETA*BETA
A(42,43)=2.*EXA
A(42,47)= BETA*BETA
A(43,2)=-.25*ETA*BETA
```

DK 0(1 - EFN SOURCE STATEMENT - IFN(S) -

```
A(43,10)= .25*ETA*BETA
A(43,38)= BETA*BETA
A(43,42)= EXA
A(43,43)=-2.*EXA-2.*BETA*BETA
A(43,44)= EXA
A(43,48)= BETA*BETA
A(44,1)= .25*ETA*BETA
A(44,3)=-.25*ETA*BETA
A(44,9)=-.25*ETA*BETA
A(44,11)=.25*ETA*BETA
A(44,39)= BETA*BETA
A(44,43)= EXA
A(44,44)=-2.*EXA-2.*BETA*BETA
A(44,45)= EXA
A(44,49)= BETA*BETA
A(45,2)= .25*ETA*BETA
A(45,4)= -.25*ETA*BETA
A(45,10)=-.25*ETA*BETA
A(45,12)= .25*ETA*BETA
A(45,40)= BETA*BETA
A(45,44)= EXA
A(45,45)= -2.*EXA-2.*BETA*BETA
A(45,46)= EXA
A(45,50)= BETA*BETA
A(46,4)= EXA*BETA
A(46,12)=-EXA*BETA
A(46,41)= BETA*BETA
A(46,45)= 2.*EXA
A(46,46)=-2.*EXA-2.*BETA*BETA+.25*ETA*ANU*BETA*BETA
A(46,51)= BETA*BETA
A(46,56)=-.25*ANU*ETA*BETA*BETA
A(47,5)=-.5*ETA*BETA
A(47,13)=.5*ETA*BETA
A(47,42)=BETA*BETA
A(47,47)=-2.*EXA-2.*BETA*BETA
A(47,48)=2.*EXA
A(47,52)=BETA*BETA
A(48,6)=-.25*ETA*BETA
A(48,14)=.25*ETA*BETA
A(48,43)= BETA*BETA
A(48,47)= EXA
A(48,48)= -2.*EXA-2.*BETA*BETA
A(48,49)= EXA
A(48,53)= BETA*BETA
A(49,5)= .25*ETA*BETA
A(49,7)= -.25*ETA*BETA
A(49,13)=-.25*ETA*BETA
A(49,15)=.25*ETA*BETA
A(49,44)= BETA*BETA
A(49,48)= EXA
A(49,49)=-2.*EXA-2.*BETA*BETA
A(49,50)= EXA
A(49,54)= BETA*BETA
A(50,6)= .25*ETA*BETA
A(50,8)=-.25*ETA*BETA
A(50,14)=-.25*ETA*BETA
```

```
A(50,16)=.25*ETA*BETA
A(50,45)= BETA*BETA
A(50,49)= EXA
A(50,50)=-2.*EXA-2.*BETA*BETA
A(50,51)= EXA
A(50,55)= BETA*BETA
A(51,8)= EXA*BETA
A(51,16)=-EXA*BETA
A(51,41)=-.25*ETA*ANU*BETA*BETA
A(51,46)= BETA*BETA
A(51,50)= 2.*EXA
A(51,51)=-2.*EXA-2.*BETA*BETA+.5*ETA*ANU*BETA*BETA
A(51,56)= BETA*BETA
A(51,61)=-.25*ETA*ANU*BETA*BETA
A(52,9)=-.5*ETA*BETA
A(52,17)=.5*ETA*BETA
A(52,47)= BETA*BETA
A(52,52)=-2.*EXA-2.*BETA*BETA
A(52,53)= 2.*EXA
A(52,57)= BETA*BETA
A(53,10)=-.25*ETA*BETA
A(53,18)= .25*ETA*BETA
A(53,48)= BETA*BETA
A(53,52)= EXA
A(53,53)=-2.*EXA-2.*BETA*BETA
A(53,54)= EXA
A(53,58)= BETA*BETA
A(54,9)= .25*ETA*BETA
A(54,11)=-.25*ETA*BETA
A(54,17)=-.25*ETA*BETA
A(54,19)= .25*ETA*BETA
A(54,49)= BETA*BETA
A(54,53)= EXA
A(54,54)=-2.*EXA-2.*BETA*BETA
A(54,55)= EXA
A(54,59)= BETA*BETA
A(55,10)= .25*ETA*BETA
A(55,12)=-.25*ETA*BETA
A(55,18)=-.25*ETA*BETA
A(55,20)= .25*ETA*BETA
A(55,50)= BETA*BETA
A(55,54)= EXA
A(55,55)=-2.*EXA-2.*BETA*BETA
A(55,56)= EXA
A(55,60)= BETA*BETA
A(56,12)= EXA*BETA
A(56,20)=-EXA*BETA
A(56,46)=-.25*ANU*ETA*BETA*BETA
A(56,51)= BETA*BETA
A(56,55)= 2.*EXA
A(56,56)=-2.*EXA-2.*BETA*BETA+.5*ETA*ANU*BETA*BETA
A(56,61)= BETA*BETA
A(56,66)=-.25*ETA*ANU*BETA*BETA
A(57,13)=-.5*ETA*BETA
A(57,21)= .5*ETA*BETA
A(57,52)= BETA*BETA
```

DK 0C1 - EFN SOURCE STATEMENT - IFN(S) -

```
A(57,57)=-2.*EXA-2.*BETA*BETA
A(57,58)= 2.*EXA
A(57,62)= BETA*BETA
A(58,14)=-.25*ETA*BETA
A(58,22)= .25*ETA*BETA
A(58,53)= BETA*BETA
A(58,57)= EXA
A(58,58)=-2.*EXA-2.*BETA*BETA
A(58,59)=EXA
A(58,63)= BETA*BETA
A(59,13)= .25*ETA*BETA
A(59,15)=-.25*ETA*BETA
A(59,21)=-.25*ETA*BETA
A(59,23)= .25*ETA*BETA
A(59,54)=BETA*BETA
A(59,58)= EXA
A(59,59)=-2.*EXA-2.*BETA*BETA
A(59,60)= EXA
A(59,64)= BETA*BETA
A(60,14)= .25*ETA*BETA
A(60,16)=-.25*ETA*BETA
A(60,22)=-.25*ETA*BETA
A(60,24)= .25*ETA*BETA
A(60,55)= BETA*BETA
A(60,59)= EXA
A(60,60)=-2.*EXA-2.*BETA*BETA
A(60,61)= EXA
A(60,65)= BETA*BETA
A(61,16)= EXA*BETA
A(61,24)=-EXA*BETA
A(61,51)=-.25*ETA*ANU*BETA*BETA
A(61,56)= BETA*BETA
A(61,60)= 2.*EXA
A(61,61)=-2.*EXA-2.*BETA*BETA+.5*ETA*ANU*BETA*BETA
A(61,66)= BETA*BETA
A(61,71)=-.25*ETA*ANU*BETA*BETA
A(62,17)= -.5*ETA*BETA
A(62,25)=  .5*ETA*BETA
A(62,57)= BETA*BETA
A(62,62)=-2.*EXA-2.*BETA*BETA
A(62,63)= 2.*EXA
A(62,67)= BETA*BETA
A(63,18)=-.25*ETA*BETA
A(63,26)= .25*ETA*BETA
A(63,58)= BETA*BETA
A(63,62)= EXA
A(63,63)=-2.*EXA-2.*BETA*BETA
A(63,64)= EXA
A(63,68)= BETA*BETA
A(64,17)= .25*ETA*BETA
A(64,19)=-.25*ETA*BETA
A(64,25)=-.25*ETA*BETA
A(64,27)= .25*ETA*BETA
A(64,59)= BETA*BETA
A(64,63)= EXA
A(64,64)=-2.*EXA-2.*BETA*BETA
```

```
A(64,65)= EXA
A(64,69)= BETA*BETA
A(65,18)= .25*ETA*BETA
A(65,20)=-.25*ETA*BETA
A(65,26)=-.25*ETA*BETA
A(65,28)= .25*ETA*BETA
A(65,60)= BETA*BETA
A(65,64)= EXA
A(65,65)=-2.*EXA-2.*BETA*BETA
A(65,66)= EXA
A(65,70)= BETA*BETA
A(66,20)= EXA*BETA
A(66,28)=-EXA*BETA
A(66,56)=-.25*ETA*ANU*BETA*BETA
A(66,61)= BETA*BETA
A(66,65)= 2.*EXA
A(66,66)=-2.*EXA-2.*BETA*BETA+.5*ETA*ANU*BETA*BETA
A(66,71)= BETA*BETA
A(66,76)=-.25*ETA*ANU*BETA*BETA
A(67,21)=-.5*ETA*BETA
A(67,62)= BETA*BETA
A(67,67)=-2.*EXA-2.*BETA*BETA
A(67,72)= BETA*BETA
A(67,68)= 2.*EXA
A(68,22)=-.25*ETA*BETA
A(68,30)= .25*ETA*BETA
A(68,63)= BETA*BETA
A(68,67)= EXA
A(68,68)=-2.*EXA-2.*BETA*BETA
A(68,69)= EXA
A(68,73)= BETA*BETA
A(69,21)= .25*ETA*BETA
A(69,23)=-.25*ETA*BETA
A(69,29)=-.25*ETA*BETA
A(69,31)= .25*ETA*BETA
A(69,64)= BETA*BETA
A(69,68)= EXA
A(69,69)=-2.*EXA-2.*BETA*BETA
A(69,70)= EXA
A(69,74)= BETA*BETA
A(70,22)= .25*ETA*BETA
A(70,24)=-.25*ETA*BETA
A(70,30)=-.25*ETA*BETA
A(70,32)= .25*ETA*BETA
A(70,65)= BETA*BETA
A(70,69)=EXA
A(70,70)=-2.*EXA-2.*BETA*BETA
A(70,71)= EXA
A(70,75)= BETA*BETA
A(71,24)= EXA*BETA
A(71,32)=-EXA*BETA
A(71,61)=-.25*ETA*ANU*BETA*BETA
A(71,66)= BETA*BETA
A(71,70) = 2.*EXA
A(71,71)=-2.*EXA-2.*BETA*BETA+.25*ETA*ANU*BETA*BETA
A(71,76)= BETA*BETA
```

```
A(72,25)=-.5*ETA*BETA
A(72,33)= .5*ETA*BETA
A(72,67)= BETA*BETA
A(72,72)=-2.*EXA-2.*BETA*BETA
A(72,73)= 2.*EXA
A(72,77)= BETA*BETA
A(73,26)=-.25*ETA*BETA
A(73,34)= .25*ETA*BETA
A(73,68)=BETA*BETA
A(73,72)= EXA
A(73,73)=-2.*EXA-2.*BETA*BETA
A(73,74)= EXA
A(73,78)= BETA*BETA
A(74,25)= .25*ETA*BETA
A(74,27)=-.25*ETA*BETA
A(74,33)=-.25*ETA*BETA
A(74,35)= .25*ETA*BETA
A(74,69)= BETA*BETA
A(74,73)= EXA
A(74,74)=-2.*EXA-2.*BETA*BETA
A(74,75)= EXA
A(74,79)= BETA*BETA
A(75,26)= .25*ETA*BETA
A(75,28)=-.25*ETA*BETA
A(75,34)=-.25*ETA*BETA
A(75,36)= .25*ETA*BETA
A(75,70)= BETA*BETA
A(75,74)= EXA
A(75,75)=-2.*EXA-2.*BETA*BETA
A(75,76)= EXA
A(75,80)= BETA*BETA
A(76,28)= EXA*BETA
A(76,36)=-EXA*BETA
A(76,66)=-.25*ANU*ETA*BETA*BETA
A(76,71)= BETA*BETA
A(76,75)= 2.*EXA
A(76,76)=-2.*EXA-2.*BETA*BETA+.25*ETA*ANU*BETA*BETA
A(77,33)=-ANU*BETA
A(77,72)= BETA*BETA
A(77,77)=-EXA-BETA*BETA+.25*ETA
A(77,78)= EXA
A(77,79)=-.25*ETA
A(78,34)=-ANU*BETA
A(78,73)= 2.*BETA*BETA
A(78,77)= EXA
A(78,78)=-2.*EXA-2.*BETA*BETA+.25*ETA
A(78,79)= EXA
A(78,80)=-.25*ETA
A(79,33)= ANU*BETA
A(79,35)=-ANU*BETA
A(79,74)= 2.*BETA*BETA
A(79,77)=-.25*ETA
A(79,78)= EXA
A(79,79)=-2.*EXA-2.*BETA*BETA+.5*ETA
A(79,80)= EXA
A(80,32)=-.5*ETA*BETA
```

```
      OK 001     -  EFN    SOURCE STATEMENT  -  IFN(S)  -

   A(80,34)= ANU*BETA
   A(80,36)=-ANU*BETA+.5*ETA*BETA
   A(80,75)= 2.*BETA*BETA
   A(80,78)=-.25*ETA
   A(80,79)= EXA
   A(80,80)=-2.*EXA-2.*BETA*BETA+.25*ETA
   DO 202 I=1,80
12 B(I)=0.
   B(3)=-.125*(1.-2.*ANU*ANU)/(1.-ANU)
   B(4)=-ANU/(1.-ANU*ANU)
   B(35)= 1./(1.-ANU)
   B(36)=-8.*ANU/(1.-ANU*ANU)
   B(37)=-2.*BETA
   B(38)=-2.*BETA
   B(39)=-2.*BETA
   B(40)=-2.*BETA
   B(41)=-1./BETA/(1.-ANU*ANU)
   B(46)= .125*BETA*ANU/(1.-ANU)
   B(76)=-ANU*BETA/(1.-ANU)
   CALL DLEQU (0,A,80,80,8,1,LUCK)
   WRITE (6,12) LUCK
12 FORMAT (I5)
   WRITE (6,24) (B(I), I=1,80)
24 FORMAT (4E16.8)
   SX(1)= (1.-ANU*ANU)*X(1)-ANU
   SX(2)= X(5)+.5*ANU*BETA*(X(47)-X(37))
   SX(3)= X(9)+.5*ANU*BETA*(X(52)-X(42))
   SX(4)= X(13)+.5*ANU*BETA*(X(57)-X(47))
   SX(5)= X(17)+.5*ANU*BETA*(X(62)-X(52))
   X(6)= X(21)+.5*ANU*BETA*(X(67)-X(57))
   SX(7)= X(25)+.5*ANU*BETA*(X(72)-X(62))
   SX(8)= X(29)+.5*ANU*BETA*(X(77)-X(67))
   SX(9)=(1.-ANU*ANU)*X(33)
   SX(10)= .5*(1.-ANU*ANU)*X(34)
   SX(11)= .5*(1.-ANU*ANU)*(X(35)-X(33))
   SX(12)= .5*(1.-ANU*ANU)*(X(36)-X(34))
   SY(1)= ANU*X(5)+.5*BETA*(X(47)-X(37))
   SY(2)= ANU*X(9)+.5*BETA*(X(52)-X(42))
   SY(3)= ANU*X(13)+.5*BETA*(X(57)-X(47))
   SY(4)= ANU*X(17)+.5*BETA*(X(62)-X(52))
   SY(5)= ANU*X(21)+.5*BETA*(X(67)-X(57))
   SY(6)= ANU*X(25)+.5*BETA*(X(72)-X(62))
   SY(7)= ANU*X(29)+.5*BETA*(X(77)-X(67))
   WRITE (6,300) SX, SY
00 FORMAT (4E20.8)
   GO TO 373
   END
E FIRST LOCATION NOT USED BY THIS PROGRAM IS 42633.
```

```
 FILE NAME 'SYSOU ' *** JOB NUMBER U0780054 ***


JOB  KENNEDY J.B.    UUW0780STRESS    0100  080    $                  M00052
          $EXECUTE        IBJOB
IBJOB VERSION 5 HAS CONTROL.
$IBJOB
$IBFTC DK 026

          DK 026     -  EEN    SOURCE STATEMENT  -  IFN(S)  -

C     DF-III ALPHA=0
      DIMENSION A(93,93), B(93), X(93),      PHI(16), SX(10), SY(8)
  373 READ (5,200) ANU, BETA, ZETA
  200 FORMAT (3F6.3)
      EQUIVALENCE (B,X)
      WRITE (6,23) ANU, BETA, ZETA
   23 FORMAT (3F8.3)
      PI= 3.1415926
      EXA= .5-.5*ANU
      ETA= .5+.5*ANU
      PHI(1)= (32./PI)*BETA/(1.+4.*BETA+3.*BETA*BETA)
      PHI(2)= 64./(PI**2)
      PHI(3)=128./(PI**3)*(2.*BETA+3.*BETA*BETA)/(1.+4.*BETA+3.*BETA**2)
      PHI(4)= (128.*BETA)/(PI**3+4.*BETA*PI**3+3.*BETA*BETA*PI**3)
      PHI(5)= (256.+512.*BETA)/(BETA*BETA*PI**2+4.*(BETA**3)*(PI**2)
     1   +3.*(BETA**4)*(PI**2))
      PHI(6)=(1.)/(PI**3*BETA*BETA)*(1024.)/(1.+4.*BETA+3.*BETA*BETA)
      PHI(7)= (6144.)/(PI**4)*(1.)/(BETA*BETA+3.*BETA**3)
      PHI(8)= (256./(PI**2*BETA))/(1.+4.*BETA+3.*BETA*BETA)
      PHI(9)= (32./PI)*(1.+2.*BETA)/(1.+4.*BETA+3.*BETA*BETA)
      PHI(10)= (1.-ANU*ANU)*ZETA
      PHI(11)= 8./(BETA**3)*PHI(3)
      PHI(12)=(24.+64.*BETA+24.*BETA**2)/(3.+12.*BETA+9.*BETA**2)
      PHI(13)= 12.*BETA**2/(PI+3.*PI*BETA)
      PHI(14)=(48./PI**3)*BETA**2/(1.+3.*BETA)
      PHI(15)= 96./PI**2/(1.+3.*BETA)
      PHI(16)= 1536./(BETA*PI**4+3.*(BETA**2)*(PI**4))
      DO 201 I=1,93
      DO 201 J=1,93
  201 A(I,J)=0
      A(1,1)=-2.-2.*EXA*BETA*BETA+.75*ETA*ANU
      A(1,2)=1.
      A(1,3)=-.25*ETA*ANU
      A(1,5)=2.*EXA*BETA*BETA
      A(1,37)=-EXA*BETA
      A(1,39)=EXA*BETA
      A(1,73)=.5*ETA*(1.-COS(PI/4.))
      A(1,74)=.5*ETA*(1.+COS(PI/4.))
      A(1,75)=.5*ETA*(1.+COS(PI/4.))
      A(1,76)=-2.*BETA*SIN(PI/8.)
      A(1,77)=-2.*BETA*SIN(3.*PI/8.)
      A(1,78)=-2.*BETA*SIN(5.*PI/8.)
      A(2,1)=1.
      A(2,2)=-2.-2.*EXA*BETA*BETA+.5*ETA*ANU
      A(2,3)=1.
```

```
      A(2,4)=-.25*ETA*ANU
      A(2,6)=2.*EXA*BETA*BETA
      A(2,38)=-EXA*BETA
      A(2,40)=EXA*BETA
      A(2,73)= .5*ETA*( COS(PI/8.)-COS(3.*PI/8.))
      A(2,74)= .5*ETA*( COS(PI/8.)+COS(3.*PI/8.))
      A(2,75)=-.5*ETA*( COS(PI/8.)+COS(3.*PI/8.))
      A(2,76)=-2.*BETA*SIN(PI/4.)
      A(2,77)=-2.*BETA*SIN(PI/4.)
      A(2,78)= 2.*BETA*SIN(PI/4.)
      A(3,1)=-.25*ETA*ANU
      A(3,2)=1.
      A(3,3)=-2.-2.*EXA*BETA*BETA+ .25*ETA*ANU
      A(3,4)=1.
      A(3,7)=2.*EXA*BETA*BETA
      A(3,39)=-EXA*BETA
      A(3,73)= .5*ETA*COS(PI/4.)
      A(3,74)=-.5*ETA*COS(PI/4.)
      A(3,75)=-.5*ETA*COS(PI/4.)
      A(3,76)=-2.*BETA*SIN(3.*PI/8.)
      A(3,77)= 2.*BETA*SIN(PI/8.)
      A(3,78)= 2.*BETA*SIN(PI/8.)
      A(3,79)= .125*ANU/(1.-ANU)
      A(3,80)= .125*ANU/(1.-ANU)
      A(3,81)= .125*ANU/(1.-ANU)
      A(4,3)= 2.*(1.-ANU*ANU)
      A(4,4)=-2.*(1.-ANU*ANU)
      A(4,79)=-1.
      A(4,80)=-1.
      A(4,81)=-1.
      A(4,73)= ANU*PI/8.
      A(4,74)=-3.*ANU*PI/8.
      A(4,75)= 5.*ANU*PI/8.
      A(4,88)= PI*BETA/16.
      A(4,89)= 3.*PI*BETA/16.
      A(4,90)= 5.*PI*BETA/16.
      A(5,1)=EXA*BETA*BETA
      A(5,5)=-2.-2.*EXA*BETA*BETA
      A(5,6)= 1.
      A(5,9)= EXA*BETA*BETA
      A(5,37)=.25*ETA*BETA
      A(5,39)=-.25*ETA*BETA
      A(5,45)=-.25*ETA*BETA
      A(5,47)= .25*ETA*BETA
      A(6,2)=EXA*BETA*BETA
      A(6,5)=1.
      A(6,6)=-2.-2.*EXA*BETA*BETA
      A(6,7)=1.
      A(6,10)=EXA*BETA*BETA
      A(6,38)=.25*ETA*BETA
      A(6,40)=-.25*ETA*BETA
      A(6,46)=-.25*ETA*BETA
      A(6,48)= .25*ETA*BETA
      A(7,3 )=EXA*BETA*BETA
      A(7,6)=1.
      A(7,7)=-2.-2.*EXA*BETA*BETA
```

DK 026 - FFN SOURCE STATEMENT - IFN(S) -

```
      A(7,8)=1.
      A(7,11)=EXA*BETA*BETA
      A(7,39)=.25*ETA*BETA
      A(7,47)=-.25*ETA*BETA
      A(8,4)= EXA*BETA*BETA
      A( 8, 7)= 2.
      A(8,8)=-2.-2.*EXA*BETA*BETA+ .25*ETA*BETA*BETA
      A(8,12)= EXA*BETA*BETA
      A( 8,16)=-.25*ETA*BETA*BETA
      A(8,40)= .5*ETA*BETA
      A( 8,76)= .5*ETA*BETA/EXA*COS(PI/8.)
      A(8,77)=-.5*ETA/EXA*SIN(PI/8.)*BETA
      A(8,78)=-.5*ETA/EXA*SIN(PI/8.)*BETA
      A(8,79)=-2.*COS(PI/16.)
      A(8,80)=-2.*COS(3.*PI/16.)
      A(8,81)=-2.*COS(5.*PI/16.)
      A(8,82)= 2.*SIN(PI/16.)+PI*BETA*BETA/(128.*(1.-ANU))
      A(8,83)= 2.*SIN(3.*PI/16.)+3.*PI*BETA*BETA/(128.*(1.-ANU))
      A(8,84)= 2.*SIN(5.*PI/16.)+5.*PI*BETA*BETA/(128.*(1.-ANU))
      A(8,88)= .5*ETA/EXA*SIN(PI/8.)*BETA
      A(8,89)= .5*ETA*BETA/EXA*COS(PI/8.)
      A(8,90)= .5*ETA*BETA/EXA*COS(PI/8.)
      A(9,5)=EXA*BETA*BETA
      A(9,9)=-2.-2.*EXA*BETA*BETA
      A(9,10)=1.
      A(9,13)=EXA*BETA*BETA
      A(9,41)=.25*ETA*BETA
      A(9,43)=-.25*ETA*BETA
      A(9,49)=-.25*ETA*BETA
      A(9,51)= .25*ETA*BETA
      A(10,6)=EXA*BETA*BETA
      A(10,9)=1.
      A(10,10)=-2.-2.*EXA*BETA*BETA
      A(10,11)=1.
      A(10,14)=EXA*BETA*BETA
      A(10,42)=.25*ETA*BETA
      A(10,44)=-.25*ETA*BETA
      A(10,50)=-.25*ETA*BETA
      A(10,52)= .25*ETA*BETA
      A(11,7)=EXA*BETA*BETA
      A(11,10)= 1.
      A(11,11)=-2.-2.*EXA*BETA*BETA
      A(11,12)= 1.
      A(11,15)=EXA*BETA*BETA
      A(11,43)=.25*ETA*BETA
      A(11,51)=-.25*ETA*BETA
      A(12, 4)=-.25*ETA*BETA*BETA
      A(12,8)= EXA*BETA*BETA
      A(12,11)= 2.
      A(12,12)=-2.-2.*EXA*BETA*BETA+.5*ETA*BETA*BETA
      A(12,16)=EXA*BETA*BETA
      A(12,20)=-.25*ETA*BETA*BETA
      A(12,79)=-2.*COS(PI/8.)
```

DK 026 - FFN SOURCE STATEMENT - IFN(S) -

```
      A(12,80)=-2.*COS(3.*PI/8.)
      A(12,81)= 2.*COS(3.*PI/8.)
      A(12,82)= 2.*SIN(PI/8.)
      A(12,83)= 2.*SIN(3.*PI/8.)
      A(12,84)= 2.*SIN(3.*PI/8.)
      A(12,76)= .5*ETA*BETA/EXA*(COS(3.*PI/16.)-COS(PI/16.))
      A(12,77)= .5*ETA*BETA/EXA*(SIN(PI/16.)+COS(3.*PI/16.))
      A(12,78)=-.5*ETA*BETA/EXA*(COS(PI/16.)+COS(5.*PI/16.))
      A(12,88)= .5*ETA*BETA/EXA*(SIN(3.*PI/16.)-SIN(PI/16.))
      A(12,89)= .5*ETA*BETA/EXA*(COS(PI/16.)-SIN(3.*PI/16.))
      A(12,90)= .5*ETA*BETA*(SIN(PI/16.)-SIN(5.*PI/16.))/EXA
      A(13,9)=EXA*BETA*BETA
      A(13,13)=-2.-2.*EXA*BETA*BETA
      A(13,14)=1.
      A(13,17)=EXA*BETA*BETA
      A(13,45)= .25*ETA*BETA
      A(13,47)=-.25*ETA*BETA
      A(13,53)=-.25*ETA*BETA
      A(13,55)= .25*ETA*BETA
      A(14,10)=EXA*BETA*BETA
      A(14,13)=1.
      A(14,14)=-2.-2.*EXA*BETA*BETA
      A(14,15)=1.
      A(14,18)=EXA*BETA*BETA
      A(14,46)= .25*ETA*BETA
      A(14,48)=-.25*ETA*BETA
      A(14,54)=-.25*ETA*BETA
      A(14,56)= .25*ETA*BETA
      A(15,11)=EXA*BETA*BETA
      A(15,14)=1.
      A(15,15)=-2.-2.*EXA*BETA*BETA
      A(15,16)=1.
      A(15,19)=EXA*BETA*BETA
      A(15,47)= .25*ETA*BETA
      A(15,55)=-.25*ETA*BETA
      A(16, 8)=-.25*ETA*BETA*BETA
      A(16,12)= EXA*BETA*BETA
      A(16,15)= 2.
      A(16,16)=-2.-2.*EXA*BETA*BETA+.5*ETA*BETA*BETA
      A(16,20)= EXA*BETA*BETA
      A(16,24)=-.25*ETA*BETA*BETA
      A(16,76)= .5*ETA*BETA/EXA*(COS(PI/4.)-COS(PI/8.))
      A(16,77)= .5*ETA*BETA/EXA*(COS(3.*PI/8.)+COS(PI/4.))
      A(16,78)= -.5*ETA*BETA/EXA*(COS(PI/4.)+COS(5.*PI/8.))
      A(16,79)=-2.*COS(3.*PI/16.)
      A(16,80)=-2.*COS(9.*PI/16.)
      A(16,81)= 2.*COS(PI/16.)
      A(16,82)= 2.*SIN(3.*PI/16.)
      A(16,83)= 2.*SIN(9.*PI/16.)
      A(16,84)= 2.*SIN(PI/16.)
      A(16,88)= .5*ETA*BETA /EXA*(SIN(PI/4.)-SIN(PI/8.))
      A(16,89)= .5*ETA*BETA/EXA*(SIN(3.*PI/4.)-SIN(3.*PI/8.))
      A(16,90)= .5*ETA*BETA/EXA*(SIN(5.*PI/4.)-SIN(5.*PI/8.))
      A(17,13)=EXA*BETA*BETA
      A(17,17)=-2.-2.*EXA*BETA*BETA
      A(17,18)=1.
```

DK 026 - EFN SOURCE STATEMENT - IFN(S) -

```
      A(17,21)=EXA*BETA*BETA
      A(17,49)= .25*ETA*BETA
      A(17,51)=-.25*ETA*BETA
      A(17,57)=-.25*ETA*BETA
      A(17,59)= .25*ETA*BETA
      A(18,14)=EXA*BETA*BETA
      A(18,17)=1.
      A(18,18)=-2.-2.*EXA*BETA*BETA
      A(18,19)=1.
      A(18,22)=EXA*BETA*BETA
      A(18,50)= .25*ETA*BETA
      A(18,52)=-.25*ETA*BETA
      A(18,58)=-.25*ETA*BETA
      A(18,60)= .25*ETA*BETA
      A(19,15)=EXA*BETA*BETA
      A(19,18)=1.
      A(19,19)=-2.-2.*EXA*BETA*BETA
      A(19,20)=1.
      A(19,23)=EXA*BETA*BETA
      A(19,51)= .25*ETA*BETA
      A(19,59)=-.25*ETA*BETA
      A(20,12)=-.25*ETA*BETA*BETA
      A(20,16)= EXA*BETA*BETA
      A(20,19)= 2.
      A(20,20)=-2.-2.*EXA*BETA*BETA+.5*ETA*BETA*BETA
      A(20,24)= EXA*BETA*BETA
      A(20,28)=-.25*ETA*BETA*BETA
      A(20,79)=-2.*COS(PI/4.)
      A(20,80)= 2.*COS(PI/4.)
      A(20,81)= 2.*COS(PI/4.)
      A(20,82)= 2.*SIN(PI/4.)
      A(20,83)= 2.*SIN(PI/4.)
      A(20,84)=-2.*SIN(PI/4.)
      A(20,76)= .5*ETA*BETA/EXA*(COS(5.*PI/16.)-COS(3.*PI/16.))
      A(20,77)= .5*ETA*BETA /EXA*(COS(PI/16.)-SIN(PI/16.))
      A(20,78)= .5*ETA*BETA/EXA*(SIN(PI/16.)+COS(PI/16.))
      A(20,88)= .5*ETA*BETA/EXA*(SIN(5.*PI/16.)-SIN(3.*PI/16.))
      A(20,89)= -.5*ETA*BETA/EXA*(COS(PI/16.)-SIN(PI/16.))
      A(20,90)=-.5*ETA*BETA/EXA*(SIN(PI/16.)+COS(PI/16.))
      A(21,17)=EXA*BETA*BETA
      A(21,21)=-2.-2.*EXA*BETA*BETA
      A(21,22)=1.
      A(21,25)=EXA*BETA*BETA
      A(21,53)= .25*ETA*BETA
      A(21,55)=-.25*ETA*BETA
      A(21,61)=-.25*ETA*BETA
      A(21,63)= .25*ETA*BETA
      A(22,18)=EXA*BETA*BETA
      A(22,21)=1.
      A(22,22)=-2.-2.*EXA*BETA*BETA
      A(22,23)=1.
      A(22,26)=EXA*BETA*BETA
      A(22,54)= .25*ETA*BETA
      A(22,56)=-.25*ETA*BETA
      A(22,62)=-.25*ETA*BETA
      A(22,64)= .25*ETA*BETA
```

DK 026 - EFN SOURCE STATEMENT - IFN(S) -

```
      A(23,19)=EXA*BETA*BETA
      A(23,22)=1.
      A(23,23)=-2.-2.*EXA*BETA*BETA
      A(23,24)=1.
      A(23,27)=EXA*BETA*BETA
      A(23,55)= .25*ETA*BETA
      A(23,63)=-.25*ETA*BETA
      A(24,16)=-.25*ETA*BETA*BETA
      A(24,20)= EXA*BETA*BETA
      A(24,23)= 2.
      A(24,24)=-2.-2.*EXA*BETA*BETA+.5*ETA*BETA*BETA
      A(24,28)= EXA*BETA*BETA
      A(24,32)=-.25*ETA*BETA*BETA
      A(24,76)= .5*ETA*BETA/EXA*(COS(3.*PI/8.)-COS(PI/4.))
      A(24,77)= .5*ETA*BETA/EXA*(COS(PI/8.)-COS(PI/4.))
      A(24,78)= .5*ETA*BETA/EXA*(COS(PI/8.)+COS(PI/4.))
      A(24,79)=-2.*COS(5.*PI/16.)
      A(24,80)= 2.*COS(PI/16.)
      A(24,81)=-2.*COS(7.*PI/16.)
      A(24,82)= 2.*SIN(5.*PI/16.)
      A(24,83)= 2.*SIN(PI/16.)
      A(24,84)=-2.*SIN(7.*PI/16.)
      A(24,88)= .5*ETA*BETA/EXA*(SIN(3.*PI/8.)-SIN(PI/4.))
      A(24,89)=-.5*ETA*BETA/EXA*(SIN(PI/8.)+SIN(PI/4.))
      A(24,90)=-.5*ETA*BETA/EXA*(SIN(PI/8.)-SIN(PI/4.))
      A(25,21)=EXA*BETA*BETA
      A(25,25)=-2.-2.*EXA*BETA*BETA
      A(25,26)=1.
      A(25,29)=EXA*BETA*BETA
      A(25,57)= .25*ETA*BETA
      A(25,59)=-.25*ETA*BETA
      A(25,65)=-.25*ETA*BETA
      A(25,67)= .25*ETA*BETA
      A(26,22)=EXA*BETA*BETA
      A(26,25)=1.
      A(26,26)=-2.-2.*EXA*BETA*BETA
      A(26,27)=1.
      A(26,30)=EXA*BETA*BETA
      A(26,58)= .25*ETA*BETA
      A(26,60)=-.25*ETA*BETA
      A(26,66)=-.25*ETA*BETA
      A(26,68)= .25*ETA*BETA
      A(27,23)=EXA*BETA*BETA
      A(27,26)=1.
      A(27,27)=-2.-2.*EXA*BETA*BETA
      A(27,28)=1.
      A(27,31)=EXA*BETA*BETA
      A(27,59)= .25*ETA*BETA
      A(27,67)=-.25*ETA*BETA
      A(28,20)=-.25*ETA*BETA*BETA
      A(28,24)= EXA*BETA*BETA
      A(28,27)= 2.
      A(28,28)=-2.-2.*EXA*BETA*BETA+.5*ETA*BETA*BETA
      A(28,32)= EXA*BETA*BETA
      A(28,36)=-.25*ETA*BETA*BETA
      A(28,76)= .5*ETA*BETA/EXA*(SIN(PI/ 6.)-COS(5.*PI/16.))
```

DK 026 - EFN SOURCE STATEMENT - IFN(S) -

```
A(28,77)= .5*ETA*BETA/EXA*(COS(5.*PI/16.)-COS(PI/16.))
A(28,78)= .5*ETA*BETA/EXA*(COS(3.*PI/16.)-SIN(PI/16.))
A(28,79)=-2.*COS(3.*PI/8.)
A(28,80)= 2.*COS(PI/8.)
A(28,81)=-2.*COS(PI/8.)
A(28,82)= 2.*SIN(3.*PI/8.)
A(28,83)=-2.*SIN(PI/8.)
A(28,84)=-2.*SIN(PI/8.)
A(28,88)=-.5*ETA*BETA/EXA*(SIN(5.*PI/16.)-COS(PI/16.))
A(28,89)=-.5*ETA*BETA/EXA*(SIN(5.*PI/16.)+SIN(PI/16.))
A(28,90)= .5*ETA*BETA/EXA*(SIN(3.*PI/16.)+COS(PI/16.))
A(29,25)=EXA*BETA*BETA
A(29,29)=-2.-2.*EXA*BETA*BETA
A(29,30)=1.
A(29,33)=EXA*BETA*BETA
A(29,61)= .25*ETA*BETA
A(29,63)=-.25*ETA*BETA
A(29,69)=-.25*ETA*BETA
A(29,71)= .25*ETA*BETA
A(30,26)=EXA*BETA*BETA
A(30,29)=1.
A(30,30)=-2.-2.*EXA*BETA*BETA
A(30,31)=1.
A(30,34)=EXA*BETA*BETA
A(30,62)= .25*ETA*BETA
A(30,64)=-.25*ETA*BETA
A(30,70)=-.25*ETA*BETA
A(30,72)= .25*ETA*BETA
A(31,27)=EXA*BETA*BETA
A(31,30)=1.
A(31,31)=-2.-2.*EXA*BETA*BETA
A(31,32)=1.
A(31,35)=EXA*BETA*BETA
A(31,63)= .25*ETA*BETA
A(31,71)=-.25*ETA*BETA
A(32,24)=-.25*ETA*BETA*BETA
A(32,28)= EXA*BETA*BETA
A(32,31)= 2.
A(32,32)=-2.-2.*EXA*BETA*BETA+ .25*ETA*BETA*BETA
A(32,36)= EXA*BETA*BETA
A(32,72)=-.5*ETA*BETA
A(32,76)=-.5*ETA*BETA/EXA*(COS(3.*PI/8.))
A(32,77)=-.5*ETA*BETA/EXA*(COS(PI/8.))
A(32,78)=-.5*ETA*BETA/EXA*(COS(PI/8.))
A(32,79)=-2.*COS(7.*PI/16.)-PI*BETA*BETA/(128.*(1.-ANU))
A(32,80)= 2.*SIN(3.*PI/16.)+3.*PI*BETA*BETA/(128.*(1.-ANU))
A(32,81)=-2.*COS(3.*PI/16.)-5.*PI*BETA*BETA/(128.*(1.-ANU))
A(32,82)= 2.* SIN(7.*PI/16.)
A(32,83)=-2.* SIN(5.*PI/16.)
A(32,84)= 2.* SIN(3.*PI/16.)
A(32,88)=-.5*ETA*BETA/EXA*COS(PI/8.)
A(32,89)= .5*ETA*BETA/EXA*SIN(PI/8.)
A(32,90)= .5*ETA*BETA/EXA*SIN(PI/8.)
A(33,29)=2.*EXA*BETA*BETA
A(33,33)=-2.-2.*EXA*BETA*BETA+.75*ETA*ANU
A(33,34)= .
```

DK 026 - FEN SOURCE STATEMENT - IFN(S) -

```
      A(33,35)=-.25*ETA*ANU
      A(33,69)= EXA*BETA
      A(33,71)=-EXA*BETA
      A(33,85)= .5*ETA*(COS(PI/4.)-1.)
      A(33,86)=-.5*ETA*(COS(PI/4.)+1.)
      A(33,87)=-.5*ETA*(COS(PI/4.)+1.)
      A(33,88)=2.*BETA*SIN(PI/8.)
      A(33,89)= 2.*BETA*COS(PI/8.)
      A(33,90)= 2.*BETA*COS(PI/8.)
      A(34,30)=2.*EXA*BETA*BETA
      A(34,33)=1.
      A(34,34)=-2.-2.*EXA*BETA*BETA+.5*ETA*ANU
      A(34,35)=1.
      A(34,36)=-.25*ETA*ANU
      A(34,70)= EXA*BETA
      A(34,72)=-EXA*BETA
      A(34,85)=.5*ETA*(COS(3.*PI/8.)-COS(PI/8.))
      A(34,86)=-.5*ETA*(COS(PI/8.)+COS(3.*PI/8.))
      A(34,87)= .5*ETA*(COS(PI/8.)-COS(5.*PI/8.))
      A(34,88)= 2.*BETA*SIN(PI/4.)
      A(34,89)= 2.*BETA*SIN(PI/4.)
      A(34,90)=-2.*BETA*SIN(PI/4.)
      A(35,31)=2.*EXA*BETA*BETA
      A(35,33)=-.25*ANU*ETA
      A(35,34)=1.
      A(35,35)=-2.-2.*EXA*BETA*BETA+ .25*ANU*ETA
      A(35,36)= 1.
      A(35,71)= EXA*BETA
      A(35,82)=-.125*ANU/(1.-ANU)
      A(35,83)= .125*ANU/(1.-ANU)
      A(35,84)=-.125*ANU/(1.-ANU)
      A(35,85)=-.5*ETA*COS(PI/4.)
      A(35,86)= .5*ETA*COS(PI/4.)
      A(35,87)= .5*ETA*COS(PI/4.)
      A(35,88)= 2.*BETA*COS(PI/8.)
      A(35,89)=-2.*BETA*SIN(PI/8.)
      A(35,90)=-2.*BETA*SIN(PI/8.)
      A(36,35)= 2.*(1.-ANU*ANU)
      A(36,36)=-2.*(1.-ANU*ANU)
      A(36,76)=-PI*BETA/16.
      A(36,77)=-3.*PI*BETA/16.
      A(36,78)=-5.*PI*BETA/16.
      A(36,82)= 1.
      A(36,83)=-1.
      A(36,84)= 1.
      A(36,85)=-PI*ANU/8.
      A(36,86)= 3.*PI*ANU/8.
      A(36,87)=-5.*PI*ANU/8.
      A(37,1)=2.*ANU*BETA
      A(37,37)=-2.*EXA-2.*BETA*BETA+.5*ETA
      A(37,38)=2.*EXA
      A(37,39)=-.5*ETA
      A(37,41)=2.*BETA*BETA
      A(37,73)=2.*BETA
      A(37,74)=2.*BETA
      A(37,75)=2.*BETA
```

```
A(37,76)=ETA/EXA*SIN(PI/8.)
A(37,77)=ETA/EXA*SIN(3.*PI/8.)
A(37,78)=ETA/EXA*SIN(5.*PI/8.)
A(38,2)=ANU*BETA
A(38,37)=EXA
A(38,38)=-2.*EXA-2.*BETA*BETA+.25*ETA
A(38,39)=EXA
A(38,40)=-.25*ETA
A(38,42)=2.*BETA*BETA
A(38,73)=2.*BETA*COS(PI/8.)
A(38,74)=2.*BETA*COS(3.*PI/8.)
A(38,75)=2.*BETA*COS(5.*PI/8.)
A(38,76)=.5*ETA/EXA*SIN(PI/4.)
A(38,77)=.5*ETA/EXA*SIN(PI/4.)
A(38,78)=-.5*ETA/EXA*SIN(PI/4.)
A(39,1)=-ANU*BETA
A(39,3)=ANU*BETA
A(39,37)=-.25*ETA
A(39,38)=EXA
A(39,39)=-2.*EXA-2.*BETA*BETA+.5*ETA
A(39,40)=EXA
A(39,43)=2.*BETA*BETA
A(39,73)=2.*BETA*COS(PI/4.)
A(39,74)=-2.*BETA*COS(PI/4.)
A(39,75)=-2.*BETA*COS(PI/4.)
A(39,76)= .5*ETA/EXA*(-SIN(PI/8.)+SIN(3.*PI/8.))
A(39,77)=.5*ETA/EXA*(-SIN(3.*PI/8.)-SIN(PI/8.))
A(39,78)=.5*ETA/EXA*(-SIN(3.*PI/8.)-SIN(PI/8.))
A(40,2)=-ANU*BETA
A(40, 4)= ANU*BETA-.5*ETA*BETA
A(40,8)= .5*ETA*BETA
A(40,38)=-.25*ETA
A(40,39)=EXA
A(40,40)=-2.*EXA-2.*BETA*BETA+ .25*ETA
A(40,44)=2.*BETA*BETA
A(40,73)= 2.*BETA*COS(3.*PI/8.)+PI/(64.*BETA*(1.-ANU))
A(40,74)=-2.*BETA*COS(PI/8.) -3.*PI/(64.*BETA*(1.-ANU))
A(40,75)= 2.*BETA*COS(PI/8.) +5.*PI/(64.*BETA*(1.-ANU))
A(40,76)=-.5*ETA/EXA*SIN(PI/4.)
A(40,77)=-.5*ETA/EXA*SIN(PI/4.)
A(40,78)= .5*ETA/EXA*SIN(PI/4.)
A(40,88)=-PI*(2.+ANU)/(128.*(1.-ANU))
A(40,89)=-3.*PI*(2.+ANU)/(128.*(1.-ANU))
A(40,90)=-5.*PI*(2.+ANU)/(128.*(1.-ANU))
A(41,1)=-.5*ETA*BETA
A(41,9)=.5*ETA*BETA
A(41,37)=BETA*BETA
A(41,41)=-2.*EXA-2.*BETA*BETA
A(41,42)=2.*EXA
A(41,45)=BETA*BETA
A(42,2)=-.25*ETA*BETA
A(42,10)=.25*ETA*BETA
A(42,38)=BETA*BETA
A(42,41)=EXA
A(42,42)=-2.*EXA-2.*BETA*BETA
A(42,43)=EXA
```

DK 026 - FFN SOURCE STATEMENT - IFN(S) -

```
A(42,46)= BETA*BETA
A(43,1)=.25*ETA*BETA
A(43,3)=-.25*ETA*BETA
A(43,9)=-.25*ETA*BETA
A(43,11)=.25*ETA*BETA
A(43,39)=BETA*BETA
A(43,42)=EXA
A(43,43)=-2.*EXA-2.*BETA*BETA
A(43,44)=EXA
A(43,47)= BETA*BETA
A(44,2)=.25*ETA*BETA
A(44,4)=-.25*ETA*BETA
A(44,10)=-.25*ETA*BETA
A(44,12)=.25*ETA*BETA
A(44,40)=BETA*BETA
A(44,43)=EXA
A(44,44)=-2.*EXA-2.*BETA*BETA
A(44,48)= BETA*BETA
A(45,5)=-.5*ETA*BETA
A(45,13)= .5*ETA*BETA
A(45,41)= BETA*BETA
A(45,45)=-2.*EXA-2.*BETA*BETA
A(45,46)= 2.*EXA
A(45,49)= BETA*BETA
A(46, 6)=-.25*ETA*BETA
A(46,14)= .25*ETA*BETA
A(46,42)= BETA*BETA
A(46,45)=EXA
A(46,46)=-2.*EXA-2.*BETA*BETA
A(46,47)=EXA
A(46,50)= BETA*BETA
A(47, 5)= .25*ETA*BETA
A(47, 7)=-.25*ETA*BETA
A(47,13)=-.25*ETA*BETA
A(47,15)= .25*ETA*BETA
A(47,43)= BETA*BETA
A(47,46)=EXA
A(47,47)=-2.*EXA-2.*BETA*BETA
A(47,48)= EXA
A(47,51)= BETA*BETA
A(48, 6)= .25*ETA*BETA
A(48, 8)=-.25*ETA*BETA
A(48,14)=-.25*ETA*BETA
A(48,16)= .25*ETA*BETA
A(48,44)= BETA*BETA
A(48,47)=EXA
A(48,48)=-2.*EXA-2.*BETA*BETA
A(48,52)= BETA*BETA
A(49, 9)=-.5*ETA*BETA
A(49,17)= .5*ETA*BETA
A(49,45)= BETA*BETA
A(49,49)=-2.*EXA-2.*BETA*BETA
A(49,50)= 2.*EXA
A(49,53)= BETA*BETA
A(50,10)=-.25*ETA*BETA
A(50,18)= .25*ETA*BETA
```

```
      A(50,46)= BETA*BETA
      A(50,49)= EXA
      A(50,50)=-2.*EXA-2.*BETA*BETA
      A(50,51)= EXA
      A(50,54)= BETA*BETA
      A(51, 9)= .25*ETA*BETA
      A(51,11)=-.25*ETA*BETA
      A(51,17)=-.25*ETA*BETA
      A(51,19)= .25*ETA*BETA
      A(51,47)= BETA*BETA
      A(51,50)= EXA
      A(51,51)=-2.*EXA-2.*BETA*BETA
      A(51,52)= EXA
      A(51,55)= BETA*BETA
      A(52,10)= .25*ETA*BETA
      A(52,12)=-.25*ETA*BETA
      A(52,18)=-.25*ETA*BETA
      A(52,20)= .25*ETA*BETA
      A(52,48)= BETA*BETA
      A(52,51)= EXA
      A(52,52)=-2.*EXA-2.*BETA*BETA
      A(52,56)= BETA*BETA
      A(53,13)=-.5*ETA*BETA
      A(53,21)= .5*ETA*BETA
      A(53,49)= BETA*BETA
      A(53,53)=-2.*EXA-2.*BETA*BETA
      A(53,54)= 2.*EXA
      A(53,57)= BETA*BETA
      A(54,14)=-.25*ETA*BETA
      A(54,22)= .25*ETA*BETA
      A(54,50)= BETA*BETA
      A(54,53)= EXA
      A(54,54)=-2.*EXA-2.*BETA*BETA
      A(54,55)= EXA
      A(54,58)= BETA*BETA
      A(55,13)= .25*ETA*BETA
      A(55,15)=-.25*ETA*BETA
      A(55,21)=-.25*ETA*BETA
      A(55,23)= .25*ETA*BETA
      A(55,51)= BETA*BETA
      A(55,54)= EXA
      A(55,55)=-2.*EXA-2.*BETA*BETA
      A(55,56)= EXA
      A(55,59)= BETA*BETA
      A(56,14)= .25*ETA*BETA
      A(56,16)=-.25*ETA*BETA
      A(56,22)=-.25*ETA*BETA
      A(56,24)= .25*ETA*BETA
      A(56,52)= BETA*BETA
      A(56,55)= EXA
      A(56,56)=-2.*EXA-2.*BETA*BETA
      A(56,60)= BETA*BETA
      A(57,17)=-.5*ETA*BETA
      A(57,25)= .5*ETA*BETA
      A(57,53)= BETA*BETA
      A(57,57)=-2.*EXA-2.*BETA*BETA
```

DK 026 - EFN SOURCE STATEMENT - IFN(S) -

```
      A(57,58)= 2.*EXA
      A(57,61)= BETA*BETA
      A(58,18)=-.25*ETA*BETA
      A(58,26)= .25*ETA*BETA
      A(58,54)= BETA*BETA
      A(58,57)= EXA
      A(58,58)=-2.*EXA-2.*BETA*BETA
      A(58,59)= EXA
      A(58,62)= BETA*BETA
      A(59,17)= .25*ETA*BETA
      A(59,19)=-.25*ETA*BETA
      A(59,25)=-.25*ETA*BETA
      A(59,27)= .25*ETA*BETA
      A(59,55)= BETA*BETA
      A(59,58)= EXA
      A(59,59)=-2.*EXA-2.*BETA*BETA
      A(59,60)= EXA
      A(59,63)= BETA*BETA
      A(60,18)= .25*ETA*BETA
      A(60,20)=-.25*ETA*BETA
      A(60,26)=-.25*ETA*BETA
      A(60,28)= .25*ETA*BETA
      A(60,56)= BETA*BETA
      A(60,59)= EXA
      A(60,60)=-2.*EXA-2.*BETA*BETA
      A(60,64)= BETA*BETA
      A(61,21)=-.5*ETA*BETA
      A(61,29)= .5*ETA*BETA
      A(61,57)= BETA*BETA
      A(61,61)=-2.*EXA-2.*BETA*BETA
      A(61,62)= 2.*EXA
      A(61,65)= BETA*BETA
      A(62,22)=-.25*ETA*BETA
      A(62,30)= .25*ETA*BETA
      A(62,58)= BETA*BETA
      A(62,61)= EXA
      A(62,62)=-2.*EXA-2.*BETA*BETA
      A(62,63)= EXA
      A(62,66)= BETA*BETA
      A(63,21)= .25*ETA*BETA
      A(63,23)=-.25*ETA*BETA
      A(63,29)=-.25*ETA*BETA
      A(63,31)= .25*ETA*BETA
      A(63,59)= BETA*BETA
      A(63,62)= EXA
      A(63,63)=-2.*EXA-2.*BETA*BETA
      A(63,64)= EXA
      A(63,67)= BETA*BETA
      A(64,22)= .25*ETA*BETA
      A(64,24)=-.25*ETA*BETA
      A(64,30)=-.25*ETA*BETA
      A(64,32)= .25*ETA*BETA
      A(64,60)= BETA*BETA
      A(64,63)= EXA
      A(64,64)=-2.*EXA-2.*BETA*BETA
      A(64,68)= BETA*BETA
```

```
A(65,25)=-.5*ETA*BETA
A(65,33)= .5*ETA*BETA
A(65,61)= BETA*BETA
A(65,65)=-2.*EXA-2.*BETA*BETA
A(65,66)= 2.*EXA
A(65,69)= BETA*BETA
A(66,26)=-.25*ETA*BETA
A(66,34)= .25*ETA*BETA
A(66,62)= BETA*BETA
A(66,65)= EXA
A(66,66)=-2.*EXA-2.*BETA*BETA
A(66,67)= EXA
A(66,70)= BETA*BETA
A(67,25)= .25*ETA*BETA
A(67,27)=-.25*ETA*BETA
A(67,33)=-.25*ETA*BETA
A(67,35)= .25*ETA*BETA
A(67,63)= BETA*BETA
A(67,66)= EXA
A(67,67)=-2.*EXA-2.*BETA*BETA
A(67,68)= EXA
A(67,71)= BETA*BETA
A(68,26)= .25*ETA*BETA
A(68,28)=-.25*ETA*BETA
A(68,34)=-.25*ETA*BETA
A(68,36)= .25*ETA*BETA
A(68,64)= BETA*BETA
A(68,67)= EXA
A(68,68)=-2.*EXA-2.*BETA*BETA
A(68,72)= BETA*BETA
A(69,33)=-2.*ANU*BETA
A(69,69)=-2.*EXA-2.*BETA*BETA+.5*ETA
A(69,70)= 2.*EXA
A(69,71)=-.5*ETA
A(69,65)= 2.*BETA*BETA
A(69,85)= 2.*BETA
A(69,86)= 2.*BETA
A(69,87)= 2.*BETA
A(69,88)= ETA/EXA*SIN(PI/8.)
A(69,89)= ETA/EXA*COS(PI/8.)
A(69,90)= ETA/EXA*COS(PI/8.)
A(70,34)=-ANU*BETA
A(70,66)= 2.*BETA*BETA
A(70,69)= EXA
A(70,70)=-2.*EXA-2.*BETA*BETA+.25*ETA
A(70,71)= EXA
A(70,72)=-.25*ETA
A(70,85)= 2.*BETA*COS(PI/8.)
A(70,86)= 2.*BETA*SIN(PI/8.)
A(70,87)=-2.*BETA*SIN(PI/8.)
A(70,88)= .5*ETA/EXA*SIN(PI/4.)
A(70,89)= .5*ETA/EXA*SIN(PI/4.)
A(70,90)=-.5*ETA/EXA*SIN(PI/4.)
A(71,33)= ANU*BETA
A(71,35)=-ANU*BETA
A(71,67)= 2.*BETA*BETA
```

DK 026 - EEN SOURCE STATEMENT - IFN(S) -

```
A(71,69)=-.25*ETA
A(71,70)= EXA
A(71,71)=-2.*EXA-2.*BETA*BETA+ .5*ETA
A(71,72)= EXA
A(71,85)= 2.*BETA*COS(PI/4.)
A(71,86)=-2.*BETA*COS(PI/4.)
A(71,87)=-2.*BETA*COS(PI/4.)
A(71,88)= .5*ETA/EXA*(COS(PI/8.)-SIN(PI/8.))
A(71,89)=-.5*ETA/EXA*(COS(PI/8.)+SIN(PI/8.))
A(71,90)=-.5*ETA/EXA*(COS(PI/8.)+SIN(PI/8.))
A(72,32)=-.5*ETA*BETA
A(72,34)= ANU*BETA
A(72,36)=-ANU*BETA+.5*ETA*BETA
A(72,68)= 2.*BETA*BETA
A(72,70)=-.25*ETA
A(72,71)= EXA
A(72,72)=-2.*EXA-2.*BETA*BETA+.25*ETA
A(72,85)= 2.*BETA*SIN(PI/8.)+PI/(64.*BETA*(1.-ANU))
A(72,86)=-2.*BETA*COS(PI/8.)-3.*PI/(64.*BETA*(1.-ANU))
A(72,87)= 2.*BETA*COS(PI/8.)+5.*PI/(64.*BETA*(1.-ANU))
A(72,88)=-.5*ETA/EXA*SIN(PI/4.)
A(72,89)=-.5*ETA/EXA*SIN(PI/4.)
A(72,90)= .5*ETA/EXA*SIN(PI/4.)
A(72,76)=-PI*(2.+ANU)/(128.*(1.-ANU))
A(72,77)=-3.*PI*(2.+ANU)/(128.*(1.-ANU))
A(72,78)=-5.*PI*(2.+ANU)/(128.*(1.-ANU))
A(73,37)= PHI(10)
A(73,38)=-2.*PHI(10)
A(73,39)= PHI(10)
A(73,73)= PHI(2)*(1.-COS(PI/8.))
A(73,74)= PHI(2)/9.*(1.-COS(3.*PI/8.))
A(73,75)= PHI(2)/25.*(1.+SIN(PI/8.))
A(73,91)= 1.
A(74,38)= PHI(10)
A(74,39)=-2.*PHI(10)
A(74,40)= PHI(10)
A(74,73)= PHI(2)*(1.-COS(PI/4.))
A(74,74)= PHI(2)/9.*(1.+COS(PI/4.))
A(74,75)= PHI(2)/25.*(1.+COS(PI/4.))
A(74,91)= 1.
A(75,39)= PHI(10)
A(75,40)=-2.*PHI(10)
A(75,73)= PHI(2)*(1.-SIN(PI/8.))
A(75,74)= PHI(2)/9.*(1.+COS(PI/8.))
A(75,75)= PHI(2)/25.*(1.-COS(PI/8.))
A(75,91)= 1.
A(76,37)=-2.*PHI(10)
A(76,38)= 2.*PHI(10)
A(76,91)= 1.
A(77, 4)=-BETA*BETA*PHI(10)
A(77,8)= 2.*BETA*BETA*PHI(10)
A(77,12)=-BETA*BETA*PHI(10).
A(77,73)= PHI(2)
A(77,74)= PHI(2)/9.
A(77,75)= PHI(2)/25.
A(77,76)= 8./(PI*BETA)
```

DK 026 - FEN SOURCE STATEMENT - IFN(S) -

```
      A(77,77)= 8./(3.*PI*BETA)
      A(77,78)= 8./(5.*PI*BETA)
      A(77,79)= 4.*PHI(2)/BETA**2*(1.-COS(PI/16.))
      A(77,80)= 4.*PHI(2)/(9.*BETA**2)*(1.-COS(3.*PI/16.))
      A(77,81)= 4.*PHI(2)/(25.*BETA*BETA)*(1.-COS(5.*PI/16.))
      A(77,82)=-4.*PHI(2)/BETA**2*SIN(PI/16.)
      A(77,83)=-4.*PHI(2)/(9.*BETA*BETA)*SIN(3.*PI/16.)
      A(77,84)=-4.*PHI(2)/(25.*BETA**2)*SIN(5.*PI/16.)
      A(77,91)= 1.
      A(77,93)=-1./BETA
      A(78, 8)=-BETA*BETA*PHI(10)
      A(78,12)= 2.*BETA*BETA*PHI(10)
      A(78,16)=-BETA*BETA*PHI(10)
      A(78,73)= PHI(2)
      A(78,74)= PHI(2)/9.
      A(78,75)= PHI(2)/25.
      A(78,76)= 16./(PI*BETA)
      A(78,77)= 16./(3.*PI*BETA)
      A(78,78)= 16./(5.*PI*BETA)
      A(78,79)= 4.*PHI(2)/BETA**2*(1.-COS(PI/8.))
      A(78,80)= 4.*PHI(2)/(9.*BETA*BETA)*(1.-SIN(PI/8.))
      A(78,81)= 4.*PHI(2)/(25.*BETA*BETA)*(1.+SIN(PI/8.))
      A(78,82)=-4.*PHI(2)/(BETA*BETA)*SIN(PI/8.)
      A(78,83)=-4.*PHI(2)/(9.*BETA*BETA)*SIN(3.*PI/8.)
      A(78,84)=-4.*PHI(2)/(25.*BETA*BETA)*COS(PI/8.)
      A(78,91)= 1.
      A(78,93)=-2./BETA
      A(79,12)=-BETA*BETA*PHI(10)
      A(79,16)= 2.*BETA*BETA*PHI(10)
      A(79,20)=-BETA*BETA*PHI(10)
      A(79,73)= PHI(2)
      A(79,74)= PHI(2)/9.
      A(79,75)= PHI(2)/25.
      A(79,76)= 24. /(PI*BETA)
      A(79,77)= 24./(3.*PI*BETA)
      A(79,78)= 24./(5.*PI*BETA)
      A(79,79)= 4.*PHI(2)/(BETA*BETA)*(1.-COS(3.*PI/16.))
      A(79,80)= 4.*PHI(2)/(9.*BETA*BETA)*(1.+SIN(PI/16.))
      A(79,81)= 4.*PHI(2)/(25.*BETA*BETA)*(1.+COS(PI/16.))
      A(79,82)=-4.*PHI(2)/(BETA*BETA)* SIN(3.*PI/16.)
      A(79,83)=-4.*PHI(2)/(9.*BETA*BETA)*COS(PI/16.)
      A(79,84)=-4.*PHI(2)/(25.*BETA*BETA)*SIN(PI/16.)
      A(79,91)= 1.
      A(79,93)=-3./BETA
      A(80,16)=-BETA*BETA*PHI(10)
      A(80,20)= 2.*BETA*BETA*PHI(10)
      A(80,24)=-BETA*BETA*PHI(10)
      A(80,73)= PHI(2)
      A(80,74)= PHI(2)/9.
      A(80,75)= PHI(2)/25.
      A(80,76)= 32./(PI*BETA)
      A(80,77)= 32./(3.*PI*BETA)
      A(80,78)= 32./(5.*PI*BETA)
      A(80,79)= 4.*PHI(2)/(BETA*BETA)*(1.-COS(PI/4.))
      A(80,80)= 4.*PHI(2)/(9.*BETA*BETA)*(1.+COS(PI/4.))
      A(80,81)= 4.*PHI(2)/(25.*BETA*BETA)*(1.+COS(PI/4.))
```

DK 026 - EFN SOURCE STATEMENT - IFN(S) -

```
A(80,82)=-4.*PHI(2)/(BETA*BETA)*SIN(PI/4.)
A(80,83)=-4.*PHI(2)/(9.*BETA*BETA)*SIN(PI/4.)
A(80,84)= 4.*PHI(2)/(25.*BETA*BETA)*SIN(PI/4.)
A(80,91)= 1.
A(80,93)=-4./BETA
A(81,20)=-BETA*BETA*PHI(10)
A(81,24)= 2.*BETA*BETA*PHI(10)
A(81,28)=-BETA*BETA*PHI(10)
A(81,73)= PHI(2)
A(81,74)= PHI(2)/9.
A(81,75)= PHI(2)/25.
A(81,76)= 40./(PI*BETA)
A(81,77)= 40./(3.*PI*BETA)
A(81,78)= 40./(5.*PI*BETA)
A(81,79)= 4.*PHI(2)/(BETA*BETA)*(1.-COS(5.*PI/16.))
A(81,80)= 4.*PHI(2)/(9.*BETA*BETA)*(1.+COS(PI/16.))
A(81,81)= 4.*PHI(2)/(25.*BETA*BETA)*(1.-SIN(PI/16.))
A(81,82)=-4.*PHI(2)/(BETA*BETA)*SIN(5.*PI/16.)
A(81,83)=-4.*PHI(2)/(9.*BETA*BETA)*SIN(PI/16.)
A(81,84)= 4.*PHI(2)/(25.*BETA*BETA)*COS(PI/16.)
A(81,91)= 1.
A(81,93)=-5./BETA
A(82,24)=-BETA*BETA*PHI(10)
A(82,28)= 2.*BETA*BETA*PHI(10)
A(82,32)=-BETA*BETA*PHI(10)
A(82,73)= PHI(2)
A(82,74)= PHI(2)/9.
A(82,75)= PHI(2)/25.
A(82,76)= 48./(PI*BETA)
A(82,77)= 48./(3.*PI*BETA)
A(82,78)= 48./(5.*PI*BETA)
A(82,79)= 4.*PHI(2)/(BETA*BETA)*(1.-COS(3.*PI/8.))
A(82,80)= 4.*PHI(2)/(9.*BETA*BETA)*(1.+COS(PI/8.))
A(82,81)= 4.*PHI(2)/(25.*BETA*BETA)*(1.-COS(PI/8.))
A(82,82)=-4.*PHI(2)/(BETA*BETA)*SIN(3.*PI/8.)
A(82,83)= 4.*PHI(2)/(9.*BETA*BETA)*SIN(PI/8.)
A(82,84)= 4.*PHI(2)/(25.*BETA*BETA)*SIN(PI/8.)
A(82,91)= 1.
A(82,93)=-6./BETA
A(83,28)=-BETA*BETA*PHI(10)
A(83,32)= 2.*BETA*BETA*PHI(10)
A(83,36)=-BETA*BETA*PHI(10)
A(83,73)= PHI(2).
A(83,74)= PHI(2)/9.
A(83,75)= PHI(2)/25.
A(83,76)= 56./(PI*BETA)
A(83,77)= 56./(3.*PI*BETA)
A(83,78)= 56./(5.*PI*BETA)
A(83,79)= 4.*PHI(2)/(BETA*BETA)*(1.-SIN(PI/16.))
A(83,80)= 4.*PHI(2)/(9.*BETA*BETA)*(1.+SIN(3.*PI/16.))
A(83,81)= 4.*PHI(2)/(25.*BETA*BETA)*(1.-COS(3.*PI/16.))
A(83,82)=-4.*PHI(2)/(BETA*BETA)*COS(PI/16.)
A(83,83)= 4.*PHI(2)/(9.*BETA*BETA)*COS(3.*PI/16.)
A(83,84)=-4.*PHI(2)/(25.*BETA*BETA)*SIN(3.*PI/16.)
A(83,91)= 1.
A(83,93)=-7./BETA
```

DK 026 - FFN SOURCE STATEMENT - IFN(S) -

```
      A(84,69)=-2.*PHI(10)
      A(84,70)= 2.*PHI(10)
      A(84,92)= 1.
      A(85,69)= PHI(10)
      A(85,70)=-2.*PHI(10)
      A(85,71)= PHI(10)
      A(85,92)= 1.
      A(85,85)= PHI(2)*(1.-COS(PI/8.))
      A(85,86)= PHI(2)/9.*(1.-SIN(PI/8.))
      A(85,87)= PHI(2)/25.*(1.+SIN(PI/8.))
      A(86,70)= PHI(10)
      A(86,71)=-2.*PHI(10)
      A(86,72)= PHI(10)
      A(86,85)= PHI(2)*(1.-COS(PI/4.))
      A(86,86)= PHI(2)/9.*(1.+COS(PI/4.))
      A(86,87)= PHI(2)/25.*(1.+COS(PI/4.))
      A(86,92)= 1.
      A(87,71)= PHI(10)
      A(87,72)=-2.*PHI(10)
      A(87,85)= PHI(2)*(1.-COS(3.*PI/8.))
      A(87,86)= PHI(2)/9.*(1.+COS(PI/8.))
      A(87,87)= PHI(2)/25.*(1.-COS(PI/8.))
      A(87,92)= 1.
      A(88,73)= BETA
      A(88,76)= 2.
      A(88,85)= BETA
      A(88,88)= 2.
      A(89,74)= BETA
      A(89,77)=-2.
      A(89,86)= BETA
      A(89,89)=-2.
      A(90,75)= BETA
      A(90,78)= 2.
      A(90,87)= BETA
      A(90,90)= 2.
      A(91,73)= PHI(1)+PHI(2)-PHI(3)
      A(91,74)=-PHI(1)/3.+PHI(2)/9.+PHI(3)/27.
      A(91,75)= PHI(1)/5.+PHI(2)/25.-PHI(3)/125.
      A(91,76)= 2.*PHI(1)/BETA
      A(91,77)= 2.*PHI(1)/(3.*BETA)
      A(91,78)= 2.*PHI(1)/(5.*BETA)
      A(91,79)= PHI(5)+PHI(6)-PHI(7)
      A(91,80)= PHI(5)/9.-PHI(6)/27.-PHI(7)/81.
      A(91,81)= PHI(5)/25.+PHI(6)/125.-PHI(7)/625.
      A(91,82)= PHI(8)+PHI(6)+PHI(7)
      A(91,83)=-PHI(8)/9.+PHI(6)/27.-PHI(7)/81.
      A(91,84)= PHI(8)/25.+PHI(6)/125.+PHI(7)/625.
      A(91,85)= PHI(1)-PHI(4)
      A(91,86)=-PHI(1)/3.+PHI(4)/27.
      A(91,87)= PHI(1)/5.-PHI(4)/125.
      A(91,88)= 2.*PHI(1)/BETA
      A(91,89)= 2.*PHI(1)/(3.*BETA)
      A(91,90)= 2.*PHI(1)/(5.*BETA)
      A(91,91)= 1.
      A(92,73)= PHI(9)+PHI(4)
      A(92,74)=-PHI(9)/3.-PHI(4)/27.
```

DK 026 - FEN SOURCE STATEMENT - IFN(S)

```
      A(92,75)= PHI(9)/5.+PHI(4)/125.
      A(92,76)= 2.*PHI(9)/BETA
      A(92,77)= 2.*PHI(9)/(3.*BETA)
      A(92,78)= 2.*PHI(9)/(5.*BETA)
      A(92,79)= PHI(8)-PHI(11)+PHI(7)
      A(92,80)= PHI(8)/9.+PHI(11)/27.+PHI(7)/81.
      A(92,81)= PHI( 8)/25.-PHI(11)/125.+PHI(7)/625.
      A(92,82)= PHI(5)-PHI(11)-PHI(7)
      A(92,83)=-PHI(5)/9.-PHI(11)/27.+PHI(7)/81.
      A(92,84)= PHI(5)/25.-PHI(11)/125.-PHI(7)/625.
      A(92,85)= PHI(9)-PHI(2)+PHI(3)
      A(92,86)=-PHI(9)/3.-PHI(2)/9.-PHI(3)/27.
      A(92,87)= PHI(9)/5.-PHI(2)/25.+PHI(3)/125.
      A(92,88)= 2.*PHI(9)/BETA
      A(92,89)= 2.*PHI(9)/(3.*BETA)
      A(92,90)= 2.*PHI(9)/(5.*BETA)
      A(92,92)=-1.
      A(93,73)=-PHI(13)+PHI(14)
      A(93, 74)= PHI(13)/3.-PHI(14)/27.
      A(93, 75)=-PHI(13)/5.+PHI(14)/125.
      A(93, 76)= 2.*PHI(13)/(3.*BETA*BETA)
      A(93, 77)= 2.*PHI(13)/(9.*BETA*BETA)
      A(93, 78)= 2.*PHI(13)/(15.*BETA*BETA)
      A(93, 79)= PHI(15)-PI*PHI(16)/4.+PHI(16)
      A(93, 80)= PHI(15)/9.+PI*PHI(16)/108.+PHI(16)/81.
      A(93, 81)= PHI(15)/25.-PI*PHI(16)/500.+PHI(16)/625.
      A(93, 82)=-PHI(15)-PI*PHI(16)/4.-PHI(16)
      A(93, 83)= PHI(15)/9.-PI*PHI(16)/108.+PHI(16)/81.
      A(93, 84)=-PHI(15)/25.-PI*PHI(16)/500.-PHI(16)/625.
      A(93, 85)=-PHI(13)+PHI(14)
      A(93, 86)= PHI(13)/3.-PHI(14)/27.
      A(93, 87)=-PHI(13)/5.+PHI(14)/125.
      A(93, 88)=-2.*PHI(13)/BETA
      A(93, 89)=-2.*PHI(13)/(3.*BETA)
      A(93, 90)=-2.*PHI(13)/(5.*BETA)
      A(93,93)=-1.
      DO 202 I=1,93
  202 B(I)=0.
      B(73)= 0.5
      B(74)= 2.0
      B(75)= 4.5
      B(77)= 8.0
      B(78)= 8.0
      B(79)= 8.0
      B(80)= 8.0
      B(81)= 8.0
      B(82)= 8.0
      B(83)= 8.0
      B(91)= PHI(12)
      B(92)= PI*PHI(1)/6.
      B(93 )= PI*PHI(13)/6.
      CALL LEQU (0,A,93,93,B,1,LUCK)
      WRITE (6,12) LUCK
   12 FORMAT (I5)
      WRITE (6,24) (B(I), I=1,93)
   24 FORMAT (4E16.8)
```

DK 026 - EFN SOURCE STATEMENT - IFN(S)

```
      SX(1)= (1.-ANU*ANU)*X(1)-ANU*(X(73)+X(74)+X(75))
      SX(2)= X(5)+.5*ANU*BETA*(X(45)-X(37))
      SX( 3)= X(9)+.5*ANU*BETA*(X(49)-X(41))
      SX( 4)= X(13)+.5*ANU*BETA*(X(53)-X(45))
      SX( 5)= X(17)+.5*ANU*BETA*(X(57)-X(49))
      SX( 6)= X(21)+.5*ANU*BETA*(X(61)-X(53))
      SX( 7)= X(25)+.5*ANU*BETA*(X(65)-X(57))
      SX( 8)= X(29)+.5*ANU*BETA*(X(69)-X(61))
      SX( 9)= (1.-ANU*ANU)*X(33)+ANU*(X(85)+X(86)+X(87))
      SX(10)= .5*(1.-ANU*ANU)*X(34)+ANU*(X(85)*COS(PI/8.)
     1  +X(86)*COS(3.*PI/8.)+X(87)*COS(5.*PI/8.))
      SY(1)= ANU*X(5)+.5*BETA*(X(45)-X(37))
      SY( 2)= ANU*X(9)+.5*BETA*(X(49)-X(41))
      SY( 3)= ANU*X(13)+.5*BETA*(X(53)-X(45))
      SY( 4)= ANU*X(17)+.5*BETA*(X(57)-X(49))
      SY( 5)= ANU*X(21)+.5*BETA*(X(61)-X(53))
      SY( 6)= ANU*X(25)+.5*BETA*(X(65)-X(57))
      SY( 7)= ANU*X(29)+.5*BETA*(X(69)-X(61))
      WRITE (6,300) SX, SY
  300 FORMAT (4E20.8)
      GO TO 373
      END
THE FIRST LOCATION NOT USED BY THIS PROGRAM IS 41450.
```